

11-2021

## **ROLE OF EBV IN NEUROINFLAMMATION: IMPLICATIONS FOR MULTIPLE SCLEROSIS PATHOGENESIS**

Asma Hassani

Follow this and additional works at: [https://scholarworks.uaeu.ac.ae/all\\_dissertations](https://scholarworks.uaeu.ac.ae/all_dissertations)

 Part of the [Medicine and Health Sciences Commons](#)

---

United Arab Emirates University

College of Medicine and Health Sciences

ROLE OF EBV IN NEUROINFLAMMATION: IMPLICATIONS FOR  
MULTIPLE SCLEROSIS PATHOGENESIS

Asma Hassani

This dissertation is submitted in partial fulfilment of the requirements for the degree  
of Doctor of Philosophy

Under the Supervision of Professor Gulfaraz Khan

November 2021

## Declaration of Original Work

I, Asma Hassani, the undersigned, a graduate student at the United Arab Emirates University (UAEU), and the author of this dissertation entitled “*Role of EBV in Neuroinflammation: Implications for Multiple Sclerosis Pathogenesis*”, hereby, solemnly declare that this dissertation is my own original research work that has been done and prepared by me under the supervision of Professor Gulfaraz Khan, in the College of Medicine and Health Sciences at UAEU. This work has not previously formed the basis for the award of any academic degree, diploma or a similar title at this or any other university. Any materials borrowed from other sources (whether published or unpublished) and relied upon or included in my dissertation have been properly cited and acknowledged in accordance with appropriate academic conventions. I further declare that there is no potential conflict of interest with respect to the research, data collection, authorship, presentation and/or publication of this dissertation.

Student's Signature:



Date: 21/11/2021

Copyright © 2021 Asma Hassani  
All Rights Reserved

## **Advisory Committee**

1) Advisor: Gulfaraz Khan

Title: Professor

Department of Medical Microbiology

College of Medicine and Health Sciences

2) Member: Basel Ramadi

Title: Professor

Department of Medical Microbiology

College of Medicine and Health Sciences

3) Member: Safa Shehab


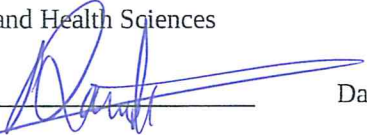
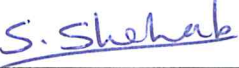
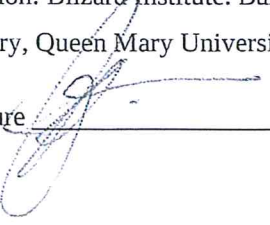
Title: Professor

Department of Anatomy

College of Medicine and Health Sciences

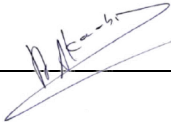
## Approval of the Doctorate Dissertation

This Doctorate Dissertation is approved by the following Examining Committee Members:

- 1) Advisor (Committee Chair): Gulfaraz Khan  
Title: Professor  
Department of Medical Microbiology  
College of Medicine and Health Sciences  
Signature  Date 24/11/2021
  
- 2) Member: Basel Ramadi  
Title: Professor  
Department of Medical Microbiology  
College of Medicine and Health Sciences  
Signature  Date 24/11/2021
  
- 3) Member: Safa Shehab  
Title: Professor  
Department of Anatomy  
College of Medicine and Health Sciences  
Signature  Date 24.11.2021
  
- 4) Member (External Examiner): Gavin Giovannoni  
Title: Professor  
Centre for Neuroscience, Surgery and Trauma  
Institution: Blizard Institute, Barts and The London School of Medicine and Dentistry, Queen Mary University of London, UK  
Signature  Date 19/10/2021

This Doctorate Dissertation is accepted by:

Dean of the College of Medicine and Health Sciences: Professor Juma Alkaabi

Signature  Date 8/12/2021

Dean of the College of Graduate Studies: Professor Ali Al-Marzouqi

Signature  Ali Hassan Date 8/12/2021

Copy \_\_\_\_ of \_\_\_\_

## Abstract

Multiple sclerosis (MS) is a demyelinating disease of the CNS with unknown cause. Individuals who are genetically predisposed and exposed to specific environmental factors have an increased risk of developing MS. Epstein-Barr virus (EBV) infection is linked to MS development, according to a large body of seroepidemiological and pathological evidence. EBV is a ubiquitous human herpesvirus that typically produces silent infection but can also cause a wide range of illnesses. A large cohort of MS and non-MS control cases has been previously examined and revealed the prevalent presence of EBV in MS. However, the role of the virus in the disease is unclear. The main objective of this research was to understand the viral dynamics *in vivo* and the consequences of peripheral infection on the CNS. To this end, a novel rabbit model of EBV, which produces latent infection comparable to the persistent infection in human carriers, was used in this study. The present dissertation contains (1) human study and (2) animal study for correlation of the results. In the human study, EBV-positive MS cases were examined for histopathological changes. In the animal study, EBV was injected intravenously in one group of animals, and PBS was injected in the control group, with and without immunosuppression. Histopathological changes and viral dynamics were evaluated in the peripheral blood, spleen, brain, and spinal cord, using molecular and histopathology techniques. A number of important aspects of EBV infection were revealed. Peripheral EBV infection led to CNS infection and promoted neuroinflammation in the form of immune aggregates. EBV infected B cells were most likely the source of CNS infection. The immune aggregates were more prevalent in immunosuppressed animals and consisted of focal accumulation of macrophages surrounded by reactive astrocytes and dispersed B and T lymphocytes. The center of aggregates exhibited signs of myelin destruction. Moreover, studying EBV infection over time revealed that the peak in viral load in the periphery and CNS corresponded to an increase in the occurrence of cellular aggregates in the brain. Additionally, altered expression of viral latent transcripts correlated with upregulation of several proinflammatory cytokines in the periphery and the CNS. Increased expression of IL-6 at the mRNA and protein level in the brain was associated with neuroinflammation. Finally, several similarities and differences were observed between the pathology in EBV positive MS cases and EBV infected rabbit CNS. Several cellular key players



contributed to both pathologies, however, the extent of infiltration of these cells and their distribution differed between the two. This work establishes the first direct *in vivo* evidence for the role of peripheral EBV infection in CNS pathology, and demonstrates the utility of a novel model for dissecting viral mechanisms involved in the development of EBV- associated diseases including MS.

**Keywords:** Epstein-Barr virus, peripheral infection, neuroinflammation, demyelination, CNS infection, multiple sclerosis, rabbit model.

## Title and Abstract (in Arabic)

دور فيروس إبشتاين بار في التهاب الأعصاب: وانعكاساته في تطور مرض التصلب

اللوحي

الملخص

التصلب العصبي المتعدد (MS) هو مرض يؤدي لإتلاف طبقة الميالين في الجهاز العصبي المركزي لأسباب غير معروفة. تزداد فرص الإصابة بمرض MS لدى الأفراد الذين لديهم قابلية وراثية ويتعرضون لعوامل بيئية معينة. وترتبط عدوى فيروس إبشتاين بار (EBV) بتطور مرض MS، وفقاً لمجموعة كبيرة من الأدلة من الدراسات الوبائية والابديميولوجية. EBV هو فيروس هربس بشري شائع ينتج عنه عادة عدوى صامتة ولكن يمكن أن يسبب أيضاً أمراض عديدة. لقد تم سابقاً دراسة مجموعة كبيرة من حالات MS وحالات غير مصابة بمرض MS، وأظهرت النتائج الوجود السائد لـ EBV في نسيج الدماغ للحالات المصابة بـ MS. ومع ذلك، فإن دور الفيروس في المرض غير واضح. وكان الهدف الرئيسي من هذا البحث هو فهم الديناميكيات الفيروسية في الجسم الحي وأثر العدوى المحيطة على الجهاز العصبي المركزي. تحقيقاً لهذه الغاية، تم استخدام في هذه الدراسة نموذج جديد لعدوى EBV في الأرانب، والذي ينتج عنه عدوى كامنة مماثلة للعدوى المستمرة في الإنسان. تحتوي هذه الرسالة على (1) دراسة بشرية و (2) دراسة حيوانية لربط النتائج، حيث تم في الدراسة البشرية فحص نسيج الدماغ المصاب بمرض MS والحامل لفيروس EBV للتغيرات النسيجية المرضية. أما في دراسة الحيوانات، فقد تم حقن فيروس EBV عن طريق الوريد في مجموعة من الأرانب، وحقن المحلول الملحي PBS في المجموعة الضابطة، مع أو بدون تثبيط المناعة. وتم تقييم التغيرات النسيجية المرضية وديناميات الفيروس في الدم المحيطي والطحال والدماغ والنخاع الشوكي باستخدام تقنيات التشريح المرضي والتقنيات الحيوية الجزيئية. وعليه أظهرت الدراسة عدداً من الجوانب الهامة لعدوى EBV، حيث أدت عدوى EBV المحيطة إلى عدوى الجهاز العصبي المركزي والتهاب الأعصاب على شكل تكتلات خلوية مناعية. وعلى الأرجح أن الخلايا البائية المصابة بـ EBV هي مصدر عدوى الجهاز العصبي المركزي. وكانت الحيوانات التي تم تثبيط مناعتها أكثر إصابة بالتكتلات الخلوية المناعية في الجهاز العصبي المركزي، وهذه التكتلات الخلوية المناعية عبارة عن تراكم بؤري للبلاعم المحاطة بالخلايا النجمية التفاعلية والخلايا الليمفاوية B و T المبعثرة. وتم ملاحظة وجود تلف لطبقة الميالين في وسط التكتلات الخلوية المناعية. علاوة على ذلك، فقد كشفت دراسة عدوى

EBV مع مرور الوقت أن ذروة الحمل الفيروسي في المحيط والجهاز العصبي المركزي تتزامن مع زيادة في حدوث التكتلات الخلوية في الدماغ. بالإضافة إلى ذلك، ترتبط التغيرات في تعبير الجينات الفيروسية بازدياد التعبير الجيني للسيتوكينات المسببة للالتهابات في المحيط والجهاز العصبي المركزي. وارتبط التهاب الأعصاب بزيادة التعبير عن IL-6 على مستوى mRNA والبروتين في الدماغ. أخيرًا، لوحظ العديد من أوجه التشابه والاختلاف بين التغيرات المرضية في نسيج الدماغ المصاب بمرض MS والحامل لفيروس EBV والجهاز العصبي المركزي للأرانب المصاب بـ EBV. ساهم عدد من الخلايا الرئيسية في كلا المرضين، على الرغم من الاختلاف في مدى انتشار هذه الخلايا وتوزيعها. ويؤسس هذا العمل أول دليل مباشر في الجسم الحي لدور عدوى EBV المحيطة في أمراض الجهاز العصبي المركزي، ويوضح فائدة نموذج حيواني جديد لدراسة الآليات الفيروسية المشاركة في تطوير الأمراض المرتبطة بـ EBV بما في ذلك مرض MS.

**مفاهيم البحث الرئيسية:** فيروس ابشتاين بار، العدوى المحيطة، الالتهاب العصبي، تلف الميالين، عدوى الجهاز العصبي المركزي، التصلب المتعدد، نموذج الأرنب.

## Acknowledgements

This project would not have been possible without the generous and selfless support of many people to whom I owe a tremendous debt of gratitude. First, I would like to express my sincere gratitude to my supervisor Prof. Gulfaraz Khan for his constant guidance, knowledge, enormous support, and patience throughout the last 7 years. I consider myself fortunate to have him as a mentor, who has been absolutely instrumental in my professional and personal growth. It is also a pleasure to thank my dissertation committee members, Prof Basel Ramadi and Prof Safa Shehab for graciously giving their time to evaluate the progress in the project, help by providing their expertise in the field of immunology and neuroanatomy and offer valuable criticism, genuine advice and support.

I am also extremely thankful to our lab technician, Pretty Philip, who has taught me the ABCs of different techniques in the lab, and for helping out during the exhausting animal work. Special thanks go to Narendran Reguraman for the enormous effort in all the animal work, injections, and sacrifice. I would also like to acknowledge the support of the lab members: Waqar Ahmed, Yasmeen Abdelmowla, Zubaida Hassan, Sadaf Rizvi, and Fatima Sulaiman. I also thank all the professors, doctors, and research technicians in the Dept. Medical Microbiology and Immunology, and my fellow postgraduate students. I am also thankful to UAEU college of graduate studies that supported me with a full scholarship throughout my PhD duration.

A big chunk of the credit goes to my parents and siblings for the endless support, prayers and patience on my absence. Finally, I am immensely grateful to my friends Meriem Rahmani, Rita Romero, Mauricio Moreno, Rana Al Alami, and Rizwan Taj, and my running group for keeping my sanity along the way.

## **Dedication**

*To my beloved parents and family*

## Table of Contents

Title .....	i
Declaration of Original Work .....	ii
Copyright .....	iii
Advisory Committee .....	iv
Approval of the Doctorate Dissertation .....	v
Abstract .....	vii
Title and Abstract (in Arabic) .....	ix
Acknowledgements .....	xi
Dedication .....	xii
Table of Contents .....	xiii
List of Tables.....	xvi
List of Figures .....	xvii
List of Abbreviations.....	xix
Chapter 1: Introduction .....	1
1.1 Overview .....	1
1.2 Introduction to Multiple Sclerosis.....	1
1.2.1 MS Pathology .....	3
1.2.2 MS Risk Factors .....	8
1.3 Introduction to Epstein-Barr Virus.....	10
1.3.1 EBV Structure and Lifecycle.....	12
1.3.2 EBV Kinetics During Primary Infection in Humans.....	15
1.3.3 The Link Between EBV and MS .....	19
1.3.4 EBV in CNS Pathologies.....	23
1.4 Introduction to the Rabbit Model of EBV Infection .....	25
1.5 Introduction to the Immunosurveillance of the CNS .....	29
1.6 The Rationale and Objectives of the Study .....	36
Chapter 2: Methods .....	38
2.1 Human Study.....	38
2.1.1 Processing of Formalin Preserved Human Brain Tissues .....	38
2.1.2 Examination of Histopathology in EBV Infected MS Brain Using Hematoxylin and Eosin .....	39
2.1.3 Examination of Demyelination in EBV Infected MS Brain Using Luxol Fast Blue .....	40
2.1.4 Examination of Inflammation in EBV Infected MS Brain Using Immunohistochemistry .....	41

2.2 Animal Study .....	44
2.2.1 Ethical Statement.....	44
2.2.2 Preparation of EBV Inoculum for Infection.....	44
2.2.3 Animals and Experimental Design.....	45
2.2.4 Isolation of PBMCs and Plasma.....	49
2.2.5 Extraction of Genomic DNA and Viral Detection and Quantitation Using Quantitative PCR.....	50
2.2.6 Examination of Histopathological Changes in the CNS Following EBV Infection Using Hematoxylin and Eosin staining .....	53
2.2.7 Examination of Inflammation in the CNS Following EBV Infection Using Immunostaining .....	53
2.2.8 Examination of EBV Infection in the Periphery and CNS Using EBER- <i>in situ</i> Hybridization .....	55
2.2.9 Extraction of Total RNA and Detection of Cellular and Viral Transcripts Using Reverse-Transcriptase PCR (RT-PCR) .....	58
2.2.10 Extraction of Total Protein and Detection of IL-2 and IL-6 in the CNS Using ELISA .....	61
2.2.11 Statistical Analysis .....	62
Chapter 3: Results .....	63
3.1 Human Study.....	63
3.1.1 Heterogeneity of MS Plaques in EBV Positive Cases.....	63
3.2 Animal Study .....	71
3.2.1 Phase 1: Examining Viral Spread from the Periphery to the CNS .....	71
3.2.2 Phase 2: Investigating the Dynamics of EBV Infection Over Time .....	90
Chapter 4: Discussion .....	110
4.1 EBV Levels Peak Within 2 Weeks of Primary Infection in Rabbits.....	111
4.2 Peripheral Infected Cells Migrate to the CNS in Rabbits .....	112
4.3 Neuropathology in the Rabbit CNS .....	114
4.3.1 The Makeup of Inflammatory Cell Aggregates in the CNS Of EBV Infected Rabbits.....	116
4.3.2 Comparison Between Pathology in EBV Positive MS Cases and Pathology in the Brain of EBV Positive Rabbits.....	120
4.4 Altered Viral Latent Transcripts and Cytokines Expression in the Periphery and the CNS .....	124
4.4.1 Correlation Between EBV Viral Transcripts and Cytokine Expression .....	124

4.4.2 Significance of Upregulated Inflammatory Cytokines During EBV Infection .....	127
Chapter 5: Conclusion.....	131
5.1 Limitations and Future Research .....	132
References .....	135
List of Publications .....	180
Appendix .....	181
Appendix I: Coating slides.....	181
Appendix II: Buffers and reagents preparation.....	181



## List of Tables

Table 1: Global number of MS cases in 2013 and 2020 .....	2
Table 2: Primary antibodies used for IHC on MS brain section .....	44
Table 3: Sequence of primers and probes used in amplifying gDNA extracted from rabbit samples .....	52
Table 4: List of antibodies used in IHC/IF on rabbit tissues.....	54
Table 5: List of fluorochrome-conjugated antibodies used for fluorescent staining on rabbit tissues .....	55
Table 6: Sequence of primers for rabbit cellular transcripts and EBV genes .....	60
Table 7: The relationship between cell-free EBV load in plasma and viral load in PBMCs and spleen .....	76
Table 8: Spearman correlation of EBV load in the CNS and viral load in the peripheral compartments (plasma, PBMCs and spleen) .....	92

## List of Figures

Figure 1: Macroscopic lesions in chronic MS .....	3
Figure 2: Demyelination of subpial grey matter in the MS brain .....	5
Figure 3: MS lesions in the white matter .....	6
Figure 4: Active MS lesions (blue area) form usually around a blood vessel .....	7
Figure 5: Various risk factors implicated in MS development and progression.....	10
Figure 6: The main components of EBV virions .....	12
Figure 7: The lifecycle of EBV .....	14
Figure 8: EBV load and antiviral immune response during primary infection.....	17
Figure 9: Animal models to study human $\gamma$ -herpesviruses .....	25
Figure 10: Trafficking of activated lymphocytes into the CNS across the BBB.....	31
Figure 11: Trafficking of immune cells into the CNS across the B-CSF-B .....	32
Figure 12: Viruses use blood and/ or peripheral nerves to access the CNS.....	33
Figure 13: Phase 1 of the animal study .....	47
Figure 14: Phase 2 of the animal study .....	49
Figure 15: Standard curve created using Namalwa gDNA .....	52
Figure 16: Standard curve established using known BSA concentrations, to estimate protein concentration from CNS homogenates.....	62
Figure 17: MS case I with chronic inactive plaque.....	64
Figure 18: MS case II with chronic inactive plaque .....	65
Figure 19: MS case III with chronic inactive plaque .....	65
Figure 20: MS case IV with chronic inactive plaque.....	66
Figure 21: Astrocytes surround demyelinated plaques .....	67
Figure 22: Microglia occupy the demyelinated lesion and surrounding non-demyelinated areas .....	68
Figure 23: Macrophages occupy the demyelinated lesion and surrounding non-demyelinated areas .....	68
Figure 24: MS case V with inactive and active plaques .....	69
Figure 25: Infiltration of T cells in MS case V .....	70
Figure 26: The relationship between demyelination and perivascular cuffing.....	70
Figure 27: IHC for PCNA in MS case V .....	71
Figure 28: Representative EBER-ISH on rabbit spleen from EBV and EBV+CsA group and their controls .....	73
Figure 29: EBV detection in the periphery of EBV inoculated rabbits .....	75
Figure 30: Cell aggregation in the rabbit CNS .....	77
Figure 31: Widespread cerebral aggregates .....	78
Figure 32: The cellular makeup of cerebral aggregates in EBV infected rabbits.....	80
Figure 33: Diffuse infiltrating immune cells in the brain parenchyma.....	81
Figure 34: Heterogeneity of cell aggregates in the brain .....	81

Figure 35: The association of brain ventricles with immune infiltrates.....	82
Figure 36: The cellular makeup of spinal cord inflammatory infiltrates in EBV infected rabbit .....	82
Figure 37: Spatial relationship between the different cells making up the aggregates.....	84
Figure 38: The impact of aggregate formation on myelin integrity in the CNS .....	85
Figure 39: The infiltration of EBV infected cells into the brain .....	87
Figure 40: The phenotype of EBV infected cells in the brain .....	89
Figure 41: EBV load in the periphery and CNS at different time points.....	91
Figure 42: CNS aggregate formation peaks at 14 and 21dpi .....	93
Figure 43: Quantification of cell aggregates in the brain.....	95
Figure 44: Prominent infiltration of macrophages and neutrophils in aggregate positive brain sections at 14 and 21dpi .....	97
Figure 45: Infiltration of the spinal cord by macrophages and neutrophils .....	98
Figure 46: Reactive glia and infiltrating immune cells in aggregate-positive brain.....	99
Figure 47: Evaluation of myelin integrity within aggregates at 14 and 21dpi.....	100
Figure 48: The relative expression of EBV transcripts in the spleen.....	101
Figure 49: The relative expression of cytokines in the spleen.....	102
Figure 50: Heat map of Spearman correlation of inflammatory and viral transcripts in the spleen.....	103
Figure 51: The relative expression of EBV transcripts in the brain.....	104
Figure 52: The relative expression of cytokines in the brain .....	104
Figure 53: Heat map of Spearman correlation of inflammatory and viral transcripts in the brain.....	105
Figure 54: The levels of IL-2 and IL-6 proteins in the brain .....	106
Figure 55: The relative expression of EBV transcripts in the spinal cord .....	107
Figure 56: The relative expression of cytokines in the spinal cord .....	107
Figure 57: Heat map of Spearman correlation of inflammatory and viral transcripts in the spinal cord .....	108
Figure 58: The levels of IL-2 and IL-6 proteins in the spinal cord.....	109

## List of Abbreviations

ADEM	Acute Disseminated Encephalomyelitis
APCs	Antigen Presenting Cells
BBB	Blood-Brain-Barrier
B-CSF-B	Blood-Cerebrospinal Fluid-Barrier
BSA	Bovine Serum Albumin
CAEBV	Chronic Active EBV Infection
CMV	Cytomegalovirus
CNS	Central Nervous System
CsA	Cyclosporin A
CSF	Cerebrospinal Fluid
Ct	Cycle Threshold
DAB	Diaminobenzidine
DMT	Disease Modifying Therapy
EA	Early Antigen
EAE	Experimental Autoimmune Encephalitis
EBER	Epstein-Barr Encoded RNAs
EBI2	Epstein-Barr Virus Induced Gene 2
EBNA	Epstein-Barr Nuclear Antigen
EBV	Epstein-Barr Virus
ELFs	Ectopic Lymphoid Follicles
FBS	Fetal Bovine Serum
FFPE	Formalin Fixed, Paraffin Embedded
GAPDH	Glyceraldehyde 3-Phosphate Dehydrogenase

GFAP	Glial Fibrillary Acidic Protein
gp	Glycoprotein
H&E	Hematoxylin and Eosin
HIAR	Heat-Induced Antigen Retrieval
HIV	Human Immunodeficiency Virus
HLA	Human Leukocyte Antigens
HLH	Hemophagocytic Lymphohistiocytosis
HSV	Herpes Simplex Virus
HVP	Herpesvirus Papio
Iba1	Ionized Calcium Binding Adaptor Molecule 1
IFN	Interferon
Ig	Immunoglobulin
IHC	Immunohistochemistry
IL	Interleukin
IM	Infectious Mononucleosis
ISH	<i>In Situ</i> Hybridization
IV	Intravenous
KSHV	Kaposi Sarcoma Herpesvirus
LCLs	Lymphoblastoid Cell Lines
LMP	Latent Membrane Protein
MAG	Myelin Associate Glycoprotein
MBP	Myelin Basic Protein
MHC	Major Histocompatibility Complex Molecules
MHV68	Murine $\gamma$ Herpesvirus 68

MMPs	Matrix Metalloproteinases
MOG	Myelin Oligodendrocyte Glycoprotein
MS	Multiple Sclerosis
NK	Natural Killer Cells
NZW	New Zealand White
PBMCs	Peripheral Blood Mononuclear Cells
PCNA	Proliferating Cell Nuclear Antigen
PD-1	Programmed Death 1
pDC	Plasmacytoid Dendritic Cells
PLP	Proteolipid Protein
PPMS	Primary Progressive Multiple Sclerosis
RRMS	Relapsing Remitting Multiple Sclerosis
RT-PCR	Reverse-Transcriptase Polymerase Chain Reaction
SAS	Subarachnoid Spaces
SARS-CoV2	Severe Acute Respiratory Syndrome Coronavirus 2
SIV	Simian Immunodeficiency Virus
SPMS	Secondary Progressive Multiple Sclerosis
Th1	T Helper1
TNF	Tumor Necrosis Factor
TMEV	Theiler's Murine Encephalomyelitis Virus
Treg	Regulatory T cells
T <sub>RM</sub>	Tissue Resident Memory T cells
VCA	Viral Capsid Antigen

## **Chapter 1: Introduction**

### **1.1 Overview**

Epstein-Barr virus (EBV) is ubiquitous in humans and causes silent infections in most people. EBV can efficiently escape and dysregulate peripheral immune response, through the exploitation and manipulation of various host cellular processes. Abnormal immune response to EBV is a defining feature of several EBV-related diseases. Due to the existence of a finely regulated CNS-periphery axis, a balanced immune system is inherent to maintaining CNS homeostasis. Immune alterations caused by EBV infection can extend beyond the periphery and disrupt CNS homeostasis. This dissertation presents research work that explores the impact of primary peripheral EBV infection on the CNS, and its implications for the link between EBV and the pathogenesis of multiple sclerosis.

### **1.2 Introduction to Multiple Sclerosis**

Multiple sclerosis (MS) is a disease that causes demyelination, or damage to myelin sheaths in the brain, spinal cord and optic nerve (Reich et al., 2018). Neuroinflammation, which is thought to be caused by autoimmunity, is fundamental in MS pathology (Bevan et al., 2018; Pikor et al., 2015). T and B lymphocytes infiltrate the central nervous system (CNS) almost always during the early stages of MS, and to a much lesser degree during the late stages (Lassmann, 2018). Yet, the understanding of what causes pathology in MS is relatively limited.

Although MS does not significantly alter the life expectancy of the patients, it does however reduce the quality of life dramatically (Koch-Henriksen et al., 2017). In fact, MS is the main contributor to non-traumatic disability among young people

(Dobson & Giovannoni, 2019). Most people with MS undergo recurrent neurological deficits followed by long periods of recovery in so-called relapsing-remitting MS (RRMS). Eventually, periods of remissions stop during secondary progressive disease (SPMS), which leads to life-long disability. A small fraction of MS patients experience progressive disability with no remission right from disease onset in primary progressive MS (PPMS) (Thompson et al., 2018).

The latest update in the Atlas of MS, generated by MS International Federation (MSIF) has revealed that the number of people living with MS in the world has escalated from 2.3 million in 2013 to 2.8 million in 2020 (Table 1) (Walton et al., 2020). Although this increase is partly attributed to improved survival and diagnosis of MS patients, it is also believed that these numbers reflect an actual rise in disease development (Wallin et al., 2019). This burden is aggravated by the lack of a cure for MS.

Table 1: Global number of MS cases in 2013 and 2020 (Walton et al., 2020)

	Number of countries included <sup>a</sup>	2013 prevalence per 100,000 population [95% CI]	2020 prevalence per 100,000 population [95% CI]	Increase; absolute (%)
Global	81	29.26 [29.21, 29.30]	43.95 [43.90, 44.01]	14.69 (50%)
African	6	5.52 [5.41, 5.62]	8.76 [8.64, 8.89]	3.24 (59%)
Americas	15	62.89 [62.72, 63.05]	117.49 [117.27, 117.71]	54.6 (87%)
E. Mediterranean	14	23.91 [23.77, 24.04]	33.00 [32.85, 33.15]	9.09 (38%)
European	35	108.25 [108.01, 108.49]	142.81 [142.53, 143.08]	34.56 (32%)
South East Asia	4	5.44 [5.41, 5.48]	8.62 [8.58, 8.66]	3.18 (58%)
Western Pacific	7	3.64 [3.61, 3.67]	4.79 [4.75, 4.82]	1.15 (32%)

CI: confidence intervals, E. Mediterranean: Eastern Mediterranean.  
<sup>a</sup>Only countries providing data for 2013 and 2020 editions of the Atlas of MS are included in the analysis. Global and WHO regional totals reported. Reported MS prevalence increased in every WHO region between the 2013 and 2020 versions of the Atlas of MS.



### 1.2.1 MS Pathology

The main pathology of MS is the presence of focal lesions of demyelination in the white matter and grey matter of the CNS (Figure 1) (Höftberger & Lassmann, 2017). These lesions, also known as plaques, are characterized by inflammation, myelin destruction, damage to oligodendrocytes and axons, neurodegeneration, and reactive astrogliosis (Filippi et al., 2018). Histopathologists use various basic and special stains and immunohistochemistry (IHC) to detect MS plaques. Hematoxylin and Eosin, Luxol Fast Blue (LFB), and IHC staining for proteolipid protein (PLP), myelin oligodendrocyte glycoprotein (MOG), myelin associated glycoprotein (MAG), and myelin basic protein (MBP) help identify areas with myelin destruction in CNS tissues. Whereas Bielschowsky silver impregnation and IHC for neurofilament protein can reveal axonal loss. Immunostaining for glial fibrillary acidic protein (GFAP) shows areas with astrogliosis, while IHC for immune cell markers such as CD68, KiM1P, CD3, CD4, CD8, CD20, and CD138 demonstrate sites of active inflammation (Lassmann, 2018).

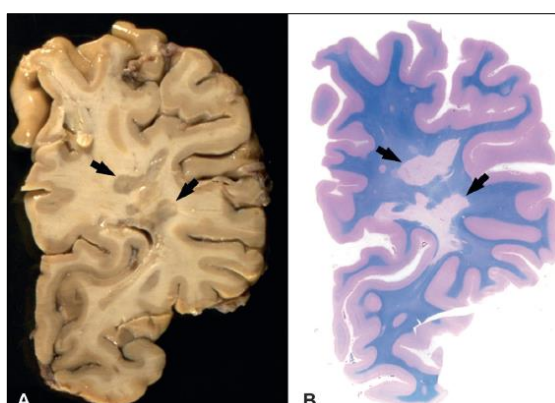


Figure 1: Macroscopic lesions in chronic MS. (A) Formalin-fixed brain hemisphere with gross appearance of demyelinated plaques (black arrows). (B) Periventricular white matter lesion is readily detectable using LFB stain (Höftberger & Lassmann, 2017)

Given the myelin-rich nature of the white matter, it was initially believed that MS plaques occur solely in the white matter. Nevertheless, several pathological studies have revealed that both white matter and grey matter are affected by demyelination in MS (Bø et al., 2003; Calabrese et al., 2010; Gilmore et al., 2009; Peterson et al., 2001; Petrova et al., 2018). Examination of autopsied MS brain and control brain samples, retrieved from the Brain Bank in Haukeland Hospital in Norway, showed that demyelinated plaques in the grey matter were significantly bigger in size than those in the white matter (Bø et al., 2003). Similar observations were made upon examining autopsied MS cerebrum, cerebellum and spinal cord tissues retrieved from MS Brain Bank in the UK (Gilmore et al., 2009).

It is unclear why demyelination affects the grey matter more than the white matter. However, it has been suggested that meningeal inflammation and increased expression of inflammatory cytokines in the cerebrospinal fluid (CSF) may play a role in increasing grey matter vulnerability (Choi et al., 2012; Howell et al., 2011; Magliozzi et al., 2018). A study on postmortem MS brain tissues found that extensive infiltration of the meningeal spaces by CD3<sup>+</sup> T cells, CD20<sup>+</sup> B cells, and CD68<sup>+</sup> macrophages among other immune cells, is associated with increased burden of lesions in the grey matter (Choi et al., 2012).

Although demyelination in the white matter can be easily detected using LFB stain, grey matter lesions are often missed due to the low sensitivity of LFB to grey matter demyelination. Instead, grey matter lesions can be seen upon immunostaining for MBP, PLP, and MOG (Bø et al., 2003; Choi et al., 2012; Howell et al., 2011). Lesions in the grey matter are characterized with neurites transection, and death of neurons. Infiltration of immune cells into demyelinated grey matter is relatively rare

(Peterson et al., 2001). Lesions in the grey matter often occur in the forebrain, the cerebellum, and in the deep grey matter nuclei, and can be detected more frequently in progressive MS (Filippi et al., 2018). The most common type of grey matter lesions is subpial demyelination (Figure 2), which develops in the subpial region and affects large area of the cerebral cortex, usually covering a number of neighboring gyri (Bø et al., 2003; Peterson et al., 2001).

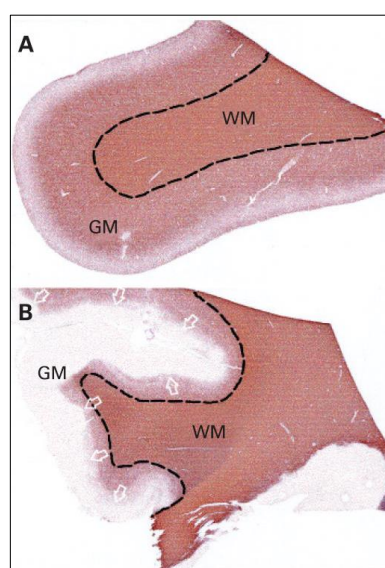


Figure 2: Demyelination of subpial grey matter in the MS brain. (A) IHC for PLP in non-MS control brain shows normal myelin integrity in the grey matter (light brown) and subcortical white matter (dark brown). (B) Immunostaining for PLP in MS brain shows a demyelinated lesion in the subpial cerebral cortex stretching into the cingulate gyrus. (Gilmore et al., 2009)

MS plaques vary in activity and are divided into acute active, chronic active, inactive, smoldering, and shadow plaques (Figure 3). Acute active lesions often occur in early MS. These lesions are hypercellular owing to the pronounced infiltration of immune cells (Figure 3A&E). Macrophages engulf remnants of myelin, and are scattered uniformly in the lesion forming “sea of macrophages” (Popescu & Lucchinetti, 2012). T and B lymphocytes are widespread in the lesion, with B cells

accumulating mainly in the perivascular cuffs. CD8<sup>+</sup> T cells are the predominant T cell subset in the lesions (Figure 4) (Hayashi et al., 1988). The extent of lymphocytes infiltration correlates with the degree of damage to axons in active lesions (Dutta & Trapp, 2011). Moreover, astrocytes increase in number and size, and GFAP staining shows numerous cell processes in active lesions (Love, 2006).

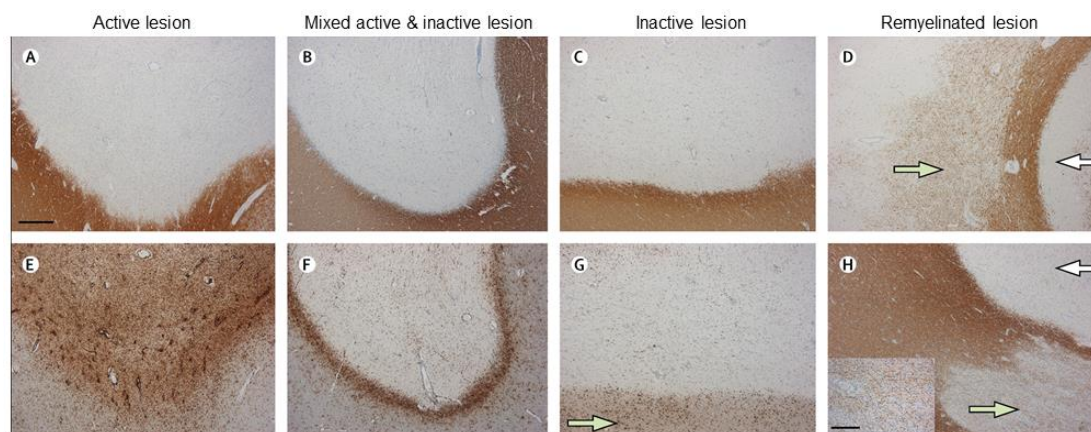


Figure 3: MS lesions in the white matter. (A&E) Early disease usually starts with active lesions. (A) IHC for MBP shows a well demarcated and completely demyelinated lesion. (E) IHC for CD68 shows pronounced infiltration of activated microglia/macrophages in the center of demyelination of active lesion. (B&F) Active lesions can evolve into mixed active and inactive. (B) IHC for MBP shows a well demarcated area of complete demyelination. (F) IHC for CD68 shows less infiltration of microglia/macrophages in the demyelinated center and a compact collection of macrophages surrounding the lesion. (C&G) MS Lesions become inactive and non-inflamed with time, as evident in the most chronic stages of MS. (C) IHC for MBP shows a demyelinated lesion. (G) IHC for CD68 shows little infiltration by macrophages in the lesion. No intense belt of macrophages is seen at the border of inactive lesions, however, the non-demyelinated area next to the lesion (green arrow) contains more macrophages than the lesion itself. (D&H) IHC for MBP demonstrates remyelinated lesions (green arrows). Remyelination can occur during any stage of the disease. However, shadow plaques, which result from incomplete remyelination with thin myelin fibers, are more common in the most chronic stages/ progressive MS. Scale bar= 200  $\mu$ m (Filippi et al., 2019)

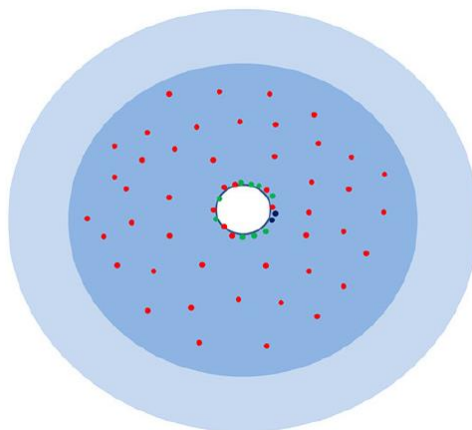


Figure 4: Active MS lesions (blue area) form usually around a blood vessel. B lymphocytes (green dots) and plasma cells (blue dots) are located in the perivascular spaces. CD8<sup>+</sup> T cells (red dots) are scattered throughout the lesion. Macrophages are found throughout the lesion (Lassmann, 2018)

Chronic active lesions are commonly detected in progressive MS. They have well-defined edges, which consist of clusters of myelin-containing macrophages. The center of the lesion is inactive and hypocellular, and contains few dispersed macrophages (Filippi et al., 2019).

In contrast to active lesions, inactive plaques contain myelin-free macrophages. They are well demarcated areas of complete demyelination and hypocellular center (Figure 3C&G) (Frischer et al., 2009). MS lesions typically shift from active, during early disease, to inactive during the later chronic stages. Inactive lesions are marked by limited macrophage infiltration, little to no inflammation, and the formation of astrocytic glial scar, which contributes to the distinct macroscopic appearance of MS lesions (Figure 1) (Lucchinetti et al., 2000).

Smoldering plaques have inactive center surrounded by a distinct hypercellular border of gradually diffusing activated microglia/macrophages and T lymphocytes (Figure 3B&F) (Höftberger & Lassmann, 2017). Finally, demyelinated plaques that undergo remyelination form shadow plaques (Figure 3D&H) (Popescu et al., 2013).

New oligodendrocytes (i.e. myelin-producing cells) are generated from oligodendrocyte progenitor cells in the CNS to form new myelin sheaths (Bradl & Lassmann, 2010). The loss of these precursor cells or failure to proliferate and/or differentiate into mature oligodendrocytes can impede remyelination (Wolswijk, 2000). Remyelination becomes less efficient with time (i.e. production of thinner myelin sheaths than the original myelin) in lesions subjected to recurrent bouts of inflammation and demyelination (Popescu et al., 2013).

### **1.2.2 MS Risk Factors**

MS development is believed to be greatly influenced by both genetics and environmental factors; however, the exact cause of MS remains unclear. The increased susceptibility to MS in Caucasians compared to other ethnic backgrounds, such as Indigenous Australians and Japanese, reflects the impact of genes on MS risk (Brum et al., 2013; Flores et al., 2012; Hammond et al., 1987). However, the concordance rate for MS is reported to be as high as 25% in genetically identical individuals (“French Research Group on MS” 1992; Willer et al., 2003). Additionally, in a recent study comparing the immune cell characteristics of Caucasian monozygotic twins with discordant MS, it was found that both MS-affected and non-affected co-twins had comparable immunological profiles (Gerdes et al., 2020). This indicates that factors other than genetics play a role in the development of MS (Fagnani et al., 2015). This has been supported by immigration studies demonstrating increased MS risk in immigrants from low MS-risk regions to regions with high MS incidence (Berg-Hansen et al., 2015; Berg-Hansen & Celius, 2015; Nasr et al., 2016).

Among the genes discovered to influence MS risk, HLA class II allele *HLADRB1\*1501* has been demonstrated to have the greatest odds ratio in conferring

susceptibility to MS (Barcellos et al., 2006; Chao et al., 2008; Ramagopalan & Ebers, 2009). HLA alleles encode MHC molecules, the surface glycoproteins on antigen presenting cells (APCs). The expression of MS risk genes is also believed to be under the influence of the epigenome including DNA methylation, histone post-translational modifications, and miRNAs activity (Celarain & Tomas-Roig, 2020; Chao et al., 2009; Gacias & Casaccia, 2014; Küçükali et al., 2015)

Additionally, given that MS incidence is higher in females than males, and in young adults (20-40 years of age) than other age groups, both female sex hormones and age are believed to be implicated in the pathogenesis of MS (Wallin et al., 2012; Ysraelit & Correale, 2019). Moreover, other factors including smoking, vitamin D status, body mass index, and infections are thought to modulate susceptibility to MS (Figure 5) (Alharbi, 2015; Hedström et al., 2013; Libbey et al., 2014; Munger et al., 2009). While there are several infectious agents suspected to be linked to MS, substantial evidence from seroepidemiological and pathological studies support the role of Epstein-Barr virus (EBV) in MS pathogenesis (Ascherio et al., 2001; Ascherio & Munger, 2010; Belbasis et al., 2015; Giovannoni et al., 2006).

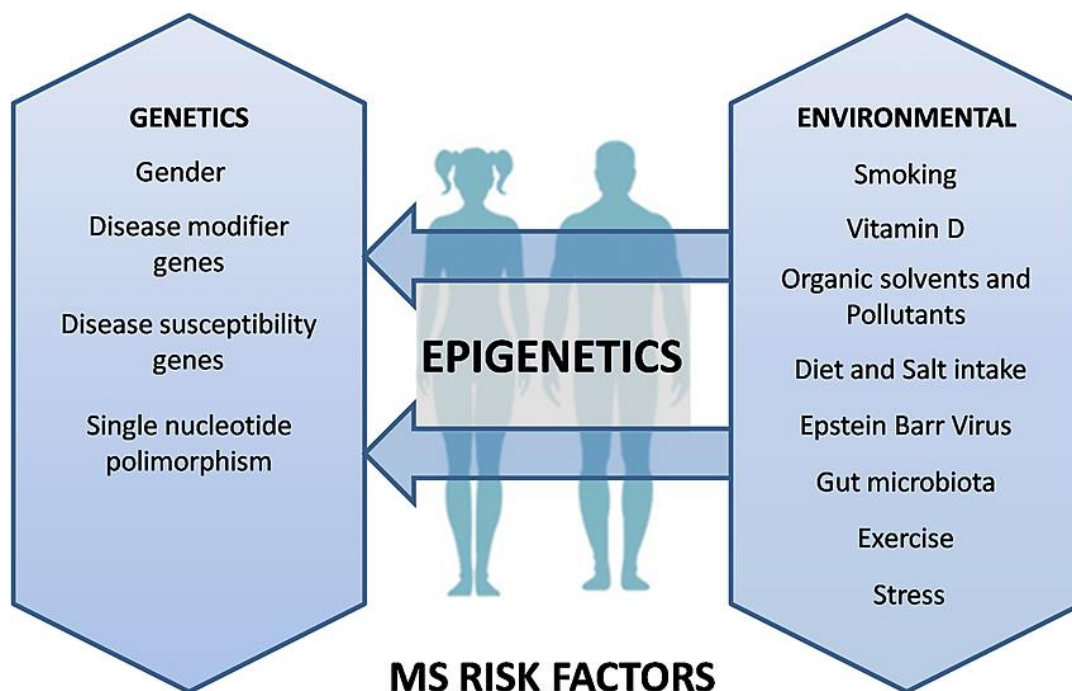


Figure 5: Various risk factors implicated in MS development and progression (Celarain & Tomas-Roig, 2020)

### 1.3 Introduction to Epstein-Barr Virus

Epstein-Barr virus (EBV) is one of the most successful pathogens persisting in humans. It targets B lymphocytes to establish a life-long reservoir (Cohen, 2020). EBV belongs to the family Herpesviridae that contain eight known viruses that infect humans; herpes simplex virus type 1 and 2 (HSV-1 and -2), varicella-zoster virus (VZV), cytomegalovirus (CMV), human herpesvirus 6 (HHV-6), human herpesvirus 7 (HHV-7), EBV and Kaposi's sarcoma herpesvirus (KSHV) (Klein et al., 2007).

EBV is carried by 95% of humans, primarily as a silent infection (Young et al., 2016). The incidence of contracting EBV is highest in children, as the first 3 years of life represent the peak period for EBV acquisition (Thorley-Lawson & Gross, 2004). Healthy Kenyan newborn, for instance, can acquire EBV as early as 3 months of age, and the virus is thought to be transmitted via mother's breast milk (Coleman et al.,



2017). However, infection can be delayed to late adolescence or early adulthood in western countries, and this late acquisition of EBV can manifest as febrile disease called infectious mononucleosis (IM) (Dunmire et al., 2018). Moreover, EBV is associated with several malignancies, such as Hodgkin's Lymphoma, Burkitt's lymphoma, nasopharyngeal carcinoma, and post-transplant lymphoproliferative disorder. Indeed, about 1.5% of all human cancer is attributed to EBV (Farrell, 2019), and the mortality from EBV-related cancers accounts for almost 2% of cancer deaths (Khan & Hashim, 2014). Unfortunately, these figures continue to rise (Khan et al., 2020).

Nevertheless, only a small fraction of infected individuals develops EBV-associated diseases. Details of why these individuals experience EBV pathologies remain ambiguous. The host's age at primary infection, genetic and environmental factors, sex hormones, and the immune system are all thought to play a role in disease development (Balfour et al., 2013; Taylor et al., 2015; Rostgaard et al., 2014).

Efficient immune response is fundamental to prevent potential EBV diseases. For instance, impaired cytotoxicity of T lymphocytes and defective degranulation due to mutations in genes involved in the formation and release of cytotoxic granules were reported in patients with chronic active EBV infection (Katano et al., 2004; Rohr et al., 2010). Additionally, EBV has been reported to infect activated CD8<sup>+</sup> T cells, interfere with their activation state and cause marked deficiency in the expression of some immune markers (e.g. CD3 and CD5) during hemophagocytic lymphohistiocytosis (HLH) (Kasahara et al., 2001; McCall et al., 2012; Toga et al., 2010; Wada et al., 2007). Another example is the dysregulated expression of over 300 genes associated with cell cycle, interferons signaling and antigen presentation in the peripheral blood during IM (Dunmire et al., 2014). This altered gene expression in

EBV infection was shown to carry similarities to that of Dengue virus infection, and inflammatory syndromes (Dunmire et al., 2014).

### 1.3.1 EBV Structure and Lifecycle

The structure of EBV virions includes four main components (Figure 6). The innermost part is a large genome (~172 kb), that is a linear double stranded DNA. Next is the icosahedral capsid coated by a layer of viral proteins, known as the tegument. Finally, the outermost part is a lipid bilayer envelope made up of host cell membrane-derived components (Smatti et al., 2018). However, EBV DNA circularizes forming episome in latently infected cells, and each infected cell contains about 10-50 copies of EBV (Shannon-Lowe et al., 2009).

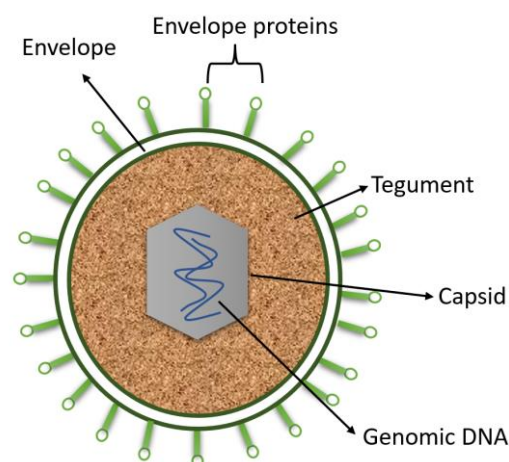


Figure 6: The main components of EBV virions. Large DNA, within a capsid, surrounded by viral tegument and cell membrane-derived envelope

EBV is mainly transmitted through saliva, and the life cycle of the virus is believed to start in the oral cavity. The tonsil is a critical site for EBV life cycle, and EBV-immune interaction (Hislop et al., 2005). In the submucosal lymphoid tissues, EBV glycoproteins, gp350/220 and gp42, bind to the cellular CD21 and MHC class II

molecules, respectively, to mediate viral entry into naïve B cells. Newly infected cells then express a set of viral proteins that help them proliferate, including 6 EBV nuclear antigens (EBNA-1, EBNA-2, EBNA-3a, EBNA-3b, EBNA-3c, and EBNA-LP), 3 latent membrane proteins (LMP-1, LMP-2a, and LMP-2b), 2 EBV non-coding RNAs (EBER-1 and EBER-2) and more than 40 viral encoded miRNAs (Weidner-Glunde et al., 2020). These cells are said to express EBV type III latency, which is fundamental for EBV's transforming capacity (Figure 7). EBV lymphomas in AIDS patients and *in vitro* EBV immortalized B cells, known as lymphoblastoid cell lines (LCLs), are good examples of type III latency (Hatton et al., 2014). EBV causes several transcriptional, metabolic and phenotypic alterations in B cells, and EBNA-2 appears to play a critical role in driving viral activation of B cells (Mrozek-Gorska et al., 2019; Pich et al., 2019). Additionally, EBV latent proteins support the persistence of infected cells and protect them from apoptosis (Fries et al., 1996; Gregory et al., 1991; Pratt et al., 2012; Price et al., 2017). The infected cells during type III latency can also produce immunosuppressive mediators, such as IL-10, TGF- $\beta$ , IL-35 and PD-L1 to suppress antiviral effector T lymphocytes, and support the activity of regulatory T cells (Treg) (Auclair et al., 2019). These strategies enable the virus to evade the immune response of the host.

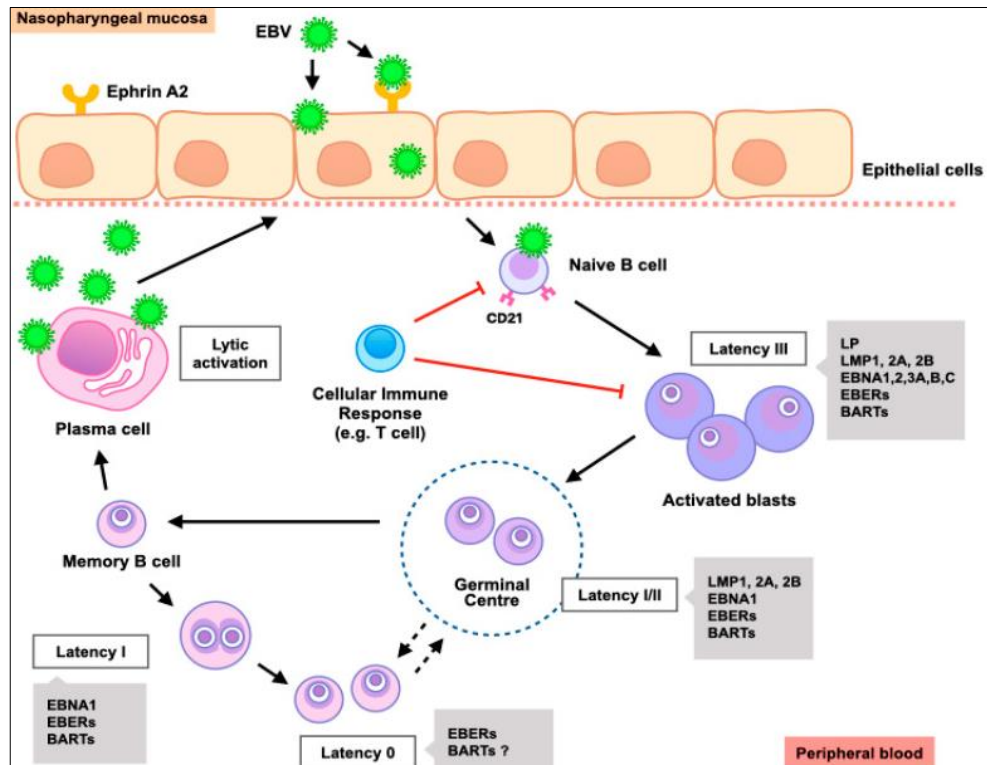


Figure 7: The lifecycle of EBV. Two main phases are recognized: latent and lytic. Various latent proteins are expressed during different types of latency (0, I, II, and III). New virus is produced during the lytic infection (Richardo et al., 2020)

EBV infected B cells express a variety of latent proteins in different body sites, and in different disease contexts. Resting memory B cells infected with EBV express latency 0 (i.e., EBERs only) in asymptomatic carriers (Figure 7). The lack of viral protein expression during latency 0 helps EBV survive undetected by the host immune system (Münz, 2019). Moreover, the expression of EBER-1 is believed to aid infected cells in spreading from lymphoid sites to peripheral blood (Hoffman et al., 2019). Actively dividing memory B cells, on the other hand, express latency I (EBERs and EBNA-1), whereas germinal center infected B cells express latency II (EBERs, EBNA-1, LMP-1, and LMP-2) (Figure 7) (Münz, 2019).

In addition to latent proteins, EBV encodes another unique set of genes required for the production of new virions. This is called the productive or lytic cycle.

This cycle helps EBV transmit to a new host. However, the active production of new infectious virus occurs only occasionally and involves over 80 lytic genes divided into immediate early (IE), early (E), and late genes (L). This cycle presumably coincides with B cell differentiation into plasma cells (Figure 7) (Murata, 2014). While the lytic cycle is highly active during the acute primary infection, the majority of the peripheral viral load is generated by the expansion of infected cells. Higher levels of latently infected cells than cell free virus were observed in the peripheral blood of newly infected individuals (Abbott et al., 2017).

The initiation of productive cycle is governed by two viral IE transactivators, BZLF-1 and BRLF-1, and is under the control of epigenetic modifications. BZLF-1 binds selectively a set of CpG methylated sequences to initiate the productive cycle (Chiu & Sugden, 2016). Moreover, BZLF-1 can be readily detected in the saliva during primary infection, and its expression correlates positively with EBV load in the oral cavity (Fagin et al., 2017). The active release of new virus lasts for several months after primary infection has ameliorated, and this prolongs virus's transmissibility period (Dunmire et al., 2018). BZLF-1 also contains some of the most immunodominant epitopes that can be detected by sera of virtually all EBV positive carriers (Goswami et al., 2017). This makes BZLF-1 a good candidate for vaccine development.

### **1.3.2 EBV Kinetics During Primary Infection in Humans**

The incubation period for EBV is about 4-6 weeks. Peripheral EBV load is significantly elevated during the acute phase of primary infection, regardless of whether it is silent or symptomatic (Abbott et al., 2017; Dunmire et al., 2018). The peak of EBV load in the blood and oral cavity coincides with the appearance of

symptoms, during primary symptomatic infection (i.e., IM) (Dunmire et al., 2015). However, the clinical manifestations of IM are not ascribed to EBV load, but rather to a perturbed immune response to the virus (Balfour et al., 2013). Unlike IM, primary silent infection shows neither disrupted CD4:CD8 ratio nor an exaggerated clonal expansion of anti-EBV CD8<sup>+</sup> T cells, despite high virus levels in the circulation (Jayasooriya et al., 2015).

During primary infection, the humoral response to EBV starts with early peaks of anti-viral capsid antigen (VCA) IgM, followed by anti-VCA IgG (Figure 8) (Abbott et al., 2017). Therefore, primary infection is commonly recognized by the detection of anti-VCA IgM and IgG, while EBV reactivation can be identified by the detection of anti-VCA IgG, and anti-EBNA-1 IgG. This EBV-specific humoral response, including titers of neutralizing antibodies, correlates with circulating viral load (Bu et al., 2016). The frequency of NK cells, also, increase during primary infection (Dunmire et al., 2015). To illustrate the importance of NK cells in EBV infection, a study on EBV infected humanized mice demonstrated that depletion of NK cells resulted in an abrupt rise in viral load in the blood and the spleen, pronounced viremia (i.e., free virus in the plasma), and enhanced expression of viral proteins associated with the lytic cycle (Chijioke et al., 2013). This implies the important role NK cells play in restricting EBV lytic infection and limiting viral load.

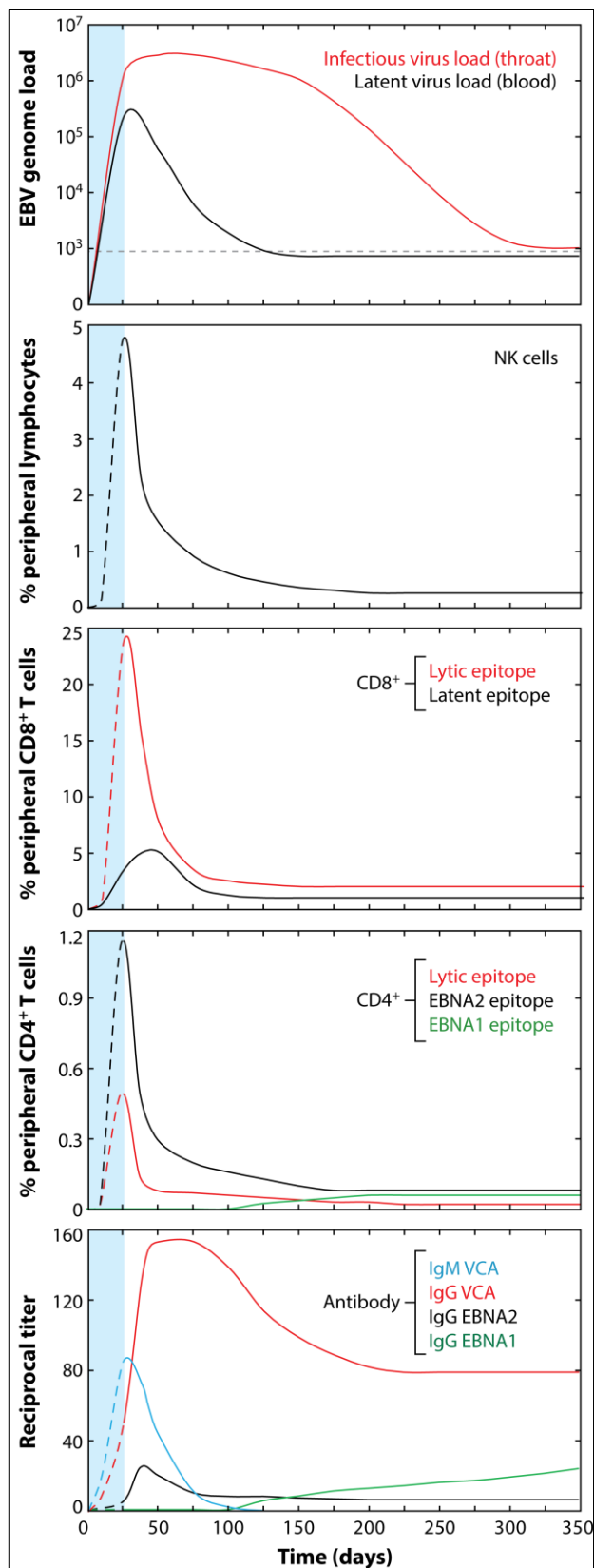


Figure 8: EBV load and antiviral immune response during primary infection. The levels of BV DNA, anti-EBV NK cells and T lymphocytes and titers of anti-EBV antibodies are indicated during acute phase and convalescence (Taylor et al., 2015)

Moreover, plasmacytoid DCs (pDCs) recognize EBV infection via the toll-like receptor 9 (TLR9), take up infected cells, and process and present viral antigens to prime naive T cells (Bickham et al., 2003; Fiola et al., 2010). However, primary symptomatic EBV infection is associated with a significant reduction in circulating pDCs, which correlates with symptoms severity (Chatterjee et al., 2019; Panikkar et al., 2015). One of the important roles that pDCs play in EBV infection is the release of IFN- $\alpha$ , which inhibits cell division of EBV infected cells, and limits viral burden (Gujer et al., 2019).

During primary symptomatic infection, the cellular response is dominated by expanded CD8<sup>+</sup> T cells and their expansion correlates with IM severity (Dunmire et al., 2015). Initially most of the expanded CD8<sup>+</sup> T cells recognize immunodominant lytic antigens, whereas response to latent antigens is delayed and occur at lower frequency (Figure 8) (Abbott et al., 2017). IM symptoms resolve once CD8<sup>+</sup> T cells return to baseline level. Subsequently, EBV-specific memory CD8<sup>+</sup> T cells remain in the circulation. Some of these cells become tissue resident memory cells (T<sub>RM</sub> cells) (i.e. CD69<sup>+</sup>CD103<sup>+</sup>CCR7<sup>-</sup>), and are retained in the tonsils ready to block any sporadic bouts of EBV reactivation (Woon et al., 2016).

Primary EBV infection is also reported to induce the expression of immune inhibitory receptors including PD-1 on antiviral CD8<sup>+</sup> T cells (Chatterjee et al., 2019). Nevertheless, these cells remain functionally active and cytotoxic. Interestingly, blocking PD-1 receptor has been shown to aggravate EBV infection and lead to the trafficking of EBV infected cells and EBV-reactive CD8<sup>+</sup> T cells into the brain causing fatal encephalitis (Chatterjee et al., 2019; Johnson et al., 2019)

In addition to CD8<sup>+</sup> T cells, EBV-specific CD4<sup>+</sup> T cells are also reported to expand in IM, and nearly 80% of these cells are cytotoxic (i.e. express perforin and



granzyme B) (Meckiff et al., 2019). In contrast, cytotoxic EBV-specific CD4<sup>+</sup> T cells in EBV long-term carriers make up only 6% of total EBV-specific CD4<sup>+</sup> T cells (Meckiff et al., 2019). Cytotoxic CD4<sup>+</sup> T cells recognizes EBV envelop proteins and lyse infected cells expressing them (Adhikary et al., 2006; Heller et al., 2006). The viral major tegument protein BNRF1 has been recently reported to contain immunodominant epitopes that are primarily targeted by cytotoxic CD4<sup>+</sup> T cells (Adhikary et al., 2020). BNRF1-reactive cytotoxic CD4<sup>+</sup> T cells help restrict EBV reactivation in healthy carriers. This efficient immune response can be employed in designing targeted immunotherapies for EBV lymphomagenesis. Another CD4<sup>+</sup> T cell subset that is affected by EBV infection is CD25<sup>high</sup> CD4<sup>+</sup> T cells. These cells normally protect against exaggerated immune responses, but in primary symptomatic EBV infection, they fall in number and frequency (Dunmire et al., 2015).

### **1.3.3 The Link Between EBV and MS**

Infection with EBV has been implicated in increased risk of MS, although the exact underlying mechanisms are poorly understood. Individuals who develop symptomatic EBV infection are particularly at higher risk of developing MS than their asymptomatic counterparts (Ascherio & Munger, 2010). A previous study on over 1000 samples from human postmortem brain slices from MS and non-MS cases revealed that EBV is present in 90% of MS cases compared to only 24% of non-MS control cases (Hassani et al., 2018). In agreement with these results, several studies have demonstrated the presence of EBV in MS brain (Moreno et al., 2018; Serafini et al., 2007; Tzartos et al., 2012). This suggests a possible link between the virus and the disease. Yet, the involvement of EBV in MS remains a subject of intense debate in the scientific community. Definitive evidence for a causative role for EBV in MS is

lacking. A number of hypotheses have been proposed to explain the association, including molecular mimicry, reactivation of MS-associated human endogenous retroviruses, bystander damage and cellular and viral miRNA interactions (Bar-Or et al., 2020; Hassani & Khan, 2019).

The following is a summary of some of the evidence implicating EBV in MS pathogenesis. First, genome-wide association studies have indicated that MS risk loci are linked to disrupted immune response to EBV latency III. The binding regions for EBV transcription factors are also over-represented in MS (Afrasiabi et al., 2019). Peripheral EBV levels and certain viral-encoded miRNAs have been shown to be linked to MS risk genes (Afrasiabi et al., 2020). However, studies on the link between MS risk and peripheral EBV load suffer inconsistencies (Afrasiabi et al., 2020; Agostini et al., 2018; Cocuzza et al., 2014). It has also been reported that increased peripheral EBV load correlates positively with the MS risk allele HLA-DRB1\*15 and negatively with the protective allele HLA-A\*02 (Agostini et al., 2018). Moreover, EBV latent protein EBNA2 is believed to interact with risk loci related to MS and other autoimmune diseases (Harley et al., 2018).

Second, serological studies have consistently demonstrated that MS patients are distinguishable from non-MS controls by significantly high serum levels of anti-EBNA-1 and anti-VCA IgG (Agostini et al., 2018; Deeba et al., 2019; Fernández-Menéndez et al., 2016). Furthermore, increased humoral response to EBV latent protein EBNA-1 is linked to brain atrophy in RRMS (Jakimovski et al., 2020; Wergeland et al., 2016). Similarly, humoral response to EBNA-2 is implicated in early stage of MS (Schlemm et al., 2016). On the other hand, serum levels of IgG specific to the lytic VCA correlates with higher levels of serum neurofilament light chain. The latter is a marker for axonal damage, and is associated with the influx of immune cells

into the CNS and disease activity (Uher et al., 2020). These observations suggest that both latent infection and viral reactivation may influence the rise in antibody responses, which act early in the disease process. Additionally, according to an analysis of *in vitro* stimulated B cells from MS peripheral blood, some MS patients display increased B cell activity and efficient antibody response to a wide range of myelin antigens (Kuerten et al., 2020). Moreover, EBNA1-specific antibodies have been shown to cross-react with the myelin antigen; MBP (Jog et al., 2020; Lünemann et al., 2008).

Third, the frequency of peripheral EBV-reactive CD8<sup>+</sup> T cells correlates with MS disease activity (Angelini et al., 2013). Antiviral cytotoxic CD8<sup>+</sup> T cells have been shown to be functionally exhausted during inactive MS and remain cytotoxic during active disease (Cencioni et al., 2017). Exhausted anti-EBV T cells presumably provide a supportive milieu for EBV reactivation during inactive disease and contribute to MS progression. Moreover, EBV-specific CD8<sup>+</sup> T cells in patients with untreated RRMS have been found to exhibit markers of senescence and terminal differentiation (CD127<sup>-</sup> KLRG1<sup>+</sup>). In contrast, patients treated with glatiramer acetate, a disease-modifying therapy (DMT), have lower frequency of exhausted T cells and activated memory B cells, which serve as EBV reservoir (Guerrera et al., 2020). These findings highlight the link between incompetent anti-EBV response and MS disease activity. The effect of DMTs on EBV-specific immune response has also been reported in MS patients treated with either IFN- $\beta$  or natalizumab (Angelini et al., 2013). The latter is a monoclonal antibody that blocks the integrin VLA-4 on immune cells surface to prevent the influx of these cells into the brain (Lopes Pinheiro et al., 2016). These DMTs have been shown to cause changes in peripheral EBV-specific CD8<sup>+</sup> T cells, but not in T cells specific for CMV (Angelini et al., 2013). Thus, these changes are

less likely to be non-specific consequences triggered by general immunomodulatory effect of DMTs on the immune system. Indeed, signs of EBV reactivation were detected *in situ* in the MS brain after the termination of natalizumab therapy. The expression of latent and lytic EBV proteins was associated with substantial neuroinflammation and demyelination (Serafini et al., 2017, 2018). These reports provide evidence that EBV, especially transcriptionally active infection is associated with pronounced immunological alterations that deeply impact the homeostasis of the CNS. Moreover, in a small clinical trial, the administration of *in vitro* expanded autologous EBV-specific T lymphocytes in patients with progressive MS, alleviated disease symptoms in some of the patients (Pender et al., 2018). This trial has significant implications on linking EBV to disease progression.

Fourth, in postmortem brain tissues, EBV-specific CD8<sup>+</sup> T cells and EBV infected cells were found to infiltrate MS lesions and the infected cells expressed both latent and lytic viral proteins (Angelini et al., 2013; Hassani et al., 2018; Serafini et al., 2019; Tzartos et al., 2012; Veroni et al., 2018). Additionally, EBV-specific CD8<sup>+</sup> T cells comprised 0.5-2.5% of total brain-infiltrating CD8<sup>+</sup> T cells. This frequency was found to be significantly higher than that of CD8<sup>+</sup> T cells recognizing peptides from MBP, CMV, or influenza virus. Further characterization of EBV-specific CD8<sup>+</sup> T cells showed expression of the degranulation marker CD107a, and perforin, and granzyme B, indicative of their cytotoxic nature (Serafini et al., 2019). This supports the notion that disruption of immunological homeostasis in the periphery brings about deleterious effects on the CNS (periphery-CNS axis). Taken together, these studies suggest that both EBV and the immune response directed at the virus are linked to MS development and progression.

### 1.3.4 EBV in CNS Pathologies

A wide range of pathological complications affecting the peripheral and central nervous systems have been observed in viral infections in immunocompetent individuals. Acute encephalitis, self-resolving aseptic meningitis, post infectious acute disseminated encephalomyelitis (ADEM) and Guillain-Barre syndrome are some of the neuropathological conditions directly or indirectly linked to viral infections including EBV (Koning et al., 2019; Tselis, 2014).

Perivascular and diffuse lymphocytic and macrophage infiltration can impact the white matter, grey matter, and meninges to variable degrees, depending on disease context. Microglia nodules can also form when virus-infected cells infiltrate the CNS. In some cases, such as in ADEM, signs of demyelination along with foamy phagocytes are prominent (Tselis, 2014). In a case of fatal EBV-HLH, necrosis, loss of neurons and gliosis are visible in the brain that is heavily infiltrated by CD8<sup>+</sup>T cells and CD68<sup>+</sup> cells. EBV infected cells also occupy various CNS niches including choroid plexus, brainstem and spinal cord (Magaki et al., 2017).

Thus, although EBV is primarily a peripheral infection, it can produce neuropathogenic effects in some cases, albeit infrequently. What causes the focal infection in the periphery to reach the CNS warrants investigation. It is possible that dysregulated immune response aids in the spread of EBV from the periphery to the nervous system. Perturbed antiviral response can also affect the CNS indirectly. For example, EBV infected humanized mice reconstituted with HLA-DR15<sup>+</sup> immune system components have been reported to exhibit poor control over the virus despite the increased activation and proliferation of T lymphocytes (Zdimerova et al., 2021). Remarkably, some T lymphocytes from these EBV infected mice have been also

shown to cross-react with the myelin antigen, MBP (Zdimerova et al., 2021). Additionally, a compromised immune system has been linked to a wide range of EBV-related CNS pathologies (Kempf et al., 2013; Lee et al., 2020; O'Neill et al., 2007).

EBV-associated neuropathologies cannot always be attributed to EBV alone. These diseases are often multifactorial, with the virus possibly being just one factor in complex etiologies. In Alzheimer's disease, for instance, some of the clonally expanded effector CD8<sup>+</sup> T cells in the CSF appear to be specific to EBV antigens EBNA-3A and BZLF-1 (Gate et al., 2020). Whether these virus-specific cells are the cause or consequence of CNS injury is unclear. Similarly, the intrathecal presence of EBV can be viewed as a cause of neurological abnormalities or as a result of underlying problem with the immune system and/or the CNS. It is not unusual for reactivated EBV to be detected in the CSF during brain pathologies triggered by non-EBV related causes such as coinfection with other viruses or bacteria, or neurosarcoidosis (Salazar et al., 2018; Weinberg et al., 2005).

Even if EBV infection may not cause the primary disease, it might exacerbate the pathology and contribute to disease worsening. For example, in HIV infected individuals, EBV can contribute to the expansion of HIV cell reservoir, that subsequently invade the CNS (McHugh et al., 2020). Alternatively, EBV may predispose HIV patients to develop neurological impairments associated with HIV. Recent reports indicate that EBV and not CMV is commonly detectable in the CSF of HIV positive viremic individuals. EBV in the CSF correlates with HIV viremia, markers of neuroinflammation and impaired BBB integrity (Lupia et al., 2020).

## 1.4 Introduction to the Rabbit Model of EBV Infection

The natural host of EBV is humans. Attempts to generate a surrogate animal model for EBV infection in humans have been made on different animals including cotton top marmosets (Shope et al., 1973), owl monkeys (Epstein et al., 1975) and humanized mice (e.g. *scid* non-obese diabetic (NOD) mice modified to contain human-like immune system) (Gujer et al., 2015). Although these animal models contributed to the understanding of EBV biology (Figure 9), they have a number of drawbacks that make recapitulation of EBV infection challenging. For example, some models do not allow the study of all types of latency, and asymptomatic viral infection (Gujer et al., 2015).

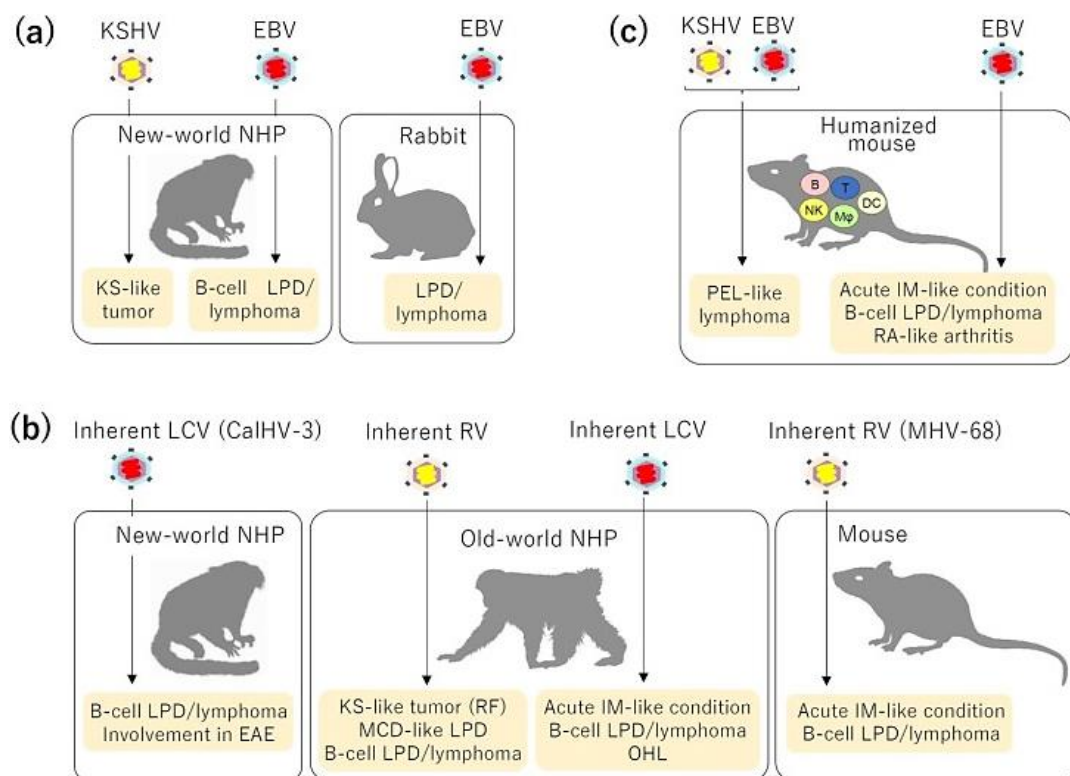


Figure 9: Animal models to study human  $\gamma$ -herpesviruses. Different approaches were used to create EBV animal models such as (a) direct inoculation into animals, (b) the use of EBV-like viruses in their natural hosts, and (c) the use of humanized mice (Fujiwara & Nakamura, 2020)

Rabbits have been revisited recently to model EBV infection. Initially, cottontail rabbits were shown to be susceptible to an EBV-like  $\gamma$ herpesvirus, called herpesvirus sylvilagus (Hesselton et al., 1988). This infection resulted in changes in the peripheral blood reminiscent of that seen in human IM. However, herpesvirus sylvilagus infection course varied between animals, depending on rabbit's age. While adult rabbits had acute disease, young animals developed lymphoid hyperplasia and inflammatory lesions in lymphoid and non-lymphoid organs including the lungs, the kidneys and salivary glands (Hesselton et al., 1988).

Moreover, when rabbits were injected with a monkey leukocyte cell line, they oddly became infected with a monkey herpesvirus that is similar to EBV. These rabbits developed lymphomas (Hayashi et al., 1994, 1995; Koirala et al., 1997). Subsequently, it was found that a variety of white rabbits (New Zealand, Japanese, and Dutch) can be infected with herpesviruses that naturally and silently infect non-human primates. Various routes of inoculation were tried and led to successful establishment of infection, and formation of lymphomas (Chen et al., 1997).

Rabbits were then utilized to study hemophagocytic syndrome, which is linked to several viruses including EBV. The hemophagocytic syndrome in rabbits was induced using herpesvirus papio (HVP), a baboon tropic virus that shares biological and genetic similarities with EBV. Both purified cell-free virus and virus-infected cells were used to infect the rabbits (Hayashi et al., 2001; Hsieh et al., 2007). Another group of rabbits was injected intravenously with EBV, derived from B95-8 cells, as a negative control for HVP infected group. The authors were surprised to see that the "negative control" rabbits had temporarily enlarged lymph nodes and spleens. Titers of anti-EBV VCA antibodies were found to be elevated in rabbits sera, and detectable levels of EBV genome in the blood confirmed EBV infection (Takashima et al., 2008).



These, otherwise healthy, EBV infected rabbits showed no symptoms, and experienced a short-term lymphocytosis. Furthermore, the splenomegaly observed between first and second week of infection was found to subside about one month later. EBV infected cells were part of the lymphocytic infiltrate in the biopsied liver, spleen, and lymph nodes. However, infected cells in the lymphoid organs were large, atypical lymphocytes as opposed to small lymphocytes seen in the liver (Takashima et al., 2008).

The authors also reported histological evidence of increased proliferation and turnover of these atypical lymphocytes in the spleen. In fact, within 2 weeks of infection the spleen had up to  $9 \times 10^4$  EBV copies/ $\mu\text{g}$  gDNA in a rabbit that was inoculated with  $1 \times 10^8$  EBV copies. Additionally, EBV levels in the periphery varied between different rabbits, and fluctuated overtime in a given animal (Takashima et al., 2008). EBV genome was either continuously undetectable, intermittently detectable, or constantly detectable. This suggests that different infection dynamics are influenced by differences in rabbits immune responses to EBV, similar to those observed in humans. Thus, EBV infection in rabbits was found to be best assessed by serological tests, rather than quantifying virus levels (Rajčáni et al., 2014).

In addition, the spleen showed enhanced expression of viral latency associated proteins, such as LMP-1 and EBNA-2, with occasional expression of the immediate early lytic protein BZLF1. Infected cells in the spleen were predominantly CD79a<sup>+</sup> B cells, and occasionally CD3<sup>+</sup> cells (Takashima et al., 2008). After monitoring these rabbits for over two years, it was found that they were persistently infected with EBV (Kanai et al., 2010). Similar to humans, the rabbit immune system does not completely eradicate EBV infection. EBV infection in rabbits was then examined using different

routes of administration and different EBV-producing cell lines (source of virus) (Okuno et al., 2010; Sano et al., 2013).

Using the oral route did not appear to cause infection (Okuno et al., 2010). Intranasal administration of more than  $3 \times 10^9$  EBV copies, however, was found to result in detectable EBV DNA in rabbit PBMCs, as well as enhanced humoral response to viral early antigen (EA) and VCA (Okuno et al., 2010). Unlike intravenous route, intranasal inoculation did not produce splenomegaly or other EBV associated gross pathologies. It also led to lower expression of LMP-1 and EBNA-2 than the intravenous route. Additionally, all infected cells in the spleen were negative for BZLF-1 (Okuno et al., 2010). These observations imply that despite using more virus, intranasal administration causes milder infection compared to intravenous inoculation.

In addition, the infectivity of EBNA-2-deficient EBV from P3HR-1 cells was compared to EBV from B95-8 cells. The EBNA2-deficient EBV was less infectious than B95-8 EBV, since infection was established in only two out of 12 inoculated rabbits (Sano et al., 2013). These observations suggest that the success of EBV infection in rabbits is somewhat determined by the route of inoculation, and cell source of the virus. Additional determining factors could include the rabbit strain and age, as well as the amount of virus used. This is because rabbits are not the natural host of EBV, and thus their susceptibility to EBV infection is likely to be suboptimal.

The susceptibility of rabbits to EBV infection was also examined in a previous study (Khan et al., 2015). EBV infection in rabbits was confirmed to produce a robust humoral response, which helps reduce viral load below detectable levels in the blood. Furthermore, the study demonstrated indirectly that cell-mediated immunity plays a role in maintaining low peripheral EBV levels in rabbits. Cyclosporin A (CsA)-mediated suppression of T cells caused significant surge in EBV level that was

previously undetectable (latent) (Khan et al., 2015). This apparent viral reactivation was associated with the expression of BZLF-1 and EBV latent genes. EBV infected cells also infiltrated the enlarged spleen and liver (Khan et al., 2015). Thus, EBV infection in rabbits resembles latent infection in asymptomatic EBV carriers, as well as EBV dynamics in transplant patients receiving immunosuppression therapy.

### **1.5 Introduction to the Immunosurveillance of the CNS**

The CNS lacks the conventional lymphatic system, and its cells do not constitutively express major histocompatibility complex (MHC) class I and class II molecules. This historically led to the idea that the CNS lacked immunosurveillance. Experiments demonstrating a decreased likelihood of rejection of allogenic tissues implanted into the brain supported the CNS immune privilege (Lopes Pinheiro et al., 2016; Medawar, 1948).

It is now, however, well-established that CNS-derived waste and antigens that are filtered by CNS interstitial fluid and CSF are drained through nasal and meningeal lymphatics by the cervical lymph nodes (Louveau et al., 2018; Manglani & McGavern, 2018). Therefore, the CNS is not completely isolated from the peripheral immune system. The illustration of CNS lymphatics has shown that what occurs in the periphery can indeed affect the CNS, and changes in the CNS can trigger an immune response in the periphery. For instance, an infection that arises in the periphery, can result in the emergence of antigen-specific memory CD8<sup>+</sup>T cells in the brain parenchyma. These cells develop T<sub>RM</sub> cell-like phenotype and persist within the brain for many months after the resolution of the peripheral infection. Brain resident CD8<sup>+</sup>T cells then perform homeostatic activities such as patrolling and defending the brain against potential invading pathogens (Urban et al., 2020). Moreover, there is

compelling evidence for the role of the adaptive immune system during brain development and in regulating behavior and cognitive functions (Filiano et al., 2015; Kipnis, 2016; Korn & Kallies, 2017). Peripheral immune system can also be associated with adverse effects of CNS infections, autoimmunity and neuroinflammation (Filiano et al., 2017; Gilli et al., 2016; Schwartz & Kipnis, 2011).

The CNS has several sites that are highly active in immunosurveillance. Regions close to brain ventricles, meninges and subarachnoid spaces (SAS) serve as potential location for the interaction between immune cells and CNS pathogens (Abbott et al., 2010). The CNS is also protected by layers of barriers; the 3 meningeal layers, the blood-brain barrier (BBB) and the blood-CSF barrier (B-CSF-B), that prevent unregulated access of immune cells or pathogens into the CNS (Russo & McGavern, 2015). The composition of CNS barriers can influence how easy a pathogen or an immune cell gains access into the CNS. While tight junctions between endothelial cells of the BBB significantly restrict entry to the CNS (Figure 10), the choroid plexus have fenestrated blood vessels that make them relatively more permeable (Figure 11) (Holman et al., 2011). For instance, circulating leukocytes can enter via the pores of fenestrated blood vessels into the choroid plexus, where they are likely to come into contact with resident APCs (e.g., DCs), and trigger an immune response. Similarly, the outermost layer of the meninges; dura mater, also holds fenestrated blood vessels. The dura mater is well exposed to the peripheral circulation and accessible to both innate and adaptive immune cell trafficking and lymphatic drainage (Mastorakos & McGavern, 2019).

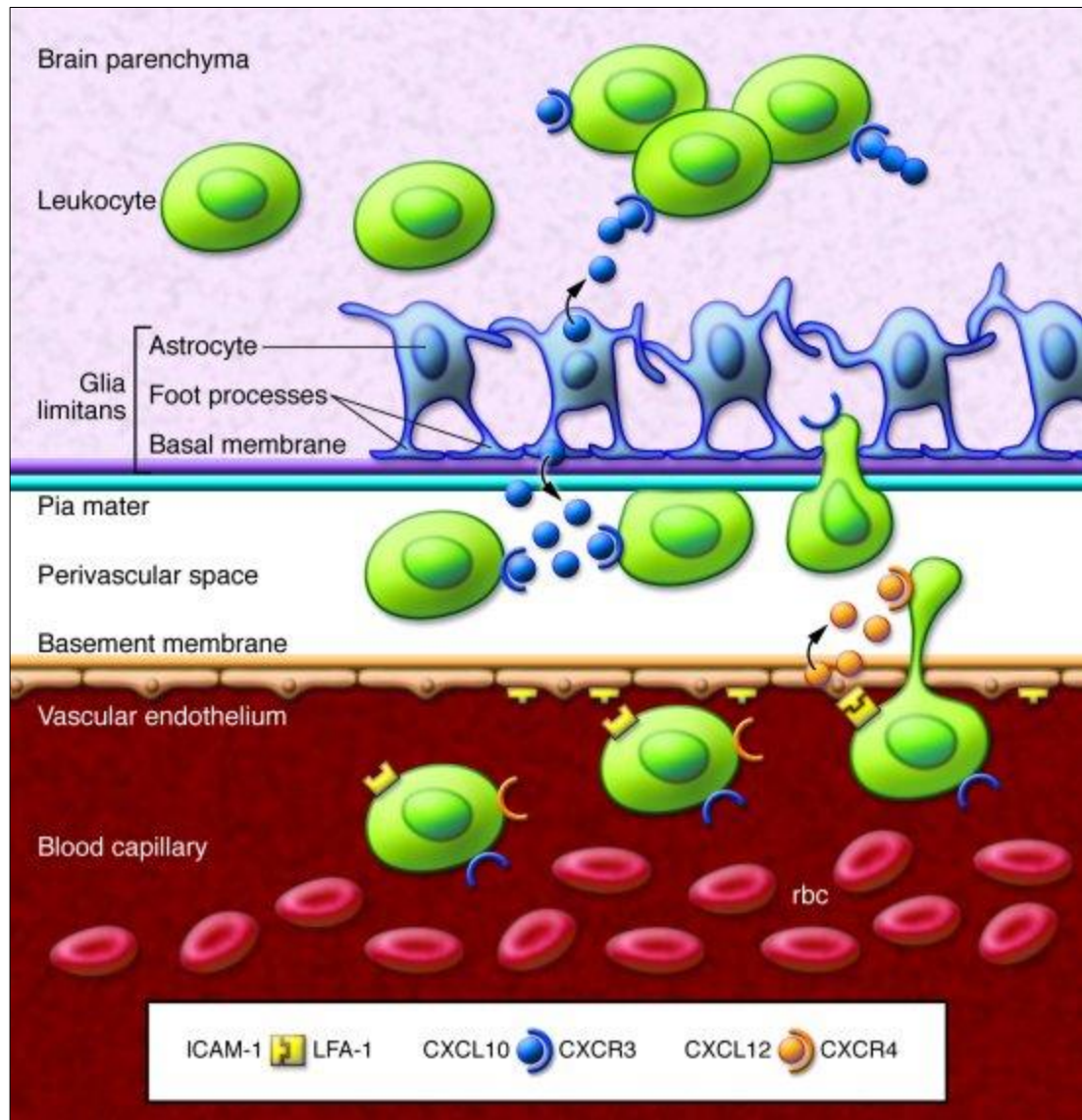


Figure 10: Trafficking of activated lymphocytes into the CNS across the BBB. The process requires multiple interactions of adhesion molecules and integrins (for rolling and attaching), and selectins (for diapedesis) and appropriate amounts of chemokines (to overcome the glia limitans of the astrocytes in the BBB) (Wilson et al., 2010)

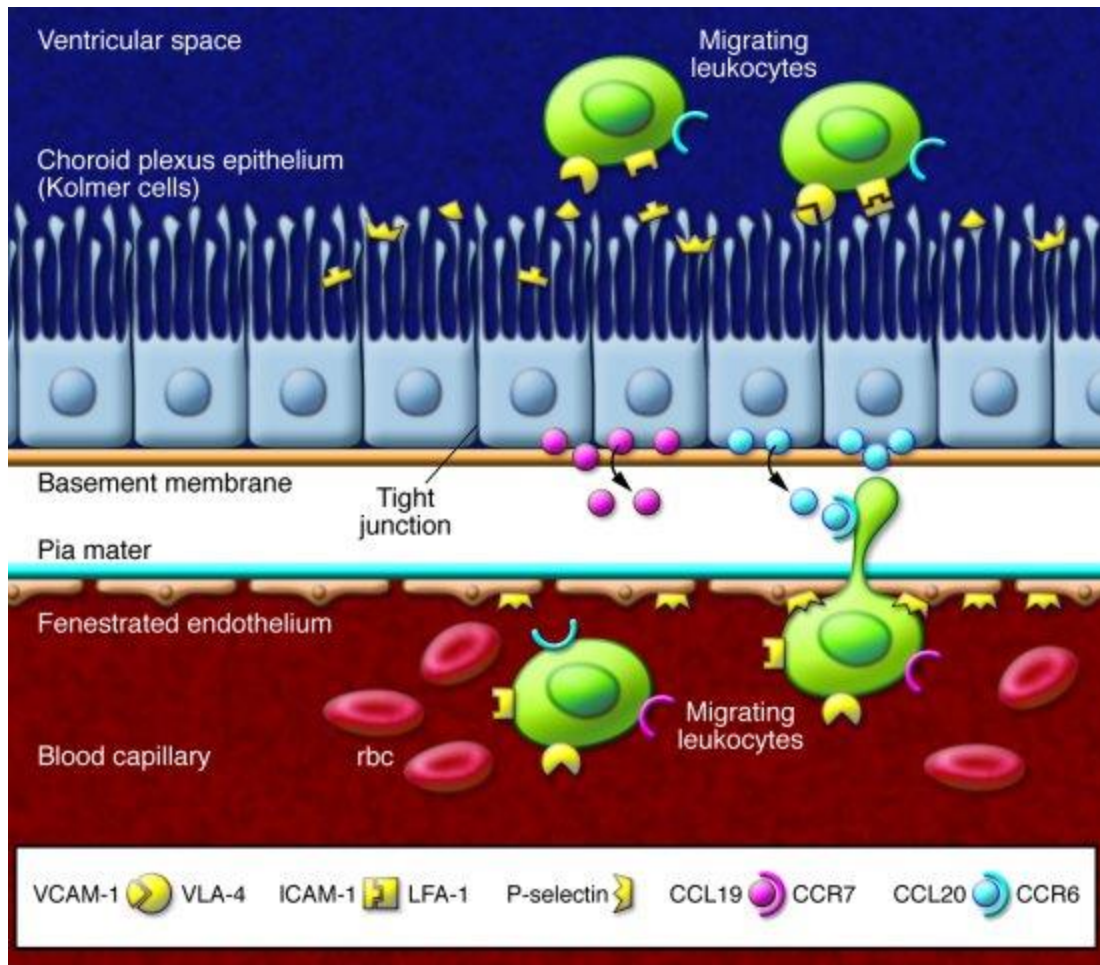


Figure 11: Trafficking of immune cells into the CNS across the B-CSF-B. Fenestrated blood vessels allow the entry of immune cells into the choroid plexus. Chemokines mediate the movement of immune cell across the tight junction-connected epithelium of the choroid plexus basement membrane (B-CSF-B). Immune cells can then circulate around the CNS, in the CSF and brain ventricles (Wilson et al., 2010)

Despite the multi-layered seals, pathogens have evolved a variety of means to breach different CNS barriers (Figure 12). For instance, some viruses simply infect the cells that make up the barrier itself to move across the barrier, while others trigger the release of products, such as matrix metalloproteinases (MMPs) that can degrade CNS barriers. MMPs can destroy astrocytic end feet and disturb extracellular matrix (ECM) around glia limitans (Ashley et al., 2017; Lind et al., 2019; Mastorakos & McGavern, 2019). On the other hand, immune cells that respond to invading pathogens release

inflammatory mediators, such as  $\text{TNF-}\alpha$  and  $\text{IL-1}\beta$ , which disrupt the integrity of the barrier, and make it leaky and easy to penetrate (Mastorakos & McGavern, 2019).

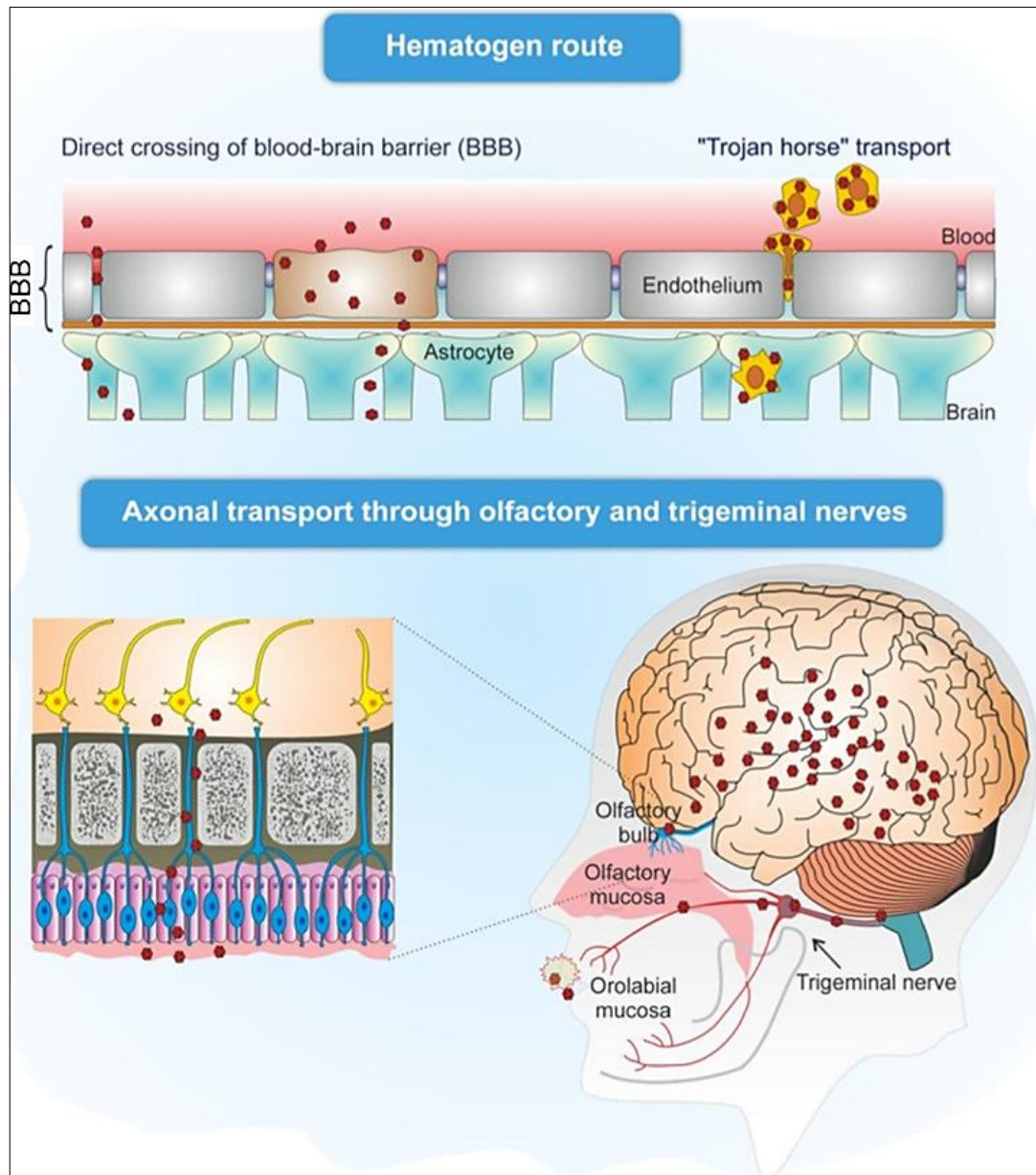


Figure 12: Viruses use blood and/ or peripheral nerves to access the CNS. The hematogenous route include damage to BBB, direct infection of BBB endothelium, and infecting leukocytes and using them as “Trojan horses”. Neuroinvasive viruses can also reach the CNS via axonal transport through peripheral sensory and motor neurons and the olfactory neurons (De Chiara et al., 2012)

Under normal conditions, limited T cell trafficking occurs across BBB. Endothelial cells downregulate the expression of adhesion molecules on the surface facing the blood vessel lumen, where immune cells circulate. Admittedly, independent of antigen specificity, a low number of activated T lymphocytes cross the BBB into the perivascular spaces (Engelhardt et al., 2017). These cells, however, do not reach the brain parenchyma. This often occurs along parenchymal postcapillaries venules. The binding of  $\alpha$ 4-integrins (e.g., VLA-4) expressed on the surface of T lymphocytes, to adhesion molecules (e.g., VCAM-1) on the surface of endothelial cells mediates T cell trafficking into the CNS. This step is blocked in MS patients receiving natalizumab; a blockade antibody that antagonizes  $\alpha$ 4-integrins (Hutchinson, 2007).

In the perivascular spaces, few T lymphocytes scan for their specific antigenic epitope-MHC complexes. In the absence of such an encounter, T lymphocytes return to the peripheral circulation or die by apoptosis. On the other hand, if perivascular macrophages, or other APCs, present to T lymphocytes their cognate antigen on MHC molecules, T lymphocytes bypasses the barrier made up by glia limitans and astrocytic basement membrane, to reach the brain parenchyma (Rossi & Constantin, 2016).

To facilitate T cells extravasation, CNS resident cells including perivascular macrophages produce matrix metalloproteinases (MMPs), such as MMP-9, to degrade astrocytes end feet. Moreover, enhanced expression of integrins, selectins and chemokine ligands on perivascular endothelial cells results in increased diapedesis of lymphocytes (Figure 10) (Ghezzi et al., 2019). Infiltrating lymphocytes release various cytokines and chemokines that promote additional infiltration of blood-derived monocytes (Rubio & Sanz-Rodriguez, 2019).

Viruses that infect the CNS cause marked chemoattraction of activated T cells into the CNS (Rubio & Sanz-Rodriguez, 2019). These immune cells that reach brain



parenchyma perform effector roles that are meant to rid the CNS from the invading pathogens. Devastating consequences, such as bystander damage to CNS cells and autoimmunity, can occur if the immune response and inflammation in the brain parenchyma are poorly regulated (Filiano et al., 2017). A deficit cellular communication between these cells can turn a protective response into a damaging one. Overproduction of inflammatory cytokines, compromised BBB integrity, continuous influx of peripheral immune cells, cell death and edema, can all lead to pathological sequelae if not resolved appropriately and timely regulated (DiSabato et al., 2016).

Some CNS resident cells, including microglia are also considered important innate immune cells. These cells are highly active; regularly scanning the surrounding environment. When activated (e.g. during brain injury), the morphology of microglia changes, and are believed to serve functions that are broadly defined as either inflammatory or reparative (Voet et al., 2018). They serve a number of different roles, including production of various soluble mediators (e.g. cytokines, chemokines, ATP, growth factors), antigen-presentation, and engulfment of cell remnants (Jha et al., 2019). Microglia can also modulate the activity of immune cells and other CNS resident cells such as astrocytes.

Astrocytes play a pivotal role in the structural support of the BBB and in a variety of other critical physiological functions (Jha et al., 2019). Both microglia and astrocytes are interdependent and influence each other's activity in health and disease (Vainchtein & Molofsky, 2020). In health, the two-way communication between astrocytes and microglia is vital for brain development, maintaining the CNS vascular unit and synaptic transmission (Jha et al., 2019). In CNS injury, this interaction can be damaging, protective or both, depending on a number of contributing factors, including

the impact of peripheral immune cells and the gut-CNS axis (Arotcarena et al., 2020; Liddelow et al., 2020). Moreover, microglia and astrocytes modulate the activity of immune cells that naturally inhabit specific areas in the CNS, and contribute to CNS immunosurveillance (Marsh et al., 2016; Ní Chasaide & Lynch, 2020).

## 1.6 The Rationale and Objectives of the Study

Inflammation, demyelination, and reactive gliosis are key components of MS pathology. Hassani and coauthors have previously demonstrated the presence of EBV in MS brain, and this viral presence was independent of presence/absence of neuroinflammation (Hassani et al., 2018). The role of the virus in MS, however, is unclear. The hypothesis of the current study was that primary EBV infection in the periphery can reach the CNS and produce pathological changes that may possibly progress to MS development. To this end, the rabbit model of EBV infection was used to understand the viral dynamics *in vivo* and the consequences of peripheral infection on the CNS. There were four main objectives for this project:

(1) Examination of pathological alterations that occur in the periphery following EBV infection.

What is the load of EBV in different peripheral compartments, e.g., spleen and whole blood? What viral genes are expressed in the periphery?

(2) Determination of pathological changes that can occur in the CNS following primary EBV infection.

What pathological changes take place (if any) in the brain and spinal cord of EBV infected rabbits? How pathological changes in the periphery (e.g., EBV load, EBV gene expression) correlate with pathological changes in the CNS? How long do these changes take to manifest after primary infection?

(3) Determining how EBV reaches the CNS.

Is cell-free virus or cell-associated virus the main mechanisms of EBV entry to the CNS? Which cells in the CNS are the targets of EBV infection and what viral genes are expressed in the infected cells?

(4) Correlating EBV infection in rabbit brain with that in human MS brain.

Is EBV infection in rabbit brain comparable to that in MS brain? Do the histopathological changes in EBV infected rabbit brain reflect those in EBV infected MS brain?

## **Chapter 2: Methods**

### **2.1 Human Study**

The human study was performed on coronal slices of postmortem human brain kindly provided by Rocky Mountain MS Center (RMMSC) Tissue Bank. RMMSC stores brain and spinal cord specimens of individuals with consent for organ donation after death. The study was approved by the local institutional ethics review board, Al Ain Medical District Human Research Ethics Committee (application number AAMD HREC 12/95). In my master's thesis, MS cases with EBV infection were identified (Hassani, 2016; Hassani et al., 2018). Here heavily infected cases were examined for histopathological changes. These observations were compared to data obtained from the animal model of EBV infection (see Section 2.2).

#### **2.1.1 Processing of Formalin Preserved Human Brain Tissues**

Formalin fixed human brain tissues were processed in a fume hood because of the well-documented toxicity of formalin. Eighteen previously identified as heavily infected cases (Hassani et al., 2018) were selected to be examined for histopathological changes. Small pieces were cut out from areas with macroscopic plaques. Tissues were placed on a filter paper and transferred into labelled histology cassettes. All cassettes were collected in formalin containing jar ready for processing.

##### **1- Dehydration.**

First, formalin was discarded, and cassettes were incubated in series of graded ethanol, 30%, 50%, 70%, and 90%, for 45 min each. Cassettes were then incubated in 2 changes of absolute ethanol, for 1 hr each. This should completely dehydrate the tissues, which is essential for xylene miscibility in the next step.

## 2- Clearing.

Tissues were cleared with xylene. Cassettes were incubated in ethanol-xylene mixture (1:1 volume ratio) for 45 min, followed by 2 changes of absolute xylene for 30 min each.

## 3- Paraffin impregnation.

Cassettes were incubated in 3 changes of pre-molten paraffin wax (Histoplast PE, Thermo) in 60°C oven, for 30 min each.

## 4- Embedding.

Tissues were then embedded into wax blocks using moulds of appropriate size. The orientation of the tissue was maintained in such a manner that the plaque surface, which was intended to be sectioned first, faced the bottom of the mould. Finally, blocks were left to solidify on a cold surface.

## 5- Microtomy.

First, each block was trimmed from all sides to remove excess wax so it could fit perfectly in microtome block holder. The surface of the blocks was also trimmed using rotary microtome at 10-15 µm thickness. Tissues were then sectioned at 5 µm thickness. The produced 'ribbons' were floated on a 42-45°C water bath and collected using silanized/coated slides to prevent tissue detachment during staining. All slides were coated with 3-aminopropyltriethoxysilane (Sigma) (Appendix I). Slides were left to dry on warm plate.

### **2.1.2 Examination of Histopathology in EBV Infected MS Brain Using Hematoxylin and Eosin**

#### 1- Dewaxing and rehydration.

Human brain sections were deparaffinized in 2 washes of xylene, 5-10 min each. Sections were then, rehydrated in 100%, 95%, 90%, 70% and 50% ethanol for 3 min

each. Sections were incubated in distilled water for 5 min, preparing them for the aqueous stain.

2- Hematoxylin staining.

Sections were stained with freshly filtered Harris hematoxylin (Shandon Instant Hematoxylin, Thermo) for 15 min, followed by rinsing in tap water to remove excess stain. For differentiation, sections were incubated in 1% HCl in 70% ethanol for 1 min, followed by blueing in running tap water for 10 min.

3- Eosin staining.

Sections were rinsed in 95% ethanol for 1 min and stained with Eosin Y (eosin in alcoholic solution, RAL diagnostics) for 30 sec. For differentiation, sections were rinsed in 95% ethanol for 30- 60 sec.

4- Mounting.

Slides were washed and dehydrated in 3 changes of absolute ethanol, and cleared in 3 changes of xylene, 5 min each. Finally, slides were mounted using xylene based DPX mounting medium (Sigma) and examined under light microscope (ZEISS Axio Scope.A1) for histopathological changes.

### **2.1.3 Examination of Demyelination in EBV Infected MS Brain Using Luxol Fast Blue**

To identify demyelinated lesions and their characteristics, human brain sections were stained with Luxol Fast Blue (LFB), an alcohol-soluble stain that is commonly used to distinguish white matter and well-myelinated areas from grey matter and demyelinated nerves in the nervous system (Carriel et al., 2017).

1- Dewaxing and rehydration.

Sections were dewaxed as described above in Section 2.1.2. Sections were then incubated in absolute ethanol, and 95% ethanol for 3 min each.

## 2- LFB staining.

First, LFB was diluted to 0.1% in 95% ethanol, and warmed in 60°C water bath for 5 min. Sections were placed in 0.1% LFB containing coplin jar covered and sealed with parafilm to prevent evaporation, and incubated in 60°C water bath overnight. Next, sections were rinsed in 95% ethanol and water to remove excess stain.

## 3- Differentiation.

Sections were differentiated in 0.05% lithium carbonate for 30 sec, followed by another 30 sec in 70% ethanol. Sections were checked under the microscope to determine if they were adequately differentiated. White matter should appear well-demarcated blue/greenish blue, and grey matter contrastingly clear. If sections were found to be poorly differentiated, rinsing in 0.05% lithium carbonate and 70% ethanol was repeated.

## 4- Counterstaining in haematoxylin.

Sections were counterstained with haematoxylin for 5 min, and briefly differentiated and blued as described in Section 2.1.2.

## 5- Mounting.

Slides were dehydrated in graded ethanol, cleared in xylene, and mounted as described in Section 2.1.2.

### **2.1.4 Examination of Inflammation in EBV Infected MS Brain Using Immunohistochemistry**

Once demyelinated areas were identified microscopically using H&E and LFB, human brain sections were stained with a number of cellular markers to determine inflammation in the brain. In addition to myelin basic protein (MBP) antibody used to confirm demyelination, CD20, CD3, CD68, PCNA, GFAP, and Iba1 antibodies were

used. Immunohistochemistry (IHC) for these cellular markers was performed as follows:

1- Dewaxing and rehydration.

Sections were dewaxed and rehydrated as described in Section 2.1.2.

2- Quenching endogenous peroxidase activity.

Because peroxidase catalyzed IHC was performed, slides were incubated in 0.5% H<sub>2</sub>O<sub>2</sub> (30% w/v, Panreac, 121076) in methanol (Panreac, 131091) for 20 min, to eliminate non-specific background staining due to inherent peroxidase enzyme activity in tissues.

3- Heat-induced antigen retrieval (HIAR).

All antibodies used here required unmasking of the epitopes. Sections were incubated in boiling 25 mM Tris-HCl-0.1% Triton X-100 (pH 9.2), on a hot plate, for 20 min. Slides were left to cool down on bench top, then rinsed in water.

4- Blocking nonspecific binding.

Sections were incubated with 5% bovine serum albumin (BSA) in washing buffer (1×PBS-0.1% Triton X-100 (Sigma)) in humidified chamber for 2 hrs.

5- Incubation with primary antibodies.

Sections were incubated with the optimal concentration of primary antibodies (Table 2) in humidified chamber, at room temperature, overnight. Sections were washed twice in the washing buffer, 5 min each.

6- Incubation with biotinylated secondary antibodies.

Sections were incubated with appropriate secondary antibodies, diluted at 1:200 in the washing buffer, in humidified chamber at room temperature for 1 hr. Sections were washed twice in the washing buffer, 5 min each. Secondary anti-rat IgG (ab97057, Abcam), anti-goat IgG (ab6885, Abcam), and anti-mouse IgG (component of Ultra-



Sensitive ABC Peroxidase Mouse IgG Staining Kit (Thermo, Cat# 32052)) were used.

Sections were washed twice in the washing buffer, 5 min each.

7- Incubation with the substrate horseradish peroxidase (HRP).

Ultra-Sensitive ABC Peroxidase Mouse IgG Staining Kit also provides the substrate HRP. ABC solution was prepared 30 min prior to its use to stabilize, by diluting each of reagent A (avidin) and reagent B (biotinylated peroxidase) 1:50 in 1×PBS, according to manufacturer's instructions. Tissues were incubated with the substrate for 30 min in a humidified tray at room temperature. Sections were washed twice in the washing buffer, 5 min each.

8- Color development.

Sections were incubated in 250 µg/ml diaminobenzidine (DAB) (Sigma Cat# D5637) in 1×PBS containing 0.02% hydrogen peroxide. Slides were incubated in DAB solution till color development was observed under microscope. If the color was thought to be underdeveloped, slides would continue incubation with DAB for maximum of 30 min. Sections were rinsed in tap water.

9- Counterstaining with hematoxylin.

Sections were incubated with hematoxylin for 2 min and subsequently differentiated and blued as described in Section 2.1.2.

10- Mounting.

Slides were dehydrated in graded ethanol, cleared in xylene, and mounted as described in Section 2.1.2.

Table 2: Primary antibodies used for IHC on MS brain section

Antibodies	Host species	Optimal Dilution	Source	Clone
Anti-MBP	Rat	1:100	ab7349/ Abcam	[12]
Anti-PCNA	Mouse	1:10000	ab29/Abcam	[PC10]
Anti-CD3	Mouse	1:100	Santa Cruz	[PC3/188A]
Anti-CD20	Mouse	1:500	Thermo	[L26]
Anti-GFAP	Mouse	1:1000	G3893/ Sigma	[G-A-5]
Anti-Iba1	Goat	1:2000	ab5076/Abcam	polyclonal

## 2.2 Animal Study

### 2.2.1 Ethical Statement

All animal work in this thesis was revised and authorized by the Institutional Review Board. Experimentation on animals was performed in adherence to the protocols and regulations approved by the Animal Research Ethics Committee of UAE University (Approval numbers: A-15-15; ERA-2018-5718).

### 2.2.2 Preparation of EBV Inoculum for Infection

Rabbits were inoculated with B95-8-derived virus. B95-8 cells are EBV immortalized B cells from marmoset monkeys (Miller et al., 1972). The virus derived from these cells is highly efficient in infecting and transforming human primary B cells *in vitro*, forming immortalized lymphoblastoid cells (Tsai et al., 2017). However, B95-8 cells do not favor spontaneous production of new virions. The lytic cycle occurs only at very low rate (Church et al., 2018; Tsai et al., 2017). Therefore, in order to harvest large amounts of infectious EBV, B95-8 cells should be exposed to stressful conditions, for example by treatment with tetradecanoyl phorbol acetate (TPA) (Hui-Yuen et al., 2011; Pan et al., 2005), or incubation at suboptimal temperatures (below 37°C) (Jones et al., 2007). Subsequently, lytic cycle is induced at higher rate, and infectious virions are increasingly shed into the media.

1. For inoculum preparation, sterile techniques were followed, and the simian cells were handled in laminar flow hood.
2. Exponentially growing B95-8 cells were seeded at  $3 \times 10^5$  cells/ml in a 75 cm<sup>2</sup> tissue culture flask. The cells were grown in complete RPMI 1640 (Gibco) including 10% heat-deactivated fetal bovine serum (FBS) (Gibco), 100 units/ml penicillin-streptomycin solution (Gibco), 0.5 µg/ml Amphotericin B, 50 µg/ml gentamycin (Hyclone), and 1× glutamine (Gibco) at 37°C, in 5% CO<sup>2</sup>.
3. At day 2 of incubation, B95-8 cells were resuspended in fresh media at  $1 \times 10^6$  cells/ml. Cells were then incubated at 33°C for 24 hr to stimulate the release of infectious EBV particles.
4. With extra care not to shake the cells, the supernatant was collected into 50 ml tube and centrifuged at 600×g for 10 min. This should help separate the source cells from the viral particles. Additional filtration was performed by passing the supernatant through 0.22 µm nylon filter (Thermo).
5. EBV copy number in the supernatant was then determined by quantitative PCR, as described in Section 2.2.5. The filtered supernatant was used for intravenous (IV) injections of rabbits.

### **2.2.3 Animals and Experimental Design**

The animal study was conducted on 4-to-8-week-old New Zealand White (NZW) rabbits. The rabbits were purchased from a local supplier and housed in the animal facility in the College of Medicine and Health Sciences (UAE University). All animals were left to acclimatize for 2 weeks. The study was divided into 2 phases: (1) examining viral spread from the periphery to the CNS, and (2) investigating the dynamics of EBV infection over time.

### **2.2.3.1 Phase 1: Examining Viral Spread from the Periphery to the CNS**

In this initial phase, a total of 24 rabbits were randomly allocated to four groups, based on the injections they received (Figure 13).

Group (1): EBV. Eight animals were intravenously (IV) injected with  $1 \times 10^7$  EBV copies, as determined by qPCR. All IV injections were administered via the marginal ear vein.

Group (2): PBS controls. Four animals were IV injected with PBS (volume equivalent to that of EBV inoculum).

Group (3): EBV+CsA. Nine animals were injected with the same viral inoculum as for group (1) and treated with daily subcutaneous injections of cyclosporin A (CsA), (20 mg/kg body weight, Sandimmune- Novartis).

Group (4): CsA controls. Three animals were IV injected with PBS and immunosuppressed using daily CsA injections as in group (3).

Rabbits were monitored daily and sacrificed at day 14 post inoculation, based on previous published work, under Ketamine-Xylazine (40 mg/kg and 5 mg/kg, respectively) anesthesia (Khan et al., 2015). Whole blood, spleen, brain, and spinal cord were collected on autopsy, and processed accordingly for molecular analysis and histopathological examination (Figure 13).

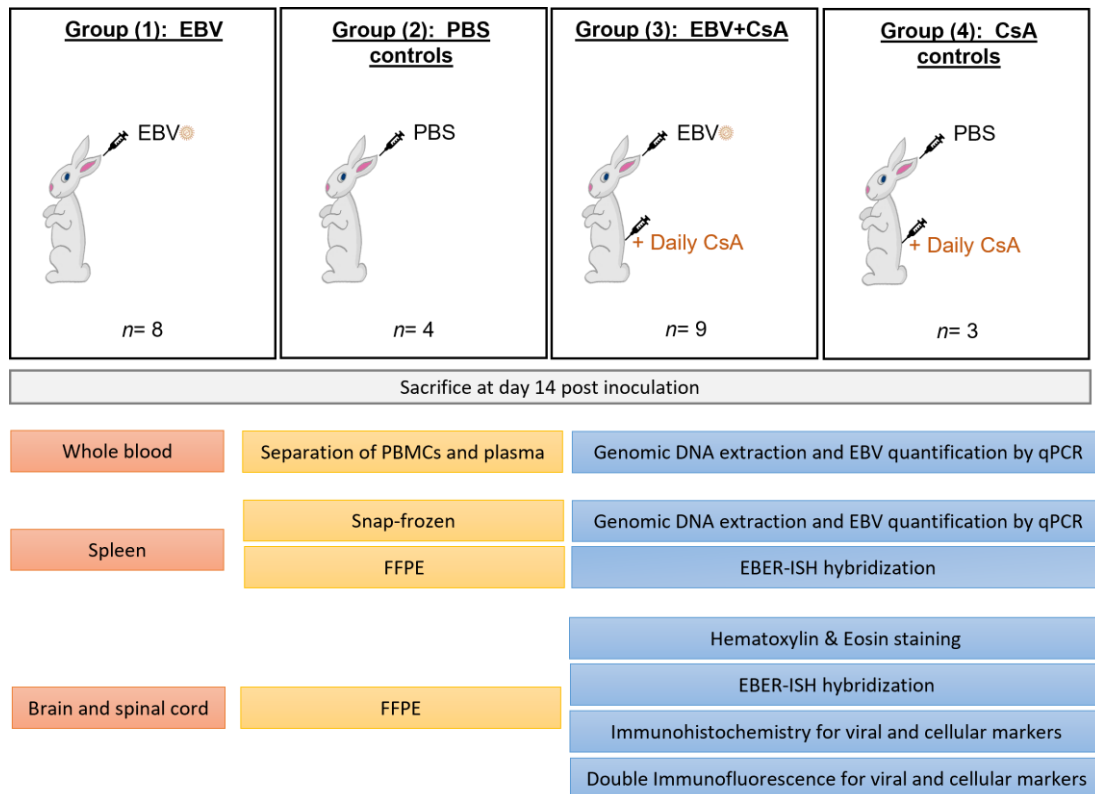


Figure 13: Phase 1 of the animal study. Examining viral spread from the periphery to the CNS. This phase included 4 groups. Group (1)/ EBV: EBV inoculated, and their controls group (2) PBS injected. Group (3)/EBV+CsA: EBV inoculated with CsA-induced immunosuppression, and their controls group (4) PBS injected with CsA-induced immunosuppression. Blood, spleen and the CNS were collected on autopsy. Blood was separated into peripheral blood mononuclear cells (PBMCs) and plasma for nucleic acid extraction and viral detection. Part of the spleen was snap-frozen in liquid nitrogen for molecular analysis, and another was fixed in 4% paraformaldehyde (PFA) for histology on formalin-fixed, paraffin-embedded (FFPE) samples. The brain and spinal cord were also fixed in 4% PFA for histology

### 2.2.3.2 Phase 2: Investigating the Dynamics of EBV Infection over Time

This second phase was confirmatory and expanded in the timeline. A total of 20 rabbits were divided into 5 groups, based on the time-point they were sacrificed at (Figure 14).

Group (1): 3dpi. Three animals were IV inoculated with EBV, and one with PBS, as described in phase 1. The 4 animals were sacrificed at day 3 post inoculation.

Group (2): 7dpi. Three animals were inoculated with EBV, and one with PBS, and sacrificed at day 7 post inoculation.

Group (3): 14dpi. Three animals were inoculated with EBV, and one with PBS, and sacrificed at day 14 post inoculation.

Group (4): 21dpi. Three animals were inoculated with EBV, and one with PBS, and sacrificed at day 21 post inoculation.

Group (5): 28dpi. Three animals were inoculated with EBV, and one with PBS, and sacrificed at day 28 post inoculation.

The sacrifice was performed under Ketamine-Xylazine anesthesia. Whole blood, spleen, brain, and spinal cord were collected on autopsy and processed accordingly for downstream molecular analysis and histopathological examination (Figure 14).

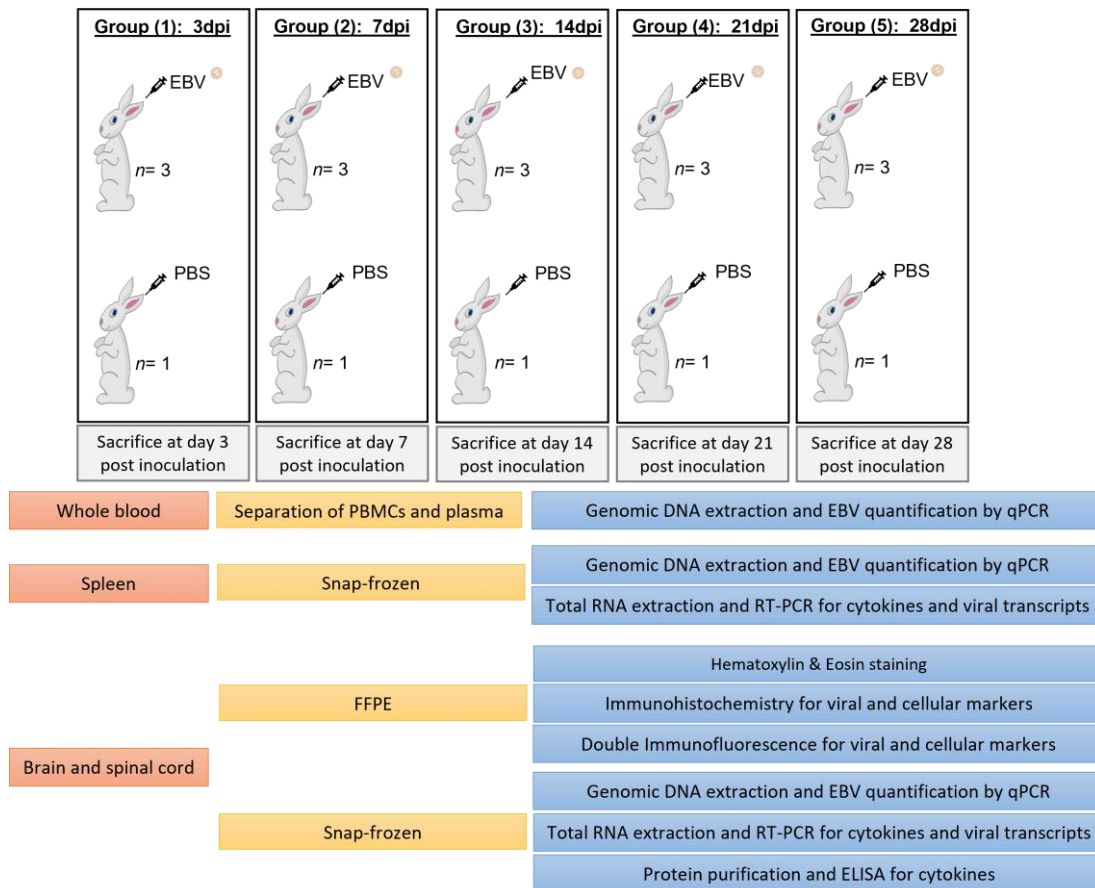


Figure 14: Phase 2 of the animal study. Investigating the dynamics of EBV infection over time. Based on the time of sacrifice post inoculation, this phase contained 5 groups made up of EBV inoculated and their PBS controls. Group (1): animals were sacrificed at day 3. Group (2): animals were sacrificed at day 7. Group (3): animals were sacrificed at day 14. Group (4): animals were sacrificed at day 21. Group (5): animals were sacrificed at day 28. Organs collected on the day of sacrifice were processed for molecular and histopathology analyses

#### 2.2.4 Isolation of PBMCs and Plasma

PBMCs and plasma were isolated from whole blood samples using density gradient centrifugation on Histopaque-1077 (Sigma).

1. On the day of sacrifice, a volume of 20-40 ml of whole blood was collected in 50 ml tubes containing 5 ml of the anticoagulant sodium citrate 4% W/V. Tubes were inverted gently to mix blood and the anticoagulant.

2. PBMCs were isolated within 1 hr of blood collection. Ficoll Histopaque and sterile phosphate buffered saline (PBS) were brought to room temperature prior to use, to avoid exposing blood cells to cold shock.
3. 10 ml blood were transferred to 50 ml tube and diluted 1:1 in PBS by pipetting up and down in the tube.
4. The diluted blood was slowly layered onto another 50 ml tube containing 10 ml Ficoll. The blood and Ficoll should not mix, and 2 separate layers should form. The samples were immediately centrifuged at 400×g for 30 min at 4°C.
5. Plasma, the top layer, was aliquoted in 1.5 Eppendorf tubes and stored at -80°C.
6. PBMCs, the buffy coat interphase, were aspirated immediately, to avoid their sedimentation, into fresh tube, and without contamination with Ficoll and the supernatant. PBMCs were washed twice with 20 ml PBS and centrifuged at 100×g for 10 min.
7. PBMCs were resuspended in PBS, checked for viability, and counted manually using trypan blue and hemacytometer.
8. Cells were resuspended at  $2 \times 10^6$  cells/ml in freezing cryoprotective media; 20% DMSO and FBS in RPMI, and aliquoted. Cryovials were kept at -80°C overnight and transferred the next day to vapor-phase liquid nitrogen tank till further analysis.

### **2.2.5 Extraction of Genomic DNA and Viral Detection and Quantitation Using Quantitative PCR**

Genomic DNA (gDNA) was extracted from PBMCs, plasma, and biopsied tissues from spleen, brain, and spinal cord using QIAamp® DNA Mini and Blood Mini Kit (QIAGEN), according to manufacturer's instructions. DNA amount and purity were determined using NanoDrop-2000c (Thermo). Conventional PCR amplification



of rabbit house-keeping gene GAPDH (Table 3) was used to determine DNA quality. PCR amplification of marmoset house-keeping gene  $\beta$ -globin (Table 3) was used to ensure that rabbit DNA samples were not contaminated with simian DNA.

PCR reaction was carried out in a volume of 30  $\mu$ l. The reaction included 1 $\times$ PCR buffer, 10 pmol of forward and reverse primers, 2 mM MgCl<sub>2</sub>, 0.05 mM deoxynucleotides (dNTPs), 1 unit Taq DNA polymerase (QIAGEN), and 100 ng gDNA. B95.8 gDNA was used as positive control, and a reaction with no DNA template was included for negative control. Applied Biosystems thermal cycler PCR System 2700 was used with the following thermal cycling conditions:

- initial denaturation step at 95°C for 5 min,
- 30 cycles of: 1 min denaturation at 95°C, 45 sec annealing at 55°C for marmoset  $\beta$ -globin and EBV BamHI primers, and at 42°C for rabbit GAPDH, and 30 sec elongation at 72°C, and
- a final extension of the full PCR product at 72°C for 5 min.

Amplicons were electrophoresed at 100 volts in 2% agarose gel stained with ethidium bromide.

For viral detection and quantitation in rabbit tissues, TaqMan qPCR for the amplification of EBV BamHI W fragment was performed using Applied Biosystems™ QuantStudio™ 7 Flex Real-Time PCR System. Each reaction was run in duplicates and prepared in a final volume of 20  $\mu$ l. The reaction contained 1 $\times$ TaqMan Universal PCR Master Mix (Applied Biosystems), 1 $\times$ primer-probe mixture (Table 3), 50 ng of DNA template, and DNase-free water. PCRs were repeated twice. Samples with undetermined Ct values were interpreted to have zero copy number for the purpose of statistical analysis.

To estimate EBV copy number in test samples, a standard curve was prepared using gDNA of Namalwa cells (CRL-1432, American Type Culture Collection). Namalwa is an EBV positive Burkitt's lymphoma cell line, with known copy number of EBV DNA in each cell (i.e., 2 integrated copies). The standard curve was made up of five 10-fold serial dilutions of Namalwa DNA (100, 10, 1, 0.1, and 0.01 ng/ $\mu$ l). The means of cycle threshold (Ct) were plotted against the logarithm of Namalwa DNA amounts (Figure 15).

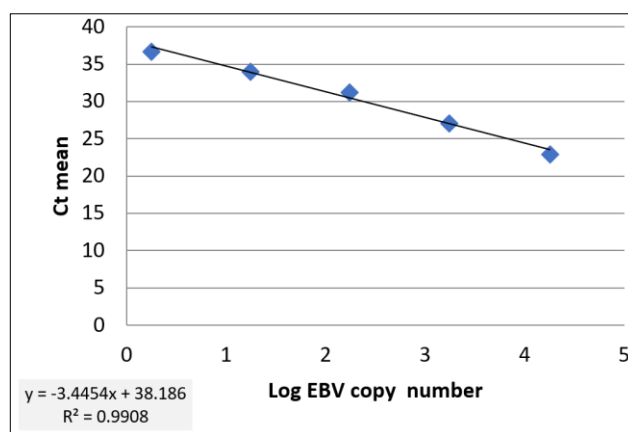


Figure 15: Standard curve created using Namalwa gDNA

Table 3: Sequence of primers and probes used in amplifying gDNA extracted from rabbit samples

Genomic fragment	Primers sequence	Product size (bp)
Marmoset $\beta$ -globin	F: 5' GAG GTT CTT TGA GTC CTT TGG 3' R: 5' CAT CAC TAA AGG CAC CGA GCA 3'	104
Rabbit GAPDH	F: 5' GGA GAA AGC TGC TAA 3' R: 5' ACG ACC TGG TCC TCG GTG TA3'	109
EBV BamHI	F: 5' CAC TTT AGA GCT CTG GAG GA 3' R: 5' TAA AGA TAG CAG CAG CGC AG 3'	152
EBV BamHI W	F: 5' GCA GCC GCC CAG TCT CT 3' R: 5' ACA GAC AGT GCA CAG GAG CCT 3' Probe: 5' (6FAM)AAA AGC TGG CGC CCT TGC CTG(TAMRA) 3'	83

### **2.2.6 Examination of Histopathological Changes in the CNS Following EBV Infection Using Hematoxylin and Eosin staining**

Brain and spinal cord collected on autopsy were fixed in 4% PFA for 1-2 weeks. The tissues were processed for embedding in paraffin wax and microtomy as described in Section 2.1.1. Brain and spinal cord tissues were cut into 5  $\mu$ m-sections and stained with H&E as described in Section 2.1.1, for basic histological evaluation.

### **2.2.7 Examination of Inflammation in the CNS Following EBV Infection Using Immunostaining**

To identify cell populations contributing to inflammation in the CNS, 5- $\mu$ m formalin-fixed, paraffin-embedded (FFPE) sections were immunostained for several cellular markers.

For chromogenic immunohistochemistry (IHC), sections were dewaxed and rehydrated, followed by blocking of endogenous peroxidase activity as described in Section 2.1.4. Next, sections were incubated in boiling 10 mM sodium citrate-0.1% Triton X-100 pH 6.0, for 10 min, for antigen unmasking. Sections were then incubated in 5% BSA in the washing buffer for 1-2 hr. Incubation with primary and secondary antibodies was performed as described in Section 2.1.4. A large number of antibodies was pre-tested on rabbit tissues to ensure specificity and determine optimal concentrations. The list of antibodies used on rabbit tissues are shown in Table 4. DAB was used for signal detection and sections were counterstained with hematoxylin.

For immunofluorescence, sections were deparaffinized, rehydrated, and subjected to HIAR. Sections were blocked in 5% BSA, and then incubated with a mixture of 2-3 diluted unconjugated primary antibodies overnight at room temperature. After washing primary antibodies off, sections were incubated in dark with appropriate fluorochrome-conjugated secondary antibodies (Table 5), for 1 hr.

Finally, sections were counterstained with DAPI, diluted at 1:5000 in washing buffer. Sections were mounted using aqueous-based Fluoromount (Sigma). Fluorescence images were captured using fluorescence microscope (Zeiss), and slides were store in dark at 4°C.

Table 4: List of antibodies used in IHC/IF on rabbit tissues

Antibodies	Host	Dilution- IHC	Dilution- IF	Source	Clone
Anti-CD3	Rat	1:250	-	ab11089/ Abcam	[CD3-12]
Anti-CD4	Mouse	1:200	-	WS0778U-100/ KingFisher Biotech	[RTHA]
Anti-CD8	Mouse	1:400	-	WS0796U-100/ KingFisher Biotech	[ISC27A]
Anti-CD21	Rabbit	1:250	1:250	ab75985/ Abcam	[EP3093]
Anti-DIG	Mouse	1:5000	-	Sigma	[D1-22]
Anti-EBI2	Rabbit	1:300	-	ab150625/ Abcam	polyclonal
Anti-EBNA1	Mouse	1:20	-	MA1-7271/ Thermo	[D810H]
Anti-GFAP	Mouse	1:1000	-	G3893/ Sigma	[G-A-5]
Anti-GFAP	Chicken	-	1:500	ab4674/ Abcam	polyclonal
Anti-Iba1	Goat	1:2000	1:100	ab5076/ Abcam	polyclonal
Anti-Rabbit IgM mu chain	Goat	1:2000	1:1000	ab97191/ Abcam	
Anti-Rabbit IgG Fc	Goat	1:3000	1:500	ab190492/ Abcam	[RMG02]
Anti-rabbit macrophage	Mouse	1:300	1:50	M0633/ Dako	[RAM11]
Anti-MBP	Rat	1:100	-	ab7349/ Abcam	[12]
Neutrophil marker	Mouse	1:200	-	sc-59376/ Santa Cruz	[RPN3/57]
Anti-PCNA	Mouse	1:10000	1:100	ab29/ Abcam	[PC10]
Anti-rat IgG-HRP conjugated	Goat	1:200	-	ab97057/ Abcam	-
Anti-goat IgG-HRP conjugated	Donkey	1:200	-	ab6885/ Abcam	-
Biotinylated anti- rabbit IgG	Goat	1:200	-	Ultra-Sensitive ABC Peroxidase Rabbit IgG Staining Kit. Cat. #: 32054. Thermo	-
Biotinylated anti- mouse IgG	Horse	1:200	-	Ultra-Sensitive ABC Peroxidase Mouse IgG Staining Kit. Cat. #: 32052. Thermo	-

Table 5: List of fluorochrome-conjugated antibodies used for fluorescent staining on rabbit tissues

Fluorochrome-conjugated antibodies	Host	Dilution	Source	Clone
Anti-DIG-FITC	Mouse	1:250	F3523/ Sigma	[D1-22]
Anti-Chicken IgY-FITC	Goat	1:200	(ab6873/ Abcam	polyclonal
Anti-Goat IgG- Rhodamine Red™-X (RRX)	Donkey	1:200	Code: 705-295-147/ Jackson ImmunoResearch	polyclonal
Anti-Goat IgG-Alexa Fluor® 647	Donkey	1:200	Code: 705-607-003/ Jackson ImmunoResearch	polyclonal
Anti-Goat IgG-Alexa Fluor® 488	Donkey	1:200	ab150129/ Abcam	polyclonal
Anti-Mouse IgG-Alexa Fluor® 555	Goat	1:200	4409S/ Cell Signaling	-
Anti-Mouse IgG-Alexa Fluor® 488	Goat	1:200	ab150117/ Abcam	-
Anti-Rabbit IgG-Alexa Fluor® 488	Goat	1:200	4412S/ Cell Signaling	-
Anti-Rabbit IgG-Alexa Fluor® 555	Goat	1:200	4413S/ Cell Signaling	-
Anti-Rat IgG-Alexa Fluor® 488	Goat	1:200	ab150157/ Abcam	Polyclonal
Anti-Rat IgG- Rhodamine Red™-X (RRX)	Donkey	1:200	Code: 712-295-153/ Jackson ImmunoResearch	polyclonal

### 2.2.8 Examination of EBV Infection in the Periphery and CNS Using EBER-*in situ* Hybridization

*In situ* hybridization for the detection of EBV encoded RNAs (EBER-ISH) was performed using two 30-nucleotide antisense probes.

#### 2.2.8.1 End-labelling Probes with Digoxin

Each one of the 2 probes was end-labelled with Digoxigenin molecule (DIG) using commercially available end-labelling kit (Cat # 03353583910, Roche) as follows:

- a- 4 µl 5×tailing buffer, containing 1 M potassium cocodylate, 125 mM Tris-HCl, 1.25 mg/ml BSA, pH 6.6,
- b- 4 µl CoCl<sub>2</sub> solution (25 mM),
- c- 1 µl Dig-dUTP (1 mM Dig-11-dUTP in ddH<sub>2</sub>O),
- d- 1 µl dATP (10 mM in ddH<sub>2</sub>O),

- e- 1  $\mu$ l terminal transferase (400 U/ $\mu$ l),
- f- 1  $\mu$ l probe (1  $\mu$ g/ $\mu$ l), and
- g- 8  $\mu$ l ddH<sub>2</sub>O was added to make up the reaction volume to 20  $\mu$ l.

After mixing the tubes well, they were incubated at 37°C in the heat block for 30 min. The reaction was stopped by adding 2  $\mu$ l of 0.2 M EDTA (pH 8.0). Finally, the volume of the labelled probe was made up to 100  $\mu$ l by adding 78  $\mu$ l sterile TE buffer (50 mM Tris-HCl, 1 mM EDTA, pH 7.6). Thus, the final concentration of the labelled probe was 10  $\mu$ g/ml. Then, the 2 labelled probes were mixed together.

#### **2.2.8.2 EBER-ISH Staining**

Once the probes were labelled, EBER-ISH was carried out as following:

1. Dewaxing.

Sections were deparaffinized in xylene as described in Section 2.1.1.

2. Dehydration.

Sections were dehydrated in graded ethanol, 70%, 90% and 100%, for 5 min each.

3. Quenching endogenous peroxidase activity.

Refer to Section 2.1.4. Sections were then dehydrated in absolute ethanol and air dried.

4. Tissue digestion using proteinase K.

In a 37°C humid incubator, sections were incubated with 100  $\mu$ g/ml proteinase K in TE buffer, for 10 min. The reaction was stopped by rinsing slides in water. Sections were then dehydrated in absolute ethanol and air dried.

5. Hybridization.

Labelled probes were diluted to 0.2 µg/ml in hybridization buffer (50% formamide, 5% dextran sulphate, 2x SSC) (Appendix II). 25 µl of this hybridization solution was added on top of the dry section. Coverslips of a dimension 32x22 cm were used to cover the tissue. The coverslips helped spread the hybridization solution over the entire tissue and eliminate evaporation. Slides were kept in a humidified chamber. Probe denaturation was performed by microwaving for 7 min at the lowest power, followed by overnight hybridization in a 42°C oven.

#### 6. Stringency wash.

Coverslips were removed and sections were washed in 2 changes of 2×SSC, for 10 min each. Slides were incubated in 2 changes of pre-warmed 0.1×SSC at 50°C, for 10 min each. At this stage the nucleotides that were not incorporated or weakly bound would be washed off. This is a critical step during EBER-ISH to eliminate non-specific probe binding. Slides were then washed in 2×SSC, followed by a wash in 1×PBS, each for 5 min.

#### 7. Incubation with anti-DIG.

Sections were incubated for 30 min at room temperature in a humidified tray with monoclonal mouse anti-DIG antibody (clone D1-22, Sigma Cat# D8156), diluted at 1:2500 in 1×PBS containing 1% horse serum (component of the Ultra-sensitive ABC peroxidase mouse IgG staining kit (Thermo)).

#### 8. Incubation with biotinylated secondary anti-mouse.

Sections were incubated for 30 min in mouse IgG (component of Ultra-Sensitive ABC Peroxidase Mouse IgG Staining Kit (Thermo, Cat# 32052)), diluted at 1:200 in 1×PBS containing 1% horse serum. Sections were washed in 3 changes of 1×PBS, 10 min each.

#### 9. Incubation with the substrate horseradish peroxidase, as described in Section 2.1.4.

10. Color development. Refer to Section 2.1.4.
11. Counterstaining with hematoxylin. Refer to Section 2.1.4.
12. Mounting. Slides were dehydrated in graded ethanol, cleared in xylene, and mounted as described in Section 2.1.2.

### **2.2.9 Extraction of Total RNA and Detection of Cellular and Viral Transcripts Using Reverse-Transcriptase PCR (RT-PCR)**

Total RNA was extracted from the spleen, brain and spinal cord using TRIzol reagent (Invitrogen).

1. Small pieces of snap-frozen tissues were homogenized in 0.5 ml TRIzol and left for 5-10 min at room temperature.
2. 0.2 ml chloroform was added to the tissue homogenate, mixed well, and incubated for 5 min at room temperature.
3. Tissue homogenates were centrifuged at 13,000×g, at 4°C, for 15 min.
4. The top transparent layer was then transferred to a new Eppendorf 2 ml-tube and mixed with 0.7 ml isopropanol. Tubes were centrifuged again at 13,000×g, at 4°C, for 10 min.
5. The supernatant was discarded, and 1 ml 70% ethanol was added. Tubes were centrifuged again at 13,000×g, at 4°C, for 5 min.
6. The supernatant was discarded, and the pellet was left to air-dry. The pellet was then resuspended in 25 µl nuclease-free water and incubated in a heat block at 55°C, for the pellet to dissolve.
7. RNA amount and purity was determined using NanoDrop-2000c (Thermo). Samples were stored at -80°C till further use.

One microgram of extracted RNA was treated with DNase I (Promega) to remove any residual DNA contamination. For this, a mixture of: 10×DNase buffer, 1



unit RNasin, and 1 unit DNase I was added to 1 µg RNA. The enzymatic reaction was carried out at 37°C for 1 hr in a thermomixer (Eppendorf). To stop DNase I activity, 2 µl stop buffer (Promega) was added to each reaction and incubated at 65°C in a thermomixer for another 10 min.

DNase-treated RNA was then checked for DNA contamination by standard PCR. PCR amplification of genomic rabbit GAPDH fragment was carried out as described above in Section 2.2.5. RNA samples that failed to amplify rabbit GAPDH fragment were deemed free of DNA contamination and suitable for reverse transcription into complementary DNA (cDNA). Reverse Transcription System kit (Promega) was used to reverse transcribe RNA. One microgram DNased RNA was incubated at 70°C for 10 min in a thermomixer. The RNA was subsequently left on ice. Reverse transcription mixture was prepared and added onto the RNA. The enzymatic reaction mixture contained: 5 mM MgCl<sub>2</sub>, 1× Reverse Transcriptase Buffer, 1 mM dNTPs, 0.5 µg random hexamers, 15 units avian myeloblastosis virus (AMV) reverse transcriptase. After 10 min incubation at room temperature, the reaction was moved to 42°C for 1 hr. The resulting cDNA was incubated at 95°C for 5 min to stop the enzymatic activity. cDNA was then moved onto ice before storing at -80°C.

SYBR Green Real-time PCR assay was performed to determine the relative mRNA expression of cellular and viral transcripts, namely, tumor necrosis factor  $\alpha$  (TNF- $\alpha$ ), interleukin-1 $\beta$  (IL-1 $\beta$ ), IL-2, IL-6, interferon- $\gamma$  (IFN- $\gamma$ ), EBER-1, EBER-2, EBNA-1, EBNA-2, LMP-1, and BZLF-1 as described in previous reports (Schnupf & Sansonetti, 2012; Tierney et al., 2015; Wang et al., 2017). The sequence of primers is shown in Table 6.

PCR reaction was run on 1 µl cDNA, using Power SYBR<sup>®</sup> Green PCR Master Mix (Applied biosystems) in a final volume of 20 µl, containing 1×PCR mix, and 10

pM forward and reverse primers. Using Applied Biosystems QuantStudio™ 7 Flex System, the reaction was initiated at 50°C for 2 min, followed by 95°C for 10 min, then 40 cycles of 15 sec at 95°C and 1 min at 60°C. To check for nonspecific amplifications, a melting curve was performed from 60-95°C. Samples were run in duplicates, and experiments were repeated twice. Relative expression was determined using comparative CT ( $\Delta\Delta C_t$ ) method. Rabbit-specific GAPDH (endogenous control), and non-infected PBS samples (experimental controls) were used as reference.

Table 6: Sequence of primers for rabbit cellular transcripts and EBV genes

Gene	Primers sequence
Rabbit GAPDH (control)	F: TGACGACATCAAGAAGGTGGTG R: GAAGGTGGAGGAGTGGGTGTC
Rabbit TNF	F: CTGCACTTCAGGGTGATCG R: CTACGTGGGCTAGAGGCTTG
Rabbit IL1	F: TTGAAGAAGAACCCGTCTCTG R: CTCATACGTGCCAGACAACACC
Rabbit IL2	F: GCCCAAGAAGGTCACAGAATTG R: TGCTGATTGATTCTCTGGTATTTCC
Rabbit IL6	F: CTACCGCTTTCCCCACTTCAG R: TCCTCAGCTCCTTGATGGTCTC
Rabbit IFN	F: TGCCAGGACACACTAACCAGAG R: TGTCACTCTCCTCTTTCCAATTCC
EBER1	F: TGCTAGGGAGGAGACGTGTGT R: TGACCGAAGACGGCAGAAAAG
EBER2	F: AACGCTCAGTGCGGTGCTA R: GAATCCTGACTTGCAAATGCTCTA
EBNA1	F: GGTCGTGGACGTGGAGAAAA R: GGTGGAGACCCGGATGATG
EBNA2	F: GCTTAGCCAGTAACCCAGCACT R: TGCTTAGAAGGTTGTTGGCATG
LMP1	F: AATTTGCACGGACAGGCATT R: AATTTGCACGGACAGGCATT
BZLF1	F: CCCAAACTCGACTTCTGAAGATGTA R: TGATAGACTCTGGTAGCTTGGTCAA

### **2.2.10 Extraction of Total Protein and Detection of IL-2 and IL-6 in the CNS Using ELISA**

Snap-frozen brain and spinal cord were used to isolate protein.

1. Ten 2.8 mm ceramic beads (Omni International) were placed in 2 ml tough tubes (Omni International).
2. 50-100 mg of the tissues were weighed and washed with ice cold sterile PBS. Excess buffer was dried with clean tissue paper.
3. Tissues were placed inside beads-containing tubes. Ice cold T-PER (tissue protein extraction reagent, Thermo) freshly mixed with a cocktail of proteases and phosphatases inhibitors (Roche) was added at 10 volumes/ gram tissue
4. Tissues were then homogenized using BeadBlaster™24 Homogenizer (Benchmark) at speed 5 for 20 sec, or until the tissue was completely disintegrated.
5. Tissue homogenates were incubated on ice for 30 min, then centrifuged at 10,000× g for 30 min at 4°C.
6. The protein-containing supernatant was collected, aliquoted and stored at -80°C.
7. Protein concentration of the supernatant was measured with the Bradford assay.
8. Using BSA as a standard, five 2-fold dilutions were prepared in 50 mM Tris. The diluted BSA standards were mixed with Protein Assay Dye Reagent Concentrate (Bio-Rad), diluted at 1:4. The mixture was incubated for 30 min at room temperature. The optical density (OD) was measured and plotted against BSA concentration as in Figure 16.

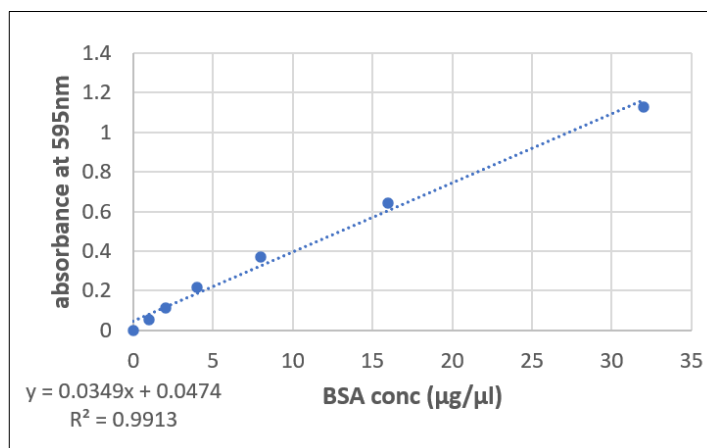


Figure 16: Standard curve established using known BSA concentrations, to estimate protein concentration from CNS homogenates

Purified proteins from the brain and spinal cord were used to estimate the amount of IL2 and IL6 using DuoSet ELISA development system kits for rabbit IL2 and IL6, according to the manufacturer's instructions (R&D Systems). All samples were assayed in duplicates, and experiments were repeated 3 times. Protein standards were provided in the kits and used to determine the quantity of cytokines in the test samples.

### 2.2.11 Statistical Analysis

Statistical analyses were performed using the GraphPad Prism Version 9.1.2 (GraphPad Software, San Diego, CA). Comparison between multiple groups was performed using one-way ANOVA or non-parametric multiple comparison,  $\alpha = 0.05$ . Comparison between two groups was done using two-tailed unpaired t-test or nonparametric Mann-Whitney test. Data was displayed as mean  $\pm$  SEM. Spearman or Pearson correlation was used to correlate between 2 variables.  $P$  value  $\leq 0.05$  was considered statistically significant.

## Chapter 3: Results

### 3.1 Human Study

#### 3.1.1 Heterogeneity of MS Plaques in EBV Positive Cases

Eighteen MS cases were classified previously as heavily infected with EBV, i.e., containing over 200 infected cells per section (Hassani et al., 2018). To study pathological changes in EBV positive MS cases, tissue blocks biopsied from areas containing macroscopic plaques were examined. On gross examination, MS plaques were well-demarcated, discolored areas. These plaques had a resistant texture that render them relatively hard to cut, compared to surrounding macroscopically normal appearing white matter. According to autopsy reports provided by RMMSC, most of these cases had moderately severe to severe burden of chronic inactive plaques.

MS plaques were evaluated by hematoxylin and eosin (H&E) stain, Luxol Fast Blue (LFB) stain, and immunohistochemistry (IHC) for myelin basic protein (MBP), CD68, Iba1, GFAP, CD20 and CD3 to identify MS plaques and determine the cellular makeup of infiltrates in the plaques (Figures 17-27) (Lassmann, 2018). Five cases were randomly selected to demonstrate a representative summary of the pathological changes and disease heterogeneity observed in the collection of EBV positive cases (Figures 17-20 and 24).

Here, the biopsied lesions in the first 4 cases represented a good example of heterogeneity although they all contained chronic inactive demyelinated plaques (Figures 17-20). The heterogeneity involved the extent of cell infiltration, changes in cell morphology, and expression level of the cellular markers used for detection. In MS cases I-IV, a well-demarcated area of hypocellularity and fibrous architecture was prominent in H&E staining (Figures 17-20). Destruction of myelin sheaths was

confirmed using LFB staining and IHC for MBP. Notably, in MS case III, thin fibers of myelin were seen within the plaque (Figure 19), implying partial remyelination, a characteristic of shadow plaques commonly detected in chronic progressive MS. Incomplete remyelination was also seen at the border of the lesion in MS case IV (Figure 20). Another common feature between the plaques in the 4 cases was the absence of infiltration by CD20<sup>+</sup> B lymphocytes and CD3<sup>+</sup> T lymphocytes. The lack of inflammation in these lesions indicated the aged inactive nature of the plaque.

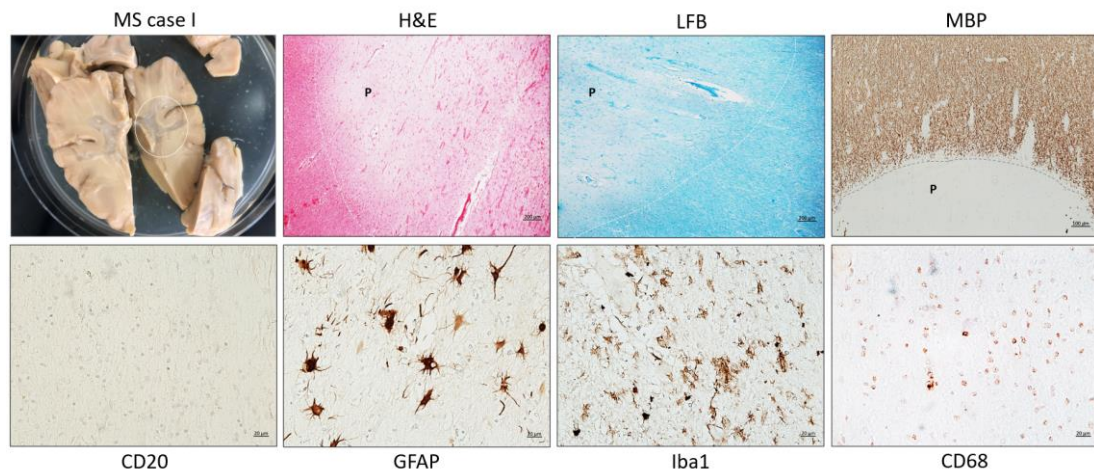


Figure 17: MS case I with chronic inactive plaque. Coronal postmortem brain slice from a 52-year-old male with moderately severe MS. This case had predominantly chronic inactive plaques, and some focal chronic active smoldering plaques. The sampled lesion is encircled. The plaque (P) is well-demarcated in H&E staining, LFB staining, and MBP immunostaining. Scale bar= 200 (for H&E and LFB) and 100  $\mu$ m (for MBP). IHC for CD20, GFAP, Iba1, and CD68 was performed to evaluate the presence/absence of B cells, astrocytes, microglia, and macrophages, respectively. Scale bar= 20  $\mu$ m

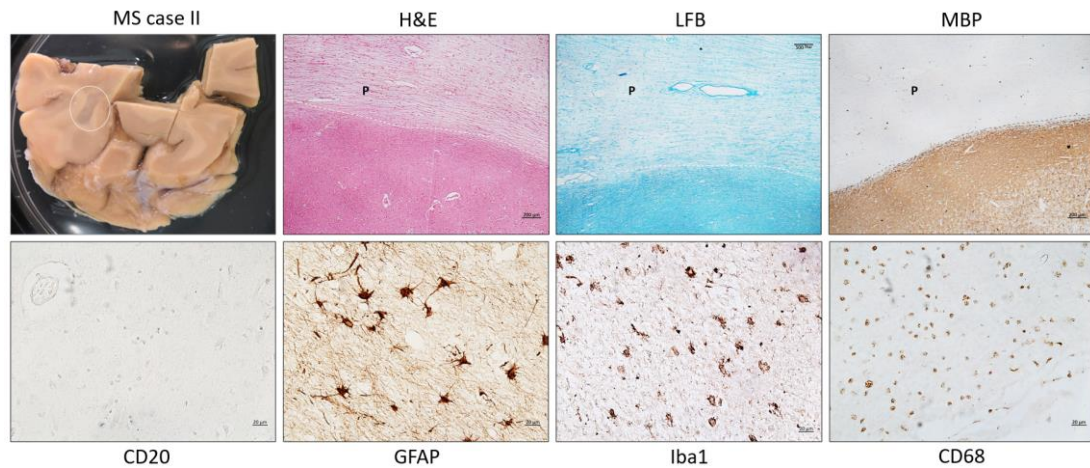


Figure 18: MS case II with chronic inactive plaque. Coronal postmortem brain slice from a 59-year-old male with moderately severe MS. The sampled lesion (P) is encircled and is evident in H&E and LFB staining and IHC for MBP. Scale bar= 200  $\mu$ m. IHC for CD20, GFAP, Iba1 and CD68 was used for characterizing the designated plaque. Scale bar= 20  $\mu$ m

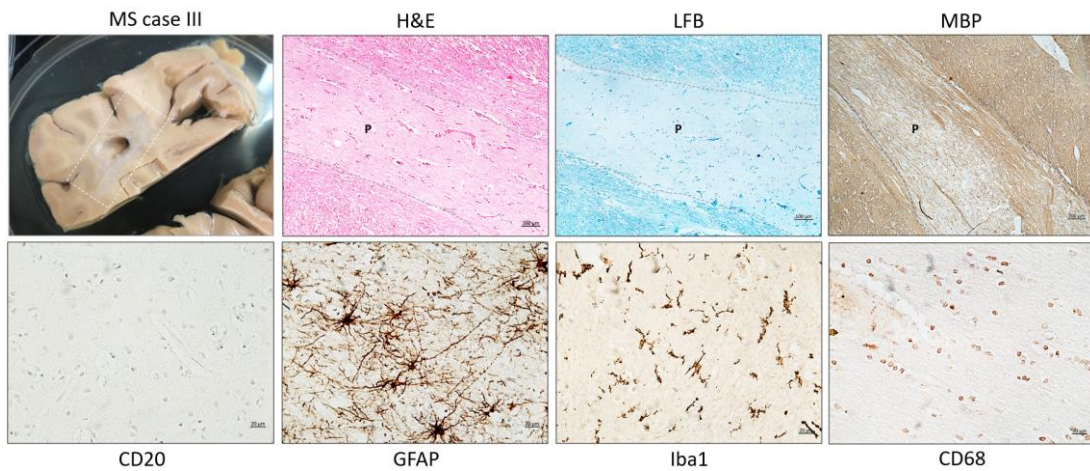


Figure 19: MS case III with chronic inactive plaque. Coronal postmortem brain slice from a female MS case. The biopsied plaque (P) was evaluated using H&E and LFB staining, and IHC for MBP, CD20, GFAP, Iba1 and CD68. Scale bars= 200 (for H&E, LFB, and MBP) and 20  $\mu$ m (for IHC for other cell markers)

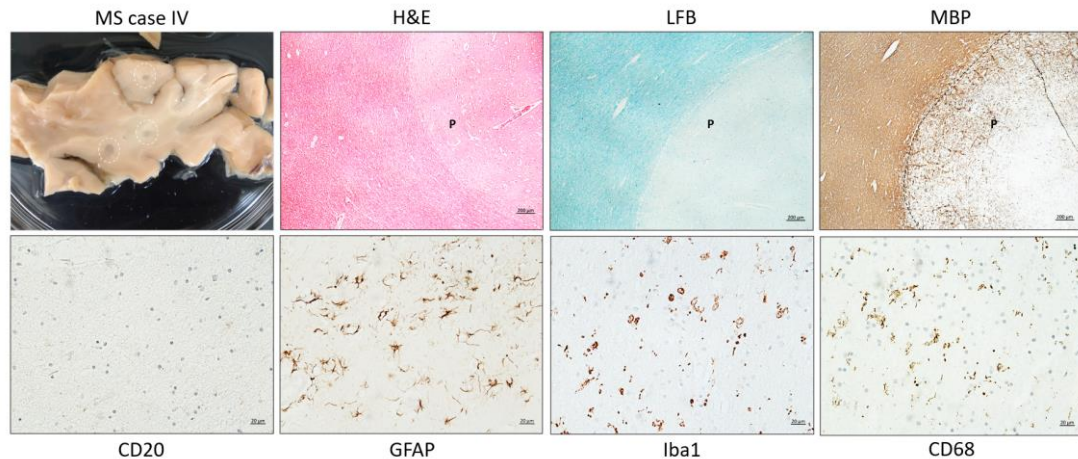


Figure 20: MS case IV with chronic inactive plaque. Coronal postmortem brain slice from a 43-year-old male with chronic inactive plaques, and chronic active smoldering plaques. The biopsied lesion (P) was evaluated using H&E and LFB staining, and IHC for MBP, CD20, GFAP, Iba1, and CD68. Scale bars= 200 (for H&E, LFB, and MBP) and 20  $\mu$ m (for IHC for other cell markers)

The hypercellular rim of the plaque contained GFAP<sup>+</sup> astrocytes. However, the expression level of GFAP and the morphology of astrocytes varied between the cases. In MS case I, the majority of astrocytes stained intensely for GFAP, suggesting relatively high protein expression and thus increased astrocytes reactivity. GFAP expression was most dense in the soma (i.e., hypertrophied astrocytes) rather than in the processes, making astrocytes processes appear shortened (Figure 17). MS case II contained a mesh of long radiating GFAP<sup>+</sup> fibers with a line of intensely immunoreactive soma (Figure 18). In MS case III, GFAP<sup>+</sup> astrocytes had elongated processes with extensive interaction with nearby processes, a feature that is commonly seen in glial scar (Figure 19). In contrast, MS case IV contained relatively lower density of astrocytes as indicated by the low expression of GFAP (Figure 20).

Additionally, the plaques in the aforementioned 4 cases contained a population of cells that were Iba1 and CD68 immunoreactive. Iba1 staining in MS case I showed



a mixture of ramified (resting) and amoeboid (activated/ phagocytic) microglia (Figure 17), while Iba1<sup>+</sup> cells in MS case II were mainly amoeboid with few taking rod-like shape (Figure 18). Most of Iba1<sup>+</sup> cells in MS case III, however, were ramified microglia (Figure 18). MS case IV contained both small and enlarged amoeboid microglia (Figure 19). CD68<sup>+</sup> cells were commonly round in shape in MS cases I-III (Figure 17-19). In MS case IV, nonetheless, CD68<sup>+</sup> cells showed a branching morphology comparable to ramified microglia (Figure 20).

In general, GFAP<sup>+</sup> astrocytes often accumulated at the borders of demyelinated plaques, while the plaque itself showed limited staining for astrocytes (Figure 21). On the other hand, Iba1<sup>+</sup> cells and CD68<sup>+</sup> cells were seen distributed unevenly throughout the demyelinated plaque and the surrounding non-demyelinated areas (Figures 22-23). Notably, microglia/macrophages were seen at higher density in the adjacent non-demyelinated area compared to the demyelinated center of the plaque (Figure 23).

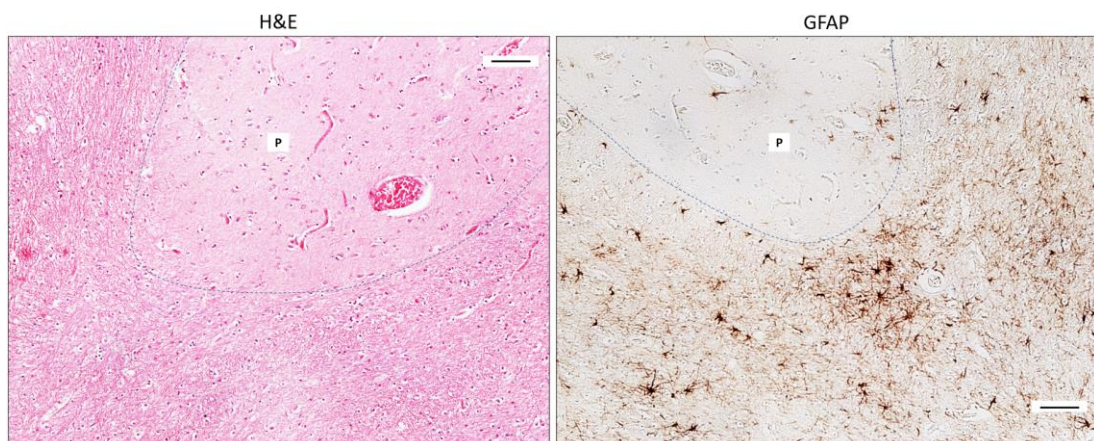


Figure 21: Astrocytes surround demyelinated plaques. The demyelinated plaque (P) evident in H&E staining contained GFAP<sup>+</sup> cells at the borders and in the area surrounding the plaque. Scale bar= 100  $\mu$ m

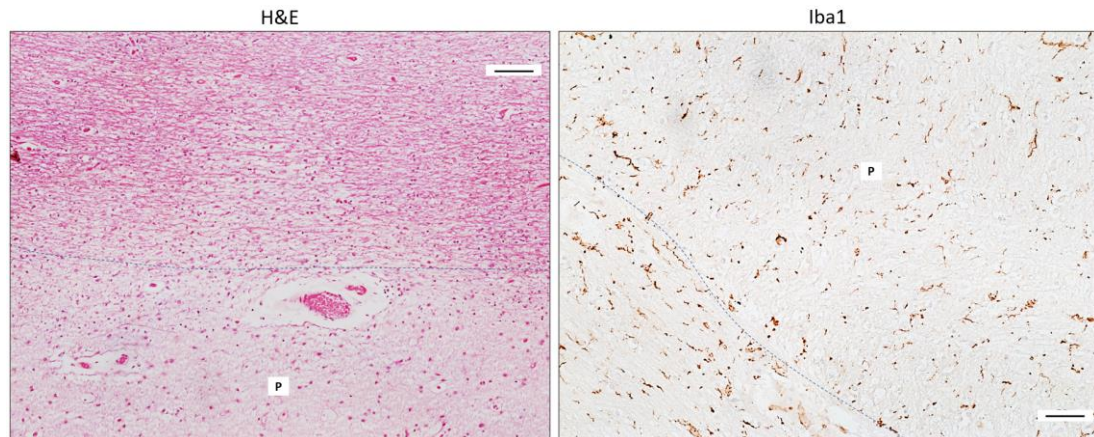


Figure 22: Microglia occupy the demyelinated lesion and surrounding non-demyelinated areas. The demyelinated plaque (P) evident in H&E staining contained Iba1<sup>+</sup> cells in the demyelinated and the surrounding normal appearing areas. Scale bar= 100  $\mu$ m

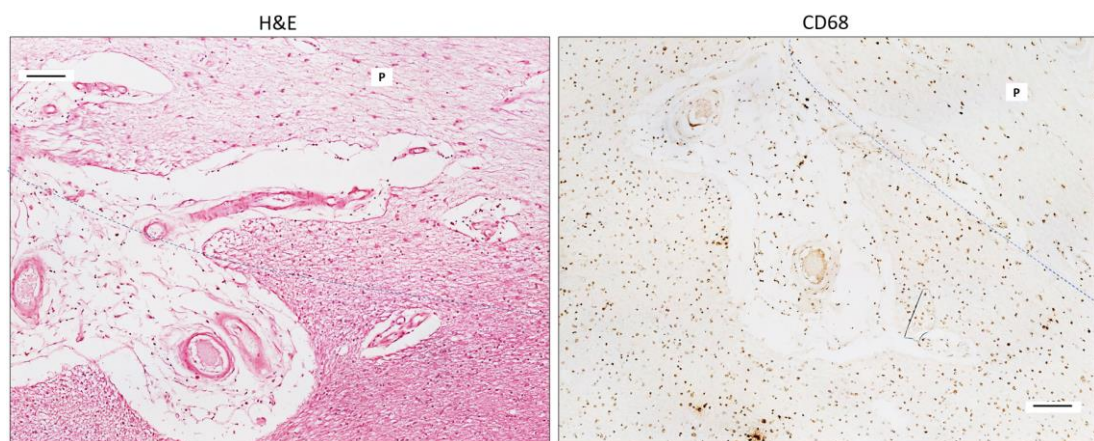


Figure 23: Macrophages occupy the demyelinated lesion and surrounding non-demyelinated areas. The demyelinated plaque (P) evident in H&E staining contained CD68<sup>+</sup> cells in the demyelinated and the surrounding normal appearing areas. Scale bar= 100  $\mu$ m

One of the heavily EBV infected MS cases showed multiple perivascular inflammatory cuffing (Figures 24-27). The inflammatory cuffings were seen in well myelinated areas (Figure 26A), poorly myelinated areas (Figures 24 and 26B) and completely demyelinated areas (Figure 26C). Demyelination was also seen in the

absence of inflammatory perivascular cuffing (Figure 26D). The perivascular cuffing was distinctly made up of CD20<sup>+</sup> B cells, few highly activated Iba1<sup>+</sup> cells and CD68<sup>+</sup> microglia/macrophages (Figure 24). The perivascular cuffing was surrounded by reactive astrocytes and their elongated GFAP<sup>+</sup> fibers and a cluster of amoeboid activated microglia. Unlike B cells, CD3<sup>+</sup> T lymphocytes were part of both the perivascular cuffs and scattered immune infiltrates in the brain parenchyma (Figure 25). Moreover, a large proportion of cells within the perivascular cuffing and diffused in the adjacent parenchyma were proliferating (PCNA<sup>+</sup>) (Figure 27).

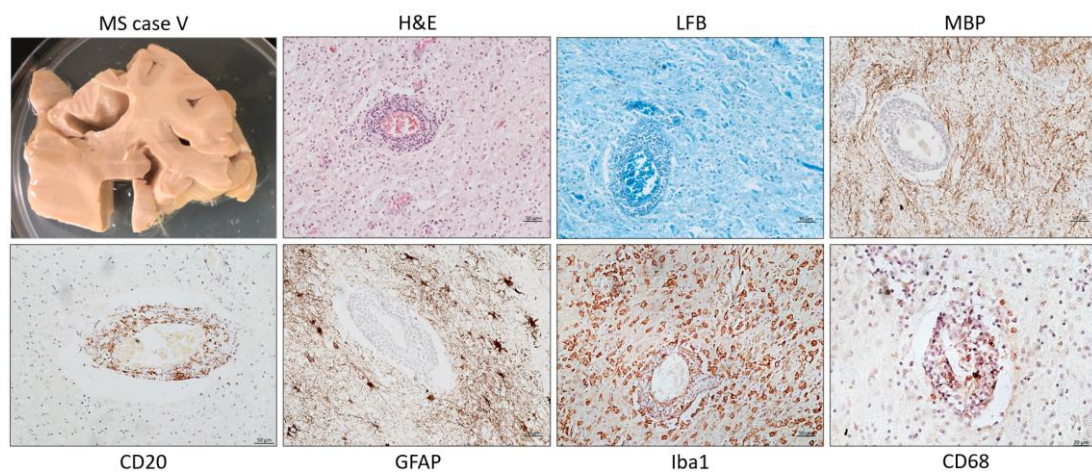


Figure 24: MS case V with inactive and active plaques. Coronal postmortem brain slice from a 32-year-old female with RRMS. The biopsied lesion (P) was evaluated using H&E and LFB staining, and IHC for MBP, CD20, GFAP, Iba1, and CD68. Scale bars= 50 and 20  $\mu$ m

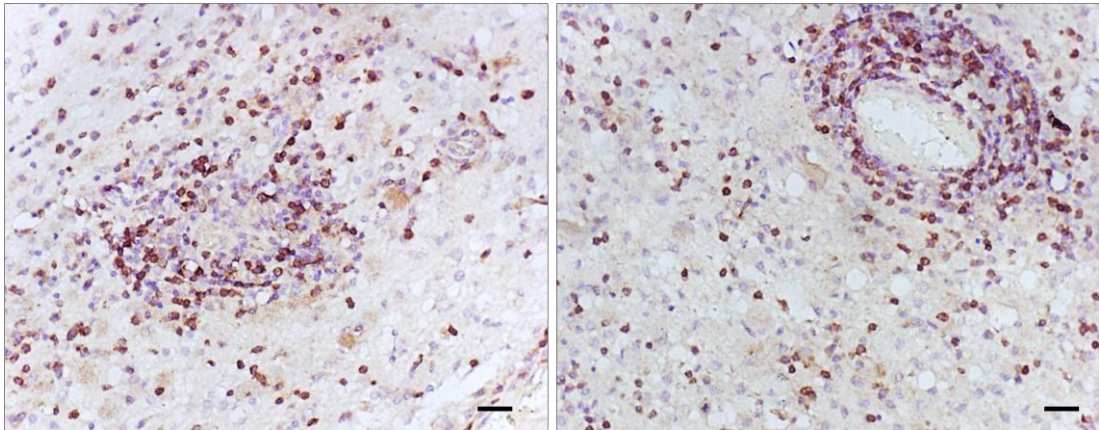


Figure 25: Infiltration of T cells in MS case V. IHC for CD3 in postmortem brain of a RRMS case. Scale bar= 20  $\mu$ m

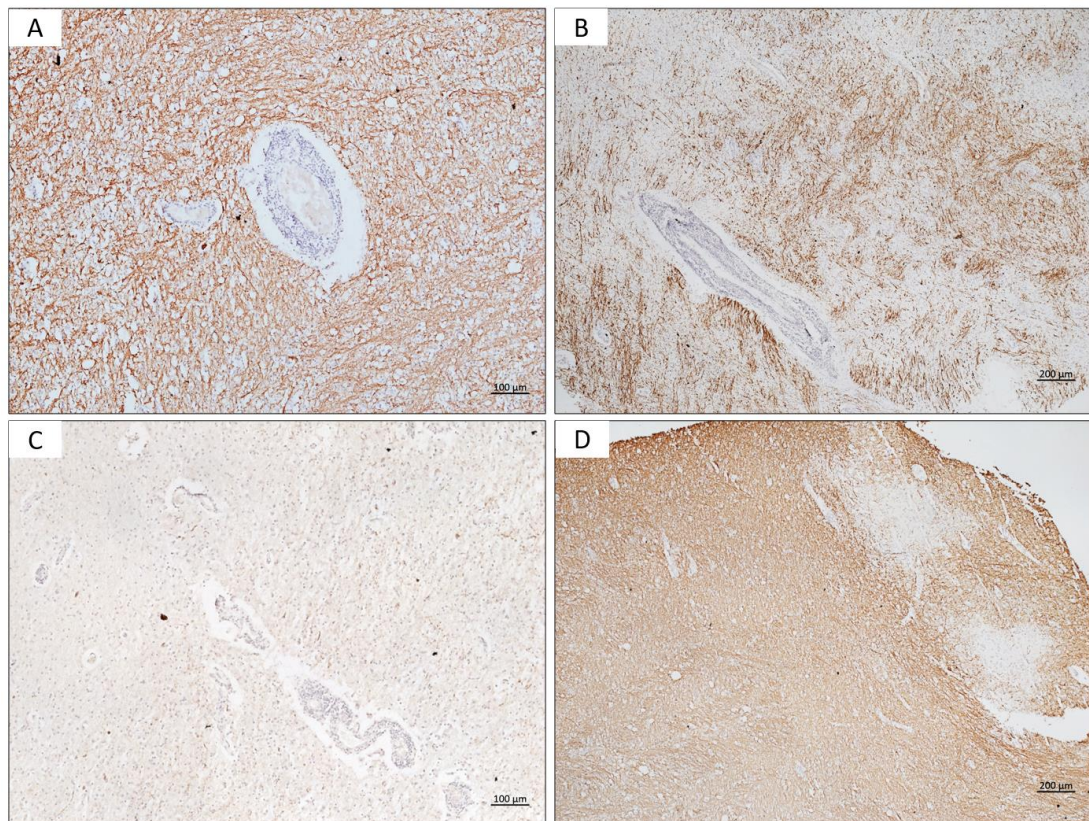


Figure 26: The relationship between demyelination and perivascular cuffing. IHC for MBP was performed to evaluate demyelination in different brain regions. Perivascular cuffing was associated with (A) myelinated, (B) poorly myelinated, and (C) completely demyelinated areas. Demyelination was observed in areas free of perivascular cuffing. Scale bars= 100 and 200  $\mu$ m

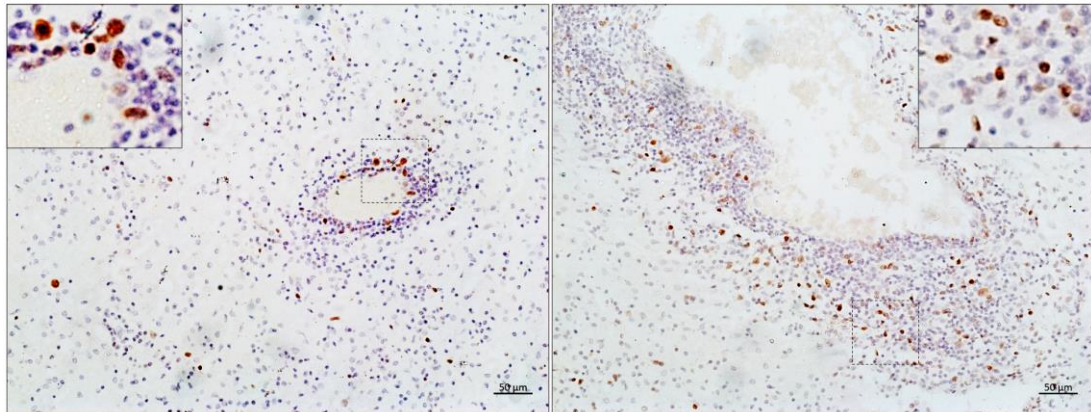


Figure 27: IHC for PCNA in MS case V. Proliferating cells were located in perivascular cuffing and diffused in the adjacent parenchyma. Scale bar= 50 µm

### 3.2 Animal Study

The animal study was carried out in 2 consecutive phases. The first phase examined the potential role of peripheral infection in causing CNS infection. The second phase examined the dynamics of viral infection and associated changes in the periphery and the CNS.

#### 3.2.1 Phase 1: Examining Viral Spread from the Periphery to the CNS

##### 3.2.1.1 EBV Inoculated Rabbits Exhibit Viremia and High Viral Load in the Periphery

The presence of EBV in the brain tissue of MS cases has been reported in several studies (Hassani et al., 2018; Moreno et al., 2018; Serafini et al., 2007; Tzartos et al., 2012). Until now, the events that cause peripheral infection to reach the brain remain poorly understood. In order to determine whether peripheral EBV infection on its own can lead to CNS infection,  $1 \times 10^7$  EBV copies were injected IV into 8 healthy NZW rabbits (EBV group). Animals were sacrificed at day 14 post inoculation.

Previously, it has been shown that injecting rabbits with EBV via IV route results in seroconversion and detectable virus in the PBMCs (Khan et al., 2015). However, EBV level in rabbits blood appear to fluctuate, and virus detectability becomes intermittent. Therefore, additional 9 rabbits were injected with EBV and immunosuppressed using CsA (EBV+CsA group). This treatment should suppress anti-EBV T cell responses and allow increased EBV replication and detection. This also was implemented to increase the likelihood of EBV spreading to the CNS.

None of the 8 animals in EBV group showed irregularities in activity or food consumption that could reflect signs of illness or neurological sequelae during the study period or at autopsy. One of the 9 animals in EBV+CsA group showed changed temperament, decreased activity, and major loss in body weight. To minimize animal suffering, this rabbit was euthanized at day 7, as opposed to the scheduled day 14. At autopsy, the spleen was found to be considerably enlarged with macroscopic white nodules in 4/9 rabbits in EBV+CsA group, but not in any of the 8 animals in the EBV group. EBV infection in the spleen was confirmed by *in situ* hybridization staining for EBV encoded RNAs (EBER-ISH) in all animals inoculated with the virus (Figure 28). No EBER signal was seen in the spleen of control rabbits that were injected with either, PBS or CsA (Figure 28).

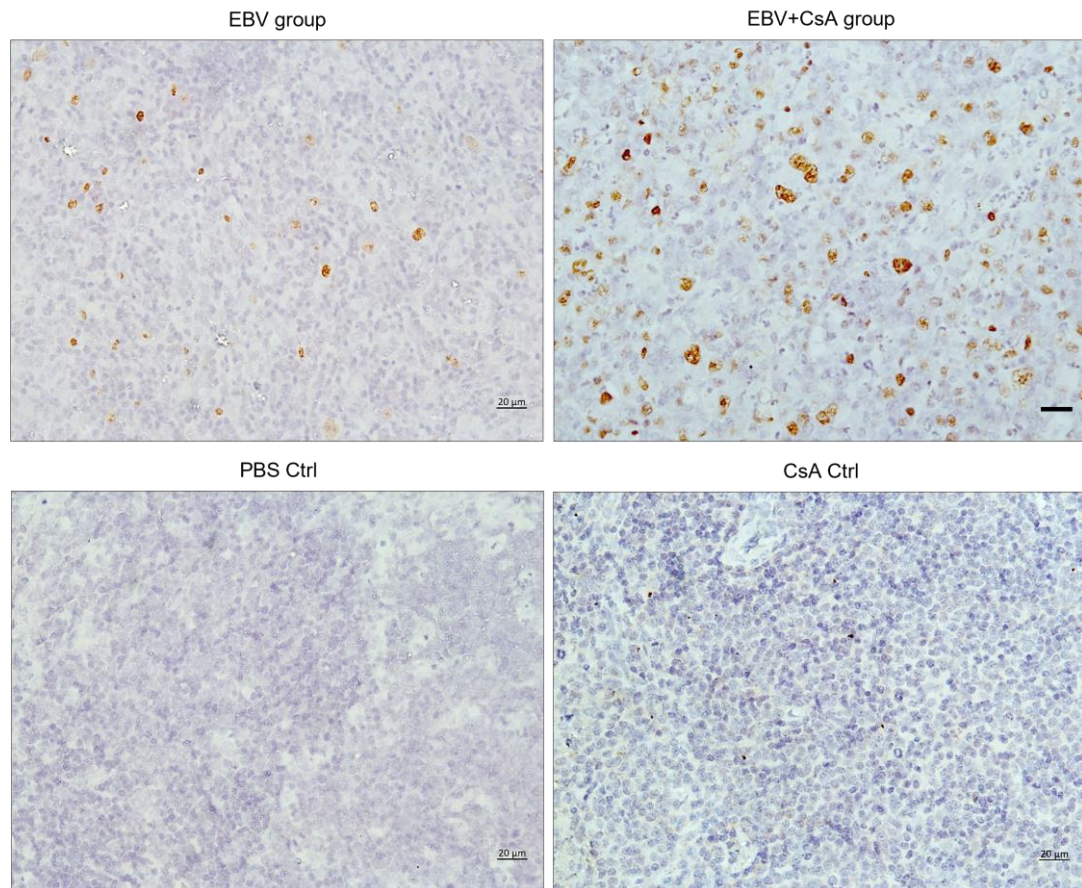


Figure 28: Representative EBER-ISH on rabbit spleen from EBV and EBV+CsA group and their controls. Scale bar=20 µm

gDNA extracted from rabbit spleen and PBMCs was then tested for EBV DNA. Rabbit DNA samples proved to be free of contamination with marmoset DNA (Figure 29A and 29D) and were of PCR amplifiable quality (Figure 29B and 29E). These results confirmed that the marmoset cell line (B95-8) used for the preparation of EBV, did not contaminate the inoculum.

EBV infection in the periphery of rabbits was further supported by the detection of the virus using TaqMan quantitative PCR. EBV genome was detected in the spleen of all rabbits in EBV (Figure 29G) and EBV+CsA (Figure 29H) groups.

Thus, peripheral EBV infection was established in 100% of animals inoculated with EBV, regardless of the immune system status.

Viremia is considered an important event in predisposing to CNS infection (Archibald & Quisling, 2013). Therefore, EBV copy number was quantified in the PBMCs and plasma. All the 8 animals in the EBV group and 8/9 animals in EBV+CsA group had quantifiable, but variable viral load in the PBMCs. The one animal in EBV+CsA group with no detectable virus in the PBMCs, was the animal which was euthanized one week prematurely. This suggests that EBV detectability in peripheral blood may be suboptimal at day 7 as opposed to day 14 post inoculation. None of the PBS/CsA controls had detectable virus.

As for plasma, 75% (6/8) of the animals in the EBV group and 78% (7/9) of EBV+CsA group were viremic (i.e., EBV DNA in plasma) (Figure 29G-H). There was also significant correlation between the levels of viremia and splenic viral load in the EBV group, but not in the EBV+CsA group (Table 7). This implies the interfering effects of immunosuppression on viremia levels. Among the 3 peripheral compartments (plasma, PBMCs and spleen), plasma had the lowest level of EBV DNA (Figure 29G-H). This indicates that lytic shedding of the virus is relatively less frequent, and most of the virus is cell-associated.



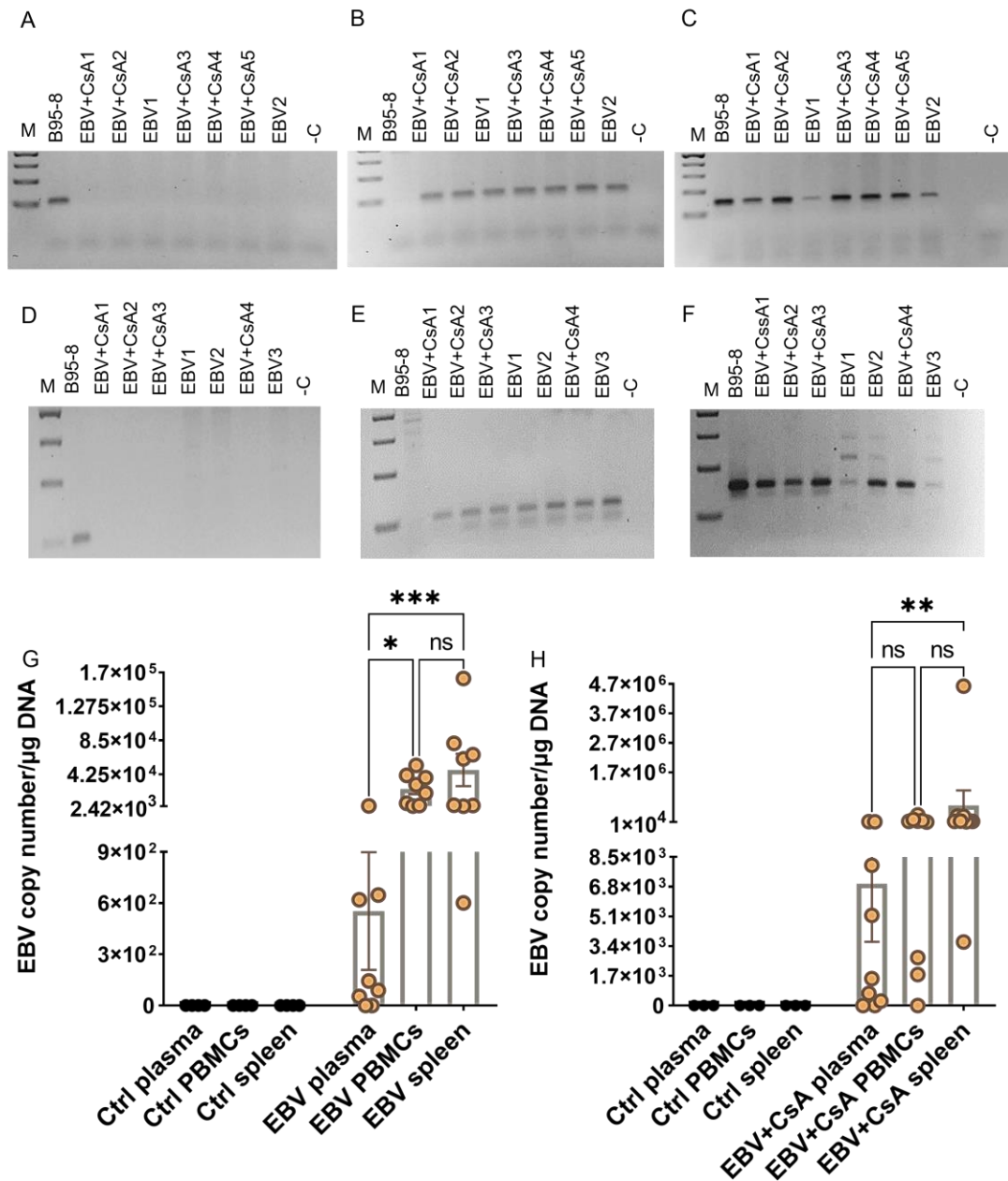


Figure 29: EBV detection in the periphery of EBV inoculated rabbits. Rabbit DNA from the spleen (A) and PBMCs (D) was free of contamination by marmoset DNA as no signal for marmoset  $\beta$ -globin, 104bp, was amplified in any of rabbit samples. Rabbit splenic (B) and PBMCs (E) DNA, but not B95-8 DNA, amplified rabbit-specific GAPDH fragment, 109bp. (C) EBV BamHI fragment, 152bp was readily detectable in 100ng splenic (C) and PBMCs (F) DNA from animals in the EBV and EBV+Csa group. Marmoset B95-8 gDNA was used as a positive control. M; 100bp marker, -C; nuclease free water as a negative control. (G-H) EBV copy number measured using qPCR in plasma, PBMCs, and spleen of rabbits in EBV group ( $n=8$ ) and PBS controls ( $n=4$ ) (G), and EBV+Csa group ( $n=9$ ) and Csa controls ( $n=3$ ) (H). Samples with undetermined EBV levels were plotted at  $y=0$ . EBV load is presented with mean  $\pm$  SEM, and comparisons were made using the nonparametric Friedman test. \*:  $p \leq 0.05$ , \*\*:  $p \leq 0.01$ , \*\*\*:  $p \leq 0.001$

Table 7: The relationship between cell-free EBV load in plasma and viral load in PBMCs and spleen. The Correlation of viremia levels with EBV load in PBMCs and spleen was performed using Spearman correlation for EBV+CsA group and Pearson correlation for EBV group

<b>EBV+CsA group</b>	plasma vs. PBMCs load	plasma vs. spleen load
Spearman r	0.2204	0.147
P (two-tailed)	0.4677	0.6323
<b>EBV group</b>	plasma vs. PBMCs load	plasma vs. spleen load
Pearson r	0.2646	0.7884
P (two-tailed)	0.5265	0.0201

### 3.2.1.2 Inflammatory Cell Aggregates Develop in The CNS Following Peripheral EBV Infection

To evaluate the impact of peripheral EBV infection on the CNS, the brain and spinal cord were examined for histopathological changes. Interestingly, widespread presence of distinct cellular aggregates consisting of inflammatory cells and microglia nodules was observed in the brain and spinal cord of (2/8) EBV and (7/9) EBV+CsA groups (Figure 30). These aggregates were not observed in any of the PBS controls. However, 2/3 CsA controls developed similar CNS aggregates. These observations suggest that peripheral EBV infection can promote neuroinflammation in some hosts, depending on the host genetics and immune system. Immunosuppression can also lead to neuroinflammation, possibly as a result of reactivation of latent infection(s) other than EBV. Additionally, the likelihood of developing neuroinflammation or cellular aggregates in the CNS appear to increase in EBV infected hosts with weakened immune system.

The cellular aggregates in the spinal cord were less frequent and smaller in size than cerebral aggregates (Figure 30). Moreover, the aggregates in the brain were widespread and present throughout the hemisphere, including the cerebrum, the meninges, and the cerebellum (Figure 31A-B). Generally, these cellular aggregates

were associated with CNS vasculature (Figure 31A). The aggregates were found to occur more frequently in the cerebrum than in the cerebellum. The aggregates also formed in both hemispheres (Figure 31C). Collectively, these observations suggest that peripheral EBV infection can lead to immune cells trafficking into the CNS and forming cellular aggregates.

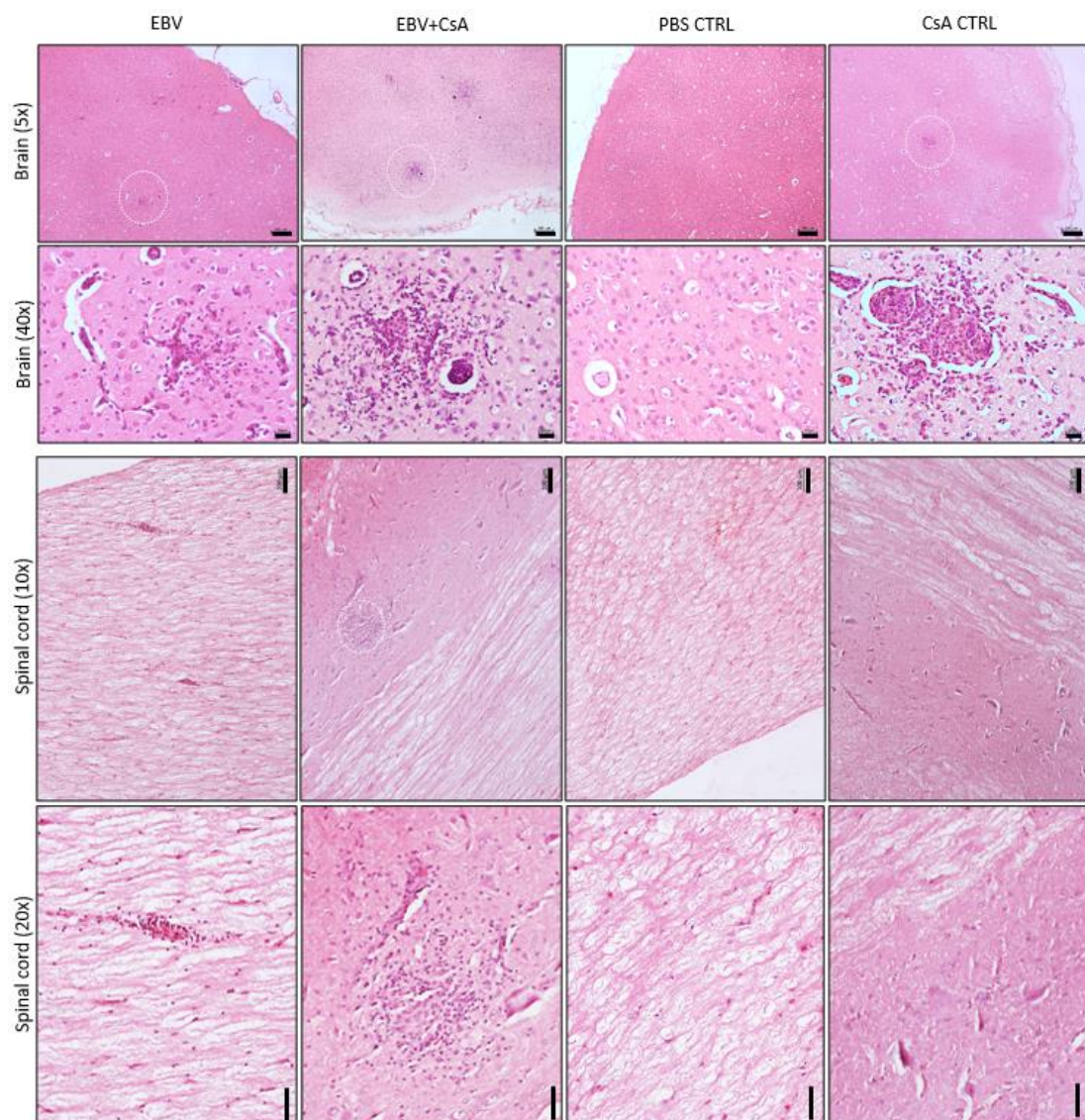


Figure 30: Cell aggregation in the rabbit CNS. H&E staining of formalin-fixed, paraffin-embedded sections of brain and spinal cord harvested from EBV, EBV+CsA and PBS/CsA control groups. Cell aggregation in the brain and spinal cord are encircled. 5× and 40× images of the brain correspond to scale bar of 200 μm and 20 μm, respectively. 10× and 20× images of the spinal cord show scale bar of 100 μm and 50 μm, respectively

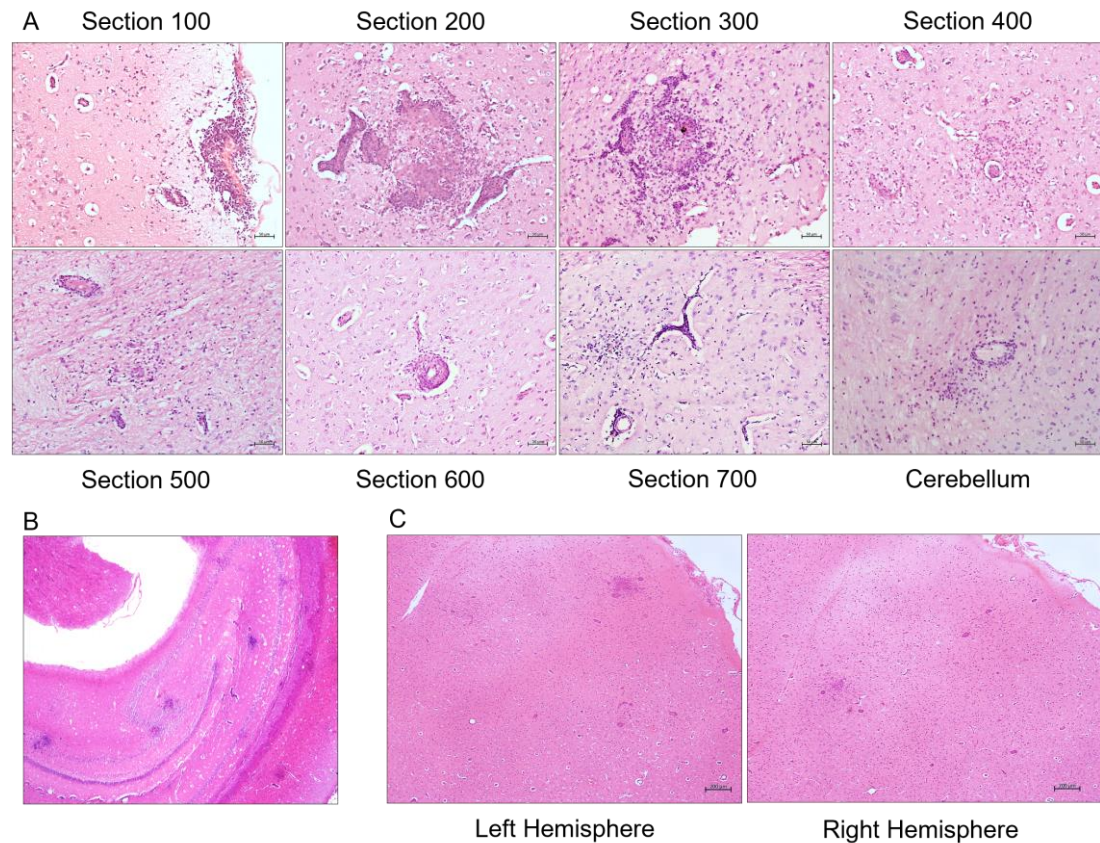


Figure 31: Widespread cerebral aggregates. (A) Representative H&E staining of series of sections from a brain hemisphere with cell aggregates. Scale bar= 50  $\mu$ m. (B) H&E staining of a cerebrum with aggregates at 2.5 $\times$  magnification. (C) Representative H&E staining of left and right hemispheres from the brain of an EBV infected rabbit that developed cerebral aggregates. Scale bar= 200  $\mu$ m

### 3.2.1.3 Inflammatory Cell Aggregates Are Made Up of a Heterogenous Cell Population

To determine the cellular makeup of the CNS aggregates, sections of the brain and spinal cord were immunostained for various cellular markers. In the brain, the cellular aggregates consisted of infiltrating macrophages (RAM11<sup>+</sup>), microglia (Iba1<sup>+</sup>), reactive astrocytes (GFAP<sup>+</sup>), and infiltrating B (CD21<sup>+</sup>) and T lymphocytes (CD3<sup>+</sup>), and neutrophils (Figure 32A). Immunostaining for myelin basic protein (MBP), however, revealed that the myelin became discontinuous in sites where cell

aggregates appeared. Additionally, cells associated with the aggregates were immunoreactive for the proliferation marker, PCNA, and various immune cell markers including CD8, IgG, and EBI2 (Figure 32B). Notably, majority of these infiltrating immune cells were also diffusely scattered in the brain parenchyma (Figure 33). Occasionally, these infiltrating immune cells formed small clusters of loosely connected cells that lacked macrophage aggregation. This implies that aggregates in a given section are at different stages of development/resolution. An example for this heterogeneity is the varying extent of T cell infiltration into different aggregates in one section (Figure 34). Lymphocytes, macrophages, neutrophils and PCNA<sup>+</sup> cells were frequently observed around the brain ventricles (Figure 35). Moreover, the small aggregates formed in the spinal cord contained the same cellular composition of aggregates formed in the brain (Figure 36).

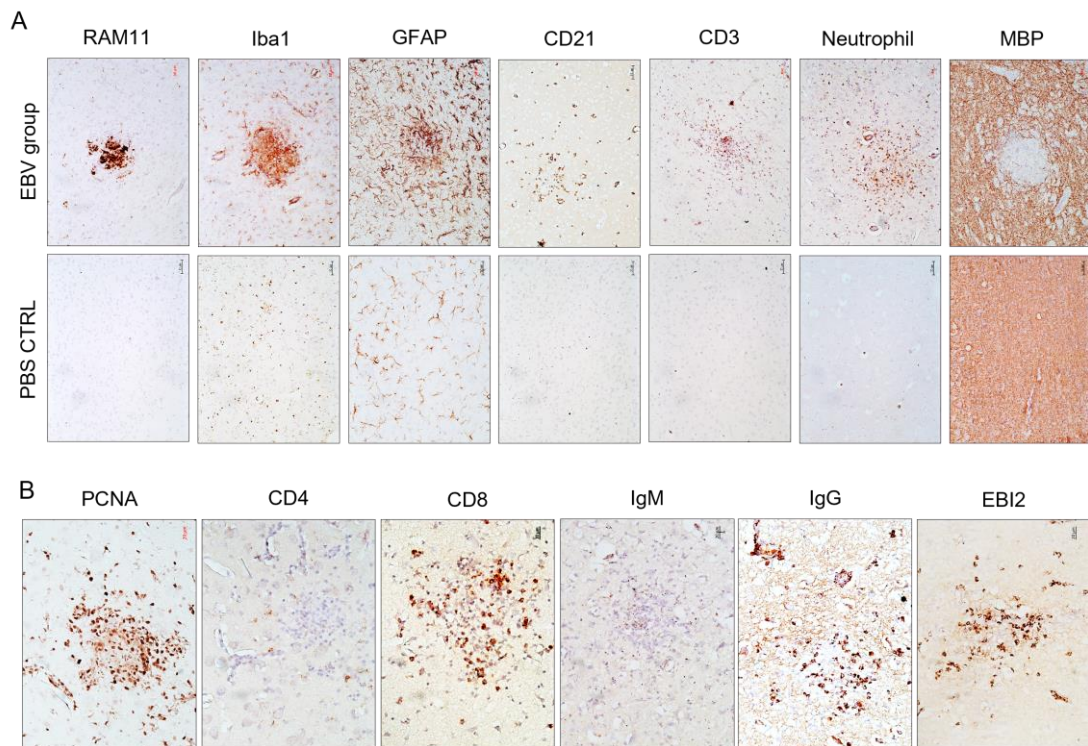


Figure 32: The cellular makeup of cerebral aggregates in EBV infected rabbits. (A) Brain sections from EBV infected rabbits with cerebral aggregates and PBS controls were stained for rabbit-specific macrophage marker RAM11, microglia marker Iba1, astrocyte marker GFAP, B cell marker CD21, T cell marker CD3, and a marker for neutrophils. Staining for myelin basic protein (MBP) was used to evaluate demyelination around cell aggregates. Scale bar=50  $\mu$ m. (B) Additional phenotypic characterization of lymphoid infiltrates by staining for the proliferation marker PCNA, T and B cell markers CD8, IgG, IgM, and Epstein-Barr virus-induced gene 2 (EBI2). Scale bar=20  $\mu$ m

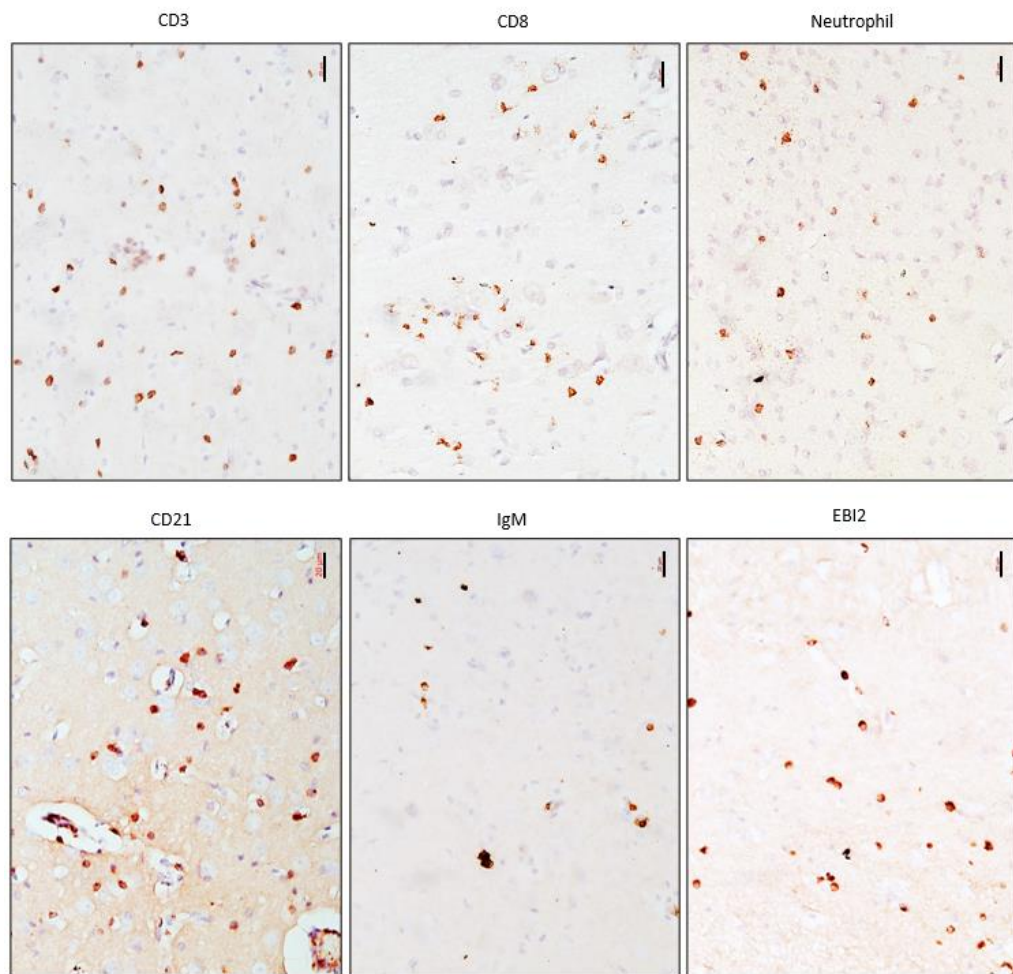


Figure 33: Diffuse infiltrating immune cells in the brain parenchyma. Inflamed brain sections from EBV infected rabbits were stained for CD3, CD8, neutrophils, CD21, IgM and EB12. Scale bar= 20  $\mu$ m

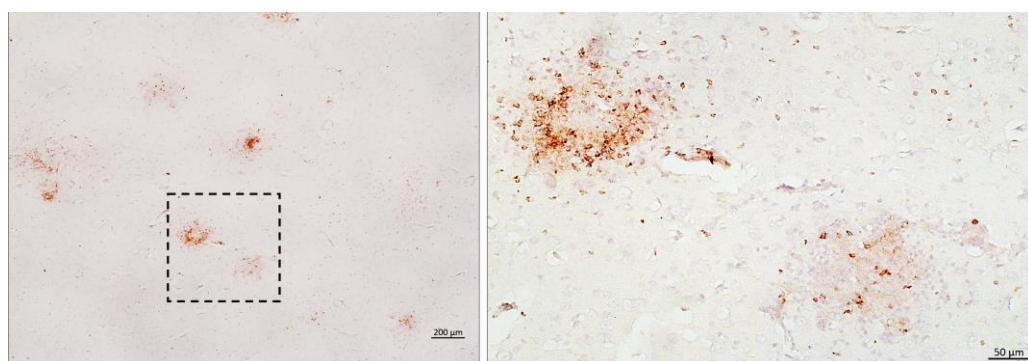


Figure 34: Heterogeneity of cell aggregates in the brain. Inflamed brain section from EBV infected rabbit was stained for CD3. On the left, the dotted square marks the 2 aggregates zoomed in on the right. Scale bar= 200  $\mu$ m in the left-hand image. Scale bar= 50  $\mu$ m in the right hand image

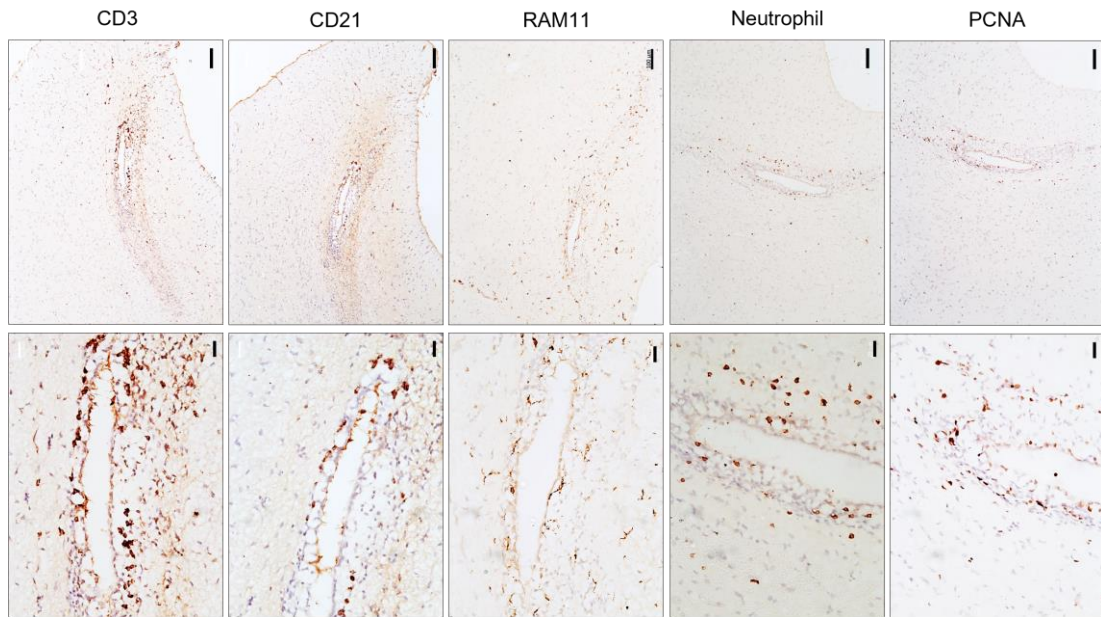


Figure 35: The association of brain ventricles with immune infiltrates. Inflamed brain sections from EBV infected rabbits were stained for CD3, CD21, RAM11, rabbit-specific neutrophil marker, and PCNA. Scale bar= 100  $\mu\text{m}$  (for the top panel), and 20  $\mu\text{m}$  (for the bottom panel)

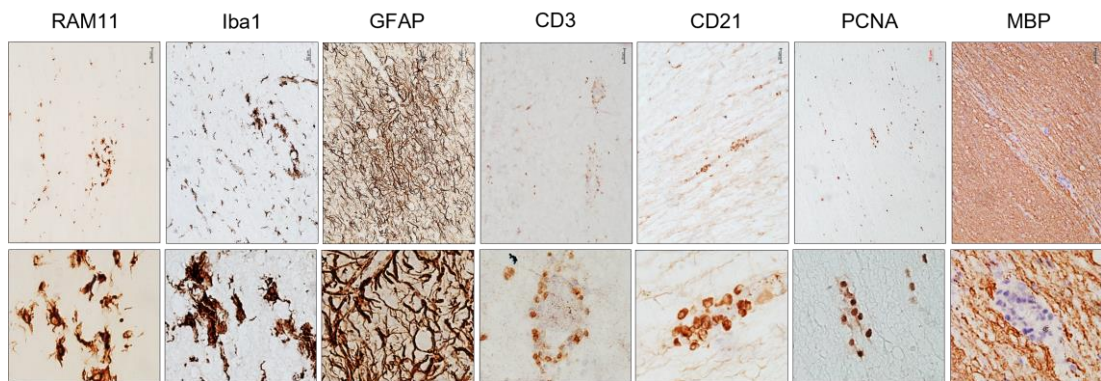


Figure 36: The cellular makeup of spinal cord inflammatory infiltrates in EBV infected rabbit. FFPE spinal cord sections were stained with rabbit-specific macrophage marker RAM11, microglia marker Iba1, astrocyte marker GFAP, T cell marker CD3, B cell marker CD21, proliferation marker PCNA and MBP. Scale bar= 50  $\mu\text{m}$



Using multiple immunofluorescence staining, the spatial relationship between different cells making up the aggregates was studied. While blood-derived macrophages (RAM11<sup>+</sup>) appeared to make up the center of most, if not all, CNS aggregates, astrocytes (GFAP<sup>+</sup>) were mainly located at the border of the aggregates (Figure 37, 1<sup>st</sup> row). Some aggregates at a different development stage contained a center of activated microglia (Iba1<sup>+</sup>), astrocytes (GFAP<sup>+</sup>) and diffuse B lymphocytes (CD21<sup>+</sup>) (Figure 37, 2<sup>nd</sup> row). Most of the aggregates with a center of macrophage/microglia (RAM11<sup>+</sup>/Iba1<sup>+</sup>) had scattered B lymphocytes (CD21<sup>+</sup>) at the outer part of the aggregates (Figure 37, 3<sup>rd</sup> row). Many of these B lymphocytes were found to be proliferating (PCNA<sup>+</sup>) (Figure 37, 4<sup>th</sup> row).

The impact of aggregate formation on myelin integrity was also examined. In the brain, aggregation of macrophages was observed to coincide with discontinuity of myelin (Figure 38A). The outer part of the aggregate, where reactive astrocytes gather, also exhibited some signs of myelin breakdown (Figure 38B). Comparable to aggregates in the brain, aggregates in the spinal cord were also associated with myelin discontinuity (Figure 38C-D). Moreover, aggregate-associated myelin disruption occurred both in the white matter and grey matter (Figure 38).

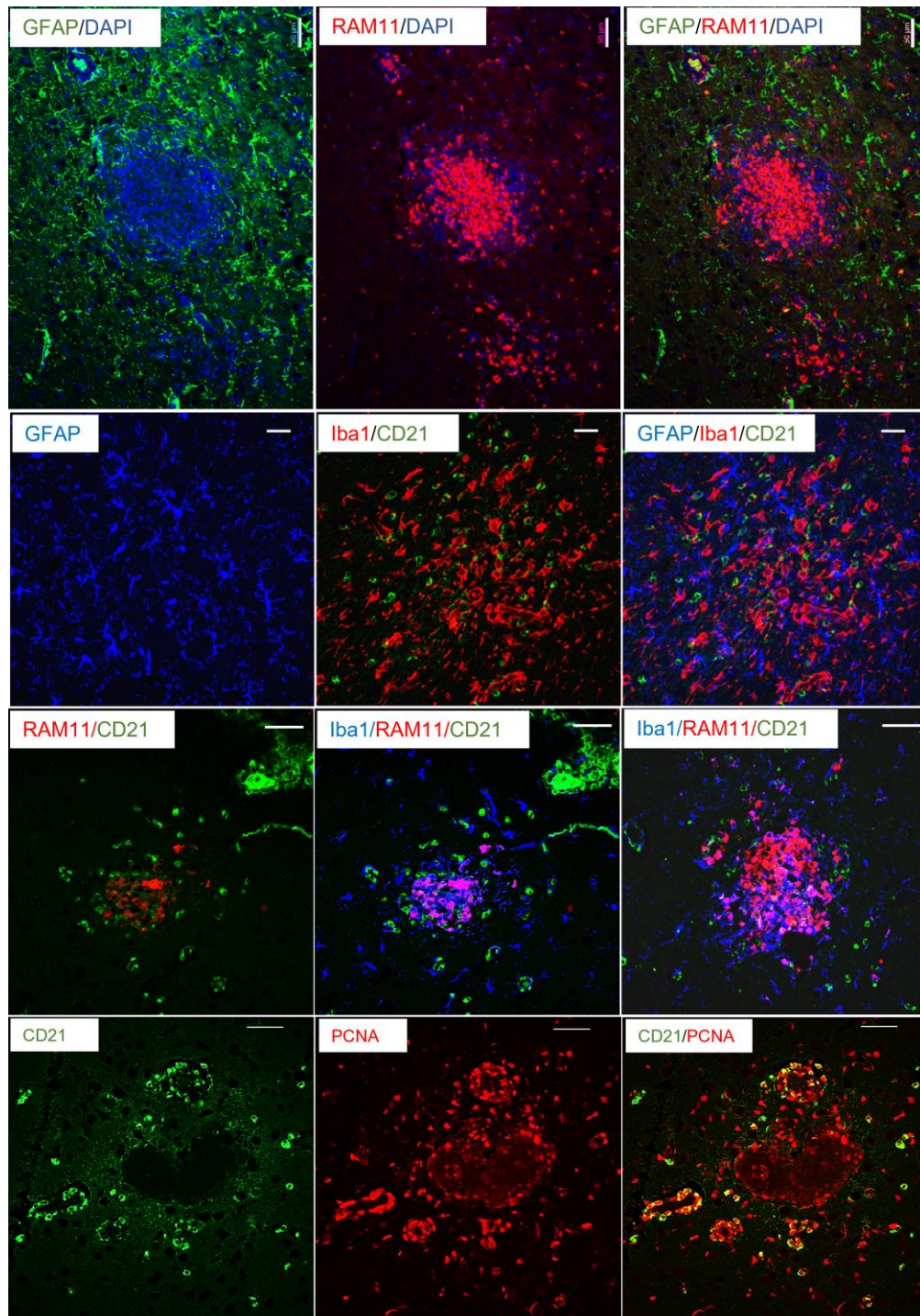


Figure 37: Spatial relationship between the different cells making up the aggregates. First row: Immunofluorescence staining of inflamed brain section with GFAP (green), RAM11 (red), and DAPI (blue). Scale bar=50  $\mu$ m. Second row: Immunofluorescence staining of inflamed brain section with GFAP (blue), Iba1 (red), and CD21 (green). Scale bar=20  $\mu$ m. Third row: Location of B cells (green) in relation to macrophages (red)/ microglia (blue) was identified by staining for CD21, RAM11 and Iba1, respectively. Scale bar=40  $\mu$ m. Fourth row: Double positive CD21 (green) and PCNA (red) depict proliferating B lymphocytes in cerebral aggregates. Scale bar=40  $\mu$ m

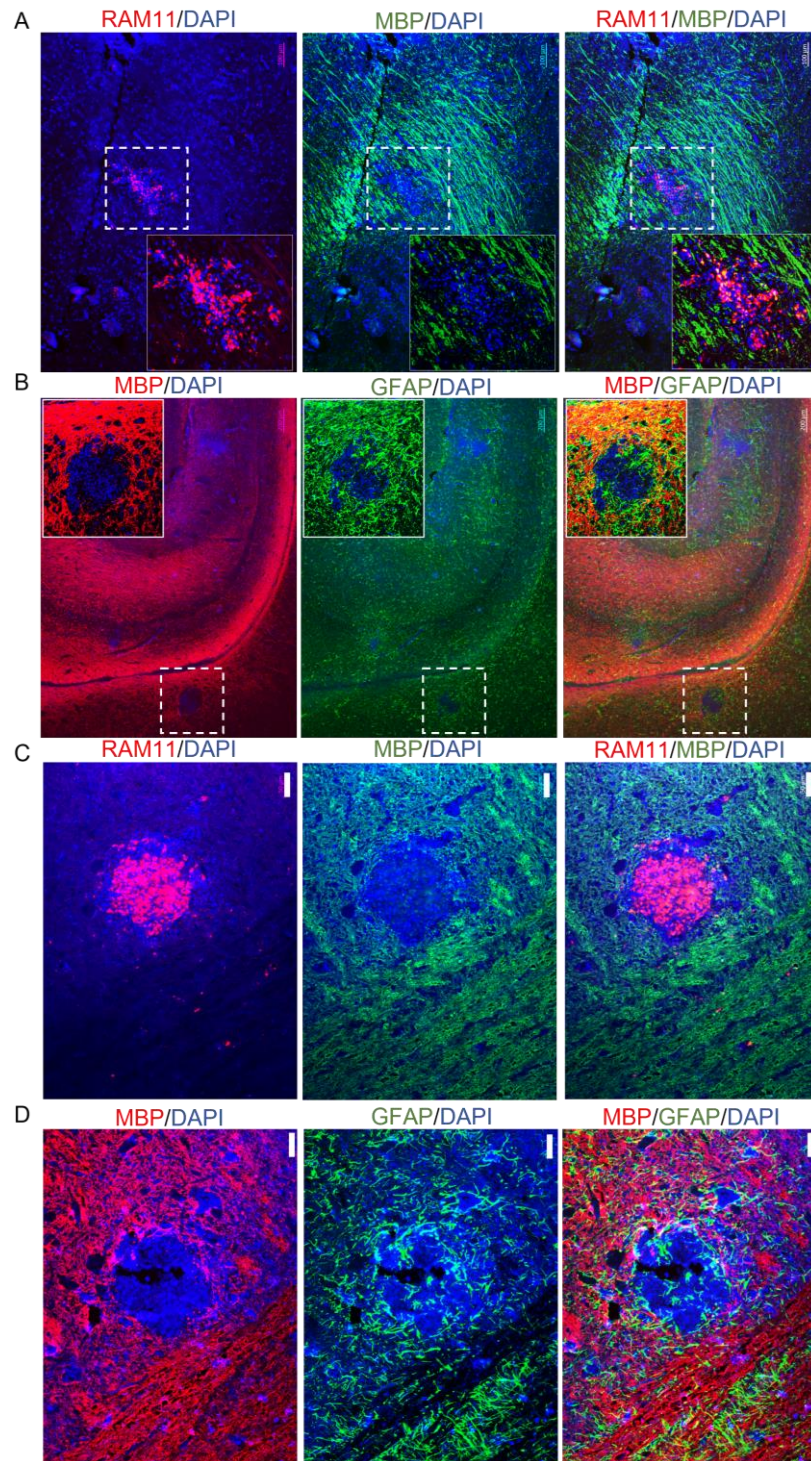


Figure 38: The impact of aggregate formation on myelin integrity in the CNS. (A) Immunofluorescence staining of inflamed brain section with RAM11 (red), MBP (green), and DAPI (blue). Scale bar=100  $\mu\text{m}$ . (B): Immunofluorescence staining of inflamed brain section with MBP (red), GFAP (green), DAPI (blue). Scale bar=200  $\mu\text{m}$ . (C) Immunofluorescence staining of a longitudinal section of inflamed spinal cord for RAM11 (red), MBP (green), and DAPI (blue). Scale bar=50  $\mu\text{m}$ . (D) Immunofluorescence staining of a longitudinal section of spinal cord for MBP (red), GFAP (green), and DAPI (blue). Scale bar=50  $\mu\text{m}$

#### **3.2.1.4 EBV Infected Cells Infiltrate the Brain of Both Immunocompetent and Immunosuppressed Animals**

EBV infection of the brain has been previously reported in MS cases (Angelini et al., 2013; Hassani et al., 2018; Magliozzi et al., 2013; Moreno et al., 2018; Serafini et al., 2007, 2019; Veroni et al., 2018). Thus, the possibility that primary peripheral infection can lead to infection of the brain was examined. Brain sections, from EBV and EBV+CsA groups and PBS/CsA controls, were stained for EBV encoded RNAs; EBERs, using EBER-ISH. EBER<sup>+</sup> cells were detected in the brain of 6/8 animals in the EBV group, and 9/9 in the EBV+CsA group, independent of the presence of cellular aggregates (Figure 39A). EBV infected cells were not seen in any of the PBS/CsA controls (Figure 39A).

In addition to EBERs, EBV infected cells expressed the latent proteins EBNA1 (Figure 39B) and EBNA2 (Figure 39C), and occasionally the immediate early lytic protein BZLF1 (Figure 39D). The distribution of transcriptionally active virus in the brain was also examined by staining a series of sections with anti-EBNA1. EBNA1<sup>+</sup> cells were seen dispersed throughout the brain. (Figure 39B). Remarkably, massive infiltration of EBNA1<sup>+</sup> cells took place in the granular layer of the cerebellum (Figure 39B). These findings indicate that primary peripheral EBV infection can be a sufficient event for EBV infected cells to infiltrate the CNS.

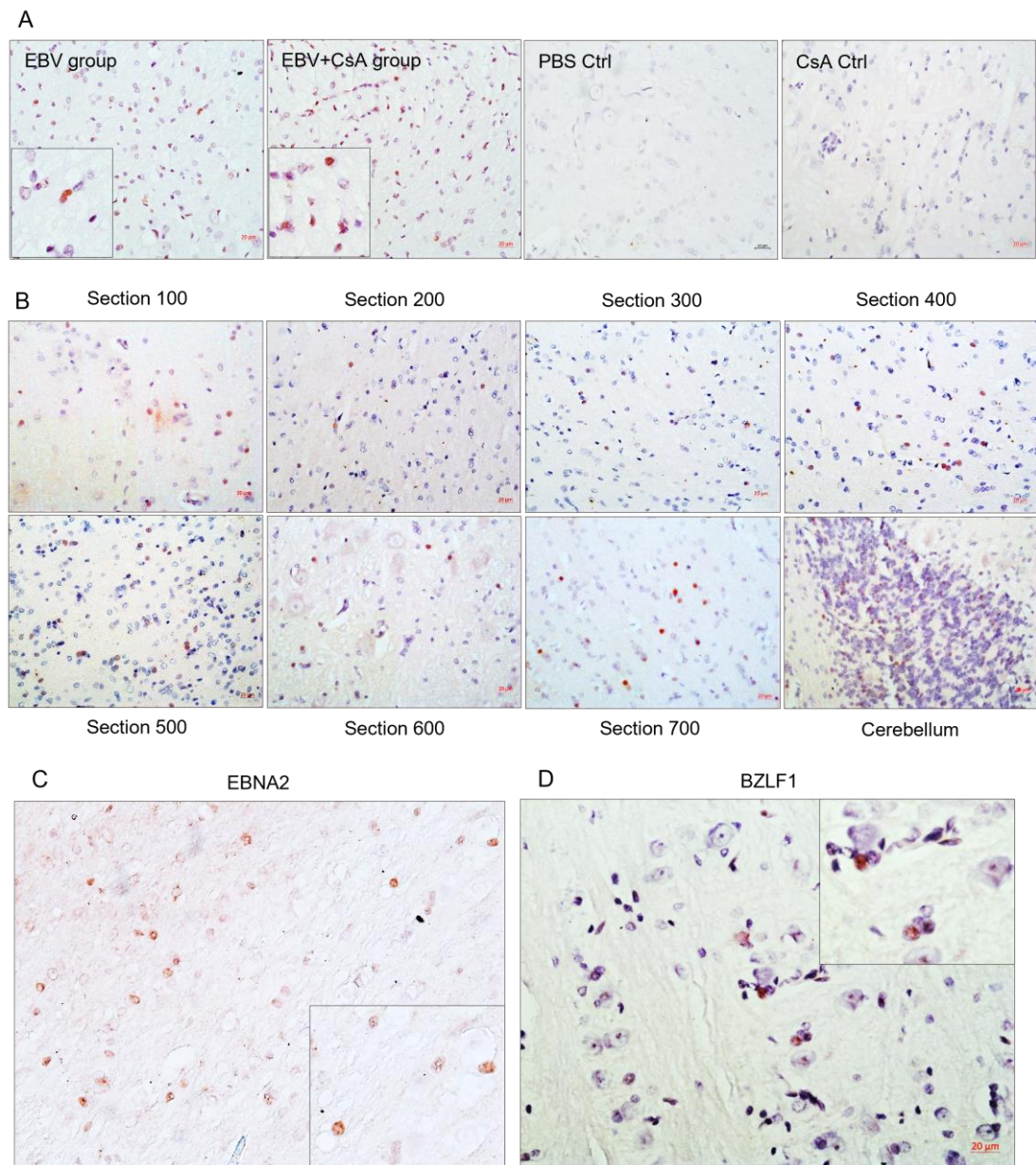


Figure 39: The infiltration of EBV infected cells into the brain. (A) Representative images of EBER-ISH on brain sections from EBV and EBV+C&A groups and their corresponding PBS/C&A controls. Scale bar=20  $\mu$ m. (B) Immunohistochemistry for EBNA1 in a series of sections from a heavily infected cerebral hemisphere and cerebellum. Scale bar=20  $\mu$ m. (C) Immunohistochemistry for EBNA2 in a heavily infected brain section. (D) Immunohistochemistry for EBNA2 in a heavily infected brain section. Scale bar=20  $\mu$ m

In humans, EBV is primarily carried by circulating IgD<sup>-</sup> CD27<sup>+</sup> isotype-switched memory B cells (Hochberg et al., 2004; Joseph et al., 2000). In the brain of MS cases, EBV was found to be carried by CD20<sup>+</sup> B cells, and GFAP<sup>+</sup> astrocytes and Iba1<sup>+</sup> microglia (Hassani et al., 2018; Serafini et al., 2010). To determine which cells are infected with EBV in the rabbit brain, double staining for EBERs and several cellular markers was performed. Although EBV infected cells were seen in close vicinity to Iba1<sup>+</sup> microglia, GFAP<sup>+</sup> astrocytes, and RAM11<sup>+</sup> macrophages, these cells did not appear to make the main cellular target for EBV infection in the brain (Figure 40A). However, many EBV positive cells were found to be either IgM<sup>+</sup> or IgG<sup>+</sup> cells (Figure 40B-C).

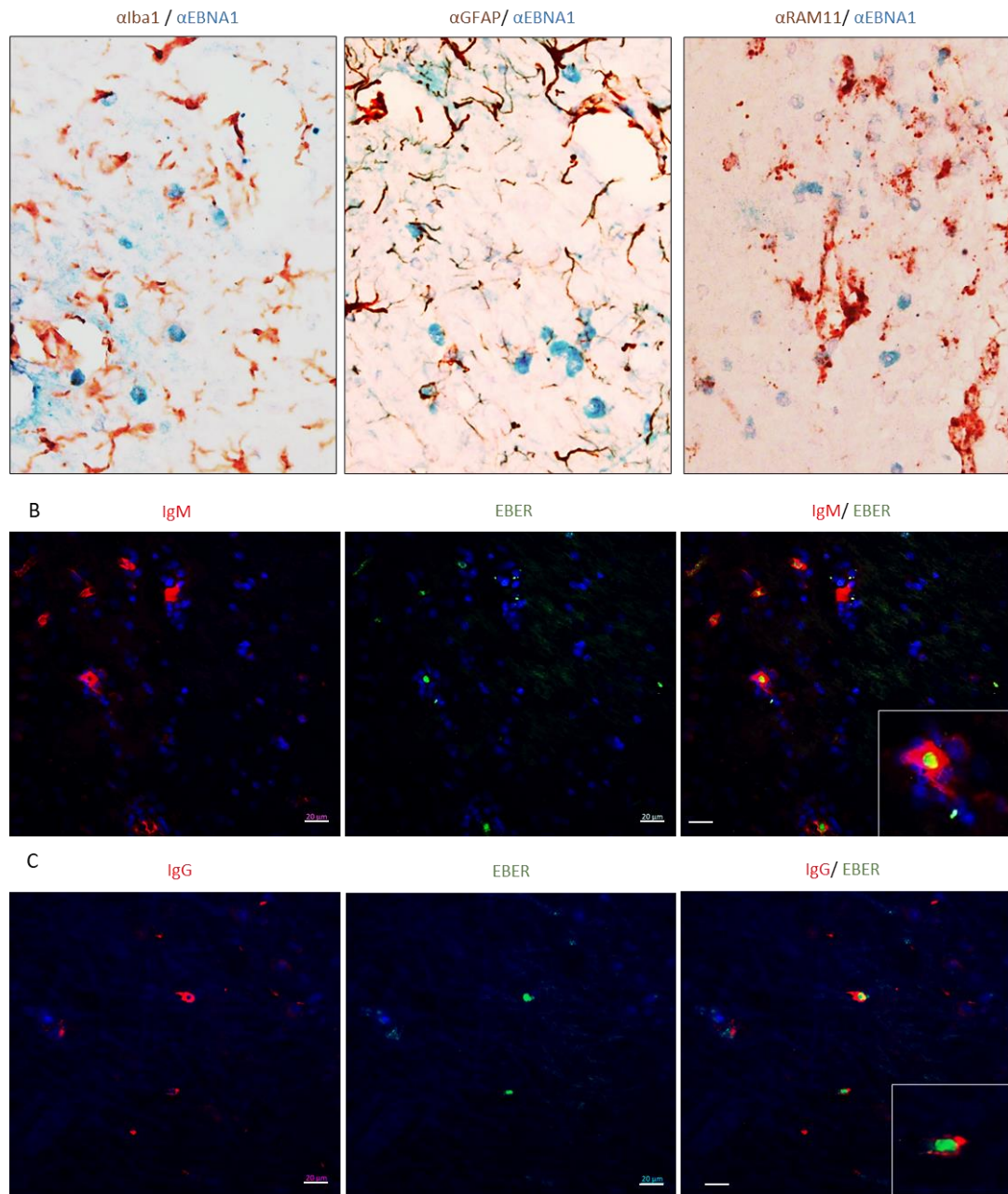


Figure 40: The phenotype of EBV infected cells in the brain. (A) Double staining for viral EBNA1 (blue) and either Iba1, GFAP, or RAM11 (brown). Scale bar=20  $\mu$ m. (B) Double staining for IgM (red) and viral EBER (green). Scale bar= 20  $\mu$ m. (C) Double staining for IgG (red) and viral EBER (green). Scale bar= 20  $\mu$ m

### **3.2.2 Phase 2: Investigating the Dynamics of EBV Infection Over Time**

#### **3.2.2.1 EBV Load Peaks at Day 14 Post Infection in Peripheral and CNS Compartments**

To evaluate infection dynamics and delineate changes in the incidence of CNS aggregates over time, a new batch of rabbits was IV inoculated with EBV and blood, spleen, brain, and spinal cord were harvested and examined at 5 time points; 3, 7, 14, 21 and 28 days post infection (dpi). Three animals were examined at each of the time points.

In the peripheral compartment, EBV was detected in the PBMCs at all time points (Figure 41A). In the spleen, however, the virus reached detectable levels by day 7 and remained detectable throughout the next 3 time points (Figure 41A). Interestingly, EBV in the plasma (indicative of viremia) could not be detected until 14 and 21dpi. As for the CNS, the virus started to become detectable in the brain by day 7 and remained detectable throughout the next 3 time points (Figure 41B). However, EBV was detected in both the brain and spinal cord simultaneously between 7 and 21dpi (Figure 41B).

Notably, the frequency of EBV detection peaked at day 14, as all 3 animals (100%) sacrificed at this time point had detectable virus. Additionally, animals at this time point exhibited significantly elevated virus load in the plasma, PBMCs, spleen and brain (Figure 41). Thus, day 14 was the optimal time point for virus detection in both the periphery and CNS.

To investigate if EBV level in the periphery is associated with CNS infection, the correlation of viral load in the spleen and blood with that in the CNS was assessed. EBV DNA load in the brain correlated significantly with both splenic and PBMCs viral load (Table 8). However, EBV load in the spinal cord correlated only moderately



with EBV levels in the plasma (viremia) (Table 8). Thus, EBV load in the PBMCs and secondary lymphoid organs, may be a determinant for virus infection of the brain. This also highlights the importance of cell-associated virus, rather than free virus (virus in the plasma), in EBV trafficking to the brain. In other words, the virus reached the brain most probably via “Trojan horses” mechanism by travelling via infected B cells.

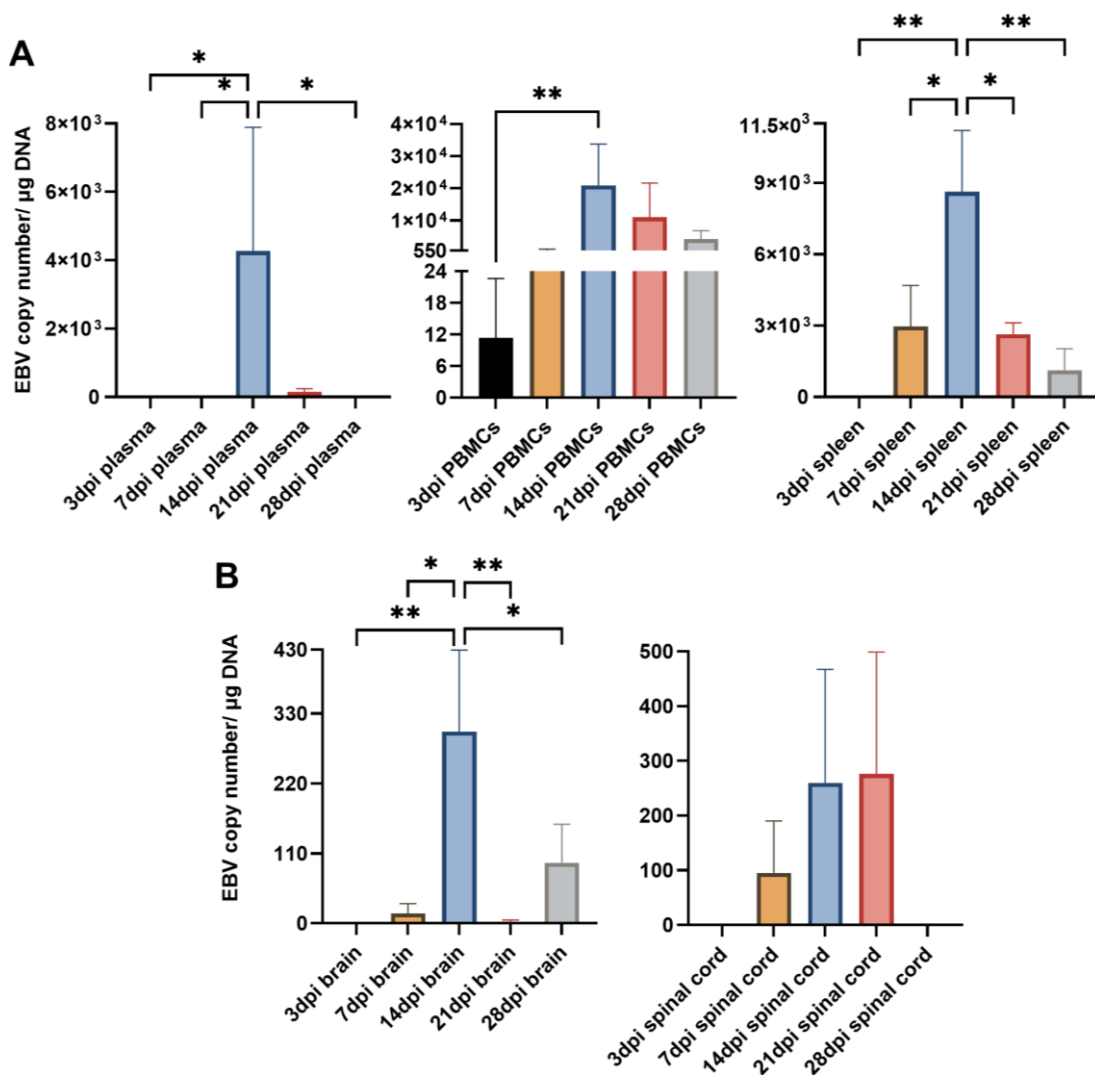


Figure 41: EBV load in the periphery and CNS at different time points. (A) EBV DNA copy number in the peripheral compartments; plasma, PBMCs and spleen. (B) EBV DNA copy number in the CNS; the brain and spinal cord. EBV copy number was determined by TaqMan qPCR at 3, 7, 14, 21 and 28dpi (n=3 rabbits/time-point) and displayed as mean  $\pm$  SEM. Comparison between groups was performed using One-Way ANOVA and non-parametric Kruskal-Wallis test. \*:  $p \leq 0.05$ , \*\*:  $p \leq 0.01$

Table 8: Spearman correlation of EBV load in the CNS and viral load in the peripheral compartments (plasma, PBMCs and spleen). Correlation coefficient ( $r$ ) and  $p$  values are indicated

	<b>EBV load in the brain vs. EBV load in plasma</b>	<b>EBV load in the brain vs. EBV load in PBMCs</b>	<b>EBV load in the brain vs. EBV load in spleen</b>
Spearman $r$	0.4128	0.686	0.7212
P (two-tailed)	0.1278	0.0065	0.0037
	<b>EBV load in the spinal cord vs. EBV load in plasma</b>	<b>EBV load in the spinal cord vs. EBV load in PBMCs</b>	<b>EBV load in the spinal cord vs. EBV load in spleen</b>
Spearman $r$	0.5582	0.2499	0.3797
P (two-tailed)	0.0202	0.3655	0.1623

### 3.2.2.2 CNS Aggregates Occurs More Frequently at Day 14 and 21 of Infection

Next, coronal sections of the brain and cross sections of the spinal cord were examined for the presence of inflammatory aggregates at 3, 7, 14, 21, and 28dpi. Mild inflammation was observed in the meninges and around blood vessels in the brain of infected animals. However, distinct cellular aggregates were readily detected in the brain and spinal cord of animals sacrificed at days 14 and 21 (Figure 42). Again, the aggregates in the spinal cord were smaller in size compared to the aggregates observed in the corresponding brain.

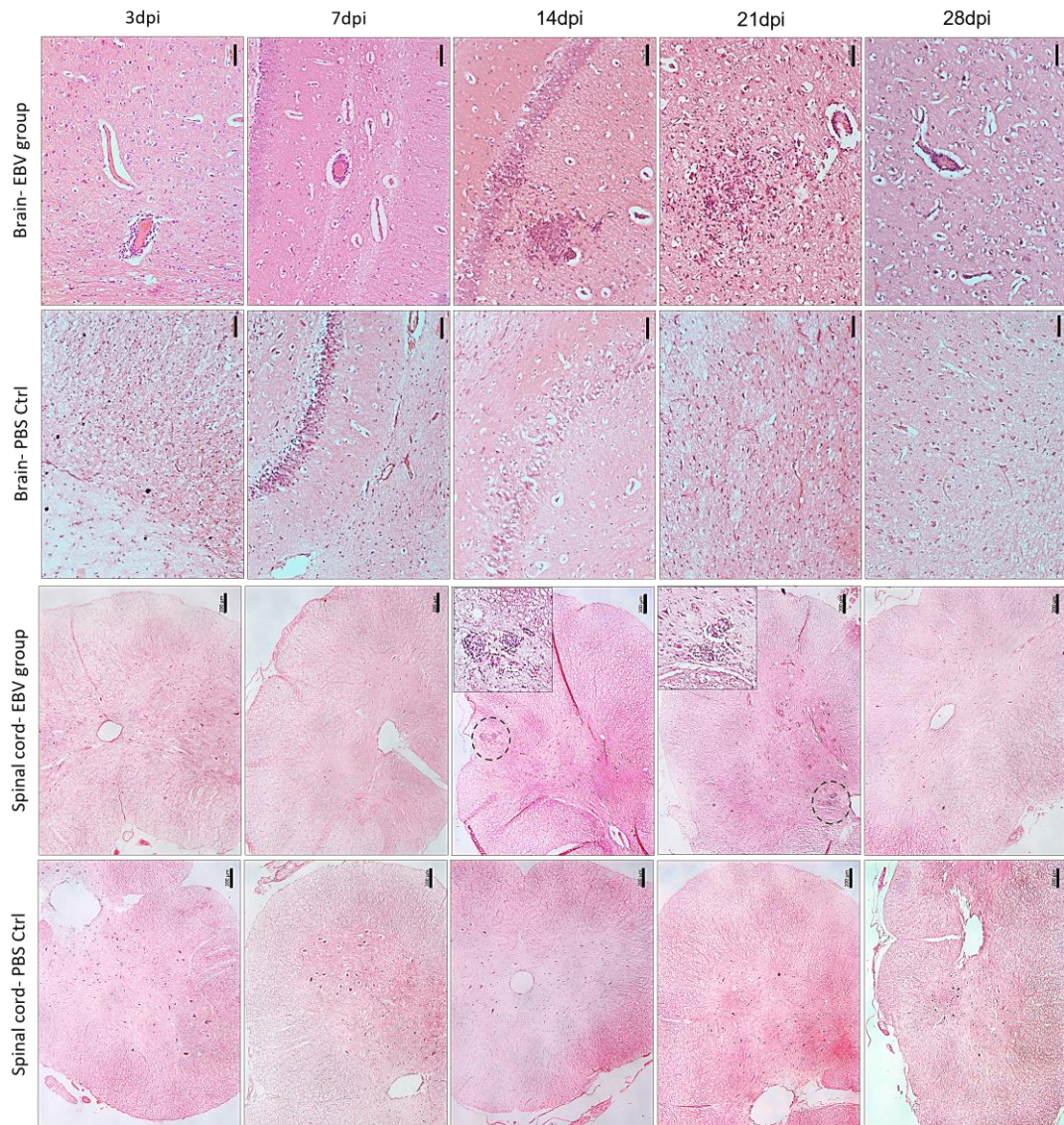


Figure 42: CNS aggregate formation peaks at 14 and 21dpi. Representative images of H&E staining of coronal brain sections (scale bar= 50  $\mu$ m) and cross sections of spinal cord (scale bar= 200  $\mu$ m) from EBV group and PBS control group (PBS Ctrl) sacrificed at 3, 7, 14, 21 and 28dpi

To determine if there was a difference in the number of cerebral aggregates at different time points, a thousand 5- $\mu$ m brain sections from each of the 3 animals at each of the five time points were cut and stained for histopathological examination. Aggregates were counted in sections at intervals of 50. The fact that aggregates were observed to have great heterogeneity in morphology, for the purpose of counting, an

aggregate in the brain parenchyma was defined as a clear continuous cluster of cells that is at least 60  $\mu\text{m}$  in diameter. The term aggregate also included any 2 cellular clusters that were connected by a thread of infiltrates. Thus, meningeal infiltrates, small vessels engorged with lymphocytes, clusters or perivascular cuffs that are less than 60  $\mu\text{m}$  in diameter, were not counted.

One out of 3 animals sacrificed at day 3 developed aggregates in the brain. Detection of these aggregates in series of sections was relatively infrequent, and when detected it was limited in number to less than 3 at best. On average, this animal developed 0.2 aggregates/0.5  $\text{cm}^2$  section. None of the 3 animals sacrificed at day 7 had detectable aggregates in the series of sections examined (Figure 43A). At day 14, 1 out of 3 animals developed aggregates in the brain. This animal had on average 2 aggregates/0.5  $\text{cm}^2$  section. At day 21, 2 out of 3 animals developed aggregates in the brain, with an average number of 1.6 aggregates/0.5  $\text{cm}^2$  section. None of the animals sacrificed at day 28 had aggregates in any of the brain sections examined (Figure 43A). Collectively, the number of aggregates in the brain reached the peak at days 14 and 21 post infection (Figure 43A).

Next, peripheral and CNS viral loads were compared between animals that developed CNS aggregates and those without aggregates. Animals with aggregates had significantly elevated levels of EBV DNA in PBMCs compared to animals without aggregates (Figure 43B). No significant difference was found in viral load in the other compartments between animals that developed aggregates and those that did not. This reflects a link between the level of cell-associated virus, but not free virus, in the peripheral blood and the presence of CNS cellular aggregates. This also indicates that viremia may not be a determinant for the development of these structures in the CNS.

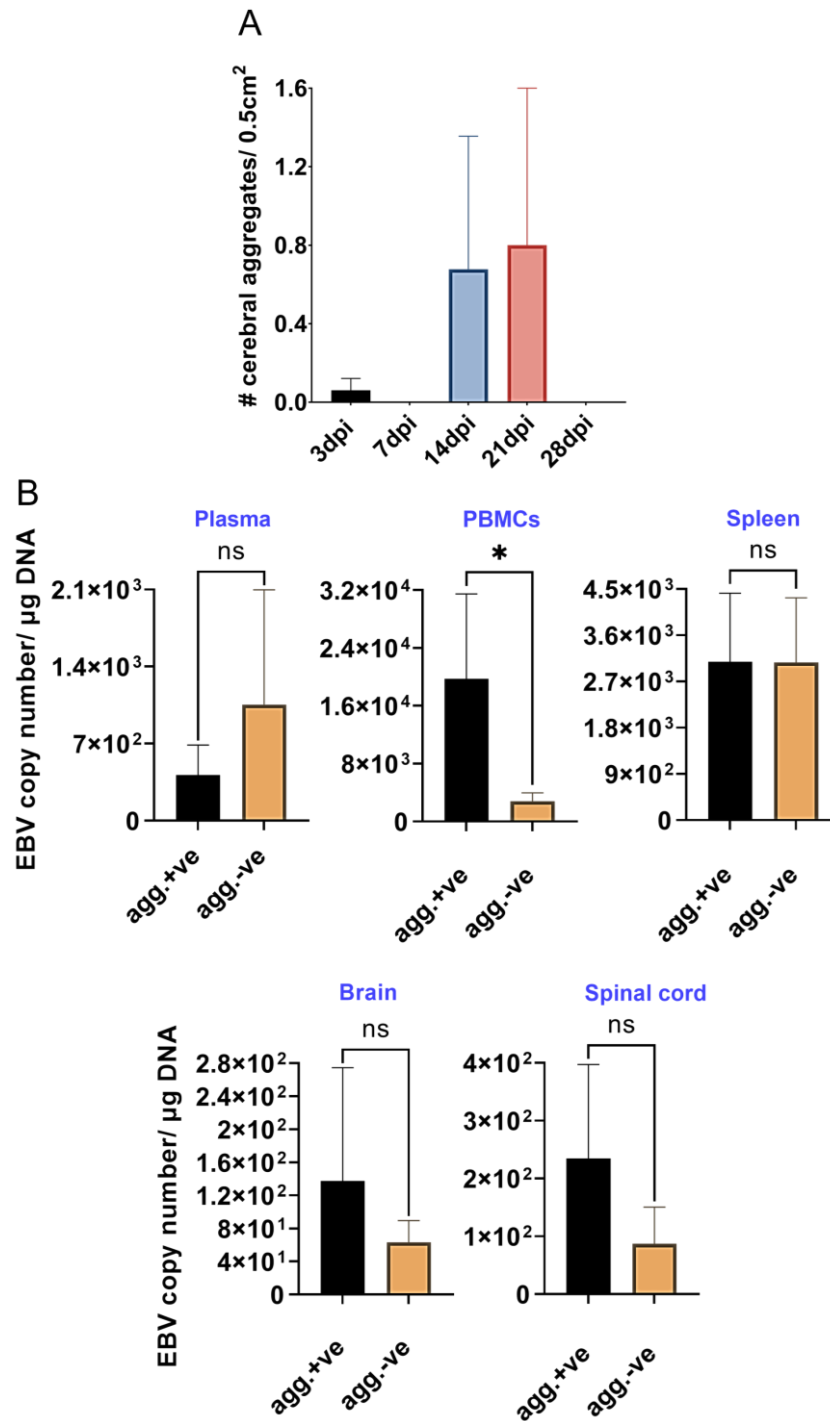


Figure 43: Quantification of cell aggregates in the brain. Aggregates were counted in one every 50 5- $\mu$ m-sections over a span of 1000 sections from EBV infected animals (n=3/ timepoint) sacrificed at 3, 7, 14, 21 and 28dpi. (A) Average number of aggregates developed at each time point. Number of cell aggregates per 0.5 cm<sup>2</sup> are displayed as mean  $\pm$ SEM. Comparisons were made using the non-parametric Kruskal-Wallis test. (B) Comparison of EBV load in plasma, PBMCs, spleen, brain and spinal cord of animals with CNS aggregates and those without, using two-tailed unpaired t test and Mann-Whitney test. ns:  $p > 0.05$ , \*:  $p \leq 0.05$ . Bars without asterisks are not significantly different

Immune cell infiltrates were also examined in the brain at different time points. Infected animals that did not develop aggregates in the brain did not exhibit pronounced infiltration of immune cells including macrophages and neutrophils (Figure 44). Macrophages (RAM11<sup>+</sup> cells) infiltrated sections with aggregates from animals sacrificed at days 3, 14 and 21 (Figure 44A). Neutrophils, on the other hand, were primarily seen in aggregate-positive sections from animals sacrificed at days 14 and 21 (Figure 44B). The corresponding spinal cord tissues also showed infiltration of macrophages and neutrophils in both transverse (Figure 45A) and longitudinal sections containing aggregates (Figure 45B).

Consistent with the findings in phase 1 of the study, aggregates formed at 14 and 21dpi were surrounded by reactive astrocytes and contained Iba1<sup>+</sup> cells and PCNA<sup>+</sup> cells (Figure 46A). Additionally, immune cells positive for CD8, EB12, and IgG were also found to infiltrate the brain parenchyma of animals that developed aggregates at 14 and 21dpi (Figure 46B).

Myelin integrity was also examined in CNS sections that were positive for aggregates, by immunostaining for MBP. In agreement with phase 1 findings, myelin discontinuity was observed within the aggregates in the brain and spinal cord at both 14 and 21dpi (Figures 45 and 47).

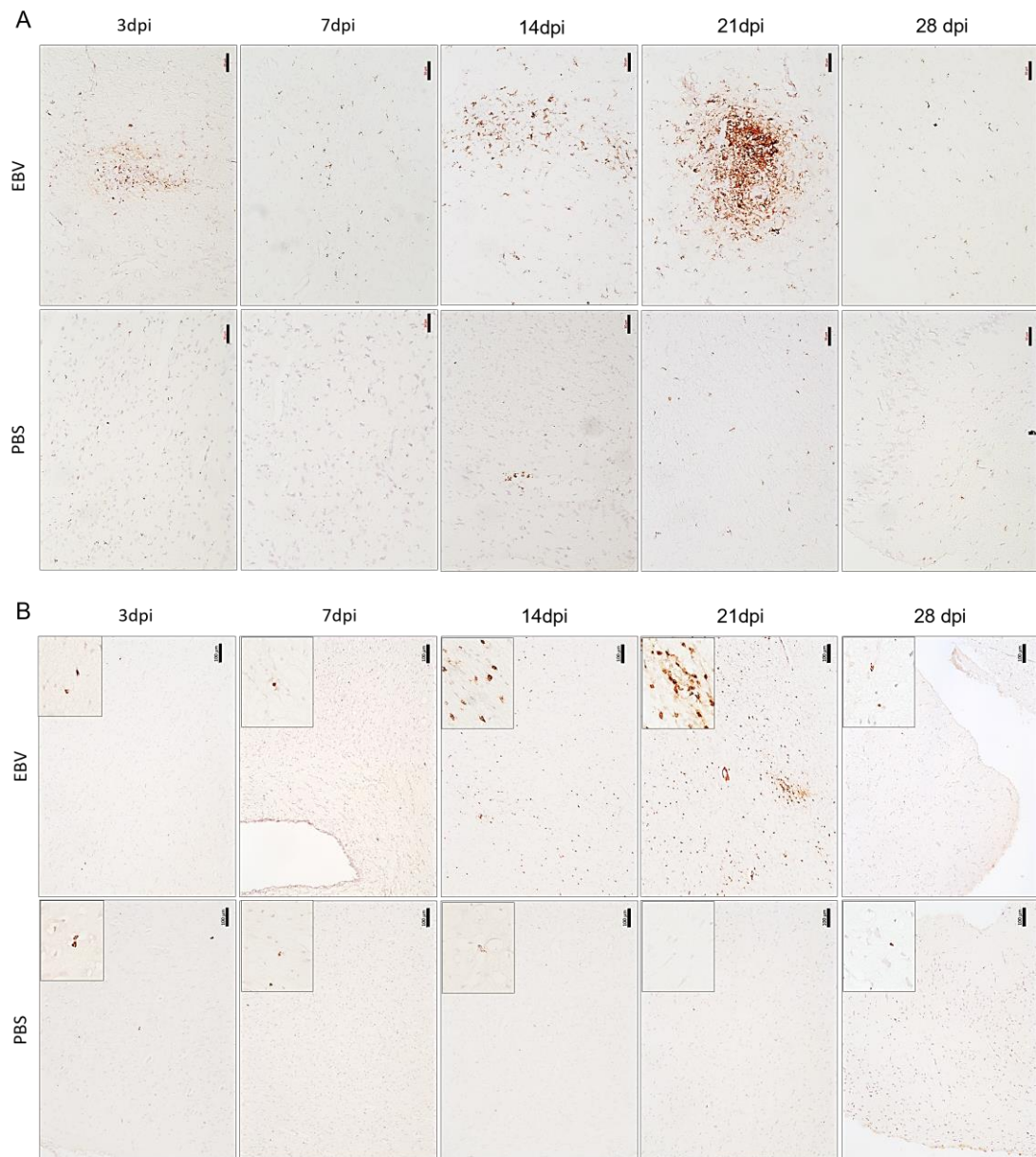


Figure 44: Prominent infiltration of macrophages and neutrophils in aggregate positive brain sections at 14 and 21dpi. (A) Immunohistochemistry staining for rabbit-specific vascular macrophages; RAM11, in EBV group and PBS controls. Scale bar=50  $\mu$ m. (B) Immunohistochemistry staining for rabbit-specific neutrophil marker in EBV group and PBS controls. Scale bar=100  $\mu$ m

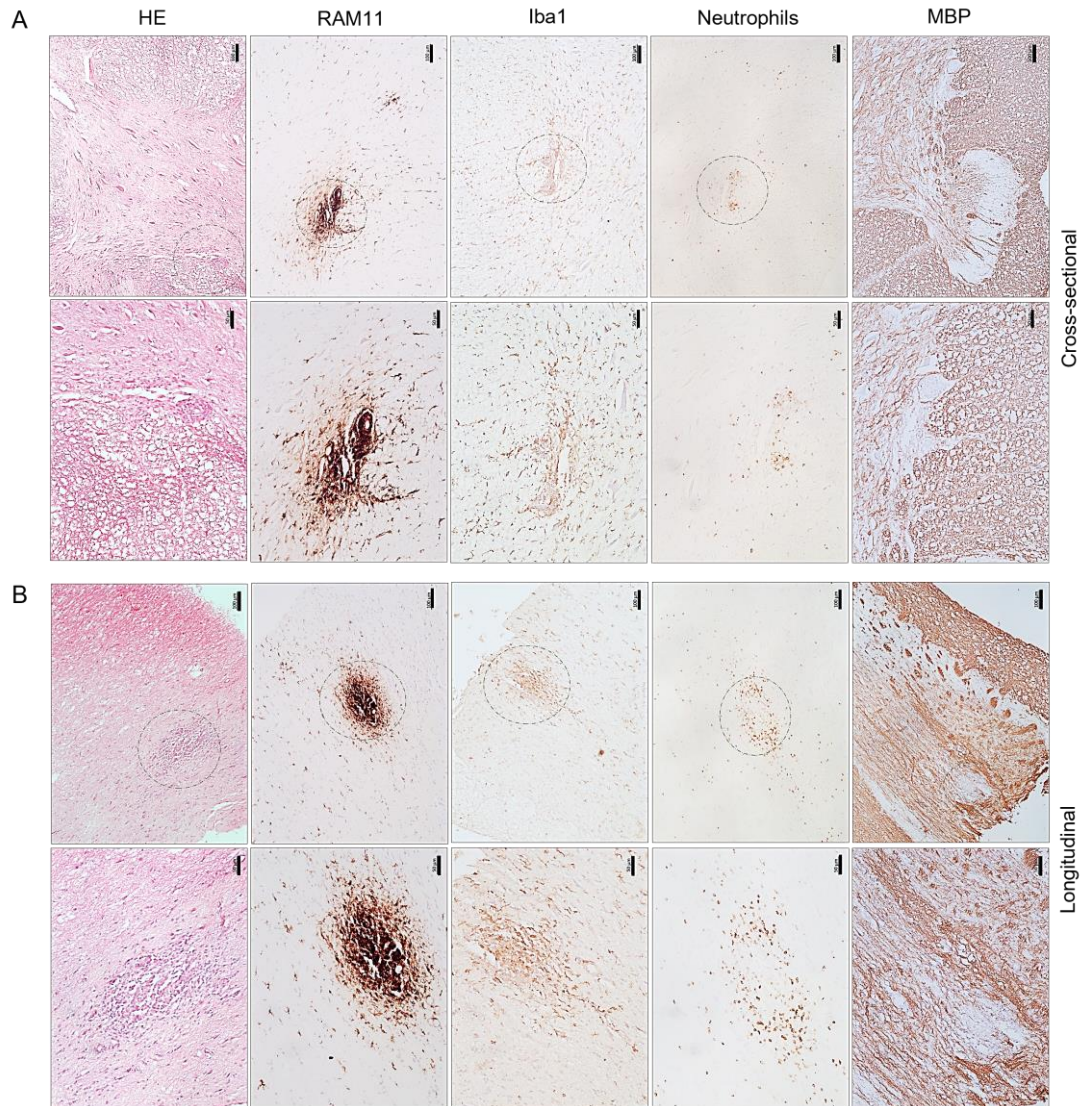


Figure 45: Infiltration of the spinal cord by macrophages and neutrophils. Spinal cord tissue from EBV infected animal sacrificed at 21dpi, cut at the (A) cross-sectional plane and (B) longitudinal plane was stained with H&E, and for rabbit-specific vascular macrophages, RAM11, microglia marker, Iba1, rabbit-specific neutrophil marker and myelin basic protein (MBP). Scale bar at lower magnification= 100  $\mu$ m. Scale bar at higher magnification= 50  $\mu$ m



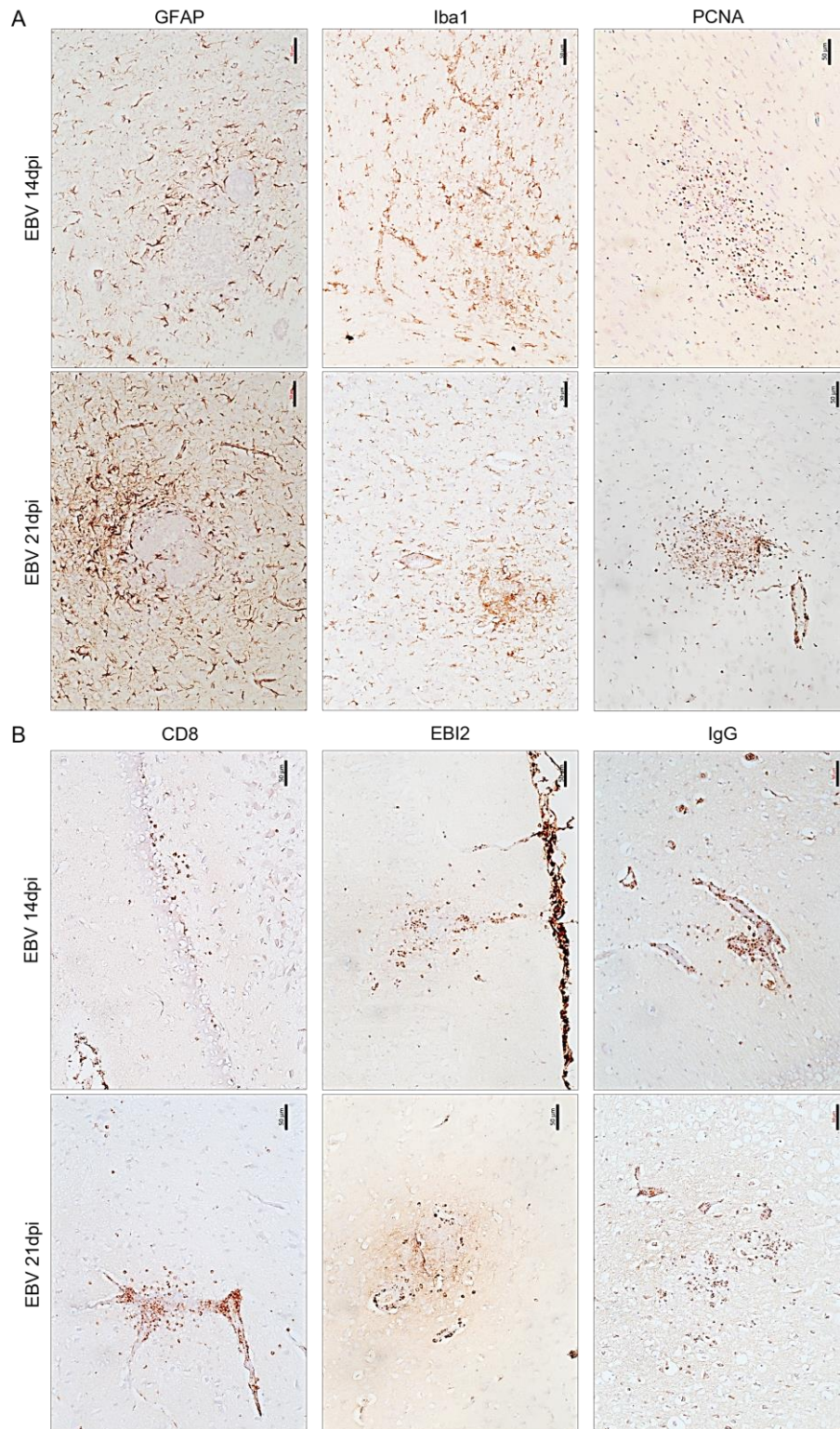


Figure 46: Reactive glia and infiltrating immune cells in aggregate-positive brain. (A) Aggregate positive brain sections from animals sacrificed at 14 and 21dpi were stained for GFAP (astrocyte marker), Iba1 (microglia marker), PCNA (proliferation marker), (B) CD8 (CD8<sup>+</sup> T cell marker), EBI2 (chemotactic receptor for lymphocytes), and IgG (marker for isotype-switched B lymphocytes). Scale bar=50 μm

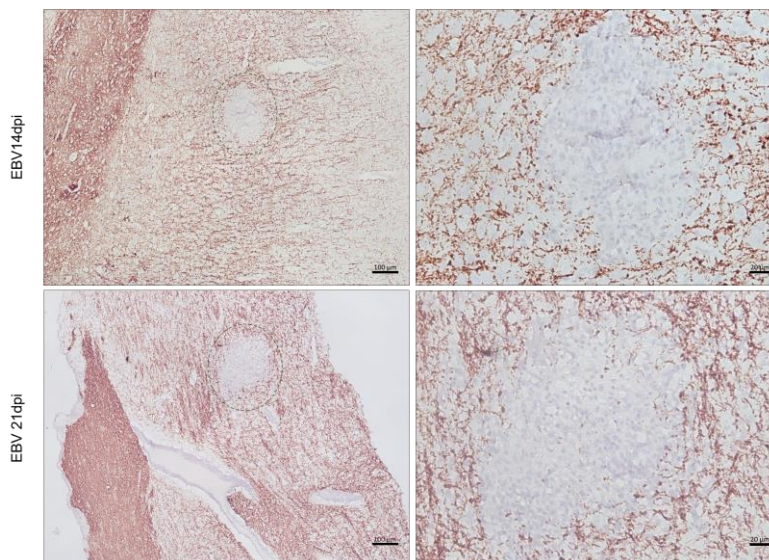


Figure 47: Evaluation of myelin integrity within aggregates at 14 and 21dpi. Brain sections containing aggregates from animals sacrificed at 14 and 21 dpi were immunostained for myelin basic protein (MBP). Scale bar at lower magnification= 100  $\mu$ m. Scale bar at higher magnification= 20  $\mu$ m

### 3.2.2.3 Peripheral EBV Infection is Associated with Changes in the Expression of Viral Latent Transcripts and Cytokines in the Periphery and the CNS

EBV infection in the periphery and the CNS may bring about changes in the expression of viral transcripts and important cytokines involved in the inflammatory and immune response. In order to understand these changes, the relative expression of viral latent transcripts namely, EBER-1/2, EBNA-1, and EBNA-2, and the cytokines tumor necrosis factor  $\alpha$  (TNF- $\alpha$ ), interleukin-1 $\beta$  (IL-1 $\beta$ ), Interferon- $\gamma$  (IFN- $\gamma$ ), interleukin-2 (IL-2) and interleukin-6 (IL-6) were quantified, using qPCR, in the spleen, brain and spinal cord, over the 5 time points of infection.

In the spleen, the majority of significant changes in the expression of viral transcripts and cytokines occurred at 7 and 28dpi (Figures 48 and 49). On average animals sacrificed at 7, 14, and 28dpi exhibited increased levels of the viral transcripts EBER-1/2, EBNA-1 and EBNA-2 than animals sacrificed at 3 and 21dpi (Figure 48).

In terms of cytokine expression, animals sacrificed at 7dpi had significantly increased levels of IFN- $\gamma$ , IL-2 and IL-6, in comparison to either non-infected controls or to animals sacrificed at other time points of infection (Figure 49). At 14dpi, the relative expression of IFN- $\gamma$  and IL-6 remained high. However, at 28dpi the infected spleen showed significant surge of the relative expression of 2 different cytokines, TNF- $\alpha$  and IL-1 $\beta$  (Figure 49). Thus, EBV infection in the spleen appears to be associated with elevated mRNA levels of IFN- $\gamma$ , IL-2 and IL-6 during week 1 and 2 of infection, and with TNF- $\alpha$  and IL-1 $\beta$  during later stage of infection, week 4.

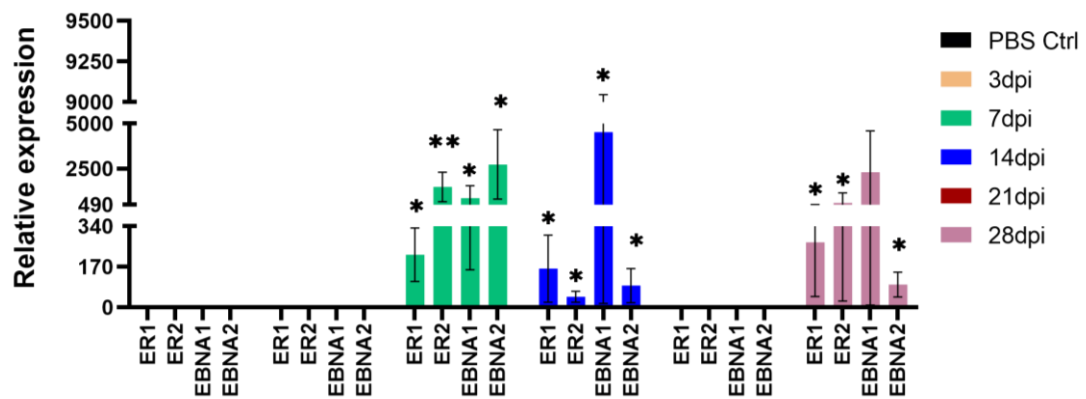


Figure 48: The relative expression of EBV transcripts in the spleen. The relative expression of EBER-1, EBER-2, EBNA-1 and EBNA-2 in the spleen tissue harvested at 3, 7, 14, 21, and 28dpi, examined using qPCR. Data displayed as mean  $\pm$ SEM. Comparisons between different time points were made using the nonparametric Kruskal-Wallis test. \*:  $p \leq 0.05$ , \*\*:  $p \leq 0.01$  compared to other time points. Bars without asterisks are not significantly different

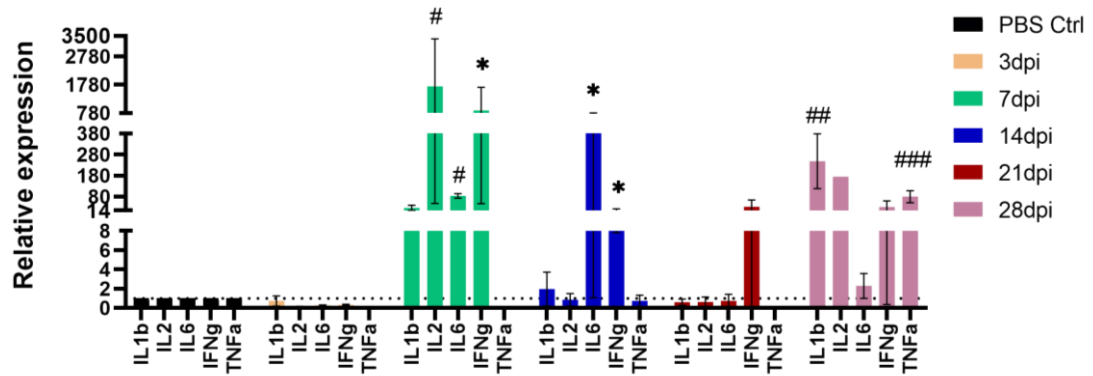


Figure 49: The relative expression of cytokines in the spleen. The relative expression of TNF- $\alpha$ , IL-1 $\beta$ , IFN $\gamma$ , IL-2, and IL-6 in the spleen tissue harvested at 3, 7, 14, 21, and 28dpi, examined using qPCR. Data displayed as mean  $\pm$ SEM. Comparisons were made using one-way ANOVA with Fisher's LSD test or the nonparametric Kruskal-Wallis test. #:  $p \leq 0.05$ , ##:  $p \leq 0.01$ , ###:  $p \leq 0.001$  compared to PBS controls. \*:  $p \leq 0.05$  compared to other time points. Bars without asterisks are not significantly different

To understand the relationship between the expression of viral transcripts and the expression of cytokines, Spearman correlation was performed. There was a strong positive correlation between the relative expression of 2 EBV RNAs, EBERs, and EBNA-2 and the relative expression of IL-1 $\beta$  and IL-6 in the infected spleen. Additionally, EBER-2 correlated positively with IL-2 and IFN- $\gamma$  (Figure 50). Therefore, increased expression of EBV transcripts, particularly the non-coding RNA EBER2 appear to be associated with increased mRNA expression of IL-1 $\beta$ , IL-2, IL-6, and IFN- $\gamma$  in the infected spleen.

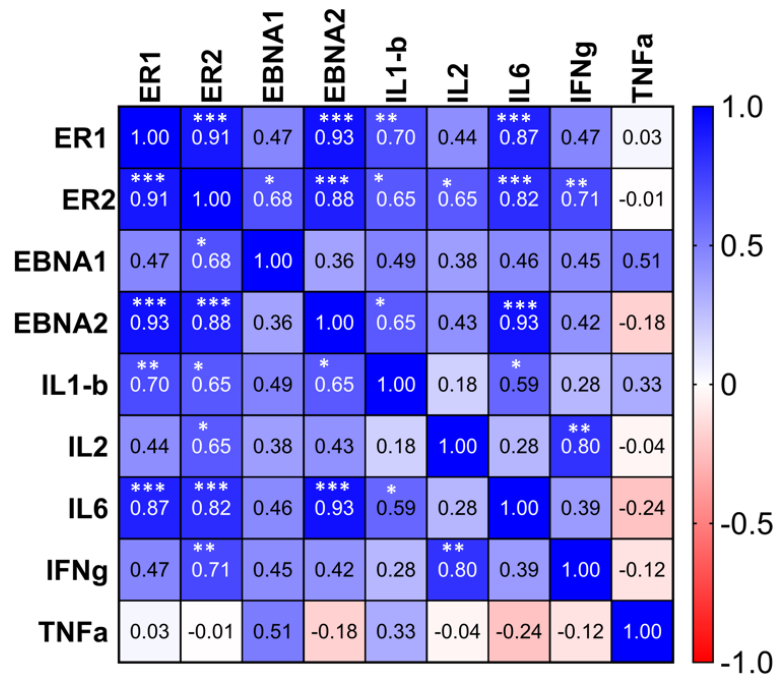


Figure 50: Heat map of Spearman correlation of inflammatory and viral transcripts in the spleen. Color mapping for positive and negative correlation are indicated in the legend on the right. \*:  $p \leq 0.05$ , \*\*:  $p \leq 0.01$ , \*\*\*:  $p \leq 0.001$

In the brain, the majority of significant changes in the expression of viral transcripts and cytokines occurred at 14 and 28dpi (Figure 51 and 52). While the relative expression of EBNA-2 and EBER-2 was elevated at 3 and 14dpi, respectively, all EBV transcripts that were analyzed were found to be significantly raised at 28dpi (Figure 51). As for cytokines, IFN- $\gamma$  and TNF- $\alpha$  were upregulated as early as 3dpi in the brain (Figure 52). At 14dpi, IL-2, IL-6, and TNF- $\alpha$  were upregulated. At 28dpi, the relative expression of TNF- $\alpha$ , IL-1 $\beta$ , and IL-2 was significantly raised in the brain (Figure 52).

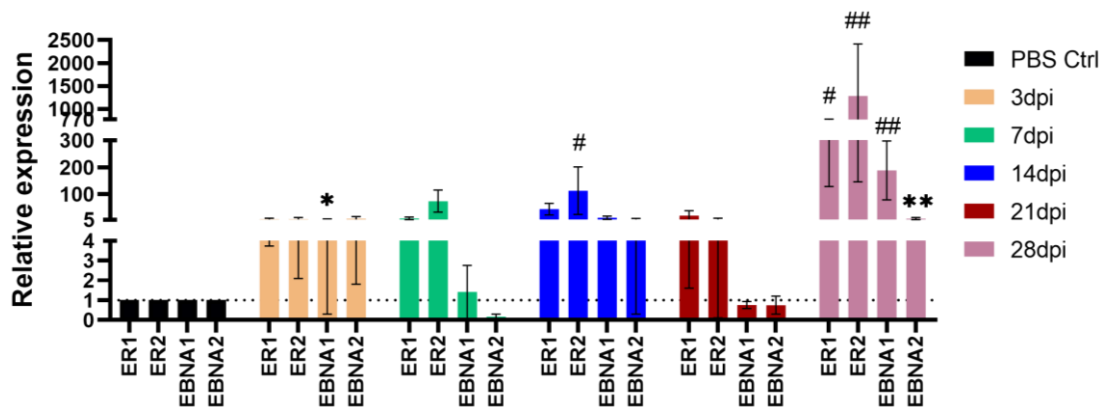


Figure 51: The relative expression of EBV transcripts in the brain. The relative expression of EBER-1, EBER-2, EBNA-1 and EBNA-2 in the brain tissue harvested at 3, 7, 14, 21, and 28dpi, examined using qPCR. Data displayed as mean  $\pm$ SEM. Comparisons were made using one-way ANOVA with Fisher's LSD test or the nonparametric Kruskal-Wallis test. #:  $p \leq 0.05$ , ##:  $p \leq 0.01$  compared to PBS controls. \*:  $p \leq 0.05$ , \*\*:  $p \leq 0.01$  compared to other time points. Bars without asterisks are not significantly different

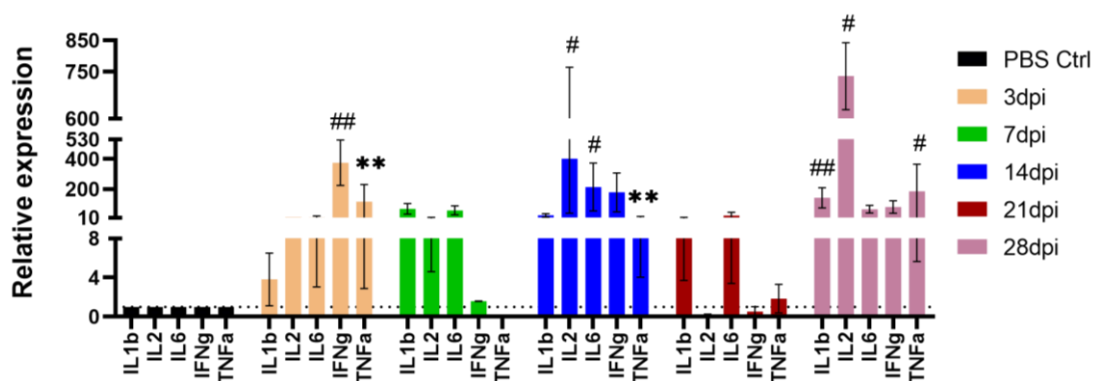


Figure 52: The relative expression of cytokines in the brain. The relative expression of TNF- $\alpha$ , IL-1 $\beta$ , IFN- $\gamma$ , IL-2, and IL-6 in the brain tissue harvested at 3, 7, 14, 21, and 28dpi, examined using qPCR. Data displayed as mean  $\pm$ SEM. Comparisons were made using one-way ANOVA with Fisher's LSD test or the nonparametric Kruskal-Wallis test. #:  $p \leq 0.05$ , ##:  $p \leq 0.01$  compared to PBS controls. \*\*:  $p \leq 0.01$  compared to other time points. Bars without asterisks are not significantly different

Heat map of Spearman correlation of viral transcripts and cytokine expression in the brain of infected animals, indicated a positive correlation between both viral RNAs EBER-1/2 and the cytokines IL-1 $\beta$ , IL-2 and IL-6 (Figure 53). There was also

a strong correlation between the relative expression of EBNA-1 and EBNA-2 and that of TNF- $\alpha$  (Figure 53). Together, these results imply that increased mRNA expression of latent EBV transcripts is accompanied by increased expression of different cytokines in the brain.

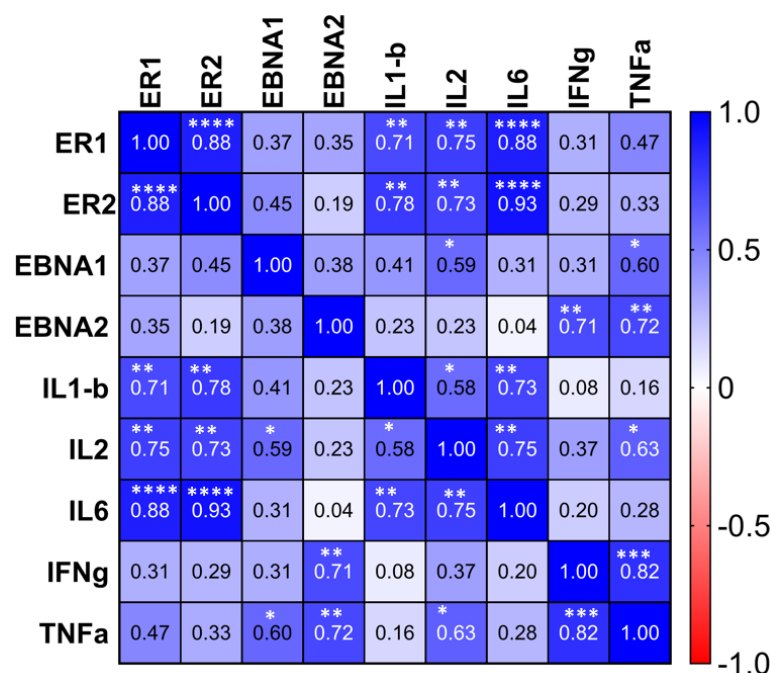


Figure 53: Heat map of Spearman correlation of inflammatory and viral transcripts in the brain. Color mapping for positive and negative correlation are indicated in the legend on the right. \*:  $p \leq 0.05$ , \*\*:  $p \leq 0.01$ , \*\*\*:  $p \leq 0.001$ , \*\*\*\*:  $p \leq 0.0001$

The impact of EBV infection on the protein levels of IL-6 and IL-2 in the brain was also examined. Generally, the levels of both IL-6 and IL-2 appeared to drop gradually at the early time points during the 1<sup>st</sup> week of infection, before starting to rise again by 14dpi (Figure 54). IL-6 level was found to be significantly higher at 14 and 21dpi, compared to either non-infected PBS controls or to earlier or later time points of infection. IL-2 level, on the other hand, dropped significantly at 7dpi (Figure

54). Thus, on the protein level, increased levels of IL-6 in the brain coincided with the time points at which aggregate occurrence peaked, while IL-2 dropped at the time point that preceded aggregate formation.

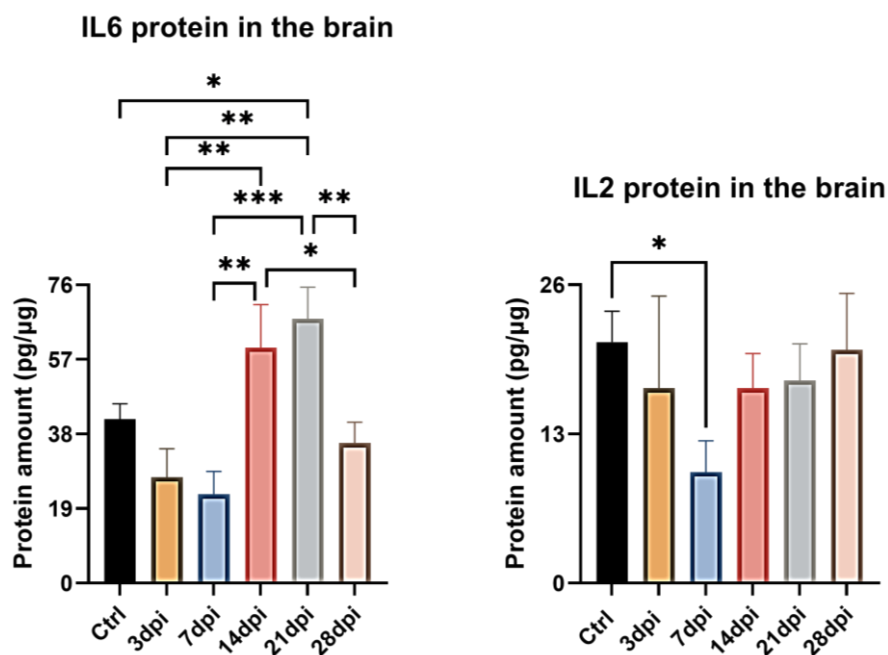


Figure 54: The levels of IL-2 and IL-6 proteins in the brain. Protein amount (pg/μg) was measured by ELISA in brain tissues harvested at 3, 7, 14, 21 and 28dpi. Data displayed as mean  $\pm$ SEM. Comparisons were made using one-way ANOVA with Fisher's LSD test or Welch and Brown-Forsythe test. \*:  $p \leq 0.05$ , \*\*:  $p \leq 0.01$ , \*\*\*:  $p \leq 0.001$ . Bars without asterisks are not significantly different

In the spinal cord, the majority of significant changes in the expression of viral transcripts and cytokines occurred at 7 and 28dpi (Figure 55 and 56). A significant increase was observed in the relative expression of EBER-1/2, and EBNA-2, but not EBNA-1 at 7dpi (Figure 55). As for cytokines, infected animals sacrificed at 3dpi had significant upregulation of IL-6 (Figure 56). IL-6 remained upregulated at 7dpi, and other cytokines including TNF- $\alpha$  and IFN- $\gamma$  became significantly upregulated at this



time point too. At 21dpi, both IL-1 $\beta$  and IL-6 were upregulated, while TNF- $\alpha$ , IL-1 $\beta$ , and IFN- $\gamma$  were significantly raised at 28dpi. No significant difference was seen in IL-2 expression (Figure 56).

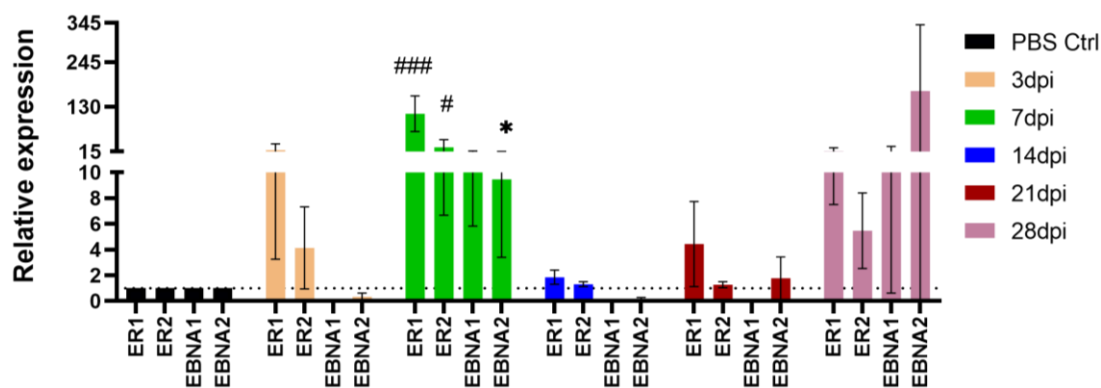


Figure 55: The relative expression of EBV transcripts in the spinal cord. The relative expression of EBER-1, EBER-2, EBNA-1 and EBNA-2 in the spinal cord tissue harvested at 3, 7, 14, 21, and 28dpi, examined using qPCR. Data displayed as mean  $\pm$ SEM. Comparisons were made using one-way ANOVA with Fisher's LSD test or the nonparametric Kruskal-Wallis test. #:  $p \leq 0.05$ , ###:  $p \leq 0.001$  compared to PBS controls. \*:  $p \leq 0.05$  compared to other time points. Bars without asterisks are not significantly different

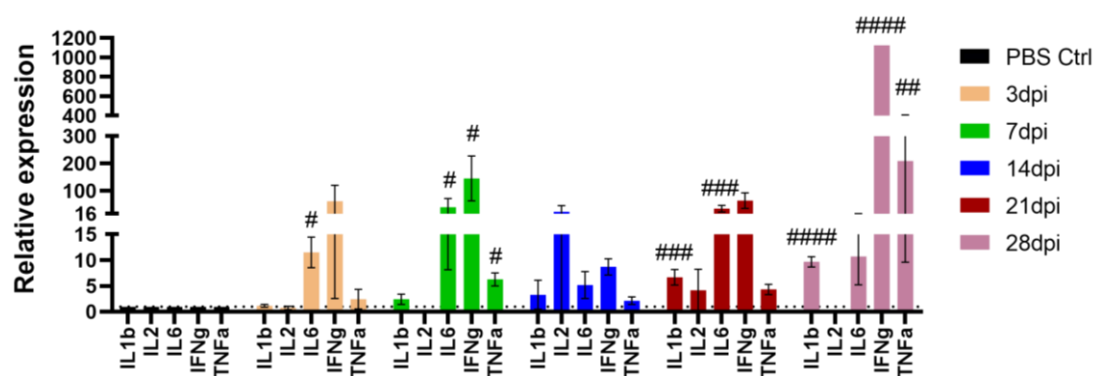


Figure 56: The relative expression of cytokines in the spinal cord. The relative expression of TNF- $\alpha$ , IL-1 $\beta$ , IFN- $\gamma$ , IL-2, and IL-6 in the spinal cord tissue harvested at 3, 7, 14, 21, and 28dpi, examined using qPCR. Data displayed as mean  $\pm$ SEM. Comparisons were made using one-way ANOVA with Fisher's LSD test or the nonparametric Kruskal-Wallis test. #:  $p \leq 0.05$ , ##:  $p \leq 0.01$ , ###:  $p \leq 0.001$ , ####:  $p \leq 0.0001$  compared to PBS controls. Bars without asterisks are not significantly different

Unlike in the spleen and brain, there was a lack of correlation between the relative expression of viral transcripts and that of cytokines in the spinal cord, as only EBNA-1 correlated moderately with TNF- $\alpha$  (Figure 57).

Notably, at the protein level, both IL-2 and IL-6 proteins dropped significantly in the spinal cord of infected animals sacrificed at 14 and 21dpi (Figure 58).

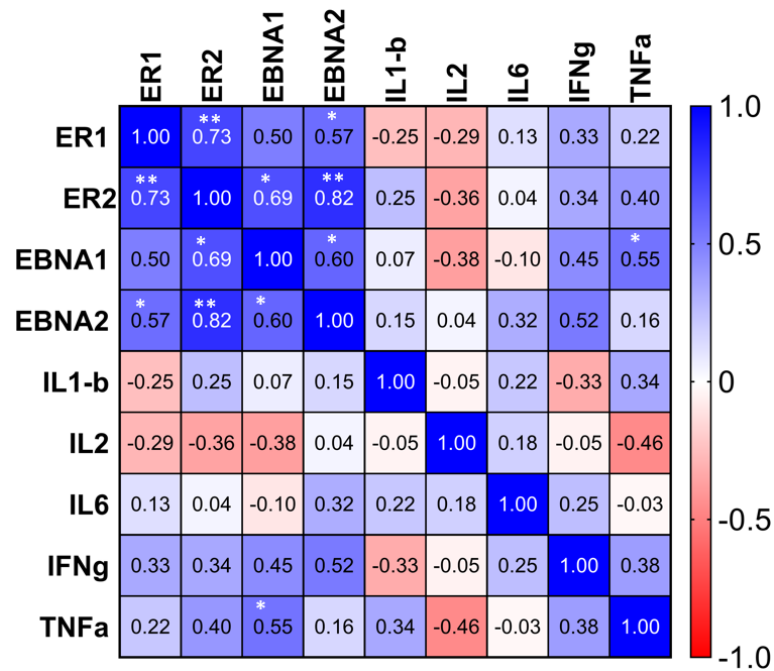


Figure 57: Heat map of Spearman correlation of inflammatory and viral transcripts in the spinal cord. Color mapping for positive and negative correlation are indicated in the legend on the right. \*:  $p \leq 0.05$ , \*\*:  $p \leq 0.01$

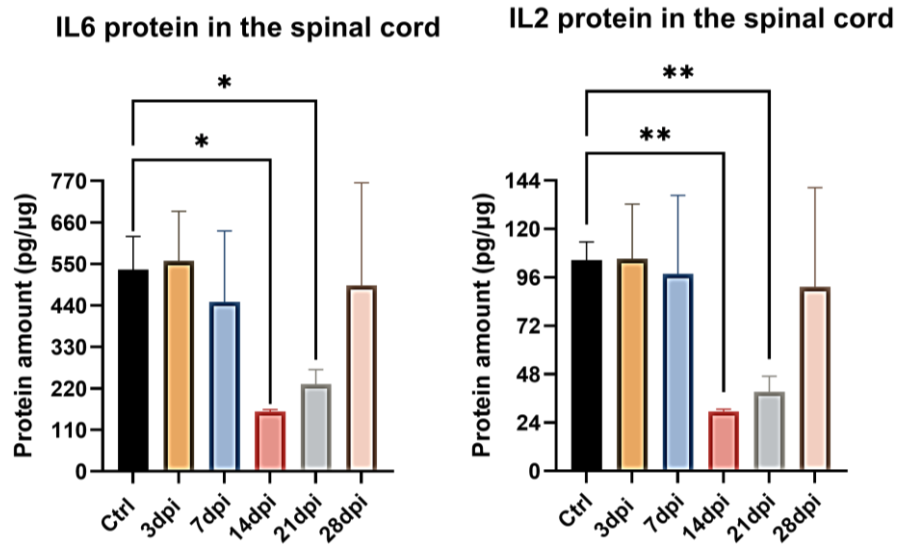


Figure 58: The levels of IL-2 and IL-6 proteins in the spinal cord. Protein amount (pg/μg) was measured by ELISA in spinal cord tissues harvested at 3, 7, 14, 21 and 28dpi. Data displayed as mean ±SEM. Comparisons were made using Welch and Brown-Forsythe test. \*:  $p \leq 0.05$ , \*\*:  $p \leq 0.01$ . Bars without asterisks are not significantly different

## Chapter 4: Discussion

Several groups have frequently demonstrated the presence of EBV in the brain of MS patients, implicating a role for the virus in the pathogenesis of this disease (Hassani et al., 2018; Moreno et al., 2018; Serafini et al., 2007). However, the dynamics of virus trafficking to the brain, and its subsequent impact on disease development and/ or progression, are poorly understood. Addressing these questions has been challenging due to the lack of a suitable animal model of EBV infection. A number of reports have recently shown that rabbits are susceptible to EBV, and the infection mimics that observed in humans (Kanai et al., 2010; Khan et al., 2015; Okuno et al., 2010; Osborne et al., 2020).

The aim of this study was to explore the neuropathogenic potential of primary peripheral EBV infection, using an *in vivo* model that closely reflects the biology of the virus in humans as much as possible. This was achieved using the unique rabbit model of EBV infection. Collectively, the data uncovered several aspects of the dynamics of EBV infection in the periphery and the CNS that was not possible before. (1) Intravenous inoculation of the virus led to widespread infection in all three peripheral compartments examined: spleen, PBMCs, and plasma. (2) Peripheral infection resulted in the virus traversing the brain. The infection in the brain correlated well with cell-associated virus load in the periphery, rather than circulating free virus in the plasma. (3) Infected cells in the brain were mainly B lymphocytes. (4) Peripheral EBV infection induced the formation of inflammatory cellular aggregates in the CNS. These aggregates were composed of blood-derived macrophages surrounded by reactive astrocytes and infiltrating B and T lymphocytes. (5) The inflammatory cellular aggregates were devoid of myelinated nerve fibers, suggesting that inflammation could

be involved in demyelination. (6) Multiple latent viral transcripts and cytokines were altered in the periphery and the CNS. The expression level of EBV transcripts correlated with the mRNA levels of cytokines.

#### **4.1 EBV Levels Peak Within 2 Weeks of Primary Infection in Rabbits**

During primary infection in rabbits, EBV load peaked at day 14 in the periphery as well as in the CNS. Also, viremia was pronounced within 2 weeks of infection. Afterwards, viral levels started to drop. This is consistent with viral dynamics in humans (Dunmire et al., 2015).

Viremia and high viral load in the PBMCs commonly occur during primary EBV infection in people, whether symptomatic or silent (Lam et al., 2018). EBV load in both the plasma and PBMCs then begin to fall gradually over time as the virus establishes latency. This coincides with a steady decline in the frequency of lytic antigen-reactive CD8<sup>+</sup> T cells and the rise of latent antigen-specific CD8<sup>+</sup> T cells. However, the frequency of polyfunctional CD4<sup>+</sup> T cells (secreting IFN- $\gamma$ , TNF- $\alpha$ , IL-2 and perforin) and polyfunctional CD8<sup>+</sup> T cells (expressing CD107a, TNF- $\alpha$  and IL-2) that react against immunodominant viral epitopes, become prominent in the circulation (Lam et al., 2018). Thus, increased polyfunctionality of T cells, and hence enhanced versatility of antiviral immune responses, may be responsible for maintaining EBV load below detectable levels after primary infection.

Indeed, reduced multifunctionality of EBV-reactive T cells has been reported to cause marked dysregulations in immune control of EBV during progressive HIV infection (Hernández et al., 2018). This has been linked to viral reactivation and EBV-driven B cell proliferation, and increased likelihood of the development of EBV lymphomas in HIV patients (Hernández et al., 2018).

Additionally, viral levels during initial infection can depend on the fitness of the immune system established by exposure to other viruses. This is a phenomenon known as heterologous immunity, where T lymphocytes develop broad response to epitopes from different antigen sources (Sharma & Thomas, 2014; Welsh et al., 2010; Welsh & Fujinami, 2007). For instance, infection with CMV prior to exposure to EBV is believed to generate more efficient anti-EBV effector immune responses compared to infection with EBV first before contracting CMV (Sohlberg et al., 2013). This cross-reactive immune response is associated with reduced frequency of EBV infected B cells (Sohlberg et al., 2013). However, the impact of heterologous immunity on EBV infection could be both beneficial and harmful, depending on the cross-reactive pathogen and on the T cell receptor repertoire in individual hosts (Aslan et al., 2017; Cornberg et al., 2010; Gil et al., 2020).

#### **4.2 Peripheral Infected Cells Migrate to the CNS in Rabbits**

Primary EBV infection during late adolescence can cause symptomatic infectious mononucleosis (IM). Both symptomatic and asymptomatic primary infection cause high viral load in the periphery. However, disrupted immunological profile is rather unique to IM (Abbott et al., 2017; Dunmire et al., 2015; Piriou et al., 2012). This emphasizes that EBV associated diseases emerge as a result of defective or exaggerated immune response to the infection.

Here, primary EBV infection was investigated in healthy rabbits, and rabbits immunosuppressed with Cyclosporine A (CsA). High viral load was detected in the peripheral compartments of all animals, but most notably in the immunosuppressed (EBV+CsA) group. This group also exhibited more than 10-fold higher levels of free virus in the plasma. However, viremia (i.e., the level of free virus) did not correlate

with brain infection. By contrast, there was a positive correlation between the level of cell-associated virus (i.e., infected cells) in the PBMCs and spleen, and brain infection. These findings support the idea that CNS infection is ascribed to migrating infected lymphocytes, most probably B cells. Nevertheless, EBV level in the spinal cord did not correlate with levels of cell-associated virus in the periphery.

Furthermore, the frequency of detecting EBV infection as well as levels of viral DNA were the highest at day 14 of infection, coinciding with the peak of immune aggregate formation. Thus, week 2 possibly represents the acute phase of EBV infection in rabbits. However, the viral load in the CNS did not differ between animals that developed aggregates and those that did not. In agreement with these results, the load of Theiler's Murine Encephalomyelitis Virus (TMEV) in the CNS of different mice strains has been shown to not correlate with disease development (Myoung et al., 2008). Instead, disease outcome correlated well with immune response to viral components. Thus, virus trafficking into the CNS is not sufficient for neuropathological changes to occur.

The migration of EBV infected cells from the periphery to the brain has only been reported recently in humanized mice developing lymphomas (Volk et al., 2020). This was achieved by inoculating humanized mice with EBV and treating them with pembrolizumab, a monoclonal antibody, used clinically to block the immune checkpoint programmed death 1 (PD-1) receptor. Subsequently, virus propagation to the CNS led to the formation of EBER-rich lymphomas in the brain. These mice had low frequency of circulating T cells, many of which were exhausted (i.e. TIM3<sup>+</sup> and LAG3<sup>+</sup> T cells) (Volk et al., 2020). Thus, surprisingly the expression of PD1 receptor on T cells appears to be important in controlling EBV systemic dissemination and restricting its neuropathogenic and malignant consequences.

### 4.3 Neuropathology in the Rabbit CNS

Unexpectedly, it was observed that up to 1/3<sup>rd</sup> and 2/3<sup>rd</sup> of healthy (without immunosuppression) rabbits infected with EBV developed inflammatory cell aggregates in the brain and the corresponding spinal cord at days 14 and 21 of infection, respectively. Why only a fraction of infected rabbits developed CNS aggregates remains to be explored. However, the results in this study suggest that EBV load in the PBMCs may partly be linked to the formation of these structures.

This observation also underscores the importance of host factors including host genetics and the fitness of the immune system in developing neuroinflammation. Indeed, susceptibility, frequency, and location of inflammatory aggregates varied between individual animals. Similarly, in experimental autoimmune encephalomyelitis (EAE), the incidence of demyelinating lesions varies between different animal strains. This variation is believed to reflect differences in the genetic background that governs whether T helper 1 (Th1) cell response or Th2 cell response dominates (Maron et al., 1999). Propensity towards this CNS autoimmunity is observed in animals with genetic background that supports Th1 cell response over Th2 cell response (Constantinescu et al., 2001; Maron et al., 1999). For example, animals that tend to overproduce Th1 cytokines such as IL-2 and IFN- $\gamma$ , with little expression of Th2 cytokines including IL-4, IL-10 and TGF- $\beta$  are readily prone to developing autoimmune-mediated neuroinflammation. By contrast, animals with an inherent response that is skewed away from the differentiation of GM-CSF and IFN- $\gamma$  producing Th17 cells are protected against developing neuroinflammation (Stojić-Vukanić et al., 2016).

Maintaining well-regulated T cell responses is crucial to prevent neuroinflammation. One way of regulating the effector response of T cells is by the



induced expression of immune checkpoints. The lack of interaction between CTLA-4 receptor, an important immune checkpoint, on activated T cell surface and its ligand B7 molecules on antigen-presenting cells (APCs) was found to render animals susceptible to the development of autoimmune-mediated neuroinflammation (Hurwitz et al., 2002). Additionally, antigen processing and peptide presentation by dendritic cells (DCs) were also found to play a role in determining whether these animals establish immune tolerance or autoreactivity to CNS (self) antigens (Steinman & Nussenzweig, 2002).

Moreover, there is some evidence suggesting that peripheral viral infections can influence the fitness of the immune system. Latent infection with CMV during adulthood, for instance, has been reported to break tolerance to CNS-specific autoimmunity in mice that were originally resistant to EAE (Milovanovic et al., 2017). Infection with influenza virus has also been found to lead to neuroinflammation in almost one third of 2D2 mice, which are genetically predisposed to EAE (Blackmore et al., 2017).

Cell aggregation also developed in Cyclosporin A (CsA)- treated non-infected rabbits. When CsA reaches the cytoplasm, it forms a complex with cyclophilin A, which obstructs calcineurin function needed for the transcription of IL-2. Without IL-2, T cell activation and expansion are halted (Flanagan et al., 1991; Fruman et al., 1992). As a result, these immunosuppressed animals can experience reactivation of endogenous opportunistic pathogens, which may subsequently trigger neuroinflammation. Alternatively, several studies have shown that CsA causes injury to pericytes and astrocytes guarding the BBB (Dohgu et al., 2000, 2004, 2010; Kochi et al., 1999; Takata et al., 2006). This leads to leakage in the CNS barrier, and results in CsA-induced neuropathology. Thus, functional characterization of cellular players

in neuroinflammation should help discriminate between changes attributed to EBV infection and those ascribed to CsA.

Additionally, inflammatory cell aggregates developed in the rabbit CNS without overt signs of neurological deficits. This is similar to what was previously observed in the intranasal infection of 129/SvEv mice with rabies CVS-F3. This CNS infection did not result in neurological manifestations, despite the occurrence of neuroinflammation, BBB breakdown and the increased expression of the proinflammatory cytokines IL-6 and TNF- $\alpha$  (Phares et al., 2006). Mice infected with the tick-borne encephalitis virus also did not manifest neurological deficits (Cornelius et al., 2020). Conversely, many neuroinvasive viruses including SARS-CoV-2, HSV-1 and influenza virus can be accompanied by neurological signs caused by virus-induced inflammation and other pathological alterations in the CNS (Boukhvalova et al., 2019; Desforges et al., 2020; Hosseini et al., 2018; Song et al., 2021; Yang et al., 2021; Zubair et al., 2020).

#### **4.3.1 The Makeup of Inflammatory Cell Aggregates in the CNS Of EBV Infected Rabbits**

Cell aggregates in the CNS of rabbits contained a heterogeneous cell population made up of brain resident cells, infiltrating macrophages, neutrophils and B and T lymphocytes. In general, aggregates were seen at dissimilar stages of evolution in a given section, and thus differed in composition. Typically, most of the aggregates had infiltrating macrophages as the prominent core surrounded by reactive astrocytes and dispersed lymphocytes. However, few aggregates lacked macrophage infiltration, but contained a cluster of reactive glia and loosely connected lymphocytes.

In rabbits, RAM11 can distinguish blood-derived macrophages from CNS-resident microglia. In mice, discriminating between infiltrating blood-derived

macrophages from CNS- resident microglia has also been established based on several markers and single cell transcriptomics (DePaula-Silva et al., 2019; Saederup et al., 2010; Yamasaki et al., 2014). In humans, on the other hand, this issue remains more complex. Tracking each of these cell populations and their subsets can help us identify their individual functions during CNS injury, viral infections and neuroinflammation.

Given the observed dense population made of infiltrating macrophages in rabbit CNS, it is of great importance to understand what roles these cells play during EBV-induced neuroinflammation. Do they contribute to CNS injury, and exacerbation of viral infection and inflammation? Or do they participate in viral clearance and recovery? Or both? Infiltration of macrophages into the CNS has been previously reported in mice infected with the coronavirus, mouse hepatitis virus strain (DePaula-Silva et al., 2019; Templeton et al., 2008). In this mouse model of coronavirus infection, blood-derived macrophages have been shown to infiltrate the infected CNS during early days of infection and mature over time to the non-classical Ly-6C<sup>+</sup> CD62L<sup>-</sup> cells. These macrophages have been shown to be associated with areas of myelin breakdown during CNS viral infection, which may suggest their pathogenic involvement in demyelination (Templeton et al., 2008). Nevertheless, their role in tissue injury is believed to be complex, as studies report their contribution to both tissue repair and inflammation (Misharin et al., 2014; Mukherjee et al., 2015; Narasimhan et al., 2019; Puchner et al., 2018). Additionally, in EAE mice, the absolute number of activated macrophages infiltrating the CNS has been found to correlate with EAE severity (Berger et al., 1997). Macrophages in these animals are also thought to support inflammation-mediated demyelination (Yamasaki et al., 2014).

In response to systemic inflammation, IL-1 $\beta$  together with TNF and angiopoietin 2 (a blood vessel-disrupting mediator), promote the recruitment of CD68<sup>+</sup>

monocytes from the periphery to populate certain niches within the CNS. These monocytes reach CNS vasculature, crawl, alter their morphology into elongated rod-shaped, and subsequently squeeze through the endothelium into the brain. They proliferate and differentiate into perivascular macrophages within the inflamed CNS (Audoy-Rémus et al., 2008).

During immunodeficiency virus-induced encephalitis in humans (HIV) and monkeys (SIV), CD163<sup>+</sup> CD14<sup>+</sup> CD16<sup>+</sup> blood monocytes are recruited into the brain, and make up a population of perivascular macrophages that are distinct from CNS-resident microglia (Kim et al., 2006). Macrophages are believed to carry HIV-1 into the CNS and mediate virus-induced neuropathogenesis (González-Scarano & Martín-García, 2005). EBV has been shown to infect human monocytes *in vitro* (Torii et al., 2017). If EBV infects rabbit monocytes in the periphery, then these monocytes, along with infected B lymphocytes, could also contribute to virus trafficking into the CNS via “Trojan horses” mechanism.

CNS-resident microglia, however, are believed to help in the clearance of cellular debris promoting resolution of inflammation in EAE (Yamasaki et al., 2014). Moreover, Microglia are also believed to offer protection against neurotropic viruses particularly during the first week of infection (Tsai et al., 2016; Wheeler et al., 2018). Exacerbation of the infection course upon microglia depletion, signifies their role in limiting viral titers in the brain. Microglia are also crucial in reducing mortality following CNS viral infections in animal models (Tsai et al., 2016; Wheeler et al., 2018). In the absence of microglia, both viral level and the expression of the cytokines IL-6 and IFN- $\beta$  increase in the brain (Wheeler et al., 2018). Additionally, microglia depletion in dengue virus-infected mice has been found to compromise antiviral response of IFN- $\gamma$ <sup>+</sup> CD8<sup>+</sup> T lymphocytes (Tsai et al., 2016). These observations imply

that microglia are essential for an efficient adaptive immune response during CNS viral infections.

Substantial contribution of astrocytes was also seen in the aggregate formation, mainly surrounding the dense clusters of macrophages (penumbra). During reactive gliosis, a subset of astrocytes known as cytotoxic A1 astrocytes become activated in response to inflammatory mediators, such as TNF and IL-1 $\alpha$ , released by activated microglia (Liddelow & Barres, 2017). A1 astrocytes have the ability of killing surrounding neuronal cells and oligodendrocytes. Inhibition of A1 astrocytes activation by microglia is now under study as a potential therapy for neurodegeneration (Park et al., 2021; Yun et al., 2018). Nevertheless, the function of astrocytes in health and disease appear to be complex, and the simple description of A1 and A2 astrocytes as “neurotoxic” and “neuroprotective”, respectively, is deemed insufficient (Escartin et al., 2021). Indeed, single-cell RNA sequencing has shown that during systemic inflammation, reactive astrocytes are transcriptionally at different sub-states based on their location in the brain (Hasel et al., 2021). Different subsets of astrocytes, in fact, experience different transcriptional changes depending on their location in the brain, and type of injury, acute or chronic (Borggrewe et al., 2021).

Moreover, astrocytes are also believed to influence the behavior of CNS infiltrating lymphocytes. For instance, reactive astrocytes are shown to secrete soluble mediators that prolong the survival of B lymphocytes within the CNS. They also help induce the expression of costimulatory molecules on the surface of B cells to improve their role as APCs (Touil et al., 2018). In response to reactive astrocytes, B cells in turn produce inflammatory cytokines that promote inflammation driven by Th1 and Th17 cells (Bar-Or et al., 2010).

Additionally, both B and T lymphocytes were associated with aggregate formation in the rabbit CNS. T lymphocytes were mainly CD8<sup>+</sup> cells, while B lymphocytes expressed proliferation marker PCNA, IgM, and IgG. The expression of EBV induced gene 2 (EBI2) was also observed in the brain. EBI2 receptor is typically expressed on activated B and T lymphocytes, and interacts with its ligand oxysterols (Hannedouche et al., 2011; Liu et al., 2011). This interaction affects the movement of lymphocytes and the subsequent immune response of antibody-producing B cells (Clottu et al., 2017; Gatto et al., 2009; Kelly et al., 2011; Pereira et al., 2009). EBI2-oxysterols interaction has also been shown to mediate the antiviral response of interferons and helps restrict replication of several viruses including EBV analogue, MHV68 (Liu et al., 2013). In the CNS, EBI2 is expressed on astrocytes, and is implicated in astrocytes movement, astrocytes-macrophages communication, and the control of inflammatory cytokine release, including IL-6 and TNF- $\alpha$ . Moreover, the expression of EBI2 has been associated with protection against myelin damage (Rutkowska, Dev, et al., 2016; Rutkowska et al., 2015, 2017, 2018; Rutkowska, O'Sullivan, et al., 2016; Velasco-Estevez et al., 2021). In rabbits, EBI2<sup>+</sup> cells were mainly located at the outer part of aggregates where myelin was often intact.

Together these cells make an important functional and structural unit that is commonly impacted in various CNS pathologies including EBV-induced CNS pathology.

#### **4.3.2 Comparison Between Pathology in EBV Positive MS Cases and Pathology in the Brain of EBV Positive Rabbits**

Several differences were observed between the pathology in EBV infected MS cases and that in EBV infected rabbit brains. Firstly, macrophages were frequently the dominant cell type within cell aggregates in the rabbit CNS. Lesions in the EBV

infected rabbits showed focal aggregation of blood-derived macrophages and microglia in the center whereas reactive astrocytes formed well defined borders around the majority of the aggregates.

By contrast, the vast majority of the collection of MS cases, regardless of the extent of EBV infection, were at an end-stage disease. These cases contained mainly chronic inactive lesions, in which inflammation was absent. Macrophages/microglia were limited within the center of the plaque. Indeed, in progressive MS cases microglia/macrophages were observed to form a dense border surrounding the demyelinated lesions in the grey matter of subpial cortex (Choi et al., 2012). The number of microglia/macrophages in the parenchyma of these patients was significantly higher than that in non-MS control brain (Choi et al., 2012).

Secondly, the aggregates in the rabbit CNS differed from MS plaques in that inflammation was present, as scattered B and T lymphocytes were readily detected, particularly in the outer part of the aggregates and diffused in the parenchyma. In MS cases, however, inflammation was seen only in a heavily infected RRMS case. This case had aggregation of immune cells in the perivascular spaces, with massive infiltration of CD3<sup>+</sup> T lymphocytes and activated amoeboid microglia, and prominent astrogliosis. CD20<sup>+</sup> B lymphocytes accumulated selectively within the perivascular cuffs. Many of these cells were proliferating, similar to those in the inflamed rabbit brain. Although, the participating cells in inflammation in this MS case may be similar to the ones present in the rabbit brain, but their extent of infiltration and anatomical distribution relative to the lesion differed.

EBV infection has been associated with the formation and/or persistence of immune aggregates in the inflamed tissue in MS and other autoimmune diseases, such as myasthenia gravis, and rheumatoid arthritis (Cavalcante et al., 2010; Croia et al.,

2013, 2014; Serafini et al., 2007). These immune aggregates were found to organize into structures reminiscent of secondary lymphoid tissues, and hence given the name ectopic lymphoid follicles (ELFs).

ELFs were previously recognized in the meninges of MS brain, and have gained attention as potential pathogenic feature of the disease (Mitsdoerffer & Peters, 2016; Pikor et al., 2015). A study on 123 cases of secondary progressive MS (SPMS) found that 40% of the progressive cases contained B cell aggregates in the meninges, which formed ELFs (Howell et al., 2011). These structures were often seen to fill several deep sulci in the brain, particularly in cases with increased concentration of demyelinated lesions in the grey matter. They comprised distinct clusters of CD20<sup>+</sup> B cells, CD138<sup>+</sup> plasma cells, CD3<sup>+</sup> T cells and CD68<sup>+</sup> macrophages intermingled with CD35<sup>+</sup> follicular dendritic cells (Howell et al., 2011; Serafini et al., 2004). Moreover, they expressed markers that determine the fate of B cells, including CXCL13, CD27, and BAFF (Magliozzi et al., 2004; Serafini et al., 2010).

Meningeal B cell ectopic follicles are believed to be linked to disease progression and damaged cerebral cortex in MS (Choi et al., 2012; Howell et al., 2011; Magliozzi et al., 2013; Pikor et al., 2015; Serafini et al., 2004). However, blocking the formation of these B cell-rich lymphoid structures in a mouse model of MS has been shown to aggravate disease course and pathology (Mitsdoerffer et al., 2021). Thus, ELFs may possibly play a dual role in MS, contributing to disease exacerbation on one hand, and immunoregulation on the other hand.

In contrast, a study on 26 primary progressive MS (PPMS) cases did not find that meningeal inflammation contained B cell ectopic follicles, despite substantial infiltration of B lymphocytes, T lymphocytes and macrophages (Choi et al., 2012). Similarly, these structures were not detected, neither in the brain collection of MS



cases, nor in the CNS of rabbits, although B lymphocytes were spatially associated with the aggregates in rabbits. Thus, cell organization observed in the aggregates in the rabbit CNS did not mimic those observed in MS ectopic lymphoid-like structures. Consistent with these observations, TMEV infection of mice CNS has been found to result in the formation of immune cell aggregates that did not exhibit typical organization of ELF, even though these aggregations consisted of dense populations of B cells (DiSano et al., 2019).

Finally, the cellular aggregates observed in the rabbit CNS were devoid of myelinated nerve fibers. Disruption of MBP in rabbits was limited to the center of the aggregates, and always associated with the presence of the aggregates. In MS cases however, areas with complete destruction of MBP in chronic inactive lesions were hypocellular and did not contain cellular aggregates. Signs of partial remyelination were also seen in some of the chronic inactive lesions. In the RRMS case, demyelination was not necessarily associated with clusters of immune cells in the perivascular spaces. Some areas with perivascular cuffs appeared to have intact myelin, while others were completely or partially demyelinated.

Disruption of myelin following peripheral viral infection is not unique to EBV. Gerbils infected with hepatitis E virus have been reported to develop acute inflammatory lesions in the CNS associated with damage to myelin (Shi et al., 2016). Rabbits infected with the same virus have also been shown to develop these myelin destroying inflammatory lesions (Tian et al., 2019). Peripheral infection with the neurotropic herpesvirus, HSV-1 can also induce neuroinflammation and cause injury to myelin in cotton rats (Boukhvalova et al., 2019). Thus, there seems a strong link between peripheral viral infections and demyelinating diseases in various species.

## **4.4 Altered Viral Latent Transcripts and Cytokines Expression in the Periphery and the CNS**

### **4.4.1 Correlation Between EBV Viral Transcripts and Cytokine Expression**

Another important finding from the rabbit model is the positive correlation between increased expression of viral latent transcripts, and the inflammatory cytokines in both the spleen and the brain. The importance of EBV latent infection in inflammation in the brain was previously examined in EAE mice using murine  $\gamma$ -herpesvirus 68 (MHV-68) that naturally infects rodents and is biologically similar to EBV (Casiraghi et al., 2015). The onset of disease course of EAE coincided with the virus establishing latency in mice, and not during the acute pre-latent infection (Casiraghi et al., 2015). Mice that were infected with latency-deficient MHV68 had significantly milder disease than those latently infected with the virus (Casiraghi et al., 2015). The latent infection in mice was found to cause increased Th1 cell infiltration into the CNS, and suppress the anti-inflammatory phenotype of T cells; regulatory T cells, both in the periphery and CNS (Casiraghi et al., 2012, 2015). Moreover, when MHV-68 infects CNS resident astrocytes and microglia, infected cells secrete several inflammatory cytokines (Taylor et al., 2003).

Furthermore, a role for EBV latent protein EBNA-1 has also been implicated in EAE. A recent study demonstrated that immunizing mice with EBV latent EBNA-1 amino acid region 411-426 could lead to neurological deficits reminiscent of EAE, and the development of MRI-confirmed cortical lesions (Jog et al., 2020). This region of EBNA-1 was also found to trigger high antibody response in individuals with relapsing-remitting and secondary progressive MS, and these antibodies cross-reacted with MBP amino acid region 205-224 (Jog et al., 2020). EBV latent transcripts were also found to be upregulated in MS lesions (Veroni et al., 2018). On the other hand,

virus reactivation in the MS brain was associated with marked neuroinflammation and demyelination leading to fatal immune reconstitution inflammatory syndrome (Serafini et al., 2017, 2018). The current study and these reports support the hypothesis that transcriptionally active EBV in the brain promotes immunological alterations.

EBV latent transcripts were also significantly upregulated in the brain and the spleen at day 28 of infection. This indicates that primary peripheral infection can result in latent persistence of EBV in the periphery and the CNS of rabbits. The spleen and the brain were reported to be the site of latent persistence of MHV68 in mice (Kang et al., 2012; Terry et al., 2000). Treating mice with CsA resulted in viral reactivation in both of these sites (Kang et al., 2012). This is consistent with the previous study showing that EBV persisted latently for months in the periphery (blood and spleen) of rabbits, and could be reactivated using CsA (Khan et al., 2015). Thus, presumably EBV reaches the brain during primary asymptomatic infection but remains dormant in the CNS tissue.

Additionally, it was observed that (1) the mRNA levels of IL-1 $\beta$  and TNF- $\alpha$  were significantly elevated at the later stage of infection; 28dpi in the spleen, brain and the spinal cord of rabbits, (2) the upregulation of IL-6 was concomitant with increased viral load in the periphery and the CNS at 14dpi, and (3) upregulated IFN- $\gamma$  was prominent during the first week and fourth week of infection.

In humans, increased EBV load during primary infection has been shown to be associated with raised levels of IL-6 (Yang & Gao, 2020). During viral reactivation, however, the expression of TNF- $\alpha$  increases. IFN- $\gamma$  and IL-10 are elevated during both primary and reactivated EBV (Yang & Gao, 2020). Increased levels of IL-6 and TNF- $\alpha$  are also detected in HIV patients with high EBV load (reactivation) (Petrara et al., 2012). In agreement with the observation that EBER2 expression correlated strongly

with IL-6 expression in the brain and the spleen, it has been previously shown that EBV2 expression *in vitro* is associated with high levels of IL-6 produced by infected B cells (Wu et al., 2007). This proinflammatory cytokine appears to be instrumental for the activation and expansion of infected B cells (Mauray et al., 2000; Wu et al., 2007).

The immune pressure over EBV infected cells governs what viral proteins are expressed. Some of the immune pressure is exerted by cytokines released by immune cells responding to the virus. Also, infected cells themselves can release soluble mediators that alter the expression of some viral proteins (Kis et al., 2010). This can offer a plausible explanation to the correlation seen between viral transcripts and cytokines expression in rabbits. For examples, IL-6 has been shown to influence EBV infected cells to downregulate the expression of the latent viral proteins EBNA-2 and LMP-1, and to undergo cell cycle arrest and subsequent death (Altmeyer et al., 1997). Additionally, the release of IFN- $\alpha$  by newly infected cells is associated with EBV expression (Jochum et al., 2012). Another example is that in *in vitro* experiments, diffused cytokines produced by CD4<sup>+</sup> T cells including IL-4, IL-10, IL-13 and IL-21, have been shown to cause EBV infected cells to switch from one type of latency to another, depending on the type of infected cells (Kis et al., 2006, 2010, 2011; Nagy et al., 2012). In other words, T cell cytokines can trigger infected cells to downregulate certain viral proteins and upregulate others. Similarly, IL-4 expression can trigger EBV reactivation in some cell types but not in others (Wang et al., 2021). This suggests that cytokine-induced up-/ downregulation of certain viral proteins is cell-specific. Moreover, IL-4 and IL-13 can induce isotype switch to IgG4 and IgE in naïve B cells, the target of EBV (Punnonen et al., 1993). This may partly explain how EBV can be involved in autoimmunity and atopy.

#### 4.4.2 Significance of Upregulated Inflammatory Cytokines During EBV Infection

The expression of IL-1 $\beta$ , TNF- $\alpha$  and IFN- $\gamma$  in the CNS is associated with impairment of BBB (Daniels et al., 2014; Förster et al., 2008; Phares et al., 2006; Tsao et al., 2001; Wong et al., 2004). CNS viral infections can trigger the production of these inflammatory cytokines, which compromises the integrity of BBB, for example by altering the expression of brain endothelia tight junction proteins (Bonney et al., 2019; Chai et al., 2014; Li et al., 2015; Minagar et al., 2003). Thus, BBB breakdown could be both a pre-requisite and consequence of CNS viral infections (Cain et al., 2017; Chai et al., 2014; Li et al., 2015). One could argue that increased mRNA levels of IL-1 $\beta$ , TNF- $\alpha$  at 28dpi may be followed by increased BBB permeability and recurrent influx of immune cells into the CNS. Whether EBV infection disrupts BBB integrity warrants further investigation. Additionally, TNF- $\alpha$  can enhance the expression of matrix metalloproteinases (MMPs) (Zeni et al., 2007). MMP2 and MMP9 proteolytically destroy dystroglycans; the receptors that secure the attachment of astrocytes end feet to brain parenchymal basement membrane (Agrawal et al., 2006). This increases the leakage of CNS barriers allowing for the influx of leukocytes into the CNS.

IL-1 $\beta$  is another cytokine that can be induced following viral infections and is required to control CNS infections (Ramos et al., 2012). Inflammasome activation and increased production of IL-1 $\beta$  has been shown in EBV infected human monocytes (Torii et al., 2017). Additionally, IL1-producing astrocytes were found to cause damage to neurons after recovery from flavivirus encephalitis (Garber et al., 2018). Administration of IL-1 $\beta$  has been demonstrated to render C57BL/6 mice susceptible to virus-induced EAE, although these mice are naturally EAE-resistant (Pullen et al.,

1995). However, abrogation of IL1 signaling is associated with defective antiviral T cell response and aggravated burden of viral disease in the CNS (Kim et al., 2012; Menu & Vince, 2011). Therefore, IL-1 $\beta$  is vital in efficient response against viruses but can also contribute to exaggerated inflammatory response.

Interferons are critical components of antiviral response and have been shown to play essential roles in halting the spread of viral infection within the CNS (Detje et al., 2009; Hwang & Bergmann, 2020). IFN- $\gamma$  signaling in the CNS plays a role in limiting viral replication and enhancing clearance of viruses, particularly neurotropic viruses (González et al., 2006; Parra et al., 1999). For example, IFN- $\gamma$  has been found to promote viral clearance from spinal cord neurons, and delay onset of CNS disease in alphavirus-infected mice (Baxter & Griffin, 2016; Binder & Griffin, 2001). On the other hand, IFN- $\gamma$  may prolong the immunopathology and thus delay recovery from CNS viral infections (Baxter & Griffin, 2016). Persistent release of IFN- $\gamma$  has been demonstrated to hinder the establishment of tissue-resident memory CD8<sup>+</sup> T cells (T<sub>RM</sub> cells) leading to prolonged retention of viruses within the CNS (Baxter & Griffin, 2020). While continuous production of IFN- $\gamma$  after amelioration of flavivirus encephalitis in mice leads to sustained activation of microglia and damage to neurons and neuronal synapses resulting in post infectious CNS disease (Garber et al., 2019). Indeed, IFN- $\gamma$  secreted by CNS infiltrating Th1 cells is highly efficient in activating microglia. Activated microglia proliferate, become bigger in size, and shift in morphology towards the less branching amoeboid cells (Ta et al., 2019). Under the influence of IFN- $\gamma$ , microglia upregulates the expression of MHC II, CD86, and IL-6, and amplify the production of TNF- $\alpha$  and reactive nitrogen species, all of which accentuate tissue injury (Browne et al., 2013; Meda et al., 1995; Murphy et al., 2010; Ta et al., 2019; Tan et al., 1999).

IFN- $\gamma$  is also indispensable for the prevention of exaggerated inflammatory response in the CNS. For instance, the loss of IFN- $\gamma$  expression facilitates EAE development in BALB/c and enhances pro-inflammatory TNF- $\alpha$  expression in the CNS (Krakowski & Owens, 1996). Similarly, elimination of IFN- $\gamma$  signaling during HSV-1 encephalitis in mice causes an abrupt surge in the levels of IL-6 and IL-17, boosts the influx of pathogenic neutrophils into the brainstem, and increases death in infected animals (Ramakrishna & Cantin, 2018).

As for the role of IFN- $\gamma$  during EBV infection, IFN- $\gamma$  released by antiviral NK cells and T cells, is pronounced at the initial site of infection within the oral cavity, where IFN- $\gamma$  limits EBV infection (Jud et al., 2017; Lotz et al., 1985; Strowig et al., 2008; Thorley-Lawson, 1981). During early days of infection, myeloid DCs recognize EBV infected cells and activate CD56<sup>bright</sup> CD16<sup>-</sup> NK cells to produce high levels of IFN- $\gamma$ . This cytokine is highly potent to obstruct the transformation of infected cells by EBV. It has also been shown to delay the expression of EBV latent protein, LMP-1, during the first week of infection *in vitro* (Strowig et al., 2008). In cultures of EBV infected cells, protein levels of IFN- $\gamma$  increases, and correlates negatively with the frequency of infected B cells (Sohlberg et al., 2013). The secretion of IFN- $\gamma$  and TNF- $\alpha$  by degranulating NK cells is also vital in eliminating EBV lytically infected cells (López-Montañés et al., 2017).

Additionally, proinflammatory IL-6 was markedly elevated in rabbits developing aggregates in the CNS. Thus, it can be argued that this cytokine is a major player in the pathogenesis of EBV-associated neuroinflammation. It is believed that IL-6 is instrumental in the development of TMEV-induced EAE disease, by promoting the generation of the pathogenic Th17 cell response, and supporting the survival of virus infected cells in the CNS (Hou et al., 2014; Kim, 2021). There were also

differences between the expression of IL-2 and IL-6 mRNAs and their protein levels in this study. This may be ascribed to short half-life of the protein, for instance when it is rapidly consumed right after its production. This can also occur when the availability of protein epitopes to capture antibody in the ELISA is suboptimal, or as a result of posttranslational modifications. Variations in biopsied region of the brain cortex, used for total RNA extraction and protein purification can also introduce discrepancies.



## Chapter 5: Conclusion

Viruses are believed to be associated with several neurodegenerative diseases; e.g., HSV in Alzheimer's disease, HHV6 and EBV in MS, and influenza virus in Parkinson's disease (De Chiara et al., 2012; Giovannoni et al., 2006; Mattson, 2004). Research on the link between latently persistent viral infections and the pathogenesis of CNS diseases is enormously expanding the understanding of possible disease pathways. The findings of this study support the role of peripheral EBV infection in promoting CNS inflammation and myelin injury.

In spite of substantial efforts over the last 6 decades in studying EBV, there are still gaps in the understanding of the details of viral pathogenesis, and key aspects of the virus life cycle. There is a pressing need to understand how the virus behaves in the host and how that affects various organ systems. The work presented in this dissertation will hopefully serve as a foundation for future research into the viral dynamics and the impact of silent EBV infection. A number of outstanding questions emerge from this project:

- Does EBV persist chronically in the CNS once it reaches there? If yes, does EBV cause recurrent bouts of immune influx into the CNS?
- Do EBV infected cells damage the CNS barriers?
- How does each cell population in the inflamed CNS contribute to viral disease or viral clearance?
- What are the underlying mechanisms for demyelination in rabbits CNS?
- What are the differences, if any, in the course of CNS viral infection between males and females, neonates and older animals?

## 5.1 Limitations and Future Research

The aim of this study was to demonstrate the nature of the link between EBV infection and MS pathogenesis. One of the main limitations of this work, is that the rabbit model used here is a model for EBV infection and not for MS, and thus interpretation of the results in relation to MS pathology should be made with caution. As an EBV model, however, rabbits are highly relevant to explore the biology of EBV as a risk factor or etiologic factor for various diseases. Another study limitation is that outbred animals were used in this study, hence the large variability in viral dynamics and heterogeneity in the extent of immune infiltration in the CNS. Admittedly, this variation mirrors the differences in host-virus interaction in humans. Additionally, the number of animals used in investigating viral dynamics over time was small. Future studies should use a bigger number of animals to address specific aspects of EBV infection. Finally, the limited availability of well-characterized antibodies specific for rabbits and suitable for fluorescence activated cell sorting (FACS) made the characterization of anti-EBV immune response challenging.

Given the lack of successful vaccines against EBV, and the multitude of diseases that the virus is associated with, this rabbit model represents a unique opportunity to explore unidentified characteristics of EBV infection and generate wealth of data of translational value to the human host. One goal of research using animal models for EBV infection is to identify critical points during EBV latency that can be targeted for therapy. The rabbit model can help determine important viral targets for the development of novel antiviral drugs, and potentially develop prophylactic and therapeutic vaccines. Moreover, EBV infection in rabbits can be utilized to identify biomarkers for EBV induced neuroinflammation and associated diseases, in the blood, serum, and CSF. This could be beneficial in identifying EBV

infected individuals at risk of CNS inflammation and introducing preventive interventions.

A significant implication of EBV infection in rabbits is that the virus promotes neuroinflammation, but other factors can influence the outcome of the infection. Vitamin D, and HLA alleles are believed to interact with EBV to shape disease susceptibility in people with MS (Giovannoni & Ebers, 2007; Teymoori-Rad et al., 2019; Wergeland et al., 2016). This is important because not every EBV positive individual develops MS, although every MS patient is EBV positive. No animal model is ideal to encompass all the factors that contribute to disease complexity. However, factors that may contribute to the heterogeneity of infection outcome between animals should be evaluated, including sex-based differences in immune response, composition of gut microbiota, and genetic factors (Erickson et al., 2018; Erny et al., 2015).

Also, research approaches to determine CNS regions with the greatest vulnerability to EBV-induced neuroinflammation are needed. This also includes the use of a combination of cell markers, as in FACS, to identify all cell subsets susceptible to EBV infection. Techniques for single cell analysis can help dissect cell-specific impact of EBV.

It is also critical to validate disease outcome in rabbits with EBV infection in humans. However, this can be tricky, as the majority of humans contract EBV silently. This makes it challenging to correlate viral kinetics during the acute infection in humans and rabbits. Alternatively, samples from IM patients can be valuable. Brain imaging of EBV infected rabbits and IM patients, even in the absence of neurological manifestations, can help validate experimental infection data. Additionally, humans

and rabbits have distinct immune cell composition (Kennedy et al., 2016), and translating animal results to humans has to be exercised with caution.

Additionally, it is essential to identify the route by which EBV infected cells enter the CNS. EBV could also infect cells that make up CNS barriers (Casiraghi et al., 2011). Alternatively, immune cells that respond to the infection can release inflammatory mediators, such as TNF- $\alpha$  and IL-1 $\beta$ , which disrupt the integrity of the CNS barriers and facilitate virus entry (Mastorakos & McGavern, 2019). Furthermore, identifying antigen specificity of the lymphoid infiltrate in rabbits CNS could further explain EBV neuropathology and identify the extent of the damage brought about by virus infected cells and immune response directed at the virus.

## References

- Abbott, N. J., Patabendige, A. A., Dolman, D. E., Yusof, S. R., & Begley, D. J. (2010). Structure and function of the blood-brain barrier. *Neurobiology of Disease*, *37*(1), 13–25. <https://doi.org/10.1016/j.nbd.2009.07.030>
- Abbott, R. J., Pachnio, A., Pedroza-Pacheco, I., Leese, A. M., Begum, J., Long, H. M., Croom-Carter, D., Stacey, A., Moss, P. A. H., Hislop, A. D., Borrow, P., Rickinson, A. B., & Bell, A. I. (2017). Asymptomatic Primary Infection with Epstein-Barr Virus: Observations on Young Adult Cases. *Journal of Virology*, *91*(21), e00382-17. <https://doi.org/10.1128/JVI.00382-17>
- Adhikary, D., Behrends, U., Moosmann, A., Witter, K., Bornkamm, G. W., & Mautner, J. (2006). Control of Epstein-Barr virus infection in vitro by T helper cells specific for virion glycoproteins. *The Journal of Experimental Medicine*, *203*(4), 995–1006. <https://doi.org/10.1084/jem.20051287>
- Adhikary, D., Damaschke, J., Mautner, J., & Behrends, U. (2020). The Epstein-Barr Virus Major Tegument Protein BNRF1 Is a Common Target of Cytotoxic CD4+ T Cells. *Journal of Virology*, *94*(15), e00284-20. <https://doi.org/10.1128/JVI.00284-20>
- Afrasiabi, A., Parnell, G. P., Fewings, N., Schibeci, S. D., Basuki, M. A., Chandramohan, R., Zhou, Y., Taylor, B., Brown, D. A., Swaminathan, S., McKay, F. C., Stewart, G. J., & Booth, D. R. (2019). Evidence from genome wide association studies implicates reduced control of Epstein-Barr virus infection in multiple sclerosis susceptibility. *Genome Medicine*, *11*(1), 26. <https://doi.org/10.1186/s13073-019-0640-z>
- Afrasiabi, A., Parnell, G. P., Swaminathan, S., Stewart, G. J., & Booth, D. R. (2020). The interaction of Multiple Sclerosis risk loci with Epstein-Barr virus phenotypes implicates the virus in pathogenesis. *Scientific Reports*, *10*(1), 193. <https://doi.org/10.1038/s41598-019-55850-z>
- Agostini, S., Mancuso, R., Guerini, F. R., D'Alfonso, S., Agliardi, C., Hernis, A., Zanzottera, M., Barizzone, N., Leone, M. A., Caputo, D., Rovaris, M., & Clerici, M. (2018). HLA alleles modulate EBV viral load in multiple sclerosis. *Journal of Translational Medicine*, *16*(1), 80. <https://doi.org/10.1186/s12967-018-1450-6>

- Agrawal, S., Anderson, P., Durbeej, M., van Rooijen, N., Ivars, F., Opdenakker, G., & Sorokin, L. M. (2006). Dystroglycan is selectively cleaved at the parenchymal basement membrane at sites of leukocyte extravasation in experimental autoimmune encephalomyelitis. *The Journal of Experimental Medicine*, 203(4), 1007–1019. <https://doi.org/10.1084/jem.20051342>
- Alharbi, F. M. (2015). Update in vitamin D and multiple sclerosis. *Neurosciences*, 20(4), 329–335. <https://doi.org/10.17712/nsj.2015.4.20150357>
- Altmeyer, A., Simmons, R. C., Krajewski, S., Reed, J. C., Bornkamm, G. W., & Chen-Kiang, S. (1997). Reversal of EBV immortalization precedes apoptosis in IL-6-induced human B cell terminal differentiation. *Immunity*, 7(5), 667–677. [https://doi.org/10.1016/s1074-7613\(00\)80387-8](https://doi.org/10.1016/s1074-7613(00)80387-8)
- Angelini, D. F., Serafini, B., Piras, E., Severa, M., Coccia, E. M., Rosicarelli, B., Ruggieri, S., Gasperini, C., Buttari, F., Centonze, D., Mechelli, R., Salvetti, M., Borsellino, G., Aloisi, F., & Battistini, L. (2013). Increased CD8+ T cell response to Epstein-Barr virus lytic antigens in the active phase of multiple sclerosis. *PLoS Pathogens*, 9(4), e1003220. <https://doi.org/10.1371/journal.ppat.1003220>
- Archibald, L. K., & Quisling, R. G. (2013). Central Nervous System Infections. *Textbook of Neurointensive Care*, 427–517. [https://doi.org/10.1007/978-1-4471-5226-2\\_22](https://doi.org/10.1007/978-1-4471-5226-2_22)
- Arotcarena, M.-L., Dovero, S., Prigent, A., Bourdenx, M., Camus, S., Porras, G., Thiolat, M.-L., Tasselli, M., Aubert, P., Kruse, N., Mollenhauer, B., Trigo Damas, I., Estrada, C., Garcia-Carrillo, N., Vaikath, N. N., El-Agnaf, O. M. A., Herrero, M. T., Vila, M., Obeso, J. A., ... Bezard, E. (2020). Bidirectional gut-to-brain and brain-to-gut propagation of synucleinopathy in non-human primates. *Brain: A Journal of Neurology*, 143(5), 1462–1475. <https://doi.org/10.1093/brain/awaa096>
- Ascherio, A., & Munger, K. L. (2010). 99th Dahlem Conference on Infection, Inflammation and Chronic Inflammatory Disorders: Epstein–Barr virus and multiple sclerosis: epidemiological evidence. *Clinical and Experimental Immunology*, 160(1), 120–124. <https://doi.org/10.1111/j.1365-2249.2010.04121.x>
- Ascherio, A., Munger, K. L., Lennette, E. T., Spiegelman, D., Hernán, M. A., Olek, M. J., Hankinson, S. E., & Hunter, D. J. (2001). Epstein-Barr virus antibodies and risk of multiple sclerosis: A prospective study. *JAMA*, 286(24), 3083–3088. <https://doi.org/10.1001/jama.286.24.3083>

- Ashley, S. L., Pretto, C. D., Stier, M. T., Kadiyala, P., Castro-Jorge, L., Hsu, T.-H., Doherty, R., Carnahan, K. E., Castro, M. G., Lowenstein, P. R., & Spindler, K. R. (2017). Matrix Metalloproteinase Activity in Infections by an Encephalitic Virus, Mouse Adenovirus Type 1. *Journal of Virology*, *91*(6), e01412-16. <https://doi.org/10.1128/JVI.01412-16>
- Aslan, N., Watkin, L. B., Gil, A., Mishra, R., Clark, F. G., Welsh, R. M., Ghersi, D., Luzuriaga, K., & Selin, L. K. (2017). Severity of Acute Infectious Mononucleosis Correlates with Cross-Reactive Influenza CD8 T-Cell Receptor Repertoires. *MBio*, *8*(6), e01841-17. <https://doi.org/10.1128/mBio.01841-17>
- Auclair, H., Ouk-Martin, C., Roland, L., Santa, P., Al Mohamad, H., Faumont, N., Feuillard, J., & Jayat-Vignoles, C. (2019). EBV Latency III–Transformed B Cells Are Inducers of Conventional and Unconventional Regulatory T Cells in a PD-L1–Dependent Manner. *The Journal of Immunology Author Choice*, *203*(6), 1665–1674. <https://doi.org/10.4049/jimmunol.1801420>
- Audoy-Rémus, J., Richard, J.-F., Soulet, D., Zhou, H., Kubes, P., & Vallières, L. (2008). Rod-Shaped Monocytes Patrol the Brain Vasculature and Give Rise to Perivascular Macrophages under the Influence of Proinflammatory Cytokines and Angiopoietin-2. *Journal of Neuroscience*, *28*(41), 10187–10199. <https://doi.org/10.1523/JNEUROSCI.3510-08.2008>
- Balfour, H. H., Odumade, O. A., Schmeling, D. O., Mullan, B. D., Ed, J. A., Knight, J. A., Vezina, H. E., Thomas, W., & Hogquist, K. A. (2013). Behavioral, virologic, and immunologic factors associated with acquisition and severity of primary Epstein-Barr virus infection in university students. *The Journal of Infectious Diseases*, *207*(1), 80–88. <https://doi.org/10.1093/infdis/jis646>
- Barcellos, L. F., Sawcer, S., Ramsay, P. P., Baranzini, S. E., Thomson, G., Briggs, F., Cree, B. C. A., Begovich, A. B., Villoslada, P., Montalban, X., Uccelli, A., Savettieri, G., Lincoln, R. R., DeLoa, C., Haines, J. L., Pericak-Vance, M. A., Compston, A., Hauser, S. L., & Oksenberg, J. R. (2006). Heterogeneity at the HLA-DRB1 locus and risk for multiple sclerosis. *Human Molecular Genetics*, *15*(18), 2813–2824. <https://doi.org/10.1093/hmg/ddl223>
- Bar-Or, A., Fawaz, L., Fan, B., Darlington, P. J., Rieger, A., Ghorayeb, C., Calabresi, P. A., Waubant, E., Hauser, S. L., Zhang, J., & Smith, C. H. (2010). Abnormal B-cell cytokine responses a trigger of T-cell-mediated disease in MS? *Annals of Neurology*, *67*(4), 452–461. <https://doi.org/10.1002/ana.21939>

- Bar-Or, A., Pender, M. P., Khanna, R., Steinman, L., Hartung, H.-P., Maniar, T., Croze, E., Aftab, B. T., Giovannoni, G., & Joshi, M. A. (2020). Epstein-Barr Virus in Multiple Sclerosis: Theory and Emerging Immunotherapies. *Trends in Molecular Medicine*, 26(3), 296–310. <https://doi.org/10.1016/j.molmed.2019.11.003>
- Baxter, V. K., & Griffin, D. E. (2016). Interferon gamma modulation of disease manifestation and the local antibody response to alphavirus encephalomyelitis. *The Journal of General Virology*, 97(11), 2908–2925. <https://doi.org/10.1099/jgv.0.000613>
- Baxter, V. K., & Griffin, D. E. (2020). Interferon-Gamma Modulation of the Local T Cell Response to Alphavirus Encephalomyelitis. *Viruses*, 12(1), 113. <https://doi.org/10.3390/v12010113>
- Belbasis, L., Bellou, V., Evangelou, E., Ioannidis, J. P. A., & Tzoulaki, I. (2015). Environmental risk factors and multiple sclerosis: An umbrella review of systematic reviews and meta-analyses. *The Lancet. Neurology*, 14(3), 263–273. [https://doi.org/10.1016/S1474-4422\(14\)70267-4](https://doi.org/10.1016/S1474-4422(14)70267-4)
- Berger, T., Weerth, S., Kojima, K., Linington, C., Wekerle, H., & Lassmann, H. (1997). Experimental autoimmune encephalomyelitis: The antigen specificity of T lymphocytes determines the topography of lesions in the central and peripheral nervous system. *Laboratory Investigation; a Journal of Technical Methods and Pathology*, 76(3), 355–364.
- Berg-Hansen, P., & Celius, E. G. (2015). Socio-economic factors and immigrant population studies of multiple sclerosis. *Acta Neurologica Scandinavica*, 132(199), 37–41. <https://doi.org/10.1111/ane.12429>
- Berg-Hansen, P., Moen, S. M., Sandvik, L., Harbo, H. F., Bakken, I. J., Stoltenberg, C., & Celius, E. G. (2015). Prevalence of multiple sclerosis among immigrants in Norway. *Multiple Sclerosis (Houndmills, Basingstoke, England)*, 21(6), 695–702. <https://doi.org/10.1177/1352458514554055>
- Bevan, R. J., Evans, R., Griffiths, L., Watkins, L. M., Rees, M. I., Magliozzi, R., Allen, I., McDonnell, G., Kee, R., Naughton, M., Fitzgerald, D. C., Reynolds, R., Neal, J. W., & Howell, O. W. (2018). Meningeal inflammation and cortical demyelination in acute multiple sclerosis. *Annals of Neurology*, 84(6), 829–842. <https://doi.org/10.1002/ana.25365>



- Bickham, K., Goodman, K., Paludan, C., Nikiforow, S., Tsang, M. L., Steinman, R. M., & Münz, C. (2003). Dendritic Cells Initiate Immune Control of Epstein-Barr Virus Transformation of B Lymphocytes In Vitro. *The Journal of Experimental Medicine*, *198*(11), 1653–1663. <https://doi.org/10.1084/jem.20030646>
- Binder, G. K., & Griffin, D. E. (2001). Interferon-gamma-mediated site-specific clearance of alphavirus from CNS neurons. *Science (New York, N.Y.)*, *293*(5528), 303–306. <https://doi.org/10.1126/science.1059742>
- Blackmore, S., Hernandez, J., Juda, M., Ryder, E., Freund, G. G., Johnson, R. W., & Steelman, A. J. (2017). Influenza infection triggers disease in a genetic model of experimental autoimmune encephalomyelitis. *Proceedings of the National Academy of Sciences*, *114*(30), E6107–E6116. <https://doi.org/10.1073/pnas.1620415114>
- Bø, L., Vedeler, C. A., Nyland, H. I., Trapp, B. D., & Mørk, S. J. (2003). Subpial demyelination in the cerebral cortex of multiple sclerosis patients. *Journal of Neuropathology and Experimental Neurology*, *62*(7), 723–732. <https://doi.org/10.1093/jnen/62.7.723>
- Bonney, S., Seitz, S., Ryan, C. A., Jones, K. L., Clarke, P., Tyler, K. L., & Siegenthaler, J. A. (2019). Gamma Interferon Alters Junctional Integrity via Rho Kinase, Resulting in Blood-Brain Barrier Leakage in Experimental Viral Encephalitis. *MBio*, *10*(4), e01675-19. <https://doi.org/10.1128/mBio.01675-19>
- Borggrewe, M., Grit, C., Vainchtein, I. D., Brouwer, N., Wesseling, E. M., Laman, J. D., Eggen, B. J. L., Kooistra, S. M., & Boddeke, E. W. G. M. (2021). Regionally diverse astrocyte subtypes and their heterogeneous response to EAE. *Glia*, *69*(5), 1140–1154. <https://doi.org/10.1002/glia.23954>
- Boukhvalova, M. S., Mortensen, E., Mbaye, A., Lopez, D., Kastrukoff, L., & Blanco, J. C. G. (2019). Herpes Simplex Virus 1 Induces Brain Inflammation and Multifocal Demyelination in the Cotton Rat *Sigmodon hispidus*. *Journal of Virology*, *94*(1), e01161-19. <https://doi.org/10.1128/JVI.01161-19>
- Bradl, M., & Lassmann, H. (2010). Oligodendrocytes: Biology and pathology. *Acta Neuropathologica*, *119*(1), 37–53. <https://doi.org/10.1007/s00401-009-0601-5>

- Browne, T. C., McQuillan, K., McManus, R. M., O'Reilly, J.-A., Mills, K. H. G., & Lynch, M. A. (2013). IFN- $\gamma$  Production by Amyloid  $\beta$ -Specific Th1 Cells Promotes Microglial Activation and Increases Plaque Burden in a Mouse Model of Alzheimer's Disease. *The Journal of Immunology*, *190*(5), 2241–2251. <https://doi.org/10.4049/jimmunol.1200947>
- Brum, D. G., Luizon, M. R., Santos, A. C., Lana-Peixoto, M. A., Rocha, C. F., Brito, M. L., Oliveira, E. M. L. de, Bichuetti, D. B., Gabbai, A. A., Diniz, D. S., Kaimen-Maciel, D. R., Comini-Frota, E. R., Wiezel, C. E. V., Muniz, Y. C. N., Costa, R. M. da S., Mendes-Junior, C. T., Donadi, E. A., Barreira, A. A., & Simões, A. L. (2013). European Ancestry Predominates in Neuromyelitis Optica and Multiple Sclerosis Patients from Brazil. *PLOS ONE*, *8*(3), e58925. <https://doi.org/10.1371/journal.pone.0058925>
- Bu, W., Hayes, G. M., Liu, H., Gemmell, L., Schmeling, D. O., Radecki, P., Aguilar, F., Burbelo, P. D., Woo, J., Balfour, H. H., & Cohen, J. I. (2016). Kinetics of Epstein-Barr Virus (EBV) Neutralizing and Virus-Specific Antibodies after Primary Infection with EBV. *Clinical and Vaccine Immunology : CVI*, *23*(4), 363–369. <https://doi.org/10.1128/CVI.00674-15>
- Cain, M. D., Salimi, H., Gong, Y., Yang, L., Hamilton, S. L., Heffernan, J. R., Hou, J., Miller, M. J., & Klein, R. S. (2017). Virus entry and replication in the brain precedes blood-brain barrier disruption during intranasal alphavirus infection. *Journal of Neuroimmunology*, *308*, 118–130. <https://doi.org/10.1016/j.jneuroim.2017.04.008>
- Calabrese, M., Filippi, M., & Gallo, P. (2010). Cortical lesions in multiple sclerosis. *Nature Reviews. Neurology*, *6*(8), 438–444. <https://doi.org/10.1038/nrneurol.2010.93>
- Carriel, V., Campos, A., Alaminos, M., Raimondo, S., & Geuna, S. (2017). Staining Methods for Normal and Regenerative Myelin in the Nervous System. *Methods in Molecular Biology (Clifton, N.J.)*, *1560*, 207–218. [https://doi.org/10.1007/978-1-4939-6788-9\\_15](https://doi.org/10.1007/978-1-4939-6788-9_15)
- Casiraghi, C., Dorovini-Zis, K., & Horwitz, M. S. (2011). Epstein-Barr virus infection of human brain microvessel endothelial cells: A novel role in multiple sclerosis. *Journal of Neuroimmunology*, *230*(1–2), 173–177. <https://doi.org/10.1016/j.jneuroim.2010.08.003>
- Casiraghi, C., Márquez, A. C., Shanina, I., & Horwitz, M. S. (2015). Latent virus infection upregulates CD40 expression facilitating enhanced autoimmunity in a model of multiple sclerosis. *Scientific Reports*, *5*, 13995. <https://doi.org/10.1038/srep13995>

- Casiraghi, C., Shanina, I., Cho, S., Freeman, M. L., Blackman, M. A., & Horwitz, M. S. (2012). Gammaherpesvirus Latency Accentuates EAE Pathogenesis: Relevance to Epstein-Barr Virus and Multiple Sclerosis. *PLOS Pathogens*, 8(5), e1002715. <https://doi.org/10.1371/journal.ppat.1002715>
- Cavalcante, P., Serafini, B., Rosicarelli, B., Maggi, L., Barberis, M., Antozzi, C., Berrih-Aknin, S., Bernasconi, P., Aloisi, F., & Mantegazza, R. (2010). Epstein-Barr virus persistence and reactivation in myasthenia gravis thymus. *Annals of Neurology*, 67(6), 726–738. <https://doi.org/10.1002/ana.21902>
- Celarain, N., & Tomas-Roig, J. (2020). Aberrant DNA methylation profile exacerbates inflammation and neurodegeneration in multiple sclerosis patients. *Journal of Neuroinflammation*, 17(1), 21. <https://doi.org/10.1186/s12974-019-1667-1>
- Cencioni, M. T., Magliozzi, R., Nicholas, R., Ali, R., Malik, O., Reynolds, R., Borsellino, G., Battistini, L., & Muraro, P. A. (2017). Programmed death 1 is highly expressed on CD8+ CD57+ T cells in patients with stable multiple sclerosis and inhibits their cytotoxic response to Epstein-Barr virus. *Immunology*, 152(4), 660–676. <https://doi.org/10.1111/imm.12808>
- Chai, Q., He, W. Q., Zhou, M., Lu, H., & Fu, Z. F. (2014). Enhancement of blood-brain barrier permeability and reduction of tight junction protein expression are modulated by chemokines/cytokines induced by rabies virus infection. *Journal of Virology*, 88(9), 4698–4710. <https://doi.org/10.1128/JVI.03149-13>
- Chao, M. J., Barnardo, M. C. N. M., Lincoln, M. R., Ramagopalan, S. V., Herrera, B. M., Dymont, D. A., Montpetit, A., Sadovnick, A. D., Knight, J. C., & Ebers, G. C. (2008). HLA class I alleles tag HLA-DRB1\*1501 haplotypes for differential risk in multiple sclerosis susceptibility. *Proceedings of the National Academy of Sciences of the United States of America*, 105(35), 13069–13074. <https://doi.org/10.1073/pnas.0801042105>
- Chao, M. J., Ramagopalan, S. V., Herrera, B. M., Lincoln, M. R., Dymont, D. A., Sadovnick, A. D., & Ebers, G. C. (2009). Epigenetics in multiple sclerosis susceptibility: Difference in transgenerational risk localizes to the major histocompatibility complex. *Human Molecular Genetics*, 18(2), 261–266. <https://doi.org/10.1093/hmg/ddn353>
- Chatterjee, B., Deng, Y., Holler, A., Nunez, N., Azzi, T., Vanoaica, L. D., Müller, A., Zdimerova, H., Antsiferova, O., Zbinden, A., Capaul, R., Dreyer, J. H., Nadal, D., Becher, B., Robinson, M. D., Stauss, H., & Münz, C. (2019). CD8+ T cells retain protective functions despite sustained inhibitory receptor expression during Epstein-Barr virus infection in vivo. *PLoS Pathogens*, 15(5), e1007748. <https://doi.org/10.1371/journal.ppat.1007748>

- Chen, H. L., Hayashi, K., Koirala, T. R., Ino, H., Fujimoto, K., Yoshikawa, Y., Choudhury, C. R., & Akagi, T. (1997). Malignant lymphoma induction in rabbits by oral inoculation of crude virus fraction prepared from Ts-B6 cells (cynomolgus B-lymphoblastoid cells harboring Epstein-Barr virus-related simian herpesvirus). *Acta Medica Okayama*, *51*(3), 141–147. <https://doi.org/10.18926/AMO/30801>
- Chijioke, O., Müller, A., Feederle, R., Barros, M. H. M., Krieg, C., Emmel, V., Marcenaro, E., Leung, C. S., Antsiferova, O., Landtwing, V., Bossart, W., Moretta, A., Hassan, R., Boyman, O., Niedobitek, G., Delecluse, H.-J., Capaul, R., & Münz, C. (2013). Human Natural Killer Cells Prevent Infectious Mononucleosis Features by Targeting Lytic Epstein-Barr Virus Infection. *Cell Reports*, *5*(6), 1489–1498. <https://doi.org/10.1016/j.celrep.2013.11.041>
- Chiu, Y. F., & Sugden, B. (2016). Epstein-Barr Virus: The Path from Latent to Productive Infection. *Annual Review of Virology*, *3*(1), 359–372. <https://doi.org/10.1146/annurev-virology-110615-042358>
- Choi, S. R., Howell, O. W., Carassiti, D., Magliozzi, R., Gveric, D., Muraro, P. A., Nicholas, R., Roncaroli, F., & Reynolds, R. (2012). Meningeal inflammation plays a role in the pathology of primary progressive multiple sclerosis. *Brain: A Journal of Neurology*, *135*(Pt 10), 2925–2937. <https://doi.org/10.1093/brain/aws189>
- Church, T. M., Verma, D., Thompson, J., & Swaminathan, S. (2018). Efficient Translation of Epstein-Barr Virus (EBV) DNA Polymerase Contributes to the Enhanced Lytic Replication Phenotype of M81 EBV. *Journal of Virology*, *92*(6), e01794-17. <https://doi.org/10.1128/JVI.01794-17>
- Clottu, A. S., Mathias, A., Sailer, A. W., Schlupe, M., Seebach, J. D., Du Pasquier, R., & Pot, C. (2017). EB12 Expression and Function: Robust in Memory Lymphocytes and Increased by Natalizumab in Multiple Sclerosis. *Cell Reports*, *18*(1), 213–224. <https://doi.org/10.1016/j.celrep.2016.12.006>
- Cocuzza, C. E., Piazza, F., Musumeci, R., Oggioni, D., Andreoni, S., Gardinetti, M., Fusco, L., Frigo, M., Banfi, P., Rottoli, M. R., Confalonieri, P., Rezzonico, M., Ferrò, M. T., Cavaletti, G., & EBV-MS Italian Study Group. (2014). Quantitative detection of Epstein-Barr virus DNA in cerebrospinal fluid and blood samples of patients with relapsing-remitting multiple sclerosis. *PloS One*, *9*(4), e94497. <https://doi.org/10.1371/journal.pone.0094497>
- Cohen, J. I. (2020). Herpesvirus latency. *The Journal of Clinical Investigation*, *130*(7), 3361–3369. <https://doi.org/10.1172/JCI136225>

- Coleman, C. B., Daud, I. I., Ogolla, S. O., Ritchie, J. A., Smith, N. A., Sumba, P. O., Dent, A. E., & Rochford, R. (2017). Epstein-Barr Virus Type 2 Infects T Cells in Healthy Kenyan Children. *The Journal of Infectious Diseases*, 216(6), 670–677. <https://doi.org/10.1093/infdis/jix363>
- Constantinescu, C. S., Hilliard, B., Ventura, E., Wysocka, M., Showe, L., Lavi, E., Fujioka, T., Scott, P., Trinchieri, G., & Rostami, A. (2001). Modulation of susceptibility and resistance to an autoimmune model of multiple sclerosis in prototypically susceptible and resistant strains by neutralization of interleukin-12 and interleukin-4, respectively. *Clinical Immunology (Orlando, Fla.)*, 98(1), 23–30. <https://doi.org/10.1006/clim.2000.4944>
- Cornberg, M., Clute, S. C., Watkin, L. B., Saccoccio, F. M., Kim, S.-K., Naumov, Y. N., Brehm, M. A., Aslan, N., Welsh, R. M., & Selin, L. K. (2010). CD8 T cell cross-reactivity networks mediate heterologous immunity in human EBV and murine vaccinia virus infections. *Journal of Immunology (Baltimore, Md.: 1950)*, 184(6), 2825–2838. <https://doi.org/10.4049/jimmunol.0902168>
- Cornelius, A. D. A., Hosseini, S., Schreier, S., Fritsch, D., Weichert, L., Michaelsen-Preusse, K., Fendt, M., & Kröger, A. (2020). Langkat virus infection affects hippocampal neuron morphology and function in mice without disease signs. *Journal of Neuroinflammation*, 17(1), 278. <https://doi.org/10.1186/s12974-020-01951-w>
- Croia, C., Astorri, E., Murray-Brown, W., Willis, A., Brokstad, K. A., Sutcliffe, N., Piper, K., Jonsson, R., Tappuni, A. R., Pitzalis, C., & Bombardieri, M. (2014). Implication of Epstein-Barr virus infection in disease-specific autoreactive B cell activation in ectopic lymphoid structures of Sjögren's syndrome. *Arthritis & Rheumatology (Hoboken, N.J.)*, 66(9), 2545–2557. <https://doi.org/10.1002/art.38726>
- Croia, C., Serafini, B., Bombardieri, M., Kelly, S., Humby, F., Severa, M., Rizzo, F., Coccia, E. M., Migliorini, P., Aloisi, F., & Pitzalis, C. (2013). Epstein-Barr virus persistence and infection of autoreactive plasma cells in synovial lymphoid structures in rheumatoid arthritis. *Annals of the Rheumatic Diseases*, 72(9), 1559–1568. <https://doi.org/10.1136/annrheumdis-2012-202352>
- Daniels, B. P., Holman, D. W., Cruz-Orengo, L., Jujjavarapu, H., Durrant, D. M., & Klein, R. S. (2014). Viral pathogen-associated molecular patterns regulate blood-brain barrier integrity via competing innate cytokine signals. *MBio*, 5(5), e01476-01414. <https://doi.org/10.1128/mBio.01476-14>

- De Chiara, G., Marocci, M. E., Sgarbanti, R., Civitelli, L., Ripoli, C., Piacentini, R., Garaci, E., Grassi, C., & Palamara, A. T. (2012). Infectious Agents and Neurodegeneration. *Molecular Neurobiology*, *46*(3), 614–638. <https://doi.org/10.1007/s12035-012-8320-7>
- Deeba, E., Koptides, D., Gaglia, E., Constantinou, A., Lambrianides, A., Pantzaris, M., Krashias, G., & Christodoulou, C. (2019). Evaluation of Epstein-Barr virus-specific antibodies in Cypriot multiple sclerosis patients. *Molecular Immunology*, *105*, 270–275. <https://doi.org/10.1016/j.molimm.2018.12.010>
- DePaula-Silva, A. B., Gorbea, C., Doty, D. J., Libbey, J. E., Sanchez, J. M. S., Hanak, T. J., Cazalla, D., & Fujinami, R. S. (2019). Differential transcriptional profiles identify microglial- and macrophage-specific gene markers expressed during virus-induced neuroinflammation. *Journal of Neuroinflammation*, *16*(1), 152. <https://doi.org/10.1186/s12974-019-1545-x>
- Desforges, M., Le Coupanec, A., Dubeau, P., Bourgooin, A., Lajoie, L., Dubé, M., & Talbot, P. J. (2020). Human Coronaviruses and Other Respiratory Viruses: Underestimated Opportunistic Pathogens of the Central Nervous System? *Viruses*, *12*(1), 14. <https://doi.org/10.3390/v12010014>
- Detje, C. N., Meyer, T., Schmidt, H., Kreuz, D., Rose, J. K., Bechmann, I., Prinz, M., & Kalinke, U. (2009). Local type I IFN receptor signaling protects against virus spread within the central nervous system. *Journal of Immunology (Baltimore, Md.: 1950)*, *182*(4), 2297–2304. <https://doi.org/10.4049/jimmunol.0800596>
- DiSabato, D. J., Quan, N., & Godbout, J. P. (2016). Neuroinflammation: The devil is in the details. *Journal of Neurochemistry*, *139*(S2), 136–153. <https://doi.org/10.1111/jnc.13607>
- DiSano, K. D., Royce, D. B., Gilli, F., & Pachner, A. R. (2019). Central Nervous System Inflammatory Aggregates in the Theiler's Virus Model of Progressive Multiple Sclerosis. *Frontiers in Immunology*, *10*, 1821. <https://doi.org/10.3389/fimmu.2019.01821>
- Dobson, R., & Giovannoni, G. (2019). Multiple sclerosis—A review. *European Journal of Neurology*, *26*(1), 27–40. <https://doi.org/10.1111/ene.13819>
- Dohgu, S., Kataoka, Y., Ikesue, H., Naito, M., Tsuruo, T., Oishi, R., & Sawada, Y. (2000). Involvement of glial cells in cyclosporine-increased permeability of brain endothelial cells. *Cellular and Molecular Neurobiology*, *20*(6), 781–786. <https://doi.org/10.1023/a:1007015228318>

- Dohgu, S., Sumi, N., Nishioku, T., Takata, F., Watanabe, T., Naito, M., Shuto, H., Yamauchi, A., & Kataoka, Y. (2010). Cyclosporin A induces hyperpermeability of the blood-brain barrier by inhibiting autocrine adrenomedullin-mediated up-regulation of endothelial barrier function. *European Journal of Pharmacology*, *644*(1–3), 5–9. <https://doi.org/10.1016/j.ejphar.2010.05.035>
- Dohgu, S., Yamauchi, A., Nakagawa, S., Takata, F., Kai, M., Egawa, T., Naito, M., Tsuruo, T., Sawada, Y., Niwa, M., & Kataoka, Y. (2004). Nitric oxide mediates cyclosporine-induced impairment of the blood-brain barrier in cocultures of mouse brain endothelial cells and rat astrocytes. *European Journal of Pharmacology*, *505*(1–3), 51–59. <https://doi.org/10.1016/j.ejphar.2004.10.027>
- Dunmire, S. K., Grimm, J. M., Schmeling, D. O., Balfour, H. H., & Hogquist, K. A. (2015). The Incubation Period of Primary Epstein-Barr Virus Infection: Viral Dynamics and Immunologic Events. *PLoS Pathogens*, *11*(12), e1005286. <https://doi.org/10.1371/journal.ppat.1005286>
- Dunmire, S. K., Odumade, O. A., Porter, J. L., Reyes-Genere, J., Schmeling, D. O., Bilgic, H., Fan, D., Baechler, E. C., Balfour, H. H., & Hogquist, K. A. (2014). Primary EBV infection induces an expression profile distinct from other viruses but similar to hemophagocytic syndromes. *PloS One*, *9*(1), e85422. <https://doi.org/10.1371/journal.pone.0085422>
- Dunmire, S. K., Verghese, P. S., & Balfour, H. H. (2018). Primary Epstein-Barr virus infection. *Journal of Clinical Virology: The Official Publication of the Pan American Society for Clinical Virology*, *102*, 84–92. <https://doi.org/10.1016/j.jcv.2018.03.001>
- Dutta, R., & Trapp, B. D. (2011). Mechanisms of neuronal dysfunction and degeneration in multiple sclerosis. *Progress in Neurobiology*, *93*(1), 1–12. <https://doi.org/10.1016/j.pneurobio.2010.09.005>
- Engelhardt, B., Vajkoczy, P., & Weller, R. O. (2017). The movers and shapers in immune privilege of the CNS. *Nature Immunology*, *18*(2), 123–131. <https://doi.org/10.1038/ni.3666>
- Epstein, M. A., zur Hausen, H., Ball, G., & Rabin, H. (1975). Pilot experiments with EB virus in owl monkeys (*Aotus trivirgatus*). III. Serological and biochemical findings in an animal with reticuloproliferative disease. *International Journal of Cancer*, *15*(1), 17–22. <https://doi.org/10.1002/ijc.2910150103>

- Erickson, M. A., Liang, W. S., Fernandez, E. G., Bullock, K. M., Thysell, J. A., & Banks, W. A. (2018). Genetics and sex influence peripheral and central innate immune responses and blood-brain barrier integrity. *PloS One*, *13*(10), e0205769. <https://doi.org/10.1371/journal.pone.0205769>
- Erny, D., Hrabě de Angelis, A. L., Jaitin, D., Wieghofer, P., Staszewski, O., David, E., Keren-Shaul, H., Mhlahkoiv, T., Jakobshagen, K., Buch, T., Schwierzeck, V., Utermöhlen, O., Chun, E., Garrett, W. S., McCoy, K. D., Diefenbach, A., Staeheli, P., Stecher, B., Amit, I., & Prinz, M. (2015). Host microbiota constantly control maturation and function of microglia in the CNS. *Nature Neuroscience*, *18*(7), 965–977. <https://doi.org/10.1038/nn.4030>
- Escartin, C., Galea, E., Lakatos, A., O’Callaghan, J. P., Petzold, G. C., Serrano-Pozo, A., Steinhäuser, C., Volterra, A., Carmignoto, G., Agarwal, A., Allen, N. J., Araque, A., Barbeito, L., Barzilai, A., Bergles, D. E., Bonvento, G., Butt, A. M., Chen, W.-T., Cohen-Salmon, M., ... Verkhratsky, A. (2021). Reactive astrocyte nomenclature, definitions, and future directions. *Nature Neuroscience*, *24*(3), 312–325. <https://doi.org/10.1038/s41593-020-00783-4>
- Fagin, U., Nerbas, L., Vogl, B., & Jabs, W. J. (2017). Analysis of BZLF1 mRNA detection in saliva as a marker for active replication of Epstein-Barr virus. *Journal of Virological Methods*, *244*, 11–16. <https://doi.org/10.1016/j.jviromet.2017.02.016>
- Fagnani, C., Neale, M. C., Nisticò, L., Stazi, M. A., Ricigliano, V. A., Buscarinu, M. C., Salvetti, M., & Ristori, G. (2015). Twin studies in multiple sclerosis: A meta-estimation of heritability and environmentality. *Multiple Sclerosis (Houndmills, Basingstoke, England)*, *21*(11), 1404–1413. <https://doi.org/10.1177/1352458514564492>
- Farrell, P. J. (2019). Epstein–Barr Virus and Cancer. *Annual Review of Pathology: Mechanisms of Disease*, *14*(1), 29–53. <https://doi.org/10.1146/annurev-pathmechdis-012418-013023>
- Fernández-Menéndez, S., Fernández-Morán, M., Fernández-Vega, I., Pérez-Álvarez, A., & Villafani-Echazú, J. (2016). Epstein-Barr virus and multiple sclerosis. From evidence to therapeutic strategies. *Journal of the Neurological Sciences*, *361*, 213–219. <https://doi.org/10.1016/j.jns.2016.01.013>
- Filiano, A. J., Gadani, S. P., & Kipnis, J. (2015). Interactions of innate and adaptive immunity in brain development and function. *Brain Research*, *1617*, 18–27. <https://doi.org/10.1016/j.brainres.2014.07.050>



- Filiano, A. J., Gadani, S. P., & Kipnis, J. (2017). How and why do T cells and their derived cytokines affect the injured and healthy brain? *Nature Reviews. Neuroscience*, *18*(6), 375–384. <https://doi.org/10.1038/nrn.2017.39>
- Filippi, M., Bar-Or, A., Piehl, F., Preziosa, P., Solari, A., Vukusic, S., & Rocca, M. A. (2018). Multiple sclerosis. *Nature Reviews. Disease Primers*, *4*(1), 43. <https://doi.org/10.1038/s41572-018-0041-4>
- Filippi, M., Brück, W., Chard, D., Fazekas, F., Geurts, J. J. G., Enzinger, C., Hametner, S., Kuhlmann, T., Preziosa, P., Rovira, À., Schmierer, K., Stadelmann, C., Rocca, M. A., & Attendees of the Correlation between Pathological and MRI findings in MS workshop. (2019). Association between pathological and MRI findings in multiple sclerosis. *The Lancet. Neurology*, *18*(2), 198–210. [https://doi.org/10.1016/S1474-4422\(18\)30451-4](https://doi.org/10.1016/S1474-4422(18)30451-4)
- Fiola, S., Gosselin, D., Takada, K., & Gosselin, J. (2010). TLR9 contributes to the recognition of EBV by primary monocytes and plasmacytoid dendritic cells. *Journal of Immunology (Baltimore, Md.: 1950)*, *185*(6), 3620–3631. <https://doi.org/10.4049/jimmunol.0903736>
- Flanagan, W. M., Corthésy, B., Bram, R. J., & Crabtree, G. R. (1991). Nuclear association of a T-cell transcription factor blocked by FK-506 and cyclosporin A. *Nature*, *352*(6338), 803–807. <https://doi.org/10.1038/352803a0>
- Flores, J., González, S., Morales, X., Yescas, P., Ochoa, A., & Corona, T. (2012). Absence of Multiple Sclerosis and Demyelinating Diseases among Lacandonians, a Pure Amerindian Ethnic Group in Mexico. *Multiple Sclerosis International*, *2012*, e292631. <https://doi.org/10.1155/2012/292631>
- Förster, C., Burek, M., Romero, I. A., Weksler, B., Couraud, P.-O., & Drenckhahn, D. (2008). Differential effects of hydrocortisone and TNF $\alpha$  on tight junction proteins in an in vitro model of the human blood–brain barrier. *The Journal of Physiology*, *586*(Pt 7), 1937–1949. <https://doi.org/10.1113/jphysiol.2007.146852>
- Fries, K. L., Miller, W. E., & Raab-Traub, N. (1996). Epstein-Barr virus latent membrane protein 1 blocks p53-mediated apoptosis through the induction of the A20 gene. *Journal of Virology*, *70*(12), 8653–8659. <https://doi.org/10.1128/JVI.70.12.8653-8659.1996>

- Frischer, J. M., Bramow, S., Dal-Bianco, A., Lucchinetti, C. F., Rauschka, H., Schmidbauer, M., Laursen, H., Sorensen, P. S., & Lassmann, H. (2009). The relation between inflammation and neurodegeneration in multiple sclerosis brains. *Brain: A Journal of Neurology*, *132*(Pt 5), 1175–1189. <https://doi.org/10.1093/brain/awp070>
- Fruman, D. A., Klee, C. B., Bierer, B. E., & Burakoff, S. J. (1992). Calcineurin phosphatase activity in T lymphocytes is inhibited by FK 506 and cyclosporin A. *Proceedings of the National Academy of Sciences*, *89*(9), 3686–3690. <https://doi.org/10.1073/pnas.89.9.3686>
- Fujiwara, S., & Nakamura, H. (2020). Animal Models for Gammaherpesvirus Infections: Recent Development in the Analysis of Virus-Induced Pathogenesis. *Pathogens (Basel, Switzerland)*, *9*(2), 116. <https://doi.org/10.3390/pathogens9020116>
- Gacias, M., & Casaccia, P. (2014). Epigenetic Mechanisms in Multiple Sclerosis. *Revista Espanola de Esclerosis Multiple*, *6*(29), 25–35.
- Garber, C., Soung, A., Vollmer, L. L., Kanmogne, M., Last, A., Brown, J., & Klein, R. S. (2019). T cells promote microglia-mediated synaptic elimination and cognitive dysfunction during recovery from neuropathogenic flaviviruses. *Nature Neuroscience*, *22*(8), 1276–1288. <https://doi.org/10.1038/s41593-019-0427-y>
- Garber, C., Vasek, M. J., Vollmer, L. L., Sun, T., Jiang, X., & Klein, R. S. (2018). Astrocytes decrease adult neurogenesis during virus-induced memory dysfunction via IL-1. *Nature Immunology*, *19*(2), 151–161. <https://doi.org/10.1038/s41590-017-0021-y>
- Gate, D., Saligrama, N., Leventhal, O., Yang, A. C., Unger, M. S., Middeldorp, J., Chen, K., Lehallier, B., Channappa, D., De Los Santos, M. B., McBride, A., Pluinage, J., Elahi, F., Tam, G. K.-Y., Kim, Y., Greicius, M., Wagner, A. D., Aigner, L., Galasko, D. R., ... Wyss-Coray, T. (2020). Clonally expanded CD8 T cells patrol the cerebrospinal fluid in Alzheimer's disease. *Nature*, *577*(7790), 399–404. <https://doi.org/10.1038/s41586-019-1895-7>
- Gatto, D., Paus, D., Basten, A., Mackay, C. R., & Brink, R. (2009). Guidance of B cells by the orphan G protein-coupled receptor EBI2 shapes humoral immune responses. *Immunity*, *31*(2), 259–269. <https://doi.org/10.1016/j.immuni.2009.06.016>

- Gerdes, L. A., Janoschka, C., Eveslage, M., Mannig, B., Wirth, T., Schulte-Mecklenbeck, A., Lauks, S., Glau, L., Gross, C. C., Tolosa, E., Flierl-Hecht, A., Ertl-Wagner, B., Barkhof, F., Meuth, S. G., Kümpfel, T., Wiendl, H., Hohlfeld, R., & Klotz, L. (2020). Immune signatures of prodromal multiple sclerosis in monozygotic twins. *Proceedings of the National Academy of Sciences*, *117*(35), 21546–21556. <https://doi.org/10.1073/pnas.2003339117>
- Ghezzi, L., Cantoni, C., Cignarella, F., Bollman, B., Cross, A. H., Salter, A., Galimberti, D., Cella, M., & Piccio, L. (2019). T cells producing GM-CSF and IL-13 are enriched in the cerebrospinal fluid of relapsing MS patients. *Multiple Sclerosis (Houndmills, Basingstoke, England)*, *26*(10), 1172–1186. <https://doi.org/10.1177/1352458519852092>
- Gil, A., Kanga, L., Chirravuri-Venkata, R., Aslan, N., Clark, F., Ghersi, D., Luzuriaga, K., & Selin, L. K. (2020). Epstein-Barr Virus Epitope-Major Histocompatibility Complex Interaction Combined with Convergent Recombination Drives Selection of Diverse T Cell Receptor  $\alpha$  and  $\beta$  Repertoires. *MBio*, *11*(2), e00250-20. <https://doi.org/10.1128/mBio.00250-20>
- Gilli, F., Li, L., & Pachner, A. R. (2016). The immune response in the CNS in Theiler's virus induced demyelinating disease switches from an early adaptive response to a chronic innate-like response. *Journal of Neurovirology*, *22*(1), 66–79. <https://doi.org/10.1007/s13365-015-0369-4>
- Gilmore, C. P., Donaldson, I., Bö, L., Owens, T., Lowe, J., & Evangelou, N. (2009). Regional variations in the extent and pattern of grey matter demyelination in multiple sclerosis: A comparison between the cerebral cortex, cerebellar cortex, deep grey matter nuclei and the spinal cord. *Journal of Neurology, Neurosurgery, and Psychiatry*, *80*(2), 182–187. <https://doi.org/10.1136/jnnp.2008.148767>
- Giovannoni, G., Cutter, G. R., Lunemann, J., Martin, R., Münz, C., Sriram, S., Steiner, I., Hammerschlag, M. R., & Gaydos, C. A. (2006). Infectious causes of multiple sclerosis. *The Lancet. Neurology*, *5*(10), 887–894. [https://doi.org/10.1016/S1474-4422\(06\)70577-4](https://doi.org/10.1016/S1474-4422(06)70577-4)
- Giovannoni, G., & Ebers, G. (2007). Multiple sclerosis: The environment and causation. *Current Opinion in Neurology*, *20*(3), 261–268. <https://doi.org/10.1097/WCO.0b013e32815610c2>
- González, J. M., Bergmann, C. C., Ramakrishna, C., Hinton, D. R., Atkinson, R., Hoskin, J., Macklin, W. B., & Stohlman, S. A. (2006). Inhibition of Interferon- $\gamma$  Signaling in Oligodendroglia Delays Coronavirus Clearance without Altering Demyelination. *The American Journal of Pathology*, *168*(3), 796–804. <https://doi.org/10.2353/ajpath.2006.050496>

- González-Scarano, F., & Martín-García, J. (2005). The neuropathogenesis of AIDS. *Nature Reviews. Immunology*, 5(1), 69–81. <https://doi.org/10.1038/nri1527>
- Goswami, R., Shair, K. H. Y., & Gershburg, E. (2017). Molecular diversity of IgG responses to Epstein-Barr virus proteins in asymptomatic Epstein-Barr virus carriers. *The Journal of General Virology*, 98(9), 2343–2350. <https://doi.org/10.1099/jgv.0.000891>
- Taylor, G. S., Long, H. M., Brooks, J. M., Rickinson, A. B., & Hislop, A. D. (2015). The immunology of Epstein-Barr virus-induced disease. *Annual Review of Immunology*, 33, 787–821. <https://doi.org/10.1146/annurev-immunol-032414-112326>
- Gregory, C. D., Dive, C., Henderson, S., Smith, C. A., Williams, G. T., Gordon, J., & Rickinson, A. B. (1991). Activation of Epstein-Barr virus latent genes protects human B cells from death by apoptosis. *Nature*, 349(6310), 612–614. <https://doi.org/10.1038/349612a0>
- Guerrera, G., Ruggieri, S., Picozza, M., Piras, E., Gargano, F., Placido, R., Gasperini, C., Salvetti, M., Buscarinu, M. C., Battistini, L., Borsellino, G., & Angelini, D. F. (2020). EBV-specific CD8 T lymphocytes and B cells during glatiramer acetate therapy in patients with MS. *Neurology(R) Neuroimmunology & Neuroinflammation*, 7(6), e876. <https://doi.org/10.1212/NXI.0000000000000876>
- Gujer, C., Chatterjee, B., Landtwing, V., Raykova, A., McHugh, D., & Münz, C. (2015). Animal models of Epstein Barr virus infection. *Current Opinion in Virology*, 13, 6–10. <https://doi.org/10.1016/j.coviro.2015.03.014>
- Gujer, C., Murer, A., Müller, A., Vanoaica, D., Sutter, K., Jacque, E., Fournier, N., Kalchschmidt, J., Zbinden, A., Capaul, R., Dzionek, A., Mondon, P., Dittmer, U., & Münz, C. (2019). Plasmacytoid dendritic cells respond to Epstein-Barr virus infection with a distinct type I interferon subtype profile. *Blood Advances*, 3(7), 1129–1144. <https://doi.org/10.1182/bloodadvances.2018025536>
- Hammond, S. R., de Wyt, C., Maxwell, I. C., Landy, P. J., English, D., McLeod, J. G., & McCall, M. G. (1987). The epidemiology of multiple sclerosis in Queensland, Australia. *Journal of the Neurological Sciences*, 80(2), 185–204. [https://doi.org/10.1016/0022-510X\(87\)90154-7](https://doi.org/10.1016/0022-510X(87)90154-7)

- Hannedouche, S., Zhang, J., Yi, T., Shen, W., Nguyen, D., Pereira, J. P., Guerini, D., Baumgarten, B. U., Roggo, S., Wen, B., Knochenmuss, R., Noël, S., Gessier, F., Kelly, L. M., Vanek, M., Laurent, S., Preuss, I., Miault, C., Christen, I., ... Sailer, A. W. (2011). Oxysterols direct immune cell migration via EBI2. *Nature*, *475*(7357), 524–527. <https://doi.org/10.1038/nature10280>
- Harley, J. B., Chen, X., Pujato, M., Miller, D., Maddox, A., Forney, C., Magnusen, A. F., Lynch, A., Chetal, K., Yukawa, M., Barski, A., Salomonis, N., Kaufman, K. M., Kottyan, L. C., & Weirauch, M. T. (2018). Transcription factors operate across disease loci, with EBNA2 implicated in autoimmunity. *Nature Genetics*, *50*(5), 699–707. <https://doi.org/10.1038/s41588-018-0102-3>
- Hasel, P., Rose, I. V. L., Sadick, J. S., Kim, R. D., & Liddelow, S. A. (2021). Neuroinflammatory astrocyte subtypes in the mouse brain. *Nature Neuroscience*, 1–13. <https://doi.org/10.1038/s41593-021-00905-6>
- Hassani, A. (November 2016). *Role of Epstein-Barr Virus in the Pathogenesis of Multiple Sclerosis*. Master, The UAE University. Al-Ain, UAE
- Hassani, A., Corboy, J. R., Al-Salam, S., & Khan, G. (2018). Epstein-Barr virus is present in the brain of most cases of multiple sclerosis and may engage more than just B cells. *PloS One*, *13*(2), e0192109. <https://doi.org/10.1371/journal.pone.0192109>
- Hassani, A., & Khan, G. (2019). Epstein-Barr Virus and miRNAs: Partners in Crime in the Pathogenesis of Multiple Sclerosis? *Frontiers in Immunology*, *10*, 695. <https://doi.org/10.3389/fimmu.2019.00695>
- Hatton, O. L., Arnold-Harris, A., Schaffert, S., Krams, S. M., & Martinez, O. M. (2014). The Interplay Between Epstein Barr Virus and B Lymphocytes: Implications for Infection, Immunity, and Disease. *Immunologic Research*, *58*(0), 268–276. <https://doi.org/10.1007/s12026-014-8496-1>
- Hayashi, K., Koirala, T. R., Ino, H., Chen, H. L., Ohara, N., Teramoto, N., Yoshino, T., Takahashi, K., Yamada, M., & Nii, S. (1995). Malignant lymphoma induction in rabbits by intravenous inoculation of Epstein-Barr-virus-related herpesvirus from HTLV-II-transformed cynomolgus leukocyte cell line (Si-IIA). *International Journal of Cancer*, *63*(6), 872–880. <https://doi.org/10.1002/ijc.2910630620>

- Hayashi, K., Ohara, N., Koirala, T. R., Ino, H., Chen, H. L., Teramoto, N., Kondo, E., Yoshino, T., Takahashi, K., & Yamada, M. (1994). HTLV-II non-integrated malignant lymphoma induction in Japanese white rabbits following intravenous inoculation of HTLV-II-infected simian leukocyte cell line (Si-IIA). *Japanese Journal of Cancer Research: Gann*, 85(8), 808–818. <https://doi.org/10.1111/j.1349-7006.1994.tb02952.x>
- Hayashi, K., Ohara, N., Teramoto, N., Onoda, S., Chen, H.-L., Oka, T., Kondo, E., Yoshino, T., Takahashi, K., Yates, J., & Akagi, T. (2001). An Animal Model for Human EBV-Associated Hemophagocytic Syndrome. *The American Journal of Pathology*, 158(4), 1533–1542. [https://doi.org/10.1016/S0002-9440\(10\)64104-1](https://doi.org/10.1016/S0002-9440(10)64104-1)
- Hayashi, T., Morimoto, C., Burks, J. S., Kerr, C., & Hauser, S. L. (1988). Dual-label immunocytochemistry of the active multiple sclerosis lesion: Major histocompatibility complex and activation antigens. *Annals of Neurology*, 24(4), 523–531. <https://doi.org/10.1002/ana.410240408>
- Hedström, A. K., Hillert, J., Olsson, T., & Alfredsson, L. (2013). Smoking and multiple sclerosis susceptibility. *European Journal of Epidemiology*, 28(11), 867–874. <https://doi.org/10.1007/s10654-013-9853-4>
- Heller, K. N., Gurer, C., & Münz, C. (2006). Virus-specific CD4+ T cells: Ready for direct attack. *The Journal of Experimental Medicine*, 203(4), 805–808. <https://doi.org/10.1084/jem.20060215>
- Hernández, D. M., Valderrama, S., Gualtero, S., Hernández, C., López, M., Herrera, M. V., Solano, J., Fiorentino, S., & Quijano, S. (2018). Loss of T-Cell Multifunctionality and TCR-V $\beta$  Repertoire Against Epstein-Barr Virus Is Associated With Worse Prognosis and Clinical Parameters in HIV+ Patients. *Frontiers in Immunology*, 9, 2291. <https://doi.org/10.3389/fimmu.2018.02291>
- Hesselton, R. M., Yang, W. C., Medveczky, P., & Sullivan, J. L. (1988). Pathogenesis of Herpesvirus sylvilagus infection in cottontail rabbits. *The American Journal of Pathology*, 133(3), 639–647.
- Hislop, A. D., Kuo, M., Drake-Lee, A. B., Akbar, A. N., Bergler, W., Hammerschmitt, N., Khan, N., Palendira, U., Leese, A. M., Timms, J. M., Bell, A. I., Buckley, C. D., & Rickinson, A. B. (2005). Tonsillar homing of Epstein-Barr virus-specific CD8+ T cells and the virus-host balance. *Journal of Clinical Investigation*, 115(9), 2546–2555. <https://doi.org/10.1172/JCI24810>

- Hochberg, D., Souza, T., Catalina, M., Sullivan, J. L., Luzuriaga, K., & Thorley-Lawson, D. A. (2004). Acute infection with Epstein-Barr virus targets and overwhelms the peripheral memory B-cell compartment with resting, latently infected cells. *Journal of Virology*, *78*(10), 5194–5204. <https://doi.org/10.1128/jvi.78.10.5194-5204.2004>
- Hoffman, B. A., Wang, Y., Feldman, E. R., & Tibbetts, S. A. (2019). Epstein–Barr virus EBER1 and murine gammaherpesvirus TMER4 share conserved in vivo function to promote B cell egress and dissemination. *Proceedings of the National Academy of Sciences*, *116*(51), 25392–25394. <https://doi.org/10.1073/pnas.1915752116>
- Höftberger, R., & Lassmann, H. (2017). Inflammatory demyelinating diseases of the central nervous system. *Handbook of Clinical Neurology*, *145*, 263–283. <https://doi.org/10.1016/B978-0-12-802395-2.00019-5>
- Holman, D. W., Klein, R. S., & Ransohoff, R. M. (2011). The blood-brain barrier, chemokines and multiple sclerosis. *Biochimica Et Biophysica Acta*, *1812*(2), 220–230. <https://doi.org/10.1016/j.bbadis.2010.07.019>
- Hosseini, S., Wilk, E., Michaelsen-Preusse, K., Gerhauser, I., Baumgärtner, W., Geffers, R., Schughart, K., & Korte, M. (2018). Long-Term Neuroinflammation Induced by Influenza A Virus Infection and the Impact on Hippocampal Neuron Morphology and Function. *The Journal of Neuroscience: The Official Journal of the Society for Neuroscience*, *38*(12), 3060–3080. <https://doi.org/10.1523/JNEUROSCI.1740-17.2018>
- Hou, W., Jin, Y. H., Kang, H. S., & Kim, B. S. (2014). Interleukin-6 (IL-6) and IL-17 Synergistically Promote Viral Persistence by Inhibiting Cellular Apoptosis and Cytotoxic T Cell Function. *Journal of Virology*, *88*(15), 8479–8489. <https://doi.org/10.1128/JVI.00724-14>
- Howell, O. W., Reeves, C. A., Nicholas, R., Carassiti, D., Radotra, B., Gentleman, S. M., Serafini, B., Aloisi, F., Roncaroli, F., Magliozzi, R., & Reynolds, R. (2011). Meningeal inflammation is widespread and linked to cortical pathology in multiple sclerosis. *Brain: A Journal of Neurology*, *134*(Pt 9), 2755–2771. <https://doi.org/10.1093/brain/awr182>
- Hsieh, W. C., Chang, Y., Hsu, M. C., Lan, B. S., Hsiao, G. C., Chuang, H. C., & Su, I. J. (2007). Emergence of Anti-Red Blood Cell Antibodies Triggers Red Cell Phagocytosis by Activated Macrophages in a Rabbit Model of Epstein-Barr Virus-Associated Hemophagocytic Syndrome. *The American Journal of Pathology*, *170*(5), 1629–1639. <https://doi.org/10.2353/ajpath.2007.060772>

- Hui-Yuen, J., McAllister, S., Koganti, S., Hill, E., & Bhaduri-McIntosh, S. (2011). Establishment of Epstein-Barr Virus Growth-transformed Lymphoblastoid Cell Lines. *Journal of Visualized Experiments : JoVE*, *57*, 3321. <https://doi.org/10.3791/3321>
- Hurwitz, A. A., Sullivan, T. J., Sobel, R. A., & Allison, J. P. (2002). Cytotoxic T lymphocyte antigen-4 (CTLA-4) limits the expansion of encephalitogenic T cells in experimental autoimmune encephalomyelitis (EAE)-resistant BALB/c mice. *Proceedings of the National Academy of Sciences*, *99*(5), 3013–3017. <https://doi.org/10.1073/pnas.042684699>
- Hutchinson, M. (2007). Natalizumab: A new treatment for relapsing remitting multiple sclerosis. *Therapeutics and Clinical Risk Management*, *3*(2), 259–268. <https://doi.org/10.2147/tcrm.2007.3.2.259>
- Hwang, M., & Bergmann, C. C. (2020). Neuronal Ablation of Alpha/Beta Interferon (IFN- $\alpha/\beta$ ) Signaling Exacerbates Central Nervous System Viral Dissemination and Impairs IFN- $\gamma$  Responsiveness in Microglia/Macrophages. *Journal of Virology*, *94*(20), e00422-20. <https://doi.org/10.1128/JVI.00422-20>
- Jakimovski, D., Ramanathan, M., Weinstock-Guttman, B., Bergsland, N., Ramasamay, D. P., Carl, E., Dwyer, M. G., & Zivadinov, R. (2020). Higher EBV response is associated with more severe gray matter and lesion pathology in relapsing multiple sclerosis patients: A case-controlled magnetization transfer ratio study. *Multiple Sclerosis (Houndmills, Basingstoke, England)*, *26*(3), 322–332. <https://doi.org/10.1177/1352458519828667>
- Jayasooriya, S., de Silva, T. I., Njie-jobe, J., Sanyang, C., Leese, A. M., Bell, A. I., McAulay, K. A., Yanchun, P., Long, H. M., Dong, T., Whittle, H. C., Rickinson, A. B., Rowland-Jones, S. L., Hislop, A. D., & Flanagan, K. L. (2015). Early Virological and Immunological Events in Asymptomatic Epstein-Barr Virus Infection in African Children. *PLoS Pathogens*, *11*(3), e1004746. <https://doi.org/10.1371/journal.ppat.1004746>
- Jha, M. K., Jo, M., Kim, J. H., & Suk, K. (2019). Microglia-Astrocyte Crosstalk: An Intimate Molecular Conversation. *The Neuroscientist: A Review Journal Bringing Neurobiology, Neurology and Psychiatry*, *25*(3), 227–240. <https://doi.org/10.1177/1073858418783959>
- Jochum, S., Ruiss, R., Moosmann, A., Hammerschmidt, W., & Zeidler, R. (2012). RNAs in Epstein-Barr virions control early steps of infection. *Proceedings of the National Academy of Sciences of the United States of America*, *109*(21), E1396-1404. <https://doi.org/10.1073/pnas.1115906109>



- Jog, N. R., McClain, M. T., Heinlen, L. D., Gross, T., Towner, R., Guthridge, J. M., Axtell, R. C., Pardo, G., Harley, J. B., & James, J. A. (2020). Epstein Barr virus nuclear antigen 1 (EBNA-1) peptides recognized by adult multiple sclerosis patient sera induce neurologic symptoms in a murine model. *Journal of Autoimmunity*, *106*, 102332. <https://doi.org/10.1016/j.jaut.2019.102332>
- Johnson, D. B., McDonnell, W. J., Gonzalez-Ericsson, P. I., Al-Rohil, R. N., Mobley, B. C., Salem, J. E., Wang, D. Y., Sanchez, V., Wang, Y., Chastain, C. A., Barker, K., Liang, Y., Warren, S., Beechem, J. M., Menzies, A. M., Tio, M., Long, G. V., Cohen, J. V., Guidon, A. C., ... Balko, J. M. (2019). A case report of clonal EBV-like memory CD4 + T cell activation in fatal checkpoint inhibitor-induced encephalitis. *Nature Medicine*, *25*(8), 1243–1250. <https://doi.org/10.1038/s41591-019-0523-2>
- Jones, R. J., Seaman, W. T., Feng, W. H., Barlow, E., Dickerson, S., Delecluse, H. J., & Kenney, S. C. (2007). Roles of lytic viral infection and IL-6 in early versus late passage lymphoblastoid cell lines and EBV-associated lymphoproliferative disease. *International Journal of Cancer*, *121*(6), 1274–1281. <https://doi.org/10.1002/ijc.22839>
- Joseph, A. M., Babcock, G. J., & Thorley-Lawson, D. A. (2000). EBV persistence involves strict selection of latently infected B cells. *Journal of Immunology (Baltimore, Md.: 1950)*, *165*(6), 2975–2981. <https://doi.org/10.4049/jimmunol.165.6.2975>
- Jud, A., Kotur, M., Berger, C., Gysin, C., Nadal, D., & Lünemann, A. (2017). Tonsillar CD56brightNKG2A+ NK cells restrict primary Epstein-Barr virus infection in B cells via IFN- $\gamma$ . *Oncotarget*, *8*(4), 6130–6141. <https://doi.org/10.18632/oncotarget.14045>
- Kanai, K., Takashima, K., Okuno, K., Kato, K., Sano, H., Kuwamoto, S., Higaki, H., Nagata, K., Sugihara, H., Kato, M., Murakami, I., & Hayashi, K. (2010). Lifelong persistent EBV infection of rabbits with EBER1-positive lymphocyte infiltration and mild sublethal hemophagocytosis. *Virus Research*, *153*(1), 172–178. <https://doi.org/10.1016/j.virusres.2010.07.026>
- Kang, H. R., Cho, H. J., Kim, S., Song, I. H., Lee, T. S., Hwang, S., Sun, R., & Song, M. J. (2012). Persistent infection of a gammaherpesvirus in the central nervous system. *Virology*, *423*(1), 23–29. <https://doi.org/10.1016/j.virol.2011.11.012>

- Kasahara, Y., Yachie, A., Takei, K., Kanegane, C., Okada, K., Ohta, K., Seki, H., Igarashi, N., Maruhashi, K., Katayama, K., Katoh, E., Terao, G., Sakiyama, Y., & Koizumi, S. (2001). Differential cellular targets of Epstein-Barr virus (EBV) infection between acute EBV-associated hemophagocytic lymphohistiocytosis and chronic active EBV infection. *Blood*, *98*(6), 1882–1888. <https://doi.org/10.1182/blood.V98.6.1882>
- Katano, H., Ali, M. A., Patera, A. C., Catalfamo, M., Jaffe, E. S., Kimura, H., Dale, J. K., Straus, S. E., & Cohen, J. I. (2004). Chronic active Epstein-Barr virus infection associated with mutations in perforin that impair its maturation. *Blood*, *103*(4), 1244–1252. <https://doi.org/10.1182/blood-2003-06-2171>
- Kelly, L. M., Pereira, J. P., Yi, T., Xu, Y., & Cyster, J. G. (2011). EB12 guides serial movements of activated B cells and ligand activity is detectable in lymphoid and nonlymphoid tissues. *Journal of Immunology (Baltimore, Md.: 1950)*, *187*(6), 3026–3032. <https://doi.org/10.4049/jimmunol.1101262>
- Kempf, C., Tinguely, M., & Rushing, E. J. (2013). Posttransplant Lymphoproliferative Disorder of the Central Nervous System. *Pathobiology*, *80*(6), 310–318. <https://doi.org/10.1159/000347225>
- Kennedy, D. E., Witte, P. L., & Knight, K. L. (2016). Bone marrow fat and the decline of B lymphopoiesis in rabbits. *Developmental and Comparative Immunology*, *58*, 30–39. <https://doi.org/10.1016/j.dci.2015.11.003>
- Khan, G., Ahmed, W., Philip, P. S., Ali, M. H., & Adem, A. (2015). Healthy rabbits are susceptible to Epstein-Barr virus infection and infected cells proliferate in immunosuppressed animals. *Virology Journal*, *12*, 28. <https://doi.org/10.1186/s12985-015-0260-1>
- Khan, G., Fitzmaurice, C., Naghavi, M., & Ahmed, L. A. (2020). Global and regional incidence, mortality and disability-adjusted life-years for Epstein-Barr virus-attributable malignancies, 1990–2017. *BMJ Open*, *10*(8), e037505. <https://doi.org/10.1136/bmjopen-2020-037505>
- Khan, G., & Hashim, M. J. (2014). Global burden of deaths from Epstein-Barr virus attributable malignancies 1990-2010. *Infectious Agents and Cancer*, *9*(1), 38. <https://doi.org/10.1186/1750-9378-9-38>
- Kim, B. S. (2021). Excessive Innate Immunity Steers Pathogenic Adaptive Immunity in the Development of Theiler's Virus-Induced Demyelinating Disease. *International Journal of Molecular Sciences*, *22*(10), 5254. <https://doi.org/10.3390/ijms22105254>

- Kim, B. S., Jin, Y. H., Meng, L., Hou, W., Kang, H. S., Park, H. S., & Koh, C. S. (2012). IL-1 signal affects both protection and pathogenesis of virus-induced chronic CNS demyelinating disease. *Journal of Neuroinflammation*, *9*, 217. <https://doi.org/10.1186/1742-2094-9-217>
- Kim, W. K., Alvarez, X., Fisher, J., Bronfin, B., Westmoreland, S., McLaurin, J., & Williams, K. (2006). CD163 identifies perivascular macrophages in normal and viral encephalitic brains and potential precursors to perivascular macrophages in blood. *The American Journal of Pathology*, *168*(3), 822–834. <https://doi.org/10.2353/ajpath.2006.050215>
- Kipnis, J. (2016). Multifaceted interactions between adaptive immunity and the central nervous system. *Science*, *353*(6301), 766–771. <https://doi.org/10.1126/science.aag2638>
- Kis, L. L., Gerasimcik, N., Salamon, D., Persson, E. K., Nagy, N., Klein, G., Severinson, E., & Klein, E. (2011). STAT6 signaling pathway activated by the cytokines IL-4 and IL-13 induces expression of the Epstein-Barr virus-encoded protein LMP-1 in absence of EBNA-2: Implications for the type II EBV latent gene expression in Hodgkin lymphoma. *Blood*, *117*(1), 165–174. <https://doi.org/10.1182/blood-2010-01-265272>
- Kis, L. L., Salamon, D., Persson, E. K., Nagy, N., Scheeren, F. A., Spits, H., Klein, G., & Klein, E. (2010). IL-21 imposes a type II EBV gene expression on type III and type I B cells by the repression of C- and activation of LMP-1-promoter. *Proceedings of the National Academy of Sciences of the United States of America*, *107*(2), 872–877. <https://doi.org/10.1073/pnas.0912920107>
- Kis, L. L., Takahara, M., Nagy, N., Klein, G., & Klein, E. (2006). IL-10 can induce the expression of EBV-encoded latent membrane protein-1 (LMP-1) in the absence of EBNA-2 in B lymphocytes and in Burkitt lymphoma- and NK lymphoma-derived cell lines. *Blood*, *107*(7), 2928–2935. <https://doi.org/10.1182/blood-2005-06-2569>
- Klein, E., Kis, L. L., & Klein, G. (2007). Epstein–Barr virus infection in humans: From harmless to life endangering virus–lymphocyte interactions. *Oncogene*, *26*(9), 1297–1305. <https://doi.org/10.1038/sj.onc.1210240>
- Koch-Henriksen, N., Laursen, B., Stenager, E., & Magyari, M. (2017). Excess mortality among patients with multiple sclerosis in Denmark has dropped significantly over the past six decades: A population based study. *Journal of Neurology, Neurosurgery, and Psychiatry*, *88*(8), 626–631. <https://doi.org/10.1136/jnnp-2017-315907>

- Kochi, S., Takanaga, H., Matsuo, H., Naito, M., Tsuruo, T., & Sawada, Y. (1999). Effect of cyclosporin A or tacrolimus on the function of blood-brain barrier cells. *European Journal of Pharmacology*, *372*(3), 287–295. [https://doi.org/10.1016/s0014-2999\(99\)00247-2](https://doi.org/10.1016/s0014-2999(99)00247-2)
- Koirala, T. R., Hayashi, K., Chen, H. L., Ino, H., Kariya, N., Yanai, H., Choudhury, C. R., & Akagi, T. (1997). Malignant lymphoma induction of rabbits with oral spray of Epstein-Barr virus-related herpesvirus from Si-IIA cells (HTLV-II-transformed Cynomolgus cell line): A possible animal model for Epstein-Barr virus infection and subsequent virus-related tumors in humans. *Pathology International*, *47*(7), 442–448. <https://doi.org/10.1111/j.1440-1827.1997.tb04522.x>
- Koning, M. T., Brik, T., Hagenbeek, R., & van den Wijngaard, I. (2019). A case of fulminant Epstein-Barr virus encephalitis in an immune-competent adult. *Journal of Neurovirology*, *25*(3), 422–425. <https://doi.org/10.1007/s13365-018-0718-1>
- Korn, T., & Kallies, A. (2017). T cell responses in the central nervous system. *Nature Reviews Immunology*, *17*(3), 179–194. <https://doi.org/10.1038/nri.2016.144>
- Krakovski, M., & Owens, T. (1996). Interferon-gamma confers resistance to experimental allergic encephalomyelitis. *European Journal of Immunology*, *26*(7), 1641–1646. <https://doi.org/10.1002/eji.1830260735>
- Küçükali, C. İ., Kürtüncü, M., Çoban, A., Çebi, M., & Tüzün, E. (2015). Epigenetics of multiple sclerosis: An updated review. *Neuromolecular Medicine*, *17*(2), 83–96. <https://doi.org/10.1007/s12017-014-8298-6>
- Kuerten, S., Lanz, T. V., Lingampalli, N., Lahey, L. J., Kleinschnitz, C., Mäurer, M., Schroeter, M., Braune, S., Ziemssen, T., Ho, P. P., Robinson, W. H., & Steinman, L. (2020). Autoantibodies against central nervous system antigens in a subset of B cell–dominant multiple sclerosis patients. *Proceedings of the National Academy of Sciences*, *117*(35), 21512–21518. <https://doi.org/10.1073/pnas.2011249117>
- Lam, J. K. P., Hui, K. F., Ning, R. J., Xu, X. Q., Chan, K. H., & Chiang, A. K. S. (2018). Emergence of CD4+ and CD8+ Polyfunctional T Cell Responses Against Immunodominant Lytic and Latent EBV Antigens in Children With Primary EBV Infection. *Frontiers in Microbiology*, *9*, 416. <https://doi.org/10.3389/fmicb.2018.00416>

- Lassmann, H. (2018). Multiple Sclerosis Pathology. *Cold Spring Harbor Perspectives in Medicine*, 8(3), a028936. <https://doi.org/10.1101/cshperspect.a028936>
- Lee, A., Bridges, L. R., Lloyd, M., Barker, R., Wren, D. R., & Galtrey, C. M. (2020). Epstein–Barr virus associated CNS lymphoproliferative disorder after long-term immunosuppression. *Practical Neurology*, 20(1), 83–86. <https://doi.org/10.1136/practneurol-2019-002356>
- Li, F., Wang, Y., Yu, L., Cao, S., Wang, K., Yuan, J., Wang, C., Wang, K., Cui, M., & Fu, Z. F. (2015). Viral Infection of the Central Nervous System and Neuroinflammation Precede Blood-Brain Barrier Disruption during Japanese Encephalitis Virus Infection. *Journal of Virology*, 89(10), 5602–5614. <https://doi.org/10.1128/JVI.00143-15>
- Libbey, J. E., Cusick, M. F., & Fujinami, R. S. (2014). Role of pathogens in multiple sclerosis. *International Reviews of Immunology*, 33(4), 266–283. <https://doi.org/10.3109/08830185.2013.823422>
- Liddelov, S. A., & Barres, B. A. (2017). Reactive Astrocytes: Production, Function, and Therapeutic Potential. *Immunity*, 46(6), 957–967. <https://doi.org/10.1016/j.immuni.2017.06.006>
- Liddelov, S. A., Marsh, S. E., & Stevens, B. (2020). Microglia and Astrocytes in Disease: Dynamic Duo or Partners in Crime? *Trends in Immunology*, 820–835. <https://doi.org/10.1016/j.it.2020.07.006>
- Lind, L., Eriksson, K., & Grahn, A. (2019). Chemokines and matrix metalloproteinases in cerebrospinal fluid of patients with central nervous system complications caused by varicella-zoster virus. *Journal of Neuroinflammation*, 16(1), 42. <https://doi.org/10.1186/s12974-019-1428-1>
- Liu, C., Yang, X. V., Wu, J., Kuei, C., Mani, N. S., Zhang, L., Yu, J., Sutton, S. W., Qin, N., Banie, H., Karlsson, L., Sun, S., & Lovenberg, T. W. (2011). Oxysterols direct B-cell migration through EB12. *Nature*, 475(7357), 519–523. <https://doi.org/10.1038/nature10226>
- Liu, S. Y., Aliyari, R., Chikere, K., Li, G., Marsden, M. D., Smith, J. K., Pernet, O., Guo, H., Nusbaum, R., Zack, J. A., Freiberg, A. N., Su, L., Lee, B., & Cheng, G. (2013). Interferon-inducible cholesterol-25-hydroxylase broadly inhibits viral entry by production of 25-hydroxycholesterol. *Immunity*, 38(1), 92–105. <https://doi.org/10.1016/j.immuni.2012.11.005>

- Lopes Pinheiro, M. A., Kooij, G., Mizee, M. R., Kamermans, A., Enzmann, G., Lyck, R., Schwaninger, M., Engelhardt, B., & de Vries, H. E. (2016). Immune cell trafficking across the barriers of the central nervous system in multiple sclerosis and stroke. *Biochimica Et Biophysica Acta*, 1862(3), 461–471. <https://doi.org/10.1016/j.bbadis.2015.10.018>
- López-Montañés, M., Alari-Pahissa, E., Sintes, J., Martínez-Rodríguez, J. E., Muntasell, A., & López-Botet, M. (2017). Antibody-Dependent NK Cell Activation Differentially Targets EBV-Infected Cells in Lytic Cycle and Bystander B Lymphocytes Bound to Viral Antigen-Containing Particles. *Journal of Immunology (Baltimore, Md.: 1950)*, 199(2), 656–665. <https://doi.org/10.4049/jimmunol.1601574>
- Lotz, M., Tsoukas, C. D., Fong, S., Carson, D. A., & Vaughan, J. H. (1985). Regulation of Epstein-Barr virus infection by recombinant interferons. Selected sensitivity to interferon-gamma. *European Journal of Immunology*, 15(5), 520–525. <https://doi.org/10.1002/eji.1830150518>
- Louveau, A., Herz, J., Alme, M. N., Salvador, A. F., Dong, M. Q., Viar, K. E., Herod, S. G., Knopp, J., Setliff, J. C., Lupi, A. L., Da Mesquita, S., Frost, E. L., Gaultier, A., Harris, T. H., Cao, R., Hu, S., Lukens, J. R., Smirnov, I., Overall, C. C., ... Kipnis, J. (2018). CNS lymphatic drainage and neuroinflammation are regulated by meningeal lymphatic vasculature. *Nature Neuroscience*, 21(10), 1380–1391. <https://doi.org/10.1038/s41593-018-0227-9>
- Love, S. (2006). Demyelinating diseases. *Journal of Clinical Pathology*, 59(11), 1151–1159. <https://doi.org/10.1136/jcp.2005.031195>
- Lucchinetti, C., Brück, W., Parisi, J., Scheithauer, B., Rodriguez, M., & Lassmann, H. (2000). Heterogeneity of multiple sclerosis lesions: Implications for the pathogenesis of demyelination. *Annals of Neurology*, 47(6), 707–717. [https://doi.org/10.1002/1531-8249\(200006\)47:6<707::aid-ana3>3.0.co;2-q](https://doi.org/10.1002/1531-8249(200006)47:6<707::aid-ana3>3.0.co;2-q)
- Lünemann, J. D., Jelčić, I., Roberts, S., Lutterotti, A., Tackenberg, B., Martin, R., & Münz, C. (2008). EBNA1-specific T cells from patients with multiple sclerosis cross react with myelin antigens and co-produce IFN-gamma and IL-2. *The Journal of Experimental Medicine*, 205(8), 1763–1773. <https://doi.org/10.1084/jem.20072397>
- Lupia, T., Milia, M. G., Atzori, C., Gianella, S., Audagnotto, S., Imperiale, D., Mighetto, L., Pirriatore, V., Gregori, G., Lipani, F., Ghisetti, V., Bonora, S., Di Perri, G., & Calcagno, A. (2020). Presence of Epstein–Barr virus DNA in cerebrospinal fluid is associated with greater HIV RNA and inflammation. *AIDS*, 34(3), 373–380. <https://doi.org/10.1097/QAD.0000000000002442>

- Magaki, S., Ostrzega, N., Ho, E., Yim, C., Wu, P., & Vinters, H. V. (2017). Hemophagocytic lymphohistiocytosis associated with Epstein-Barr virus in the central nervous system. *Human Pathology*, *59*, 108–112. <https://doi.org/10.1016/j.humpath.2016.07.033>
- Magliozzi, R., Columba-Cabezas, S., Serafini, B., & Aloisi, F. (2004). Intracerebral expression of CXCL13 and BAFF is accompanied by formation of lymphoid follicle-like structures in the meninges of mice with relapsing experimental autoimmune encephalomyelitis. *Journal of Neuroimmunology*, *148*(1–2), 11–23. <https://doi.org/10.1016/j.jneuroim.2003.10.056>
- Magliozzi, R., Howell, O. W., Nicholas, R., Cruciani, C., Castellaro, M., Romualdi, C., Rossi, S., Pitteri, M., Benedetti, M. D., Gajofatto, A., Pizzini, F. B., Montemezzi, S., Rasia, S., Capra, R., Bertoldo, A., Facchiano, F., Monaco, S., Reynolds, R., & Calabrese, M. (2018). Inflammatory intrathecal profiles and cortical damage in multiple sclerosis. *Annals of Neurology*, *83*(4), 739–755. <https://doi.org/10.1002/ana.25197>
- Magliozzi, R., Serafini, B., Rosicarelli, B., Chiappetta, G., Veroni, C., Reynolds, R., & Aloisi, F. (2013). B-cell enrichment and Epstein-Barr virus infection in inflammatory cortical lesions in secondary progressive multiple sclerosis. *Journal of Neuropathology and Experimental Neurology*, *72*(1), 29–41. <https://doi.org/10.1097/NEN.0b013e31827bfc62>
- Manghani, M., & McGavern, D. B. (2018). New advances in CNS immunity against viral infection. *Current Opinion in Virology*, *28*, 116–126. <https://doi.org/10.1016/j.coviro.2017.12.003>
- Maron, R., Hancock, W. W., Slavin, A., Hattori, M., Kuchroo, V., & Weiner, H. L. (1999). Genetic susceptibility or resistance to autoimmune encephalomyelitis in MHC congenic mice is associated with differential production of pro- and anti-inflammatory cytokines. *International Immunology*, *11*(9), 1573–1580. <https://doi.org/10.1093/intimm/11.9.1573>
- Marsh, S. E., Abud, E. M., Lakatos, A., Karimzadeh, A., Yeung, S. T., Davtayan, H., Fote, G. M., Lau, L., Weinger, J. G., Lane, T. E., Inlay, M. A., Poon, W. W., & Blurton-Jones, M. (2016). The adaptive immune system restrains Alzheimer's disease pathogenesis by modulating microglial function. *Proceedings of the National Academy of Sciences of the United States of America*, *113*(9), E1316–1325. <https://doi.org/10.1073/pnas.1525466113>
- Mastorakos, P., & McGavern, D. (2019). The anatomy and immunology of vasculature in the central nervous system. *Science Immunology*, *4*(37), eaav0492. <https://doi.org/10.1126/sciimmunol.aav0492>

- Mattson, M. P. (2004). Infectious agents and age-related neurodegenerative disorders. *Ageing Research Reviews*, 3(1), 105–120. <https://doi.org/10.1016/j.arr.2003.08.005>
- Mauray, S., Fuzzati-Armentero, M. T., Trouillet, P., Rüegg, M., Nicoloso, G., Hart, M., Aarden, L., Schapira, M., & Duchosal, M. A. (2000). Epstein-Barr virus-dependent lymphoproliferative disease: Critical role of IL-6. *European Journal of Immunology*, 30(7), 2065–2073. [https://doi.org/10.1002/1521-4141\(200007\)30:7<2065::AID-IMMU2065>3.0.CO;2-W](https://doi.org/10.1002/1521-4141(200007)30:7<2065::AID-IMMU2065>3.0.CO;2-W)
- McCall, C. M., Mudali, S., Arceci, R. J., Small, D., Fuller, S., Gocke, C. D., Vuica-Ross, M., Burns, K. H., Borowitz, M. J., & Duffield, A. S. (2012). Flow Cytometric Findings in Hemophagocytic Lymphohistiocytosis. *American Journal of Clinical Pathology*, 137(5), 786–794. <https://doi.org/10.1309/AJCPP40MEXWYRLPN>
- McHugh, D., Myburgh, R., Caduff, N., Spohn, M., Kok, Y. L., Keller, C. W., Murer, A., Chatterjee, B., Rühl, J., Engelmann, C., Chijioke, O., Quast, I., Shilaih, M., Strouvelle, V. P., Neumann, K., Menter, T., Dirnhofer, S., Lam, J. K., Hui, K. F., ... Münz, C. (2020). EBV renders B cells susceptible to HIV-1 in humanized mice. *Life Science Alliance*, 3(8), e202000640. <https://doi.org/10.26508/lsa.202000640>
- Meckiff, B. J., Ladell, K., McLaren, J. E., Ryan, G. B., Leese, A. M., James, E. A., Price, D. A., & Long, H. M. (2019). Primary EBV Infection Induces an Acute Wave of Activated Antigen-Specific Cytotoxic CD4 + T Cells. *Journal of Immunology*, 203(5), 1276–1287. <https://doi.org/10.4049/jimmunol.1900377>
- Meda, L., Cassatella, M. A., Szendrei, G. I., Otvos, L., Baron, P., Villalba, M., Ferrari, D., & Rossi, F. (1995). Activation of microglial cells by beta-amyloid protein and interferon-gamma. *Nature*, 374(6523), 647–650. <https://doi.org/10.1038/374647a0>
- Medawar, P. B. (1948). Immunity to homologous grafted skin; the fate of skin homografts transplanted to the brain, to subcutaneous tissue, and to the anterior chamber of the eye. *British Journal of Experimental Pathology*, 29(1), 58–69.
- Menu, P., & Vince, J. E. (2011). The NLRP3 inflammasome in health and disease: The good, the bad and the ugly. *Clinical and Experimental Immunology*, 166(1), 1–15. <https://doi.org/10.1111/j.1365-2249.2011.04440.x>



- Miller, G., Shope, T., Lisco, H., Stitt, D., & Lipman, M. (1972). Epstein-Barr Virus: Transformation, Cytopathic Changes, and Viral Antigens in Squirrel Monkey and Marmoset Leukocytes. *Proceedings of the National Academy of Sciences*, 69(2), 383–387.
- Milovanovic, J., Popovic, B., Milovanovic, M., Kvestak, D., Arsenijevic, A., Stojanovic, B., Tanaskovic, I., Krmpotic, A., Arsenijevic, N., Jonjic, S., & Lukic, M. L. (2017). Murine Cytomegalovirus Infection Induces Susceptibility to EAE in Resistant BALB/c Mice. *Frontiers in Immunology*, 8, 192. <https://doi.org/10.3389/fimmu.2017.00192>
- Minagar, A., Long, A., Ma, T., Jackson, T. H., Kelley, R. E., Ostanin, D. V., Sasaki, M., Warren, A. C., Jawahar, A., Cappell, B., & Alexander, J. S. (2003). Interferon (IFN)-beta 1a and IFN-beta 1b block IFN-gamma-induced disintegration of endothelial junction integrity and barrier. *Endothelium: Journal of Endothelial Cell Research*, 10(6), 299–307. <https://doi.org/10.1080/10623320390272299>
- Misharin, A. V., Cuda, C. M., Saber, R., Turner, J. D., Gierut, A. K., Haines, G. K., Berdnikovs, S., Filer, A., Clark, A. R., Buckley, C. D., Mutlu, G. M., Budinger, G. R. S., & Perlman, H. (2014). Non-classical Ly6C<sup>+</sup> monocytes drive the development of inflammatory arthritis in mice. *Cell Reports*, 9(2), 591–604. <https://doi.org/10.1016/j.celrep.2014.09.032>
- Mitsdoerffer, M., Di Liberto, G., Dötsch, S., Sie, C., Wagner, I., Pfaller, M., Kreutzfeldt, M., Fräßle, S., Aly, L., Knier, B., Busch, D. H., Merkler, D., & Korn, T. (2021). Formation and immunomodulatory function of meningeal B cell aggregates in progressive CNS autoimmunity. *Brain: A Journal of Neurology*, 144(6), 1697–1710. <https://doi.org/10.1093/brain/awab093>
- Mitsdoerffer, M., & Peters, A. (2016). Tertiary Lymphoid Organs in Central Nervous System Autoimmunity. *Frontiers in Immunology*, 7, 451. <https://doi.org/10.3389/fimmu.2016.00451>
- Moreno, M. A., Or-Geva, N., Aftab, B. T., Khanna, R., Croze, E., Steinman, L., & Han, M. H. (2018). Molecular signature of Epstein-Barr virus infection in MS brain lesions. *Neurology(R) Neuroimmunology & Neuroinflammation*, 5(4), e466. <https://doi.org/10.1212/NXI.0000000000000466>
- Mrozek-Gorska, P., Buschle, A., Pich, D., Schwarzmayr, T., Fechtner, R., Scialdone, A., & Hammerschmidt, W. (2019). Epstein–Barr virus reprograms human B lymphocytes immediately in the prelatent phase of infection. *Proceedings of the National Academy of Sciences*, 116(32), 16046–16055. <https://doi.org/10.1073/pnas.1901314116>

- Mukherjee, R., Kanti Barman, P., Kumar Thatoi, P., Tripathy, R., Kumar Das, B., & Ravindran, B. (2015). Non-Classical monocytes display inflammatory features: Validation in Sepsis and Systemic Lupus Erythematosus. *Scientific Reports*, 5(1), 13886. <https://doi.org/10.1038/srep13886>
- Multiple sclerosis in 54 twinships: Concordance rate is independent of zygoty. French Research Group on Multiple Sclerosis. (1992). *Annals of Neurology*, 32(6), 724–727. <https://doi.org/10.1002/ana.410320604>
- Munger, K. L., Chitnis, T., & Ascherio, A. (2009). Body size and risk of MS in two cohorts of US women. *Neurology*, 73(19), 1543–1550. <https://doi.org/10.1212/WNL.0b013e3181c0d6e0>
- Münz, C. (2019). Latency and lytic replication in Epstein–Barr virus-associated oncogenesis. *Nature Reviews Microbiology*, 17(11), 691–700. <https://doi.org/10.1038/s41579-019-0249-7>
- Murata, T. (2014). Regulation of Epstein-Barr virus reactivation from latency. *Microbiology and Immunology*, 58(6), 307–317. <https://doi.org/10.1111/1348-0421.12155>
- Murphy, A. C., Lalor, S. J., Lynch, M. A., & Mills, K. H. G. (2010). Infiltration of Th1 and Th17 cells and activation of microglia in the CNS during the course of experimental autoimmune encephalomyelitis. *Brain, Behavior, and Immunity*, 24(4), 641–651. <https://doi.org/10.1016/j.bbi.2010.01.014>
- Myoung, J., Bahk, Y. Y., Kang, H. S., Dal Canto, M. C., & Kim, B. S. (2008). Anticapsid immunity level, not viral persistence level, correlates with the progression of Theiler’s virus-induced demyelinating disease in viral P1-transgenic mice. *Journal of Virology*, 82(11), 5606–5617. <https://doi.org/10.1128/JVI.02442-07>
- Nagy, N., Ádori, M., Rasul, A., Heuts, F., Salamon, D., Ujvári, D., Madapura, H. S., Leveau, B., Klein, G., & Klein, E. (2012). Soluble factors produced by activated CD4+ T cells modulate EBV latency. *Proceedings of the National Academy of Sciences of the United States of America*, 109(5), 1512–1517. <https://doi.org/10.1073/pnas.1120587109>
- Narasimhan, P. B., Marcovecchio, P., Hamers, A. A. J., & Hedrick, C. C. (2019). Nonclassical Monocytes in Health and Disease. *Annual Review of Immunology*, 37(1), 439–456. <https://doi.org/10.1146/annurev-immunol-042617-053119>

- Nasr, Z., Majed, M., Rostami, A., Sahraian, M. A., Minagar, A., Amini, A., McGee, J. C., & Etemadifar, M. (2016). Prevalence of multiple sclerosis in Iranian emigrants: Review of the evidence. *Neurological Sciences: Official Journal of the Italian Neurological Society and of the Italian Society of Clinical Neurophysiology*, *37*(11), 1759–1763. <https://doi.org/10.1007/s10072-016-2641-7>
- Ní Chasaide, C., & Lynch, M. A. (2020). The role of the immune system in driving neuroinflammation. *Brain and Neuroscience Advances*, *4*, 2398212819901082. <https://doi.org/10.1177/2398212819901082>
- Okuno, K., Takashima, K., Kanai, K., Ohashi, M., Hyuga, R., Sugihara, H., Kuwamoto, S., Kato, M., Sano, H., Sairenji, T., Kanzaki, S., & Hayashi, K. (2010). Epstein-Barr virus can infect rabbits by the intranasal or peroral route: An animal model for natural primary EBV infection in humans. *Journal of Medical Virology*, *82*(6), 977–986. <https://doi.org/10.1002/jmv.21597>
- O’Neill, B. P., Vernino, S., Dogan, A., & Giannini, C. (2007). EBV-associated lymphoproliferative disorder of CNS associated with the use of mycophenolate mofetil. *Neuro-Oncology*, *9*(3), 364–369. <https://doi.org/10.1215/15228517-2007-004>
- Osborne, A. J., Atkins, H. M., Balogh, K. K., Brendle, S. A., Shearer, D. A., Hu, J., Sample, C. E., & Christensen, N. D. (2020). Antibody-Mediated Immune Subset Depletion Modulates the Immune Response in a Rabbit (*Oryctolagus cuniculus*) Model of Epstein-Barr Virus Infection. *Comparative Medicine*, *70*(5), 312–322. <https://doi.org/10.30802/AALAS-CM-20-000019>
- Pan, Y.-R., Fang, C.-Y., Chang, Y.-S., & Chang, H.-Y. (2005). Analysis of Epstein-Barr virus gene expression upon phorbol ester and hydroxyurea treatment by real-time quantitative PCR. *Archives of Virology*, *150*(4), 755–770. <https://doi.org/10.1007/s00705-004-0431-7>
- Panikkar, A., Smith, C., Hislop, A., Tellam, N., Dasari, V., Hogquist, K. A., Wykes, M., Moss, D. J., Rickinson, A., Balfour, H. H., & Khanna, R. (2015). Cytokine-Mediated Loss of Blood Dendritic Cells During Epstein-Barr Virus-Associated Acute Infectious Mononucleosis: Implication for Immune Dysregulation. *The Journal of Infectious Diseases*, *212*(12), 1957–1961. <https://doi.org/10.1093/infdis/jiv340>

- Park, J. S., Kam, T. I., Lee, S., Park, H., Oh, Y., Kwon, S. H., Song, J. J., Kim, D., Kim, H., Jhaldiyal, A., Na, D. H., Lee, K. C., Park, E. J., Pomper, M. G., Pletnikova, O., Troncoso, J. C., Ko, H. S., Dawson, V. L., Dawson, T. M., & Lee, S. (2021). Blocking microglial activation of reactive astrocytes is neuroprotective in models of Alzheimer's disease. *Acta Neuropathologica Communications*, 9(1), 78. <https://doi.org/10.1186/s40478-021-01180-z>
- Parra, B., Hinton, D. R., Marten, N. W., Bergmann, C. C., Lin, M. T., Yang, C. S., & Stohlman, S. A. (1999). IFN-gamma is required for viral clearance from central nervous system oligodendroglia. *Journal of Immunology (Baltimore, Md.: 1950)*, 162(3), 1641–1647.
- Pender, M. P., Csurhes, P. A., Smith, C., Douglas, N. L., Neller, M. A., Matthews, K. K., Beagley, L., Rehan, S., Crooks, P., Hopkins, T. J., Blum, S., Green, K. A., Ioannides, Z. A., Swayne, A., Aftab, B. T., Hooper, K. D., Burrows, S. R., Thompson, K. M., Coulthard, A., & Khanna, R. (2018). Epstein-Barr virus-specific T cell therapy for progressive multiple sclerosis. *JCI Insight*, 3(22), e124714. <https://doi.org/10.1172/jci.insight.124714>
- Pereira, J. P., Kelly, L. M., Xu, Y., & Cyster, J. G. (2009). EBI2 mediates B cell segregation between the outer and centre follicle. *Nature*, 460(7259), 1122–1126. <https://doi.org/10.1038/nature08226>
- Peterson, J. W., Bö, L., Mörk, S., Chang, A., & Trapp, B. D. (2001). Transected neurites, apoptotic neurons, and reduced inflammation in cortical multiple sclerosis lesions. *Annals of Neurology*, 50(3), 389–400. <https://doi.org/10.1002/ana.1123>
- Petrara, M. R., Cattelan, A. M., Zanchetta, M., Sasset, L., Freguja, R., Gianesin, K., Cecchetto, M. G., Carmona, F., & De Rossi, A. (2012). Epstein-Barr virus load and immune activation in human immunodeficiency virus type 1-infected patients. *Journal of Clinical Virology: The Official Publication of the Pan American Society for Clinical Virology*, 53(3), 195–200. <https://doi.org/10.1016/j.jcv.2011.12.013>
- Petrova, N., Carassiti, D., Altmann, D. R., Baker, D., & Schmierer, K. (2018). Axonal loss in the multiple sclerosis spinal cord revisited. *Brain Pathology (Zurich, Switzerland)*, 28(3), 334–348. <https://doi.org/10.1111/bpa.12516>
- Phares, T. W., Kean, R. B., Mikheeva, T., & Hooper, D. C. (2006). Regional differences in blood-brain barrier permeability changes and inflammation in the apathogenic clearance of virus from the central nervous system. *Journal of Immunology (Baltimore, Md.: 1950)*, 176(12), 7666–7675. <https://doi.org/10.4049/jimmunol.176.12.7666>

- Pich, D., Mrozek-Gorska, P., Bouvet, M., Sugimoto, A., Akidil, E., Grundhoff, A., Hamperl, S., Ling, P. D., & Hammerschmidt, W. (2019). First Days in the Life of Naive Human B Lymphocytes Infected with Epstein-Barr Virus. *MBio*, *10*(5), e01723-19. <https://doi.org/10.1128/mBio.01723-19>
- Pikor, N. B., Prat, A., Bar-Or, A., & Gommerman, J. L. (2015). Meningeal Tertiary Lymphoid Tissues and Multiple Sclerosis: A Gathering Place for Diverse Types of Immune Cells during CNS Autoimmunity. *Frontiers in Immunology*, *6*, 657. <https://doi.org/10.3389/fimmu.2015.00657>
- Piriou, E., Asito, A. S., Sumba, P. O., Fiore, N., Middeldorp, J. M., Moormann, A. M., Ploutz-Snyder, R., & Rochford, R. (2012). Early age at time of primary Epstein-Barr virus infection results in poorly controlled viral infection in infants from Western Kenya: Clues to the etiology of endemic Burkitt lymphoma. *The Journal of Infectious Diseases*, *205*(6), 906–913. <https://doi.org/10.1093/infdis/jir872>
- Popescu, B. F. G., & Lucchinetti, C. F. (2012). Pathology of demyelinating diseases. *Annual Review of Pathology*, *7*, 185–217. <https://doi.org/10.1146/annurev-pathol-011811-132443>
- Popescu, B. F. G., Pirko, I., & Lucchinetti, C. F. (2013). Pathology of multiple sclerosis: Where do we stand? *Continuum (Minneapolis, Minn.)*, *19*(4 Multiple Sclerosis), 901–921. <https://doi.org/10.1212/01.CON.0000433291.23091.65>
- Pratt, Z. L., Zhang, J., & Sugden, B. (2012). The latent membrane protein 1 (LMP1) oncogene of Epstein-Barr virus can simultaneously induce and inhibit apoptosis in B cells. *Journal of Virology*, *86*(8), 4380–4393. <https://doi.org/10.1128/JVI.06966-11>
- Price, A. M., Dai, J., Bazot, Q., Patel, L., Nikitin, P. A., Djavadian, R., Winter, P. S., Salinas, C. A., Barry, A. P., Wood, K. C., Johannsen, E. C., Letai, A., Allday, M. J., & Luftig, M. A. (2017). Epstein-Barr virus ensures B cell survival by uniquely modulating apoptosis at early and late times after infection. *ELife*, *6*, e22509. <https://doi.org/10.7554/eLife.22509>
- Puchner, A., Saferding, V., Bonelli, M., Mikami, Y., Hofmann, M., Brunner, J. S., Caldera, M., Goncalves-Alves, E., Binder, N. B., Fischer, A., Simader, E., Steiner, C.-W., Leiss, H., Hayer, S., Niederreiter, B., Karonitsch, T., Koenders, M. I., Podesser, B. K., O'Shea, J. J., ... Blüml, S. (2018). Non-classical monocytes as mediators of tissue destruction in arthritis. *Annals of the Rheumatic Diseases*, *77*(10), 1490–1497. <https://doi.org/10.1136/annrheumdis-2018-213250>

- Pullen, L. C., Park, S. H., Miller, S. D., Dal Canto, M. C., & Kim, B. S. (1995). Treatment with bacterial LPS renders genetically resistant C57BL/6 mice susceptible to Theiler's virus-induced demyelinating disease. *Journal of Immunology (Baltimore, Md.: 1950)*, *155*(9), 4497–4503.
- Punnonen, J., Aversa, G., Cocks, B. G., McKenzie, A. N., Menon, S., Zurawski, G., de Waal Malefyt, R., & de Vries, J. E. (1993). Interleukin 13 induces interleukin 4-independent IgG4 and IgE synthesis and CD23 expression by human B cells. *Proceedings of the National Academy of Sciences of the United States of America*, *90*(8), 3730–3734.  
<https://doi.org/10.1073/pnas.90.8.3730>
- Rajčáni, J., Szenthe, K., Ďurmanová, V., Tóth, A., Ásványi, B., Pitlik, E., Stipkovits, L., & Szathmary, S. (2014). Epstein-Barr Virus (HHV-4) Inoculation to Rabbits by Intranasal and Oral Routes Results in Subacute and/or Persistent Infection Dissimilar to Human Disease. *Intervirology*, *57*(5), 254–269.  
<https://doi.org/10.1159/000360223>
- Ramagopalan, S. V., & Ebers, G. C. (2009). Multiple sclerosis: Major histocompatibility complexity and antigen presentation. *Genome Medicine*, *1*(11), 105. <https://doi.org/10.1186/gm105>
- Ramakrishna, C., & Cantin, E. M. (2018). IFN $\gamma$  inhibits G-CSF induced neutrophil expansion and invasion of the CNS to prevent viral encephalitis. *PLoS Pathogens*, *14*(1), e1006822. <https://doi.org/10.1371/journal.ppat.1006822>
- Ramos, H. J., Lanteri, M. C., Blahnik, G., Negash, A., Suthar, M. S., Brassil, M. M., Sodhi, K., Treuting, P. M., Busch, M. P., Norris, P. J., & Gale, M. (2012). IL-1 $\beta$  signaling promotes CNS-intrinsic immune control of West Nile virus infection. *PLoS Pathogens*, *8*(11), e1003039.  
<https://doi.org/10.1371/journal.ppat.1003039>
- Reich, D. S., Lucchinetti, C. F., & Calabresi, P. A. (2018). Multiple Sclerosis. *The New England Journal of Medicine*, *378*(2), 169–180.  
<https://doi.org/10.1056/NEJMra1401483>
- Richardo, T., Prattapong, P., Ngernsombat, C., Wisetyaningsih, N., Iizasa, H., Yoshiyama, H., & Janvilisri, T. (2020). Epstein-Barr Virus Mediated Signaling in Nasopharyngeal Carcinoma Carcinogenesis. *Cancers*, *12*(9), E2441. <https://doi.org/10.3390/cancers12092441>

- Rohr, J., Beutel, K., Maul-Pavicic, A., Vraetz, T., Thiel, J., Warnatz, K., Bondzio, I., Gross-Wieltsch, U., Schündeln, M., Schütz, B., Woessmann, W., Groll, A. H., Strahm, B., Pagel, J., Speckmann, C., Janka, G., Griffiths, G., Schwarz, K., zur Stadt, U., & Ehl, S. (2010). Atypical familial hemophagocytic lymphohistiocytosis due to mutations in UNC13D and STXBP2 overlaps with primary immunodeficiency diseases. *Haematologica*, *95*(12), 2080–2087. <https://doi.org/10.3324/haematol.2010.029389>
- Rossi, B., & Constantin, G. (2016). Live Imaging of Immune Responses in Experimental Models of Multiple Sclerosis. *Frontiers in Immunology*, *7*, 506. <https://doi.org/10.3389/fimmu.2016.00506>
- Rostgaard, K., Wohlfahrt, J., & Hjalgrim, H. (2014). A Genetic Basis for Infectious Mononucleosis: Evidence From a Family Study of Hospitalized Cases in Denmark. *Clinical Infectious Diseases*, *58*(12), 1684–1689. <https://doi.org/10.1093/cid/ciu204>
- Rubio, N., & Sanz-Rodriguez, F. (2019). Theiler's murine encephalomyelitis virus infection of astrocytes induces the expression of chemokines which attract activated but not resting T lymphocytes. *Journal of Neurovirology*, *25*(6), 844–852. <https://doi.org/10.1007/s13365-019-00776-5>
- Russo, M., & McGavern, D. B. (2015). Immune surveillance of the CNS following infection and injury. *Trends in Immunology*, *36*(10), 637–650. <https://doi.org/10.1016/j.it.2015.08.002>
- Rutkowska, A., Dev, K. K., & Sailer, A. W. (2016). The Role of the Oxysterol/EBI2 Pathway in the Immune and Central Nervous Systems. *Current Drug Targets*, *17*(16), 1851–1860. <https://doi.org/10.2174/1389450117666160217123042>
- Rutkowska, A., O'Sullivan, S. A., Christen, I., Zhang, J., Sailer, A. W., & Dev, K. K. (2016). The EBI2 signalling pathway plays a role in cellular crosstalk between astrocytes and macrophages. *Scientific Reports*, *6*, 25520. <https://doi.org/10.1038/srep25520>
- Rutkowska, A., Preuss, I., Gessier, F., Sailer, A. W., & Dev, K. K. (2015). EBI2 regulates intracellular signaling and migration in human astrocyte. *Glia*, *63*(2), 341–351. <https://doi.org/10.1002/glia.22757>
- Rutkowska, A., Sailer, A. W., & Dev, K. K. (2017). EBI2 receptor regulates myelin development and inhibits LPC-induced demyelination. *Journal of Neuroinflammation*, *14*(1), 250. <https://doi.org/10.1186/s12974-017-1025-0>

- Rutkowska, A., Shimshek, D. R., Sailer, A. W., & Dev, K. K. (2018). EBI2 regulates pro-inflammatory signalling and cytokine release in astrocytes. *Neuropharmacology*, *133*, 121–128. <https://doi.org/10.1016/j.neuropharm.2018.01.029>
- Saederup, N., Cardona, A. E., Croft, K., Mizutani, M., Coteleur, A. C., Tsou, C. L., Ransohoff, R. M., & Charo, I. F. (2010). Selective chemokine receptor usage by central nervous system myeloid cells in CCR2-red fluorescent protein knock-in mice. *PloS One*, *5*(10), e13693. <https://doi.org/10.1371/journal.pone.0013693>
- Salazar, R., Hypolite, T., Bixby, E., & Nguyen, A. (2018). Co-occurrence of neurosarcoidosis and intrathecal reactivation of Epstein-Barr virus. *Multiple Sclerosis and Related Disorders*, *25*, 297–299. <https://doi.org/10.1016/j.msard.2018.08.021>
- Sano, H., Nagata, K., Kato, K., Kanai, K., Yamamoto, K., Okuno, K., Kuwamoto, S., Higaki-Mori, H., Sugihara, H., Kato, M., Murakami, I., Kanzaki, S., & Hayashi, K. (2013). EBNA-2 -deleted Epstein-Barr virus from P3HR-1 can infect rabbits with lower efficiency than prototype Epstein-Barr virus from B95-8. *Intervirology*, *56*(2), 114–121. <https://doi.org/10.1159/000343753>
- Schlemm, L., Giess, R. M., Rasche, L., Pfuhl, C., Wakonig, K., Behrens, J. R., Scheibenbogen, C., Bellmann-Strobl, J., Paul, F., Reimer, U., & Ruprecht, K. (2016). Fine specificity of the antibody response to Epstein-Barr nuclear antigen-2 and other Epstein-Barr virus proteins in patients with clinically isolated syndrome: A peptide microarray-based case-control study. *Journal of Neuroimmunology*, *297*, 56–62. <https://doi.org/10.1016/j.jneuroim.2016.05.012>
- Schnupf, P., & Sansonetti, P. J. (2012). Quantitative RT-PCR profiling of the Rabbit Immune Response: Assessment of Acute Shigella flexneri Infection. *PLOS ONE*, *7*(6), e36446. <https://doi.org/10.1371/journal.pone.0036446>
- Schwartz, M., & Kipnis, J. (2011). A conceptual revolution in the relationships between the brain and immunity. *Brain, Behavior, and Immunity*, *25*(5), 817–819. <https://doi.org/10.1016/j.bbi.2010.12.015>
- Serafini, B., Rosicarelli, B., Franciotta, D., Magliozzi, R., Reynolds, R., Cinque, P., Andreoni, L., Trivedi, P., Salvetti, M., Faggioni, A., & Aloisi, F. (2007). Dysregulated Epstein-Barr virus infection in the multiple sclerosis brain. *The Journal of Experimental Medicine*, *204*(12), 2899–2912. <https://doi.org/10.1084/jem.20071030>



- Serafini, B., Rosicarelli, B., Magliozzi, R., Stigliano, E., & Aloisi, F. (2004). Detection of ectopic B-cell follicles with germinal centers in the meninges of patients with secondary progressive multiple sclerosis. *Brain Pathology (Zurich, Switzerland)*, *14*(2), 164–174. <https://doi.org/10.1111/j.1750-3639.2004.tb00049.x>
- Serafini, B., Rosicarelli, B., Veroni, C., Mazzola, G. A., & Aloisi, F. (2019). Epstein-Barr Virus-Specific CD8 T Cells Selectively Infiltrate the Brain in Multiple Sclerosis and Interact Locally with Virus-Infected Cells: Clue for a Virus-Driven Immunopathological Mechanism. *Journal of Virology*, *93*(24), e00980-19. <https://doi.org/10.1128/JVI.00980-19>
- Serafini, B., Scorsi, E., Rosicarelli, B., Rigau, V., Thouvenot, E., & Aloisi, F. (2017). Massive intracerebral Epstein-Barr virus reactivation in lethal multiple sclerosis relapse after natalizumab withdrawal. *Journal of Neuroimmunology*, *307*, 14–17. <https://doi.org/10.1016/j.jneuroim.2017.03.013>
- Serafini, B., Severa, M., Columba-Cabezas, S., Rosicarelli, B., Veroni, C., Chiappetta, G., Magliozzi, R., Reynolds, R., Coccia, E. M., & Aloisi, F. (2010). Epstein-Barr virus latent infection and BAFF expression in B cells in the multiple sclerosis brain: Implications for viral persistence and intrathecal B-cell activation. *Journal of Neuropathology and Experimental Neurology*, *69*(7), 677–693. <https://doi.org/10.1097/NEN.0b013e3181e332ec>
- Serafini, B., Zandee, S., Rosicarelli, B., Scorsi, E., Veroni, C., Larochelle, C., D'Alfonso, S., Prat, A., & Aloisi, F. (2018). Epstein-Barr virus-associated immune reconstitution inflammatory syndrome as possible cause of fulminant multiple sclerosis relapse after natalizumab interruption. *Journal of Neuroimmunology*, *319*, 9–12. <https://doi.org/10.1016/j.jneuroim.2018.03.011>
- Shannon-Lowe, C., Adland, E., Bell, A. I., Delecluse, H.-J., Rickinson, A. B., & Rowe, M. (2009). Features distinguishing Epstein-Barr virus infections of epithelial cells and B cells: Viral genome expression, genome maintenance, and genome amplification. *Journal of Virology*, *83*(15), 7749–7760. <https://doi.org/10.1128/JVI.00108-09>
- Sharma, S., & Thomas, P. G. (2014). The two faces of heterologous immunity: Protection or immunopathology. *Journal of Leukocyte Biology*, *95*(3), 405–416. <https://doi.org/10.1189/jlb.0713386>
- Shi, R., Soomro, M. H., She, R., Yang, Y., Wang, T., Wu, Q., Li, H., & Hao, W. (2016). Evidence of Hepatitis E virus breaking through the blood–brain barrier and replicating in the central nervous system. *Journal of Viral Hepatitis*, *23*(11), 930–939. <https://doi.org/10.1111/jvh.12557>

- Shope, T., Dechairo, D., & Miller, G. (1973). Malignant lymphoma in cottontop marmosets after inoculation with Epstein-Barr virus. *Proceedings of the National Academy of Sciences of the United States of America*, 70(9), 2487–2491. <https://doi.org/10.1073/pnas.70.9.2487>
- Smatti, M. K., Al-Sadeq, D. W., Ali, N. H., Pintus, G., Abou-Saleh, H., & Nasrallah, G. K. (2018). Epstein-Barr Virus Epidemiology, Serology, and Genetic Variability of LMP-1 Oncogene Among Healthy Population: An Update. *Frontiers in Oncology*, 8, 211. <https://doi.org/10.3389/fonc.2018.00211>
- Sohlberg, E., Saghafian-Hedengren, S., Rasul, E., Marchini, G., Nilsson, C., Klein, E., Nagy, N., & Sverremark-Ekström, E. (2013). Cytomegalovirus-seropositive children show inhibition of in vitro EBV infection that is associated with CD8+CD57+ T cell enrichment and IFN- $\gamma$ . *Journal of Immunology (Baltimore, Md.: 1950)*, 191(11), 5669–5676. <https://doi.org/10.4049/jimmunol.1301343>
- Song, E., Zhang, C., Israelow, B., Lu-Culligan, A., Prado, A. V., Skriabine, S., Lu, P., Weizman, O.-E., Liu, F., Dai, Y., Szigeti-Buck, K., Yasumoto, Y., Wang, G., Castaldi, C., Heltke, J., Ng, E., Wheeler, J., Alfajaro, M. M., Levavasseur, E., ... Iwasaki, A. (2021). Neuroinvasion of SARS-CoV-2 in human and mouse brain. *The Journal of Experimental Medicine*, 218(3), e20202135. <https://doi.org/10.1084/jem.20202135>
- Steinman, R. M., & Nussenzweig, M. C. (2002). Avoiding horror autotoxicus: The importance of dendritic cells in peripheral T cell tolerance. *Proceedings of the National Academy of Sciences of the United States of America*, 99(1), 351–358. <https://doi.org/10.1073/pnas.231606698>
- Stojić-Vukanić, Z., Pilipović, I., Vujnović, I., Nacka-Aleksić, M., Petrović, R., Arsenović-Ranin, N., Dimitrijević, M., & Leposavić, G. (2016). GM-CSF-Producing Th Cells in Rats Sensitive and Resistant to Experimental Autoimmune Encephalomyelitis. *PLoS One*, 11(11), e0166498. <https://doi.org/10.1371/journal.pone.0166498>
- Strowig, T., Brilot, F., Arrey, F., Bougras, G., Thomas, D., Muller, W. A., & Münz, C. (2008). Tonsillar NK cells restrict B cell transformation by the Epstein-Barr virus via IFN-gamma. *PLoS Pathogens*, 4(2), e27. <https://doi.org/10.1371/journal.ppat.0040027>
- Ta, T. T., Dikmen, H. O., Schilling, S., Chausse, B., Lewen, A., Hollnagel, J. O., & Kann, O. (2019). Priming of microglia with IFN- $\gamma$  slows neuronal gamma oscillations in situ. *Proceedings of the National Academy of Sciences of the United States of America*, 116(10), 4637–4642. <https://doi.org/10.1073/pnas.1813562116>

- Takashima, K., Ohashi, M., Kitamura, Y., Ando, K., Nagashima, K., Sugihara, H., Okuno, K., Sairenji, T., & Hayashi, K. (2008). A new animal model for primary and persistent Epstein-Barr virus infection: Human EBV-infected rabbit characteristics determined using sequential imaging and pathological analysis. *Journal of Medical Virology*, *80*(3), 455–466. <https://doi.org/10.1002/jmv.21102>
- Takata, F., Dohgu, S., Yamauchi, A., Sumi, N., Nakagawa, S., Naito, M., Tsuruo, T., Shuto, H., & Kataoka, Y. (2006). Inhibition of transforming growth factor-beta production in brain pericytes contributes to cyclosporin A-induced dysfunction of the blood-brain barrier. *Cellular and Molecular Neurobiology*, *27*(3), 317–328. <https://doi.org/10.1007/s10571-006-9125-x>
- Tan, J., Town, T., Paris, D., Mori, T., Suo, Z., Crawford, F., Mattson, M. P., Flavell, R. A., & Mullan, M. (1999). Microglial Activation Resulting from CD40-CD40L Interaction After  $\beta$ -Amyloid Stimulation. *Science*, *286*(5448), 2352–2355. <https://doi.org/10.1126/science.286.5448.2352>
- Taylor, W. R., Rasley, A., Bost, K. L., & Marriott, I. (2003). Murine gammaherpesvirus-68 infects microglia and induces high levels of pro-inflammatory cytokine production. *Journal of Neuroimmunology*, *136*(1-2), 75–83. [https://doi.org/10.1016/s0165-5728\(03\)00011-0](https://doi.org/10.1016/s0165-5728(03)00011-0)
- Templeton, S. P., Kim, T. S., O'Malley, K., & Perlman, S. (2008). Maturation and Localization of Macrophages and Microglia During Infection with a Neurotropic Murine Coronavirus. *Brain Pathology (Zurich, Switzerland)*, *18*(1), 40–51. <https://doi.org/10.1111/j.1750-3639.2007.00098.x>
- Terry, L. A., Stewart, J. P., Nash, A. A., & Fazakerley, J. K. (2000). Murine gammaherpesvirus-68 infection of and persistence in the central nervous system. *Journal of General Virology*, *81*(11), 2635–2643. <https://doi.org/10.1099/0022-1317-81-11-2635>
- Teymoori-Rad, M., Mozhgani, S.-H., Zarei-Ghobadi, M., Sahraian, M. A., Nejati, A., Amiri, M. M., Shokri, F., & Marashi, S. M. (2019). Integrational analysis of miRNAs data sets as a plausible missing linker between Epstein-Barr virus and vitamin D in relapsing remitting MS patients. *Gene*, *689*, 1–10. <https://doi.org/10.1016/j.gene.2018.12.004>
- Thompson, A. J., Baranzini, S. E., Geurts, J., Hemmer, B., & Ciccarelli, O. (2018). Multiple sclerosis. *The Lancet*, *391*(10130), 1622–1636. [https://doi.org/10.1016/S0140-6736\(18\)30481-1](https://doi.org/10.1016/S0140-6736(18)30481-1)

- Thorley-Lawson, D. A. (1981). The transformation of adult but not newborn human lymphocytes by Epstein Barr virus and phytohemagglutinin is inhibited by interferon: The early suppression by T cells of Epstein Barr infection is mediated by interferon. *Journal of Immunology (Baltimore, Md.: 1950)*, *126*(3), 829–833.
- Thorley-Lawson, D. A., & Gross, A. (2004). Persistence of the Epstein-Barr virus and the origins of associated lymphomas. *The New England Journal of Medicine*, *350*(13), 1328–1337. <https://doi.org/10.1056/NEJMra032015>
- Tian, J., Shi, R., Liu, T., She, R., Wu, Q., An, J., Hao, W., & Soomro, M. H. (2019). Brain Infection by Hepatitis E Virus Probably via Damage of the Blood-Brain Barrier Due to Alterations of Tight Junction Proteins. *Frontiers in Cellular and Infection Microbiology*, *9*, 52. <https://doi.org/10.3389/fcimb.2019.00052>
- Tierney, R. J., Shannon-Lowe, C. D., Fitzsimmons, L., Bell, A. I., & Rowe, M. (2015). Unexpected patterns of Epstein-Barr virus transcription revealed by a high throughput PCR array for absolute quantification of viral mRNA. *Virology*, *474*, 117–130. <https://doi.org/10.1016/j.virol.2014.10.030>
- Toga, A., Wada, T., Sakakibara, Y., Mase, S., Araki, R., Tone, Y., Toma, T., Kurokawa, T., Yanagisawa, R., Tamura, K., Nishida, N., Taneichi, H., Kanegane, H., & Yachie, A. (2010). Clinical significance of cloned expansion and CD5 down-regulation in Epstein-Barr Virus (EBV)-infected CD8+ T lymphocytes in EBV-associated hemophagocytic lymphohistiocytosis. *The Journal of Infectious Diseases*, *201*(12), 1923–1932. <https://doi.org/10.1086/652752>
- Torii, Y., Kawada, J.-I., Murata, T., Yoshiyama, H., Kimura, H., & Ito, Y. (2017). Epstein-Barr virus infection-induced inflammasome activation in human monocytes. *PloS One*, *12*(4), e0175053. <https://doi.org/10.1371/journal.pone.0175053>
- Touil, H., Kobert, A., Lebeurrier, N., Rieger, A., Saikali, P., Lambert, C., Fawaz, L., Moore, C. S., Prat, A., Gommerman, J., Antel, J. P., Itoyama, Y., Nakashima, I., Bar-Or, A., & Canadian B Cell Team in MS. (2018). Human central nervous system astrocytes support survival and activation of B cells: Implications for MS pathogenesis. *Journal of Neuroinflammation*, *15*(1), 114. <https://doi.org/10.1186/s12974-018-1136-2>
- Tsai, M. H., Lin, X., Shumilov, A., Bernhardt, K., Feederle, R., Poirey, R., Kopp-Schneider, A., Pereira, B., Almeida, R., & Delecluse, H.-J. (2017). The biological properties of different Epstein-Barr virus strains explain their association with various types of cancers. *Oncotarget*, *8*(6), 10238–10254. <https://doi.org/10.18632/oncotarget.14380>

- Tsai, T. T., Chen, C. L., Lin, Y. S., Chang, C. P., Tsai, C. C., Cheng, Y. L., Huang, C. C., Ho, C. J., Lee, Y. C., Lin, L. T., Jhan, M. K., & Lin, C. F. (2016). Microglia retard dengue virus-induced acute viral encephalitis. *Scientific Reports*, 6, 27670. <https://doi.org/10.1038/srep27670>
- Tsao, N., Hsu, H. P., Wu, C. M., Liu, C. C., & Lei, H. Y. (2001). Tumour necrosis factor-alpha causes an increase in blood-brain barrier permeability during sepsis. *Journal of Medical Microbiology*, 50(9), 812–821. <https://doi.org/10.1099/0022-1317-50-9-812>
- Tselis, A. C. (2014). Epstein-Barr virus infections of the nervous system. *Handbook of Clinical Neurology*, 123, 285–305. <https://doi.org/10.1016/B978-0-444-53488-0.00013-4>
- Tzartos, J. S., Khan, G., Vossenkamper, A., Cruz-Sadaba, M., Lonardi, S., Sefia, E., Meager, A., Elia, A., Middeldorp, J. M., Clemens, M., Farrell, P. J., Giovannoni, G., & Meier, U.-C. (2012). Association of innate immune activation with latent Epstein-Barr virus in active MS lesions. *Neurology*, 78(1), 15–23. <https://doi.org/10.1212/WNL.0b013e31823ed057>
- Uher, T., McComb, M., Galkin, S., Srpova, B., Oechtering, J., Barro, C., Tyblova, M., Bergsland, N., Krasensky, J., Dwyer, M., Havrdova, E. K., Posova, H., Vaneckova, M., Zivadinov, R., Horakova, D., Kuhle, J., & Ramanathan, M. (2021). Neurofilament levels are associated with blood-brain barrier integrity, lymphocyte extravasation, and risk factors following the first demyelinating event in multiple sclerosis. *Multiple sclerosis (Houndmills, Basingstoke, England)*, 27(2), 220–231. <https://doi.org/10.1177/1352458520912379>
- Urban, S. L., Jensen, I. J., Shan, Q., Pewe, L. L., Xue, H. H., Badovinac, V. P., & Harty, J. T. (2020). Peripherally induced brain tissue-resident memory CD8 + T cells mediate protection against CNS infection. *Nature Immunology*, 21(8), 938–949. <https://doi.org/10.1038/s41590-020-0711-8>
- Vainchtein, I. D., & Molofsky, A. V. (2020). Astrocytes and Microglia: In Sickness and in Health. *Trends in Neurosciences*, 43(3), 144–154. <https://doi.org/10.1016/j.tins.2020.01.003>
- Velasco-Estevez, M., Koch, N., Klejbor, I., Laurent, S., Dev, K. K., Szutowicz, A., Sailer, A. W., & Rutkowska, A. (2021). EBI2 Is Temporarily Upregulated in MO3.13 Oligodendrocytes during Maturation and Regulates Remyelination in the Organotypic Cerebellar Slice Model. *International Journal of Molecular Sciences*, 22(9), 4342. <https://doi.org/10.3390/ijms22094342>

- Veroni, C., Serafini, B., Rosicarelli, B., Fagnani, C., & Aloisi, F. (2018). Transcriptional profile and Epstein-Barr virus infection status of laser-cut immune infiltrates from the brain of patients with progressive multiple sclerosis. *Journal of Neuroinflammation*, *15*(1), 18. <https://doi.org/10.1186/s12974-017-1049-5>
- Voet, S., Prinz, M., & van Loo, G. (2018). Microglia in Central Nervous System Inflammation and Multiple Sclerosis Pathology. *Trends in Molecular Medicine*, *25*(2), 112–123. <https://doi.org/10.1016/j.molmed.2018.11.005>
- Volk, V., Theobald, S. J., Danisch, S., Khailaie, S., Kalbarczyk, M., Schneider, A., Bialek-Waldmann, J., Krönke, N., Deng, Y., Eiz-Vesper, B., Dragon, A. C., von Kaysenberg, C., Lienenklaus, S., Bleich, A., Keck, J., Meyer-Hermann, M., Klawonn, F., Hammerschmidt, W., Delecluse, H.-J., ... Stripecte, R. (2020). PD-1 Blockade Aggravates Epstein-Barr Virus+ Post-Transplant Lymphoproliferative Disorder in Humanized Mice Resulting in Central Nervous System Involvement and CD4+ T Cell Dysregulations. *Frontiers in Oncology*, *10*, 614876. <https://doi.org/10.3389/fonc.2020.614876>
- Wada, T., Kurokawa, T., Toma, T., Shibata, F., Tone, Y., Hashida, Y., Kaya, H., Yoshida, T., & Yachie, A. (2007). Immunophenotypic analysis of Epstein-Barr virus (EBV)-infected CD8(+) T cells in a patient with EBV-associated hemophagocytic lymphohistiocytosis. *European Journal of Haematology*, *79*(1), 72–75. <https://doi.org/10.1111/j.1600-0609.2007.00868.x>
- Wallin, M. T., Culpepper, W. J., Coffman, P., Pulaski, S., Maloni, H., Mahan, C. M., Haselkorn, J. K., Kurtzke, J. F., & Veterans Affairs Multiple Sclerosis Centres of Excellence Epidemiology Group. (2012). The Gulf War era multiple sclerosis cohort: Age and incidence rates by race, sex and service. *Brain: A Journal of Neurology*, *135*(Pt 6), 1778–1785. <https://doi.org/10.1093/brain/aws099>
- Wallin, M. T., Culpepper, W. J., Nichols, E., Bhutta, Z. A., Gebrehiwot, T. T., Hay, S. I., Khalil, I. A., Krohn, K. J., Liang, X., Naghavi, M., Mokdad, A. H., Nixon, M. R., Reiner, R. C., Sartorius, B., Smith, M., Topor-Madry, R., Werdecker, A., Vos, T., Feigin, V. L., & Murray, C. J. L. (2019). Global, regional, and national burden of multiple sclerosis 1990–2016: A systematic analysis for the Global Burden of Disease Study 2016. *The Lancet Neurology*, *18*(3), 269–285. [https://doi.org/10.1016/S1474-4422\(18\)30443-5](https://doi.org/10.1016/S1474-4422(18)30443-5)

- Walton, C., King, R., Rechtman, L., Kaye, W., Leray, E., Marrie, R. A., Robertson, N., La Rocca, N., Uitdehaag, B., van der Mei, I., Wallin, M., Helme, A., Angood Napier, C., Rijke, N., & Baneke, P. (2020). Rising prevalence of multiple sclerosis worldwide: Insights from the Atlas of MS, third edition. *Multiple Sclerosis (Houndmills, Basingstoke, England)*, 26(14), 1816–1821. <https://doi.org/10.1177/1352458520970841>
- Wang, C., Wang, H., Zhang, Y., Guo, W., Long, C., Wang, J., Liu, L., & Sun, X. (2017). Berberine inhibits the proliferation of human nasopharyngeal carcinoma cells via an Epstein-Barr virus nuclear antigen 1-dependent mechanism. *Oncology Reports*, 37(4), 2109–2120. <https://doi.org/10.3892/or.2017.5489>
- Wang, G., Zarek, C., Chang, T., Tao, L., Lowe, A., & Reese, T. A. (2021). Th2 Cytokine Modulates Herpesvirus Reactivation in a Cell Type Specific Manner. *Journal of Virology*, , 95(8), e01946-20. <https://doi.org/10.1128/JVI.01946-20>
- Weidner-Glunde, M., Kruminis-Kaszkiel, E., & Savanagouder, M. (2020). Herpesviral Latency-Common Themes. *Pathogens (Basel, Switzerland)*, 9(2), 125. <https://doi.org/10.3390/pathogens9020125>
- Weinberg, A., Bloch, K. C., Li, S., Tang, Y.-W., Palmer, M., & Tyler, K. L. (2005). Dual Infections of the Central Nervous System with Epstein-Barr Virus. *The Journal of Infectious Diseases*, 191(2), 234–237. <https://doi.org/10.1086/426402>
- Welsh, R. M., Che, J. W., Brehm, M. A., & Selin, L. K. (2010). Heterologous immunity between viruses. *Immunological Reviews*, 235(1), 244–266. <https://doi.org/10.1111/j.0105-2896.2010.00897.x>
- Welsh, R. M., & Fujinami, R. S. (2007). Pathogenic epitopes, heterologous immunity and vaccine design. *Nature Reviews Microbiology*, 5(7), 555–563. <https://doi.org/10.1038/nrmicro1709>
- Wergeland, S., Myhr, K.-M., Løken-Amsrud, K. I., Beiske, A. G., Bjerve, K. S., Hovdal, H., Midgard, R., Kvistad, S. S., Holmøy, T., Riise, T., & Torkildsen, Ø. (2016). Vitamin D, HLA-DRB1 and Epstein-Barr virus antibody levels in a prospective cohort of multiple sclerosis patients. *European Journal of Neurology*, 23(6), 1064–1070. <https://doi.org/10.1111/ene.12986>
- Wheeler, D. L., Sariol, A., Meyerholz, D. K., & Perlman, S. (2018). Microglia are required for protection against lethal coronavirus encephalitis in mice. *The Journal of Clinical Investigation*, 128(3), 931–943. <https://doi.org/10.1172/JCI97229>

- Willer, C. J., Dyment, D. A., Risch, N. J., Sadovnick, A. D., Ebers, G. C., & Canadian Collaborative Study Group. (2003). Twin concordance and sibling recurrence rates in multiple sclerosis. *Proceedings of the National Academy of Sciences*, *100*(22), 12877–12882. <https://doi.org/10.1073/pnas.1932604100>
- Wilson, E. H., Weninger, W., & Hunter, C. A. (2010). Trafficking of immune cells in the central nervous system. *The Journal of Clinical Investigation*, *120*(5), 1368–1379. <https://doi.org/10.1172/JCI41911>
- Wolswijk, G. (2000). Oligodendrocyte survival, loss and birth in lesions of chronic-stage multiple sclerosis. *Brain: A Journal of Neurology*, *123* ( Pt 1), 105–115. <https://doi.org/10.1093/brain/123.1.105>
- Wong, D., Dorovini-Zis, K., & Vincent, S. R. (2004). Cytokines, nitric oxide, and cGMP modulate the permeability of an in vitro model of the human blood-brain barrier. *Experimental Neurology*, *190*(2), 446–455. <https://doi.org/10.1016/j.expneurol.2004.08.008>
- Woon, H. G., Braun, A., Li, J., Smith, C., Edwards, J., Sierro, F., Feng, C. G., Khanna, R., Elliot, M., Bell, A., Hislop, A. D., Tangye, S. G., Rickinson, A. B., Gebhardt, T., Britton, W. J., & Palendira, U. (2016). Compartmentalization of Total and Virus-Specific Tissue-Resident Memory CD8<sup>+</sup> T Cells in Human Lymphoid Organs. *PLOS Pathogens*, *12*(8), e1005799. <https://doi.org/10.1371/journal.ppat.1005799>
- Wu, Y., Maruo, S., Yajima, M., Kanda, T., & Takada, K. (2007). Epstein-Barr Virus (EBV)-Encoded RNA 2 (EBER2) but Not EBER1 Plays a Critical Role in EBV-Induced B-Cell Growth Transformation. *Journal of Virology*, *81*(20), 11236–11245. <https://doi.org/10.1128/JVI.00579-07>
- Yamasaki, R., Lu, H., Butovsky, O., Ohno, N., Rietsch, A. M., Cialic, R., Wu, P. M., Doykan, C. E., Lin, J., Cotleur, A. C., Kidd, G., Zorlu, M. M., Sun, N., Hu, W., Liu, L., Lee, J. C., Taylor, S. E., Uehlein, L., Dixon, D., ... Ransohoff, R. M. (2014). Differential roles of microglia and monocytes in the inflamed central nervous system. *The Journal of Experimental Medicine*, *211*(8), 1533–1549. <https://doi.org/10.1084/jem.20132477>
- Yang, A. C., Kern, F., Losada, P. M., Agam, M. R., Maat, C. A., Schmartz, G. P., Fehlmann, T., Stein, J. A., Schaum, N., Lee, D. P., Calcuttawala, K., Vest, R. T., Berdnik, D., Lu, N., Hahn, O., Gate, D., McNerney, M. W., Channappa, D., Cobos, I., ... Wyss-Coray, T. (2021). Dysregulation of brain and choroid plexus cell types in severe COVID-19. *Nature*, *595*(7868), 565–571. <https://doi.org/10.1038/s41586-021-03710-0>



- Yang, Y., & Gao, F. (2020). Clinical characteristics of primary and reactivated Epstein-Barr virus infection in children. *Journal of Medical Virology*, 10.1002/jmv.26202. <https://doi.org/10.1002/jmv.26202>
- Young, L. S., Yap, L. F., & Murray, P. G. (2016). Epstein-Barr virus: More than 50 years old and still providing surprises. *Nature Reviews. Cancer*, 16(12), 789–802. <https://doi.org/10.1038/nrc.2016.92>
- Ysraelit, M. C., & Correale, J. (2019). Impact of sex hormones on immune function and multiple sclerosis development. *Immunology*, 156(1), 9–22. <https://doi.org/10.1111/imm.13004>
- Yun, S. P., Kam, T. I., Panicker, N., Kim, S., Oh, Y., Park, J. S., Kwon, S. H., Park, Y. J., Karuppagounder, S. S., Park, H., Kim, S., Oh, N., Kim, N. A., Lee, S., Brahmachari, S., Mao, X., Lee, J. H., Kumar, M., An, D., ... Ko, H. S. (2018). Block of A1 astrocyte conversion by microglia is neuroprotective in models of Parkinson's disease. *Nature Medicine*, 24(7), 931–938. <https://doi.org/10.1038/s41591-018-0051-5>
- Zdimerova, H., Murer, A., Engelmann, C., Raykova, A., Deng, Y., Gujer, C., Rühl, J., McHugh, D., Caduff, N., Naghavian, R., Pezzino, G., Capaul, R., Zbinden, A., Ferlazzo, G., Lünemann, J. D., Martin, R., Chatterjee, B., & Münz, C. (2021). Attenuated immune control of Epstein-Barr virus in humanized mice is associated with the multiple sclerosis risk factor HLA-DR15. *European Journal of Immunology*, 51(1), 64–75. <https://doi.org/10.1002/eji.202048655>
- Zeni, P., Doepker, E., Schulze-Topphoff, U., Schulze Topphoff, U., Huewel, S., Tenenbaum, T., & Galla, H.-J. (2007). MMPs contribute to TNF-alpha-induced alteration of the blood-cerebrospinal fluid barrier in vitro. *American Journal of Physiology. Cell Physiology*, 293(3), C855-864. <https://doi.org/10.1152/ajpcell.00470.2006>
- Zubair, A. S., McAlpine, L. S., Gardin, T., Farhadian, S., Kuruvilla, D. E., & Spudich, S. (2020). Neuropathogenesis and Neurologic Manifestations of the Coronaviruses in the Age of Coronavirus Disease 2019: A Review. *JAMA Neurology*, 77(8), 1018–1027. <https://doi.org/10.1001/jamaneurol.2020.2065>

## List of Publications

### Relevant

*Hassani A*, Reguraman N, Shehab S, Khan G. Primary Peripheral Epstein-Barr virus infection can lead to CNS infection and neuroinflammation in a rabbit model: Implications for multiple sclerosis pathogenesis. *Frontiers in Immunology*, 12, 5035 DOI:10.3389/fimmu.2021.764937

Reguraman N, *Hassani A*, Philip P, Khan G. Uncovering early events in primary Epstein-Barr virus infection using a rabbit model. *Scientific reports*, 11(1), 21220. <https://doi.org/10.1038/s41598-021-00668-x>

*Hassani A*, Khan G. Epstein-Barr Virus and Neuroinflammation. In: *Translational Neuroimmunology*. (Edited by Nima Rezaei), Elsevier, 2021, Vol 7, Chapter 8 [In press]

Khan G, *Hassani A*. Epstein-Barr Virus in Multiple Sclerosis. In: *Multiple Sclerosis*. (Edited by Stavros J. Baloyannis). InTech 2019. DOI:10.5772/intechopen.85222

*Hassani A*, Khan G. Epstein-Barr virus and miRNAs: partners in crime in the pathogenesis of multiple sclerosis? *Frontiers in Immunol* 2019; 10:695. <https://doi.org/10.3389/fimmu.2019.00695>

*Hassani A*, Corboy JR, Al-Salam S, Khan G. Epstein-Barr virus is present in the brain of most cases of multiple sclerosis and may engage more than just B cells. *PloS One*. 2018 Feb 2;13: e0192109. <https://doi.org/10.1371/journal.pone.0192109>

### Other

*Hassani A*, Khan G. Human-Animal Interaction and the Emergence of SARS-CoV-2. *JMIR Public Health Surveill* 2020;6(4):e22117. <https://doi.org/10.2196/22117>

## Appendix

### Appendix I: Coating slides

#### A- Coating histology slides:

- 1- Slides were washed in water for 30 min
- 2- Slides were immersed in acetone (Panreac, 361007) for 5 min
- 3- Slides were incubated in 2% 3-aminopropyltriethoxysilane in acetone for another 5 min
- 4- Slides were rinsed in distilled water for a minute and eventually left to air dry overnight

### Appendix II: Buffers and reagents preparation

#### B- Preparation of hybridization buffer

Five milliliter hybridization buffer was prepared by mixing:

- 1- 2.5 ml formamide deionized (Sigma Cat# F9037). This blocks RNases activity, which improves RNA stability
- 2- 1 ml 25% dextran sulphate (Sigma Cat# D8906). This enhances probe concentration owing to its capacity to displace water
- 3- 500  $\mu$ l 20x SSC (saline sodium citrate, pH7.0. 1 L: 175.3 g NaCl (3 M) + 88.2 g sodium citrate + 800 mL sterile dH<sub>2</sub>O). This buffer regulates stringency
- 4- 125  $\mu$ l 2 M Tris-HCl pH 7.5
- 5- 875  $\mu$ l ddH<sub>2</sub>O

#### C- Preparation of 10xPBS (phosphate buffered saline):

10x in 1 L ddH<sub>2</sub>O: 80 g NaCl, 2 g KCl, 14.4 g Na<sub>2</sub>HPO<sub>4</sub>, 2.4 g KH<sub>2</sub>PO<sub>4</sub>; pH 7.4.

#### D- Preparation of DAB:

One gram of DAB powder was dissolved in 40 ml water with ~5 drops of HCl (ACS reagent, 37%, Sigma, 258148) to facilitate DAB dissolving.